

SIRT1; A Novel Antithrombotic Target in Cardiovascular Disease?

MARIA ROSARIO BLANCO LOPEZ

A thesis submitted for the Degree of Doctor of
Philosophy (PhD)

Department of Life Sciences
Manchester Metropolitan University

2024

Abstract

Platelets play a pivotal role in atherothrombosis, the primary cause of heart attacks and ischaemic strokes. As a consequence, antiplatelet drugs provide an important reduction in cardiovascular events. However, adverse bleeding events and variable patient responses limit the safety and efficacy of current antithrombotic treatments, which generates the clinical need to develop novel therapeutical approaches.

Sirtuin 1 (SIRT1) is an NAD⁺ dependent deacetylase protective against oxidative damage. Individuals at high risk of atherothrombosis, such as diabetic and obese patients, display reduced SIRT1 levels, which were associated with enhanced thrombus formation in a murine model of arterial thrombosis. However, the importance of SIRT1 in regulating haemostasis and thrombosis has not been evaluated. The aim of this study was to assess the potential use of the SIRT1 selective agonist SRT1720 as a novel antithrombotic therapy by evaluating the effect of SIRT1 activation on platelet and endothelial function.

First, the expression of all sirtuins was confirmed in platelets. Then, different platelet functional assays with SRT1720-treated (10 μ M) platelet-rich plasma were performed. Using plate-based aggregometry, it was demonstrated that SIRT1 activation attenuates platelet aggregation induced with TRAP-6, collagen and ADP. Further evaluation of the role of SIRT1 in platelet activation showed that SRT1720 decreases fibrinogen and PAC-1 binding, which indicates that this drug reduces integrin α IIb β 3 activation. Moreover, SIRT1 activation decreased the percentage of platelets that release dense granules, while no effects were observed in α -granule secretion. *In vitro* arterial thrombus formation assays demonstrated that SRT1720 reduces the area covered by the thrombi on collagen.

Considering the decrease in thrombus formation caused by SRT1720, the effect of SIRT1 activation in platelet functions dependent on integrin α IIb β 3 “outside-in” signalling and cytoskeletal reorganisation was explored. Activation of SIRT1 inhibited platelet adhesion and spreading on collagen and fibrinogen, but it did not alter the tubulin ring. Incubation with SRT1720 disrupted the actin cytoskeleton of basal and activated platelets and significantly reduced actin polymerization after stimulation. The results from this study also demonstrate that SRT1720 reduces the late stage of clot retraction, which suggests that SIRT1 activation could potentiate the bioavailability of fibrinolytics inside of the thrombi by reducing its density. To investigate the signalling behind the effects of SRT1720 in integrin α IIb β 3 activity and cytoskeletal rearrangement, the phosphorylation status of key

regulators, including Y773- β 3, S3-cofilin-1, Y397-FAK, and S19-MLC2, was assessed in resting and activated platelets following SIRT1 activation. Although the phosphorylation levels of these proteins changed upon platelet agonist stimulation, SRT1720 had no effect. Thus, the precise mechanism by which SIRT1 exerts its effects in platelets remains unclear.

To evaluate the global effect of SIRT1 activation in thrombosis and haemostasis, the impact of SRT1720 in healthy and dysfunctional human coronary artery endothelial cells (HCAECs) was also investigated. This study confirmed that HCAECs express SIRT1 and revealed that SRT1720 is not toxic at a dose of 3 μ M or lower. SRT1720 (0.1 - 3 μ M) failed to reverse TNF- α -induced NF- κ B nuclear translocation in HCAEC. In a gap closure assay, a high but non-toxic dose of SRT1720 (3 μ M) significantly reduced HCAEC migration. Investigation of the mechanism behind these effects revealed that HCAEC F-actin levels remained unaltered upon TNF- α and SRT1720 treatment (0.1 - 3 μ M). Using a FITC-dextran permeability assay, it was identified that SIRT1 activation is protective against LPS-induced hyperpermeability in HCAEC. To assess the role of SIRT1 in the context of atherosclerosis and thromboinflammation *in vitro*, the effect of a panel of endothelial dysfunction inducers, including IL-6 (50 ng/mL), LPS (100 ng/mL), TNF- α (10 ng/mL) and H₂O₂ (100 μ M), was tested in HCAEC, revealing that LPS was the best molecule to induce dysfunction. The effect of SIRT1 activation on thrombosis was tested *in vitro* using an endothelialised arterial flow model, revealing that the area covered by the thrombi on the HCAEC treated with SRT1720 in the presence of LPS was significantly reduced versus the vehicle control. To elucidate the mechanism behind these protective effects, the impact of SIRT1 activation on the mRNA expression of endothelial regulators of haemostasis in healthy and dysfunctional HCAEC was evaluated using RT-qPCR. SRT1720 (1 μ M) increased NOS3 mRNA levels only in healthy HCAEC, while it was unable to recover NOS3 LPS-induced downregulation. By contrast, DDAH1 mRNA levels were increased by SRT1720 in the presence of LPS. Moreover, SIRT1 activation increased THBD mRNA expression in LPS-treated and healthy HCAEC.

In conclusion, the investigation performed for this thesis indicates that SIRT1 activation could be a novel alternative to current antiplatelet agents and a potential adjuvant drug during fibrinolytic therapy. Moreover, the protective effects of SIRT1 activation observed in HCAEC suggest that SIRT1 agonists could be useful to prevent endothelial dysfunction.

Acknowledgements

I would like to express my deep gratitude to my supervisory team for their constant support throughout my PhD journey, ensuring I always put my wellbeing first. Dr Sarah Jones and Dr Amanda Unsworth, thank you for guiding me during this research project and giving me the space to grow as a scientist, allowing me to develop critical and creative thinking while feeling always supported. You are the best mentors I could have ever asked for and will always be role models for me.

Thank you to all the members of the MMU Cardiovascular Research Group, especially my colleagues of the Thrombosis Group, for your feedback, motivation and genuine interest in my research. I also want to thank everyone in the MMU Department of Life Sciences who has somehow contributed to the development of this thesis, even if it was through a pat on the back on a day my experiments failed. Some of you are not only great colleagues but also close friends. Sophie, Razan, Marta, Marilena, Chloe, Anna and Rabea, I feel very lucky to have shared this experience with you.

I am also extremely grateful to all the members of the Ghevaert Group at Cambridge Stem Cell Institute, for allowing me to spend some time in their lab doing amazing research and for being so welcoming. Also during my research stay in Cambridge, I had the immense fortune to meet Andrea, Íñigo, Marcos and Duncan, and to reconnect with Lidia, Alberto and Mati. Apart from great friends, you are all extremely bright and kind. I deeply admire you. Special thanks to Andrea, Mati and Lidia, who were there for me in a very difficult moment in my life. Wherever we go, we know we will always be there for each other.

Huge thanks to my friends Pablo and Elli, who always took care of me and included me in their lovely life. You made Manchester my home and I consider you my family. I also want to thank my best friends in Spain, or should I say sisters? Caye, Nati, María, Lucía and Sara. You always seemed to be right next to me in the good and bad moments, even though you were 1248.26 km away. Thank you for the countless moments of laughter we spent together. I am very lucky to have you.

Last and most importantly, I want to thank my parents, Cristina and Conrado, and my grandparents, Memé and Pepé, for always believing in me and giving me the chance to pursue a career in science. I could not have done this without your emotional support. I love you very much. Pepé, I dedicate this thesis to you.

Table of contents

Abstract.....	1
Acknowledgements	3
Presentations	8
List of Tables.....	10
List of Figures	11
Abbreviations	20
Chapter 1. General introduction.....	26
1.1 Platelet production	26
1.2 Platelet structure	26
1.2.1 Cytoskeleton	28
1.3 Platelet function.....	31
1.3.1 Primary haemostasis	31
1.3.2 Secondary Haemostasis	33
1.4 Platelet signalling	36
1.4.1 Adhesion receptors	36
1.4.2 G-protein coupled receptors.....	39
1.5 Vascular endothelial cell structure.....	44
1.6 Vascular endothelial cell function	45
1.7 Cardiovascular disease	48
1.7.1 Endothelial dysfunction	48
1.7.2 Atherosclerosis and atherothrombosis.....	53
1.7.3 Antithrombotic treatments.....	56
1.8 Posttranslational modifications	61
1.8.1 Lysine acetyltransferases	62
1.8.2 Lysine deacetylases	65
1.8.3 Targeting acetylation in atherosclerosis.....	66
1.9 SIRT1 pharmacological modulators.....	68
1.10 Aims and objectives.....	69
Chapter 2. Materials and methods	70

2.1 Pharmacological modulation of SIRT1	70
2.2 Platelet agonists	70
2.3 Human blood extraction and preparation	70
2.3.1 Phlebotomy	70
2.3.2 Preparation of platelet-rich plasma and washed platelets.....	71
2.4 Plate-Based Aggregometry	71
2.5 Flow cytometry	72
2.5.1 Platelet activation markers	73
2.5.2 Actin polymerisation assay	73
2.6 Platelet adhesion and spreading assay	74
2.7 Scanning Electron Microscopy	75
2.8 Investigation of the platelet marginal band	76
2.9 Clot retraction	77
2.10 Western Blotting	78
2.10.1 F/G actin ratio	79
2.10.2 Platelet signalling	80
2.11 Arterial thrombus formation <i>in vitro</i> on collagen	80
2.12 HCAEC dysfunction inducers	82
2.13 HCAEC culture	83
2.14 HCAEC immunofluorescence	84
2.14.1 SIRT1 expression	84
2.14.2 Actin staining.....	84
2.14.3 NF- κ B subcellular location and actin polymerisation	85
2.14.4 Evaluation of HCAEC eNOS levels post-thrombosis model.....	86
2.15 MTS assay	87
2.16 Cell migration assay	87
2.17 Endothelial permeability assay	88
2.18 Endothelialised arterial thrombus formation <i>in vitro</i>	89
2.19 Quantitative reverse transcription polymerase chain reaction	92

2.19.1	Treatments, extraction and purification.....	92
2.19.2	Reverse transcription	92
2.19.3	Real-time quantitative Polymerase Chain Reaction (RT-qPCR)	93
2.19.4	Primer design and sequences	93
2.19.5	Primer efficiencies.....	95
2.20	Statistical Analysis	96
Chapter 3. SIRT1 activation reduces platelet reactivity and thrombus formation in vitro		
.....		97
3.1	Introduction	97
3.2	Hypothesis, chapter aim and objectives.....	99
3.3	Results	100
3.3.1	All SIRT1s are present in human platelets	100
3.3.2	SIRT1 activation reduces platelet aggregation	102
3.3.3	SRT1720 reduces integrin α IIb β 3 activation	106
3.3.4	SRT1720 reduces dense granule release but does not affect α -granule secretion	109
3.3.5	SIRT1 activation reduces thrombus formation <i>in vitro</i>	112
3.4	Discussion	114
Chapter 4. SIRT1 activation disrupts actin cytoskeleton dynamics, decreasing platelet spreading and clot retraction		122
4.1	Introduction	122
4.2	Hypothesis, chapter aim and objectives.....	125
4.3	Results	126
4.3.1	SRT720 inhibits platelet adhesion and spreading in static conditions	126
4.3.2	SRT1720 disrupts the platelet cytoskeleton	129
4.3.3	SIRT1 activation reduces the F-actin pool in activated platelets.....	131
4.3.4	SIRT1 activation has no effect on platelet microtubule reorganisation.....	133
4.3.5	SIRT1 activation attenuates the late stage of platelet clot retraction.....	136
4.3.6	The role of SIRT1 in platelet signalling.....	138
4.4	Discussion	146
Chapter 5. Protective effects of SIRT1 on endothelial function		153

5.1 Introduction	153
5.2 Hypothesis, chapter aim and objectives.....	157
5.3 Results	158
5.3.1 SIRT1 is present in HCAEC	158
5.3.2 The effect of SRT1720 on HCAEC viability.....	160
5.3.3 The role of SIRT1 in endothelial cell function	162
5.3.3.4 SRT1720 reduces LPS-induced HCAEC permeability.....	168
5.3.4 The impact of SIRT1 activation on endothelial regulation of thrombus formation <i>in vitro</i>	172
5.3.5 Transcriptional effects of SIRT1 in arterial endothelial cells	176
5.4 Discussion	182
<i>Chapter 6. General discussion</i>	<i>191</i>
6.1 Key findings.....	191
6.1.1 SIRT1 is a key regulator of platelet function.....	191
6.1.2 SIRT1 activation has antithrombotic effects in platelets and endothelial cells, reducing <i>in vitro</i> thrombus formation	192
6.1.3 SIRT1 prevents LPS-induced endothelial dysfunction by reducing HCAEC permeability	194
6.1.4 SIRT1 activation did not compensate for the downregulation in eNOS protein and mRNA expression caused by LPS in HCAEC.....	195
6.1.5 SIRT1 regulates platelet spreading and HCAEC migration.....	196
6.1.6 SIRT1 activators as novel antithrombotics.....	198
6.2 Limitations and future directions.....	204
6.3 Conclusion	211
<i>Chapter 7. References</i>	<i>212</i>
<i>Appendix</i>	<i>272</i>
Primer efficiencies	272

Conferences and presentations

2021

- **International Society on Thrombosis and Haemostasis (ISTH) Virtual Congress**
Attendee
- **Platelet Society Virtual Meeting**
Attendee
- **Thromboinflammation Workshop at the University of Manchester**
Poster presentation

2022

- **Platelet Summer School, Reading**
Attendee
- **ECCR Symposium, Manchester**
Poster presentation
- **Small Vessel Disease Symposium, Manchester**
Poster presentation
- **Platelet Society Meeting, Hull**
Poster presentation

2023

- **Joint EUPLAN and Platelet Society Meeting, Bristol**
Poster presentation
- **Cell Biology of MKs and Platelets GRS and GRC, Lucca**
Poster presentation
- **BAS-BSCR Meeting, Manchester**
Poster presentation
- **Northern Vascular Biology Forum, Manchester**
Oral and poster presentations (Best Talk Award)

2024

- **MMU Summer Symposium, Manchester**
Oral and poster presentations (Best Poster Award)

Publications

- Drysdale, A., Blanco-Lopez, M., White, S. J., Unsworth, A. J. and Jones, S. (2024) 'Differential Proteoglycan Expression in Atherosclerosis Alters Platelet Adhesion and Activation'. *International Journal of Molecular Sciences*, 25(2) p. 950.
- Nock, S. H., Blanco-Lopez, M. R., Stephenson-Deakin, C., Jones, S. and Unsworth, A. J. (2024) 'Pim Kinase Inhibition Disrupts CXCR4 Signalling in Megakaryocytes and Platelets by Reducing Receptor Availability at the Surface'. *International Journal of Molecular Sciences*, 25(14) p. 7606.
- Nock, S., Hutchinson, J. L., Blanco-Lopez, M., Naseem, K., Jones, S., Mundell, S. J., Unsworth, A. J. (Accepted: 2024) 'Constitutive surface expression of the Thromboxane A2 receptor is Pim kinase-dependent'. *Journal of Thrombosis and Haemostasis* (under temporary embargo).

List of Tables

Table 1.1. Different types of G-protein α subunits and their functions.....	40
Table 1.2. Adhesion molecules involved in the maintenance of endothelial junctions.	45
Table 1.3. Classification of KAT in types and families and their subcellular location in human cells. In brackets and grey, are the former names of the different KATs. KAT, lysine acetyltransferase; KDAC, lysine deacetylases; α TAT1, α -tubulin N-acetyltransferase; CBP, CREB-binding protein; CRM1, chromosomal maintenance 1 or exportin 1; NAA60, N- α -acetyltransferase 60; NcoA, nuclear receptor coactivator; Tf, transcription factors.....	64
Table 1.4. SIRT1-specific modulators.....	69
Table 2.1. Platelet agonists used in experiments and supplier information.....	70
Table 2.2. Antibodies used for testing platelet activation markers using flow cytometry.....	73
Table 2.3. Antibodies used for Western blotting. mAb, monoclonal antibody.....	78
Table 2.4. Molecules used to induce endothelial dysfunction in HCAEC and suppliers.	82
Table 2.5. Primers used for RT-qPCR. F = forward, R = reverse.	95

List of Figures

Figure 1.1. Ultrastructure of an unstimulated platelet. Created in BioRender.com.	28
Figure 1.2. Coiling of the marginal band following platelet activation and microtubule depolymerisation. Created in BioRender.com.	30
Figure 1.3. Platelets in primary haemostasis. The healthy endothelium releases prostacyclin (PGI ₂), nitric oxide (NO) and CD39 to inhibit platelet activation. After vascular injury, primary haemostasis is initiated by the collagen-VWF complex, which promotes platelet initial adhesion. The binding of GPVI and integrin $\alpha 2\beta 1$ to collagen contributes to platelet adhesion and activation. Activated platelets spread and release secondary mediators through degranulation, which activates and recruits other platelets to the injury site. Then, the binding of fibrinogen to the activated integrin $\alpha IIb\beta 3$ allows platelet-platelet interactions, leading to aggregation and eventually thrombus formation. Created in BioRender.com.....	32
Figure 1.4. Summary of the coagulation cascade enzymatic reactions and negative feedback mechanisms. The coagulation cascade can be initiated via the intrinsic pathway, which requires platelet contact with an activating surface, or the extrinsic pathway, which is triggered by endothelial and subendothelial TF exposure upon vascular trauma. Both of these signalling pathways converge in the production of thrombin (FIIa) and the conversion of fibrinogen (FI) into fibrin (FIa). Fibrin clot formation is limited by negative feedback mechanisms, including the inactivation of TF and thrombin by AT; the binding of thrombin to THBD and the subsequent formation of the PC-PS complex, which blocks FVIIa; the inhibition of TF by TFPI in the presence of PS; and the degradation of fibrin by plasmin, which is created via the enzymatic conversion of plasminogen by tPA and uPA. Created in Biorender.com.	35
Figure 1.5. Summary of the main signalling pathways in platelets. Activation of GPVI, GPIb-IX-V or GPCRs initiates the phospholipase C (PLC) signalling pathway, which allows the conversion of phosphatidylinositol (4,5)-bisphosphate (PIP) into diacylglycerol (DAG) and inositol triphosphate (IP3). Then, DAG activates the protein kinase C (PKC), leading to “inside-out” signalling and the activation of integrin $\alpha IIb\beta 3$, while IP3 causes calcium (Ca ²⁺) mobilisation and granule release. Activated integrin $\alpha IIb\beta 3$ binds to fibrinogen, which results in “outside-in” signalling. TP – thromboxane receptor. Created with BioRender.com.	43
Figure 1.6. The basic structure of endothelial cells and the ECM. The main components of the ECM are collagen, proteoglycans, laminin and elastin. Created in Biorender.com.	44
Figure 1.7. Endothelial regulation of haemostasis. The release of NO, PGI ₂ and CD39 by healthy endothelial cells prevents platelet activation and adhesion. The molecular mechanisms involved in the negative regulation of coagulation are the irreversible binding and clearance of ATIII to thrombin (FIIa) and FXa; the presentation of FIIa to thrombomodulin by EPCR to generate activated protein C (APC), which complex with PS inhibits FVa and FVIIIa; and the release of TFPI, which binds to FXa and neutralises the TF-FVIIa complex, subsequently inhibiting the activation of FX in the extrinsic pathway. Endothelial cells contribute to fibrinolysis by secreting u-PA and t-PA, which convert plasminogen into plasmin, allowing the metabolization of fibrin into fibrin degradation products (FDPs). Created in BioRender.com.....	47
Figure 1.8. Molecular mechanisms of eNOS uncoupling. The three main mechanisms of eNOS uncoupling are BH4 or L-arginine deficiency, ADMA accumulation and eNOS S-glutathionylation.	49
Figure 1.9. Molecular mechanisms involved in endothelial dysfunction. Upon an injury or infection, endothelial cells produce the vasoconstrictor TXA ₂ . In response to inflammation, endothelial cells contract, which increases vascular permeability. Continuous exposure to inflammatory molecules, DAMPS or antigens, such as LPS, increases ROS levels, which reduces NO production. Activation of NF- κ B changes the endothelial transcriptome. Endothelial cells present leukocyte adhesion molecules on their surface, including E-selectin, ICAM-1 and VCAM-1, allowing leukocyte capture, rolling and extravasation. Moreover, dysfunctional endothelial cells express different cytokines, contributing further to the inflammatory cascade. Constant inflammation leads to cell death,	

causing denudation of the endothelium. Immobilisation of circulating VWF on the exposed ECM allows platelet adhesion and activation via the GPIb-IX-V complex. VWF release from the Weibel-Palade bodies is also increased, which facilitates the action of FVIIIa by acting as a carrier. The release of TF by endothelial cells activates the extrinsic coagulation pathway. Finally, fibrinolysis is inhibited due to an increase in the production of PAI-1, which translates into the inactivation of uPA and tPA. As a consequence, the thrombotic risk in healthy areas of the vessels increases. 52

Figure 1.10. Contribution of platelets to atherosclerosis and atherothrombosis. Atherosclerosis usually develops in the areas of the arteries with disturbed flow, such as the branching arterial regions, and is characterized by chronic vascular inflammation and oxidative stress, which leads to endothelial dysfunction. As a consequence, the antithrombotic effects of endothelial cells are impaired. In this prothrombotic scenario, activated platelets adhere to the vascular wall, contributing to the development of an atherosclerotic plaque. Plaque rupture or erosion leads to thrombus formation, which can either cause a total or partial occlusion of the vessel or travel towards arteries nearby. Created in Biorender.com. 55

Figure 1.11. Mechanism of action of currently available antiplatelet drugs. Aspirin prevents TXA2 synthesis via irreversible inhibition of COX; Vorapaxar is a PAR-1 antagonist; Clopidogrel, prasugrel, elinogrel, ticagrelor and cangrelor inhibit the P2Y12 ADP receptor and Glencicimab is an antibody that binds and blocks GPVI, preventing the binding of ligands and GPVI dimerisation. Created in Biorender.com. 60

Figure 1.12 Classes and subcellular location KDACs. In terms of cellular location, KDACs are more diverse than KATs. HDACs are mainly located in the nucleus, except class IIb HDACs. Contrarily, SIRT1s can be found in the cytoplasm, mitochondria or nucleus. These differences in subcellular distribution suggest that HDACs and SIRT1s play distinct roles in cell functions. Created in Biorender.com. 66

Figure 2.1. Representative images of platelets spread on non-coated wells and wells coated with collagen or fibrinogen. All wells were blocked with 1% BSA-PBS. The non-coated wells were used as a negative control for platelet adhesion and spreading. 74

Figure 2.2. Morphological classification of platelets based on the grade of spreading. From the least (left) to the most (right) spread, cells were categorised into 3 groups: adhered, filopodia forming platelets and lamellipodia forming platelets. 75

Figure 2.3. Morphological classification of the platelet marginal band. In the resting state, microtubules form a ring-like structure (A), while platelet activation leads to coiling (B). 77

Figure 2.4. Basic operation of the *in vitro* arterial thrombosis model on collagen. Blood was added to the 3 mL reservoir syringes (right) before the activation of the programmable pump, which withdraws the liquid from the slide channels at a shear stress representative of the arterial environment. Blood flowed over the collagen coated Ibidi slides and images of the thrombi were captured in real-time and at the end of the assay. Residual blood and Tyrodes-HEPES buffer were accumulated in the output 20 mL syringes (left) and disposed of according to the health and safety regulations. Created in BioRender.com. 81

Figure 2.5. Example of nuclear NF-κB analysis on ImageJ. Masks of the nucleus were created on the DAPI images (A) and overlaid on the GFP images (B) to measure NF-κB presence in the nucleus. 86

Figure 2.6. Seeding HCAEC for the scratch assay. HCAEC were grown O/N on Ibidi 2-well cell culture inserts (AI), which were then removed (AII), leaving a space between the cells. Representative images of the gap (B) were acquired using the 10x objective of the ZEISS Primovert inverted microscope (Carl Zeiss Microscopy Limited). 88

Figure 2.7. Principle of the endothelial permeability assay. FITC-dextran would only be present in the receiver tray if the permeability of the HCAEC monolayer is increased as a result of endothelial dysfunction. Created in BioRender com. 89

Figure 2.8. Representative image of a confluent HCAEC monolayer in the Ibidi VI 0.1 μ-slides. Images were taken with the 20x (left) and 10x (right) objectives of the ZEISS Primovert inverted microscope (Carl Zeiss Microscopy Limited, Cambridge, UK). 90

Figure 2.9. Endothelialised thrombus formation model set up. Reservoir syringes on the right, two connected Ibidi slides coated with HCAEC and collagen, respectively, on the microscope in the middle, and the multi-syringe pump on the left. Created in BioRender.com.....	90
Figure 2.10. Picture of the endothelialised arterial thrombus formation model setting.	91
Figure 2.11. Example of Weka trainable segmentation. Using an 8-bit image, the Weka segmentation tool from ImageJ was trained to differentiate the thrombi (red) from the HCAEC (green) and background (purple) using a reference image. The classifier was then saved and applied to the rest of the images of that dataset.	91
Figure 3.1. All proteins from the SIRT family were detected in human platelets by Western Blotting. Washed platelet lysates from 3 different donors (D1-D3) were immunoblotted with antibodies against SIRT1-7. Protein detection was performed using an HRP-labelled antibody and chemiluminescence. In the case of SIRT1, two bands were observed: one at 82 kDa and the other at 120 kDa, corresponding to SIRT1 and O-GlcNAc-SIRT1, respectively (A). The presence of SIRT2 isoform 1 (43 kDa) and isoform 2 (39 kDa) (B), SIRT3 (C), SIRT4 (D), SIRT5 (E), SIRT6 (F) and SIRT7 (G) were also confirmed in human platelets. MW=molecular weight.	101
Figure 3.2. SIRT1 activation reduces platelet aggregation in response to TRAP-6. PRP was incubated with different concentrations of SRT1720 (0.01 - 10 μ M) or vehicle (V, 0.1% DMSO) for 10 (A) and 60 (B) minutes. Then, platelet aggregation was induced with TRAP-6 (0.1 - 10 μ M). Absorbance was measured at 450 nm and the aggregation percentage was calculated. Dose-response curves were constructed (I) and aggregation stimulated by 3 μ M TRAP-6 was compared (II) using One-Way ANOVA. Data represent mean \pm SEM. ****p<0.0001. N=6.....	103
Figure 3.3. SIRT1 activation reduces platelet aggregation in response to collagen. PRP was incubated with different concentrations of SRT1720 (0.01 - 10 μ M) or vehicle (V, 0.1% DMSO) for 10 (A) and 60 (B) minutes. Then, platelet aggregation was induced with collagen (0.1 - 10 μ g/mL). Absorbance was measured at 450 nm and the aggregation percentage was calculated. Dose-response curves were constructed (I) and aggregation stimulated by 0.3 μ g/mL of collagen was compared (II) using One-Way ANOVA. Data represent mean \pm SEM. **p<0.01. N=6.	104
Figure 3.4. SIRT1 activation reduces ADP-induced platelet aggregation. PRP was incubated with different concentrations of SRT1720 (0.01 - 10 μ M) or vehicle (V, 0.1% DMSO) for 10 (A) and 60 min (B). Then, platelet aggregation was induced with ADP (0.1 - 10 μ M). Absorbance was measured at 450 nm and the aggregation percentage was calculated. Dose-response curves were constructed (I) and aggregation stimulated by 1 μ M ADP was compared (II) using One-Way ANOVA. Data represent mean \pm SEM. *p<0.05. N=6.	105

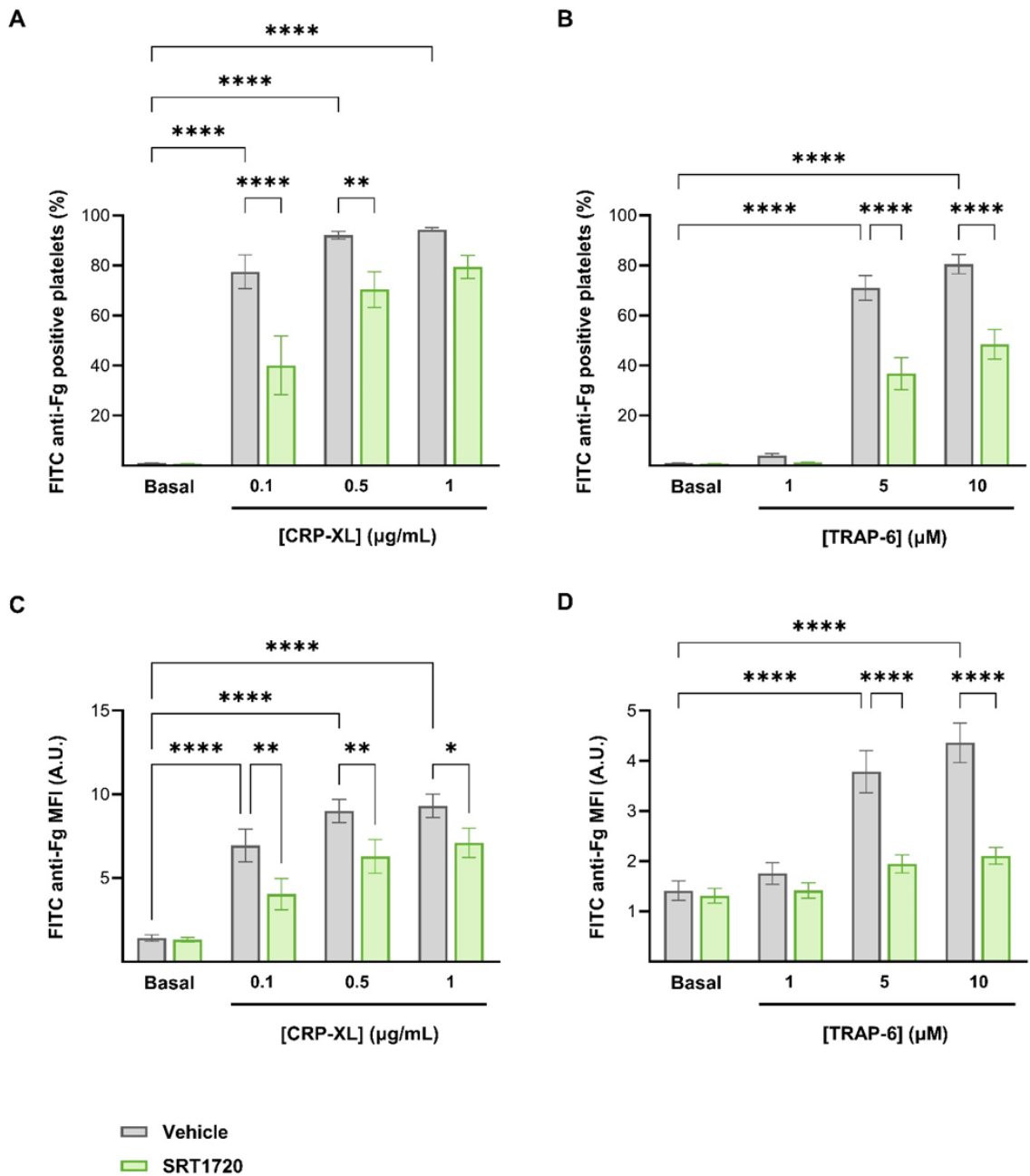


Figure 3.5. SRT1720 inhibits fibrinogen binding to platelets. PRP was incubated with SRT1720 (10 μ M) or vehicle (0.1% DMSO) for 10 min at 37°C and platelet activation induced with different concentrations of CRP-XL (A, C) and TRAP-6 (B, D) for 20 min at RT in the presence of FITC anti-fibrinogen. Fibrinogen binding was quantified using flow cytometry. Data is represented as the percentage of FITC anti-fibrinogen positive platelets (A, B) and MFI (C, D). The platelet gate was established based on size and CD42 positive staining. Data was analysed using the FlowLogic software and compared by Two-way ANOVA. Data represent mean \pm SEM. * p <0.05, ** p <0.01, *** p <0.0001 N=6. Fg = fibrinogen. 107

Figure 3.6. SRT1720 inhibits platelet integrin α 2b β 3 activation. PRP was incubated with SRT1720 (10 μ M) or vehicle (0.1% DMSO) for 10 min at 37°C and platelet activation was induced with different concentrations of CRP-XL (A, C) and TRAP-6 (B, D) for 20 min at RT in the presence of FITC anti-PAC-1. PAC-1 binding to the active conformation of the integrin α IIb β 3 was quantified using flow cytometry. Data is represented as the percentage of FITC anti-PAC-1 positive platelets (A, B) and MFI (C, D). The platelet gate was established based on size and CD42 positive staining. Data was analysed using the FlowLogic software and compared by Two-way ANOVA. Data represent mean \pm SEM. * p <0.05, *** p <0.001, **** p <0.0001. N=6. 108

- Figure 3.7.** SRT1720 reduced the number of platelets that release dense granules in response to CRP-XL. PRP was treated with SRT1720 (10 μ M) or vehicle (0.1% DMSO) for 10 min at 37°C prior to platelet stimulation with different concentrations of CRP-XL (A, C) and TRAP-6 (B, D) for 20 min at RT in the presence of a PE-CD63 antibody. Dense granule secretion was determined by measuring CD63 surface levels in platelets using flow cytometry. The platelet gate was established based on size and CD42 positive staining. Data was analysed using the FlowLogic software and compared by Two-way ANOVA. Data presented as mean \pm SEM. * p <0.05, ** p <0.01, *** p <0.001, **** p <0.0001. N=6. 110
- Figure 3.8.** P-selectin exposure, a marker for platelet α -granule release, remained unaffected after SIRT1 activation. PRP was treated with SRT1720 (10 μ M) or vehicle (0.1% DMSO) for 10 min at 37°C prior to platelet stimulation with different concentrations of CRP-XL (A, C) and TRAP-6 (B, D) for 20 min at RT in the presence of a PE-Cy5-CD62P antibody. α -granule secretion was determined by measuring CD62P surface levels in platelets using flow cytometry. The platelet gate was established based on size and CD42 positive staining. Data was analysed using the FlowLogic software and compared by Two-way ANOVA. Data is presented as mean \pm SEM. **** p <0.0001. N=7 111
- Figure 3.9.** SIRT1 activation inhibits thrombus formation on collagen-coated slides after 10 and 30 min of treatment, recovering after 60 min. Whole blood was incubated with SRT1720 (10 μ M) or vehicle (0.1% DMSO) for 10, 30 and 60 min, and exposed to collagen at an arterial shear rate (15 dynes/cm²) for 8 min. Images of DIOC-6-labelled platelets were taken every 10 seconds using the CELENA[®] S Logos Biosystems microscope. Area coverage of vehicle and SRT1720-treated samples were quantified using the Image J software at the different time points (D) and the average thrombi size, thrombi number and area coverage were compared at the end of the assay by One-way ANOVA (A, B, C). Data represent mean \pm SEM. * p <0.05. Representative images shown (E). N=6 (A, B, C) and N=3 (D)..... 113
- Figure 4.1.** SIRT1 activation inhibits platelet spreading and adhesion on collagen. ADP-sensitive platelets were incubated with SRT1720 (10 μ M) or vehicle (V, 0.1% DMSO) for 10 min and exposed to collagen (10 μ g/mL) for 45 min at 37°C. Platelets were labelled with Alexa 488-phalloidin. Images of adherent platelets for analysis were captured using the 20x objective on the CELENA[®] S Logos Biosystems microscope. Representative images taken on the 63x oil immersion lens of the Thunder microscope are shown. The image J software was used to morphologically classify platelets depending on the formation of filopodia or lamellipodia (B) and calculate the number of adhered platelets per field of view (A), the mean platelet area (C) and the percentage area covered by platelets (D). Statistical differences were assessed by t-test (A, C, D) and Repeated Measures Two-Way ANOVA (B). Scale bar is 50 μ m. Data represent mean \pm SEM. * p <0.05, ** p <0.01, *** p <0.001, **** p <0.0001. N=6. 127
- Figure 4.2.** SIRT1 activation inhibits platelet spreading and adhesion on fibrinogen. ADP-sensitive platelets were incubated with SRT1720 (10 μ M) or vehicle (V, 0.1% DMSO) for 10 min and exposed to fibrinogen (100 μ g/mL) for 45 min at 37°C. Platelets were labelled with Alexa 488-phalloidin. Images of adherent platelets for analysis were captured using the 20x objective on the CELENA[®] S Logos Biosystems microscope. Representative images taken on the 63x oil immersion lens of the Thunder microscope are shown. The image J software was used to morphologically classify platelets depending on the formation of filopodia or lamellipodia (B) and calculate the number of adhered platelets per field of view (A), the mean platelet area (C) and the percentage area covered by platelets (D). Statistical differences were assessed by t-test (A, C, D) and RM Two-Way ANOVA (B). Scale bar is 50 μ m. Data represent mean \pm SEM. * p <0.05, ** p <0.01. N=5..... 128
- Figure 4.3.** SRT1720 altered the platelet cytoskeleton. Platelets were treated with SRT1720 (10 μ M) or vehicle (0.1% DMSO) for 10 min followed by a 3-min incubation with TRAP-6 (10 μ M) or PBS (0.1%) and span down into poly-L-lysine-coated coverslips at 1450xg for 5 min. Adhered platelets were treated with cytoskeleton stabilisation buffer to conserve the structure of microfilaments and microtubules. Samples were fixed, dehydrated, and dried before mounting them on a stub and coating them with gold. Scanning Electron Microscopy was performed, and pictures of the platelet cytoskeleton were taken using the Zeiss Crossbeam 350 FIB-SEM microscope and a 20,000x magnification. SIRT1 activation disrupted the platelet cytoskeleton, as shown in the representative

- images (A), and significantly reduced platelet area coverage in both basal and TRAP-6 activated platelets (B). Platelet area coverage was quantified on ImageJ. Statistical differences were assessed by One-way ANOVA (B). Scale bar is 1 μ m. Data represent mean \pm SEM. ** p <0.01. N=2. 130
- Figure 4.4.** Measurement of filamentous actin levels revealed that SIRT1 activation decreases platelet actin polymerisation upon stimulation with TRAP-6. PRP (A, B, C) or ADP-sensitive platelets (D, E) were treated with SRT1720 (10 μ M) or vehicle (0.1% DMSO) for 10 minutes. Actin polymerization was induced by activating platelets with TRAP-6 (10 μ M) for 3 min. F-actin levels were detected using flow cytometry by staining fixed platelets with Alexa488-phalloidin (A, B, C) or generating lysates of the globular (G) and filamentous (F) components of the cytoskeleton to detect β -actin using western blotting (D, E). Flow cytometry (B, C) and Western Blotting (D) results showed a decrease in F-actin levels in SRT1720-treated platelets versus vehicle control (A, E). Differences in MFI (A) and the F/G actin ratio (E) were measured using FlowLogic and ImageJ, respectively, and analysed by One-way ANOVA. Only statistically significant differences are shown. Data represent mean \pm SEM. *** p <0.0001. N=5. G=globular actin; F=filamentous actin. 132
- Figure 4.5.** SIRT1 activation with SRT1720 does not alter platelet microtubule formation. ADP-sensitive platelets were treated with SRT1720 (10 μ M) or vehicle (0.1% DMSO) for 10 minutes. Tubulin polymerization was induced by activating platelets with TRAP-6 (10 μ M) for 3 min. Polymerised tubulin levels were tested by generating lysates using a cytoskeleton stabilisation buffer and separating using centrifugation the soluble tubulin (T) from the insoluble microtubules (MT). Evaluation of the ratio of globular and polymerised tubulin was performed by Western Blotting. Differences in the MT/T ratio were measured on ImageJ and analysed by One-way ANOVA, revealing that SRT1720 did not affect tubulin polymerisation in platelets. Only statistically significant differences were shown. Data represent mean \pm SEM. N=5. T= β -tubulin; MT=microtubules. 134
- Figure 4.6.** The platelet marginal band remains unaffected after SIRT1 activation. PRP was incubated for 10 min with SRT1720 (10 μ M) or vehicle (V, 0.1% DMSO) before platelet activation with TRAP-6 (0.1 μ M) for 3 min. Platelets were fixed in suspension and added to poly-L-Lysine coated coverslips. Platelet cytoskeleton was stained using Alexa488-conjugated phalloidin for F-actin (green) and Alexa647-conjugated anti- β -tubulin antibody for visualisation of the marginal band (red). Images were taken in the 100x oil immersion objective of the STELLARIS confocal microscope. Platelets with an intact marginal band were counted using ImageJ and differences were analysed by One-way ANOVA. Data represent mean \pm SEM. N=6. 135
- Figure 4.7.** SIRT1 pharmacological activation with SRT1720 inhibits the late stage of clot retraction. PRP and RBC diluted in Tyrode's with glucose were treated with SRT1270 (10 μ M) or vehicle (V, 0.1% DMSO) for 10 minutes at 37°C. Platelet aggregation was induced with thrombin (1 U/mL) and clot retraction was monitored for 1 hour at 37°C. The percentage of clot retraction was calculated using the fractional area occupied by the clots at 10-min intervals (A) using RM Two-way ANOVA. The weight of the clots after 60 min was compared by Paired t-test (B). Representative images of the clots at the beginning (C) and the end (D) of the assay are shown. Data represent mean \pm SEM. * p <0.05, ** p <0.01. N=6. 137
- Figure 4.8.** SRT1720 causes no significant changes in the phosphorylation of the integrin α IIb β 3 tail. Human washed platelets were pretreated for 30 min with or without SRT1720 (10 μ M) and activated with CRP-XL (1 μ g/mL) for 90 and 180 seconds or TRAP-6 (10 μ M) for 30 and 90 seconds. Platelets were lysed in SDS Laemmli sample buffer and Western Blotting was performed using an antibody against Y773 in the integrin α 2b β 3 tail. Actin was used to confirm equal loading. Representative blots and quantified data are shown. Levels of phosphorylation were quantified and expressed as a ratio of the vehicle control (0.1% DMSO). Differences were analysed by One-way ANOVA. Data represent mean \pm SEM. ** p <0.01 *** p <0.001. N=4. 139
- Figure 4.9.** SIRT1 activation had no effect on platelet MLC2 phosphorylation. Human washed platelets were pretreated for 30 min with or without SRT1720 (10 μ M) and activated with CRP-XL (1 μ g/mL) for 90 and 180 seconds or TRAP-6 (10 μ M) for 30 and 90 seconds. Platelets were lysed in SDS Laemmli sample buffer and Western Blotting was performed using an antibody against S19-MLC2.

β -actin was used as a loading control. Representative blots (I) and quantified data (II) are shown. Levels of phosphorylation were quantified and expressed as a ratio of the vehicle control (0.1% DMSO). Differences were analysed by One-way ANOVA. Data represent mean \pm SEM ** $p < 0.01$ *** $p < 0.001$. N=4. 141

Figure 4.10. SIRT1 activation had no effect on platelet FAK autophosphorylation. Human washed platelets were pretreated for 30 min with or without SRT1720 (10 μ M) and activated with CRP-XL (1 μ g/mL) for 90 and 180 seconds or TRAP-6 (10 μ M) for 30 and 90 seconds. Platelets were lysed in SDS Laemmli sample buffer and Western Blotting was performed using an antibody against Y397-FAK. Total FAK was used as a loading control. Representative blots (I) and quantified data (II) are shown. Levels of phosphorylation were quantified and expressed as a ratio of the vehicle control (0.1% DMSO). Differences were analysed by One-way ANOVA. Data represent mean \pm SEM. ** $p < 0.01$ *** $p < 0.001$. N=4. 143

Figure 4.11. SIRT1 activation did not affect cofilin-1 phosphorylation levels in platelets. Human washed platelets were pretreated for 30 min with or without SRT1720 (10 μ M) and activated with CRP-XL (1 μ g/mL) for 90 and 180 seconds or TRAP-6 (10 μ M) for 30 and 90 seconds. Platelets were lysed in SDS Laemmli sample buffer and Western Blotting was performed using an antibody against S3 in cofilin-1. Total cofilin was used as a loading control. Representative blots (I) and quantified data (II) are shown. Levels of phosphorylation were quantified and expressed as a ratio of the vehicle control (0.1% DMSO). Differences were analysed by One-way ANOVA. Data represent mean \pm SEM. ** $p < 0.01$ *** $p < 0.001$. N=4. 145

Figure 5.1. SIRT1 is present in HCAEC, but its expression does not significantly change with an acute TNF- α treatment. HCAEC were treated with TNF- α (10 ng/mL) or vehicle (V, 0.1% PBS) for 20 and 60 minutes (A). Samples were fixed, incubated with a primary antibody against SIRT1 and stained with an Alexa488 secondary antibody, rhodamine-phalloidin and DAPI. An IgG control was included in the assay (B). Images were taken in the STELLARIS 5 confocal microscope using the 40x oil immersion objective. SIRT1 mean fluorescence intensity was quantified with the ImageJ software and changes in the expression of this enzyme were compared between conditions by One-Way ANOVA (C). Data represent mean \pm SEM. N=3. 159

Figure 5.2. SRT1720 10 μ M decreases HCAEC viability. HCAEC were treated with SRT1720 10 μ M for 24 hours, fixed and stained with DAPI and Rhodamine Phalloidin. Samples were imaged using the 20x objective of the STELLARIS 5 Confocal microscope. Representative images are shown (A). In Figure All, it can be observed that SRT1720 10 μ M reduced the size of the cells (1) and led to gaps in the cell monolayer (2), indicating that high concentrations of this drug could affect cell viability. To test this, HCAEC were incubated with different concentrations of SRT1720 (0.1 - 10 μ M) or vehicle (V, 0.1% DMSO). After 24 (A), 48 (B) or 72 hours (C) of treatment, an MTS assay was performed. SDS at 0.1% was used as a cell death positive control. According to the kit recommendations, MTS reagent was added to every condition and incubated for 2 hours at 37°C. Absorbance at 490 nm was measured. The absorbance of the vehicle was considered 100% of cell viability. Conditions were measured in duplicate. Data represent mean \pm SEM. **** $p < 0.0001$. N=3. 161

Figure 5.3. SIRT1 activation for 4 hours failed to prevent NF- κ B nuclear translocation. HCAEC were cultured in a 96-well plate and dysfunction was induced with TNF- α (10 ng/mL) for 20 min. SRT1720 (0.1 – 3 μ M) or vehicle (0.1% DMSO) were added to the wells for 4 h. HCAEC were fixed, permeabilised and incubated with an NF- κ B primary antibody. Nuclei were stained with DAPI and NF- κ B was labelled using an Alexa 488 secondary antibody. Images were taken with the 20x objective of the CELENA® S microscope. Using ImageJ, masks of the nuclei were created and the median green fluorescence intensity in that area was quantified to measure NF- κ B nuclear presence. Differences were compared by One-Way ANOVA. Data represent mean \pm SEM. * $p < 0.05$. N=3. 163

Figure 5.4. SRT1720 reduced HCAEC migration in a dose-dependent way but only significantly at 3 μ M. Cells were cultured in Ibidi 2-well inserts in a clear-bottomed 24-well plate until confluency. On the day of the assay, the inserts were removed and media supplemented with SRT1720 (0.3, 1 or 3 μ M) or vehicle (0.1% DMSO) was added. Cell migration was monitored for 20 hours by taking images

every 10 minutes using the 20x objective of the HoloMonitor Live Cell Imaging System. Images were analysed using the HoloMonitor App Suite cell imaging software (AI, BI, BII) and ImageJ (AII). Representative images of the gap after 10 and 20 hours are shown (C). Data represent mean \pm SEM. * p <0.05, ** p <0.01, *** p <0.001. N=5. 165

Figure 5.5. SRT1720 does not alter actin polymerisation in HCAEC. Cells were treated with a range of SRT1720 concentrations (0.1 – 3 μ M) or vehicle (V, 0.1% DMSO) and endothelial dysfunction was induced with TNF- α (10 ng/mL). A healthy vehicle control was also included in the assay. Samples were stained with DAPI and rhodamine phalloidin and pictures were taken in the 10x objective of the CELENA[®] S microscope. Representative images are shown (A). The number of nuclei and the rhodamine mean fluorescence were quantified using ImageJ. The fluorescent signal was normalised by the nuclei count (B). No changes in actin polymerisation were observed between HCAEC treated with SRT1720 and vehicle conditions. Data represent mean \pm SEM. N=3. 167

Figure 5.6. SRT1720 protected HCAEC from LPS damage by reducing the permeability of the cell monolayer. HCAEC were seeded in 96-well inserts until confluency and treated with SRT1720 (1 μ M) with and without TNF- α at 1 μ g/mL (A) or LPS at 1 μ g/mL (B) for 24 hours. FITC-dextran was added to the inserts according to the indications of the *in vitro* vascular permeability kit from Merck and incubated for 2 hours. The FITC fluorescence of the media in the inserts and the bottom well was measured in the GloMax microplate reader and compared between conditions by One-Way ANOVA. N=4. 169

Figure 5.7. LPS increased VCAM and reduced NOS3 mRNA levels. HCAEC were grown in a 12-well plate and serum-starved O/N. Then, treatment with different endothelial dysfunction inducers, including IL-6 (50 ng/mL), LPS (100 ng/mL), TNF- α (10 ng/mL), H₂O₂ (100 μ M), or 0.1% PBS (H), was performed for 24 hours. After a PBS wash, RNA was extracted and purified. cDNA was obtained and qPCR was performed to test the expression of SIRT1 (A), VCAM (B), PTGS2 (C) and NOS3 (D). GAPDH and RPLPO were used as housekeeper genes. The mRNA fold change was calculated using the $\Delta\Delta$ Ct method using the average vehicle Δ Ct of the biological replicates as a control. Data was obtained from three technical replicates. Data represent mean \pm SEM. * p <0.05, ** p <0.01. N=4..... 171

Figure 5.8. Treatment of HCAEC with SRT1720 significantly reduced thrombus formation induced by LPS on the cells, but not on collagen. HCAEC were cultured in Ibidi μ -Slides VI 0.1 until confluent then treated with LPS (100 ng/mL) in the presence of SRT1720 (1 μ M) or vehicle (0.1% DMSO) for 24 hours. Using an *in vitro* thrombus formation model, untreated DIOC6-stained human blood was flowed first over the cell monolayer (A) and then over a collagen-coated slide (B), representative images of the different channels are shown. Images were taken in the 10x objective of the CELENA[®] S Logos Biosystems microscope. Thrombi size (I), number (II) and area coverage (III) were quantified in both slides using the Weka Trainable Segmentation on ImageJ and compared by One-Way ANOVA. Data represent mean \pm SEM. * p <0.05. N=4. 173

Figure 5.9. SIRT1 pharmacological activation with SRT1720 did not recover eNOS levels after LPS damage in HCAEC. HCAEC were cultured in Ibidi μ -Slides VI 0.1 until confluent and damaged with LPS (100 ng/mL) in the presence of SRT1720 (1 μ M) or vehicle (0.1% DMSO) for 24 hours. Using an *in vitro* thrombus formation model, untreated DIOC6-stained human blood was flowed over the cell monolayer. Samples were fixed, incubated with an eNOS antibody and stained with DAPI and an Alexa647 secondary antibody. Images were taken in the 40x objective of the STELLARIS 5 Confocal microscope. The magenta mean fluorescence intensity was quantified using ImageJ, normalised by the nuclei number and used as a measurement of eNOS expression. Differences between conditions were compared by One-Way ANOVA. Data represent mean \pm SEM. * p <0.05. N=4. 175

Figure 5.10. SIRT1 contributes to endothelial health through an increase in NOS3 and DDAH1 mRNA expression. HCAEC were grown in a 12-well plate and serum-starved O/N. Cells were treated with SRT1720 (0.3 and 1 μ M) with and without LPS (100 ng/mL) for 24 hours. RNA was extracted, purified and reverse-transcribed into cDNA. qPCR was performed to assess the expression of the genes ENTPD1 (A), NOS3 (BI), DDAH1 (BII), PTGS1 (C) and PTGS2 (D). GAPDH and RPLPO were used as housekeeper genes. mRNA fold change was calculated using the $\Delta\Delta$ Ct method using the average

vehicle Δ Ct of the biological replicates as a control. Data was obtained from three technical replicates. Data represent mean \pm SEM. *p<0.05, **p<0.01. N=5.	179
Figure 5.11. SRT1720 does not affect VWF expression in static HCAEC. HCAEC were cultured in a 12-well plate and serum-starved O/N. Cells were treated with SRT1720 (0.3 and 1 μ M) in the presence and absence of LPS (100 ng/mL) for 24 hours. RNA was extracted, purified and reverse-transcribed into cDNA. qPCR was performed to assess the expression of the VWF. GAPDH and RPLPO were used as housekeeper genes. mRNA fold change was calculated using the $\Delta\Delta$ Ct method using the average vehicle Δ Ct of the biological replicates as a control. Data was obtained from three technical replicates. Data represent mean \pm SEM. *p<0.05, **p<0.01. N=5.	180
Figure 5.12. SIRT1 activation increases thrombomodulin (THBD) mRNA expression. Cells were treated with SRT1720 (0.3 and 1 μ M) in the presence and absence of LPS (100 ng/mL) for 24 hours. RNA was extracted, purified and reverse-transcribed into cDNA. qPCR was performed to assess the expression of thrombomodulin (THBD). GAPDH and RPLPO were used as housekeeper genes. mRNA fold change was calculated using the $\Delta\Delta$ Ct method using the average vehicle Δ Ct of the biological replicates as a control. Data was obtained from three technical replicates. Data represent mean \pm SEM. *p<0.05, **p<0.01. N=3.....	181
Figure 6.1. Summary of the effects of specific SIRT1 activation with SRT1720 in platelets and endothelial cells. In platelets, SRT1720 (10 μ M) attenuated platelet aggregation in response to TRAP-6, collagen and ADP. SIRT1 activation also reduced dense granule release upon CRP-XL stimulation and decreased fibrinogen binding to the integrin α IIb β 3. Moreover, SRT1720 reduced F-actin levels, although whether this is a consequence of the decrease in integrin “outside-in” signalling or SIRT1 has a direct effect on actin polymerisation via deacetylation of ABPs remains unclear. As a consequence, SIRT1 alters platelet actin cytoskeletal rearrangement, reducing platelet adhesion and spreading to both collagen and fibrinogen and decreasing clot retraction. Regarding the effects in endothelial cells, SRT1720 (1 μ M) increased the mRNA levels of eNOS and DDAH1 in healthy and dysfunctional HCAECs, respectively. SRT1720 also increased THBD transcription in both healthy and LPS-treated HCAEC, which indicates that SIRT1 activation negatively regulates coagulation. LPS-treated HCAEC. Finally, higher doses of SRT1720 (3 μ M) diminished HCAEC migration in a gap closure assay. However, the mechanism behind this effect is still unknown. Overall, SIRT1 activation has an antithrombotic effect, which was demonstrated in our <i>in vitro</i> arterial thrombus formation experiments on both collagen and LPS-treated HCAEC. Created in BioRender.com	203

Abbreviations

ABP – Actin binding protein

Abs – Absorbance

ACD – Acid Citrate Dextrose

ADMA – Asymmetric dimethylarginine

ADP – Adenosine diphosphate

AEE – Aspirin eugenol ester

AMP – Adenosine monophosphate

AMPK – AMP-activated protein kinase

APOE – Apolipoprotein E

aPTT – Activated partial thromboplastin time

α TAT1 – Alpha tubulin acetyltransferase 1

ATC – Antithrombotic Trialists' Collaboration

ATP – Adenosine triphosphate

AUC – Area under the curve

BH₄ – Tetrahydrobiopterin

BH₂ – Dihydrobiopterin

Bp – Base pairs

CBP – CREB-binding protein

CD39 – Ectonucleoside triphosphate diphosphohydrolase 1 (protein)

cDNA – Complementary DNA

COX – Cyclooxygenase

CYP – Cytochrome P450

cDNA – complementary DNA

CD62P – P-selectin

COX1 – Prostaglandin-endoperoxide synthase 1

COX2 – Prostaglandin-endoperoxide synthase 2

CRM1 – Chromosomal maintenance 1

CRP-XL – Collagen-Related Peptide Crosslinked

CVD – Cardiovascular disease

DAG – Diacylglycerol

DDAH1 – Dimethylarginine dimethylaminohydrolase 1

DMSO – Dimethyl sulfoxide

DNA – Deoxyribonucleic acid

DPBS – Dulbecco's phosphate-buffered saline

EGTA – Ethyleneglycol-bis(β -aminoethyl)-N,N,N',N'-tetraacetic Acid

eNOS – Endothelial nitric oxide synthase

ENTPD1 – Ectonucleoside triphosphate diphosphohydrolase 1 (gene)

FAK – Focal adhesion kinase

FBS – Foetal bovine serum

FCS – Foetal calf serum

Fg – Fibrinogen

FOXO – Forkhead box O class

FSC – Forward scatter

GS – Goat serum

H – Hour

HCAEC – Human coronary artery endothelial cell

HDAC – Histone deacetylase

Hep – Heparin-like proteoglycans

ICAM-1 – Intercellular Adhesion Molecule 1

ILK – Integrin Linked Kinase

IP3 – Inositol 1,4,5-trisphosphate

ITAM – Immunoreceptor tyrosine-based activation motif

KAT – Lysine acetyltransferase

KDAC – Lysine deacetylase

KO – Knock-out

LPS – Lipopolysaccharide

LTA – Light transmission aggregometry

Ltd – Limited

MBP – Microtubule binding protein

MFI – Mean fluorescence intensity

Mg – Milligrams

Min – Minutes

MTS – 3-(4,5-dimethylthiazol-2-yl)-5-(3-carboxymethoxyphenyl)-2-(4-sulfophenyl)-2H-tetrazolium

MW – Molecular weight

NAA60 – N-alpha-acetyltransferase 60

NAD – Nicotinamide adenine dinucleotide

NADPH – Nicotinamide adenine dinucleotide phosphate

NcoA – Nuclear receptor coactivator

NF-κB – Nuclear Factor-κB

NO – Nitric oxide

NOS3 – Nitric oxide synthase 3

Nfr2 – Nuclear factor erythroid 2-related factor 2

NSAID – Non-steroidal anti-inflammatory drug

O/N – Over night

PAI-1 – Plasminogen activator inhibitor-1

PAF-R – Platelet-activating factor receptor

PCSK9 – Proprotein convertase subtilisin/kexin type 9

PGE₂ – Prostaglandin E₂

PGI₂ – Prostacyclin

PI3K – Phosphoinositide 3-kinases

PIP – Phosphatidylinositol

PIPES – 2,2'-(Piperazine-1,4-diyl)di(ethane-1-sulfonic acid)

PKC – Protein kinase C

PLC – Phospholipase C

PMSF – Phenylmethylsulfonyl fluoride

PPP – Platelet poor plasma

PRP – Platelet rich plasma

PS – Phosphatidylserine

PSGL-1 – P-selectin glycoprotein ligand-1

PT – Prothrombin time

PTGS1 – Prostaglandin-endoperoxide synthase 1

PTGS2 – Prostaglandin-endoperoxide synthase 2

PTM – Posttranslational modification

PVDF – Polyvinylidene Fluoride

Rac1 – Ras-related C3 botulinum toxin substrate 1

Rasa3 – Ras GTPase-activating protein 3

RBC – Red blood cell

rH – Recombinant human

RNA – Ribonucleic acid

ROS – Reactive oxygen species

Rpm – Revolutions per minute

RT – Room temperature

RT-qPCR – Real-time quantitative polymerase chain reaction

RM – Repeated measures

S – Serine

SDS – Sodium dodecyl sulfate

SEM – Scanning electron microscopy

SEM – Standard error of the mean

SFK – Src family kinases

SiRNA – Small interfering RNA

SIRT – Sirtuin

SOD2 – Superoxide dismutase 2

SRC – Steroid receptor coactivator

SSC – Side scatter

SSG – S-glutathionylation

TBP – Tubulin binding protein

T2DM – Type II diabetes mellitus

TE – Tris-EDTA

TF – Tissue factor

Tf – Transcription factor

TFPI – Tissue factor pathway inhibitor

THBD – Thrombomodulin

TJ – Tight junctions

TLR4 – Toll-like receptor 4

T_m – Melting temperature

TMS – 3,4',5-tetramethoxy-trans-stilbene

TP – Thromboxane receptor

tPA – Tissue-type plasminogen activator

TRAP 2°P TIMI 50 – Trial to Assess the Effects of SCH 530348 in Preventing Heart Attack and Stroke in Patients with Atherosclerosis

TXA₂ – Thromboxane A₂

u-PA – Urokinase plasminogen activator

VCAM – Vascular cell adhesion molecule

VE-Cadherin – Vascular endothelial-cadherin

VEGF – Vascular endothelial growth factor

v/v – Volume/volume

VWF – Von Willebrand factor

WHO – World Health Organisation

Y – Tyrosine

Chapter 1. General introduction

1.1 Platelet production

Platelets are the smallest cells of the human body, with 2 to 3 μm of diameter and an average lifespan of 7 to 10 days. They are produced via the fragmentation of megakaryocytes in the sinusoidal walls of the bone marrow (Machlus and Italiano, 2013) or the lung (Lefrançois et al., 2017). Since 1882, the role of platelets in the regulation of haemostasis has been well-established (Mazzarello et al., 2001). However, over the past decade a large body of evidence has demonstrated that platelets play a key role in other biological processes, such as immune (Ali et al., 2015) and inflammatory responses (Sonmez and Sonmez, 2017; Scherlinger et al., 2023).

Disruptions in the blood flow, endothelial dysfunction or the increase of inflammatory molecules in the bloodstream by cardiovascular risk factors, such as hypercholesterolemia, diabetes or infections, lead to platelet activation (Lechner et al., 2020; Libby, 2021). In this scenario, platelets contribute to atherogenesis through the release of inflammatory mediators and the recruitment of monocytes into the affected area of the vasculature (Badimon et al., 2012; Chatterjee and Gawaz, 2017). After the rupture or erosion of an atherosclerotic plaque, platelets initiate thrombus formation, leading to myocardial infarction or ischaemic stroke (Asada et al., 2020). Therefore, investigating platelet biology and novel pharmacological tools to modulate platelet function is crucial for the prevention of cardiovascular diseases (CVDs) and the management of atherothrombotic events (Majithia and Bhatt, 2019).

1.2 Platelet structure

Platelets are anucleate cells comprising a plasma membrane, the membrane complex, the cytoskeleton and the organelles.

The platelet plasma membrane is a bilayer of phospholipids characterised by a plethora of surface receptors, which are crucial for the complex signalling that regulates platelet function (Hashemzadeh et al., 2023) (Figure 1.1).

The membrane complex is formed by the Open Canalicular System (OCS) and the Dense Tubular System (DTS). The OCS is an intricate network of channels connected to the platelet surface that was created through the invagination of the plasma

membrane (Ghoshal and Bhattacharyya, 2014; Selvadurai and Hamilton, 2018) (Figure 1.1). The main function of this system is to allow the release of the contents of the granules and the exchange of material between the extracellular space and the cytoplasm of platelets. Moreover, the OCS plays a key role in spreading by promoting filopodia formation and is where plasma membrane glycoproteins are primarily stored (Jonathan N. Thon and Italiano, 2012; Thomas, 2019).

The DTS is a set of closed channels similar to a smooth endoplasmic reticulum that serves as calcium storage, making this cation available in different localised areas of the cell whenever required (Figure 1.1). This system is crucial for platelet function, as all stages of thrombus formation are associated with a peak in platelet intracellular calcium (Ghoshal and Bhattacharyya, 2014; Anand and Harper, 2020).

The platelet cytoskeleton can be divided into the membrane skeleton and the cytoplasmic core cytoskeleton, which is mainly formed by actin filaments, microtubules and myosin (Shin et al., 2017) (Figure 1.1). Cytoskeletal reorganisation is regulated by a complex network of signalling pathways, which trigger platelet shape change, stable adhesion and the extension of pseudopodia (Kobsar and Eigenthaler, 2006; Zaninetti et al., 2020).

Platelets also have mitochondria (Y. Ma et al., 2023), peroxisomes, lysosomes and granules, which constitute the organelles. Platelet granules are classified into three different groups depending on their contents. The most abundant are the α -granules, followed by the dense granules and the recently discovered T-granules (J. N. Thon et al., 2012) (Figure 1.1).

Platelet α -granules contain soluble mediators and membrane receptors, such as α IIb β 3 and P-selectin (CD62P). Proteomic studies have demonstrated the presence of more than 300 soluble proteins in α -granules, which are involved in haemostasis, inflammation and wound healing (Maynard et al., 2010). The most important haemostatic proteins stored in α -granules are platelet factor 4 (PF4), fibrinogen, fibronectin, von Willebrand factor (VWF), factor V, factor XI and factor XIII. Moreover, these granules contain several anti-coagulation proteins, such as tissue factor pathway inhibitor (TFPI) or plasminogen (Heijnen and van der Sluijs, 2015).

The main components of dense granules are adenosine 5'-triphosphate (ATP), adenosine 5'-diphosphate (ADP), CD63, pyrophosphate, calcium and catecholamines,

such as serotonin and histamine (Jurk, 2017). While the contents of α -granules contribute to platelet adhesion, dense granules are more important for the secondary feedback that sustains platelet aggregation via the secretion of the soluble cargo (Y. Chen et al., 2018).

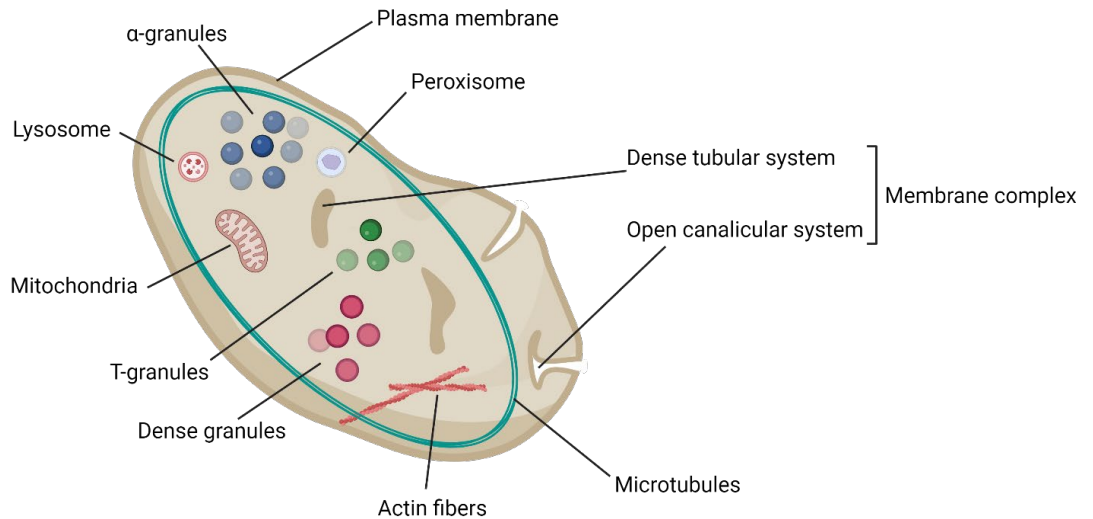


Figure 1.1. Ultrastructure of an unstimulated platelet. Created in BioRender.com.

1.2.1 Cytoskeleton

The platelet cytoskeleton is responsible for the maintenance of the discoid shape in the resting state and the change in morphology that occurs after activation in response to vascular injury. Platelet cytoskeletal machinery is formed by actin, tubulin and many other regulatory proteins that bind to the microfilaments or microtubules to coordinate the cytoskeletal rearrangement that leads to spreading and marginal band coiling (Jonathan N. Thon and Italiano, 2012). Upon stimulation, the platelet shape drastically changes through cytoskeletal rearrangements to cover the injury site, connect with the fibrin mesh of the thrombi and stop bleeding, allowing wound healing via clot retraction (Falet, 2017). The structures that form the platelet cytoskeleton will be described in the following sections.

1.2.1.1 Actin microfilaments

Unstimulated platelets have a cytoplasmic network formed by filamentous actin (F-actin). Subcortical actin filaments are cross-linked with spectrin and connect with the platelet plasma membrane through multiple filamin A-CD42 and talin-integrin α IIb β 3 attachment points. This structure is called the

membrane skeleton (Patel-Hett et al., 2011). Upon platelet activation, spectrin is degraded by calcium-dependent proteases, which release the actin filaments and start actin cytoskeleton reorganisation (Falet, 2017).

On adhesive surfaces, such as collagen, fibrinogen, fibronectin or VWF, actin microfilaments suffer a dramatic reorganisation and platelets become flattened, emitting filopodia and lamellipodia, which are characterised by the presence of actin stress-fibres. This event, known as spreading, is associated with an increase in actin polymerisation regulated by different actin-binding proteins (ABPs), such as cofilin, gelsolin, profilin, vasodilator-stimulated phosphoprotein (VASP), Wiskott-Aldrich syndrome protein (WASP) and the Arp2/3 complex (Bearer et al., 2002; Dasgupta and Thiagarajan, 2020).

Other platelet actin-rich structures are actin nodules and podosomes. Actin nodules are spherical structures containing vinculin and talin required for platelet-platelet interactions at the early stage of platelet adhesion and spreading. Podosomes are short-life F-actin structures with high expression of integrins, Src family kinases (SFKs) and the ARP2/3 complex. Both nodule and podosome formation are dependent on WASP (Poulter et al., 2015).

Platelet actin rearrangements are important not only for platelet adhesion, aggregation and coverage of the damaged area of the vessel but also during clot retraction. The interaction between the filopodia actin fibres and myosin IIA is essential to condense the fibrin mesh and reduce the size of the thrombi, which avoids the obstruction of the vessel, contributes to injury healing and prevents infections (Fox, 2001).

1.2.1.2 Microtubules

As platelets are anucleate cells, they lack a microtubule-organising centre. In non-activated platelets, α and β tubulin are present in the marginal band, which is a subcortical ring-shaped structure that gives platelets their characteristic discoid shape (Sadoul, 2015). Platelet stimulation leads to the centralisation, elongation and coiling of the tubulin ring, which drives the transition to a spherical platelet shape. This allows faster circulation of the platelets through the bloodstream and better exposure of the receptors to bind to the extracellular matrix (Moskalensky et al., 2018).

The coiling of the tubulin ring is regulated by three major tubulin-binding proteins (TBPs): dynein, dynactin and kinesins. The dynein-dynactin complex participates in the extension of the marginal band through microtubule elongation, promoting the formation of the coil. Kinesins, namely kinesins 1 and 4, antagonise dynein motor action in resting platelets to stabilise the marginal band and mediate the transport of vesicular structures through the microtubules. Other important proteins in microtubule function are formins, which connect the actin microfilaments with the tubulin cytoskeleton (Green et al., 2020).

In unstimulated platelets, the ring-shape of the marginal band is maintained due to the antagonistic motion of dynein and kinesin. After platelet activation, kinesin stops generating resistance to dynein and microtubules slide and elongate. This microtubule extension allows centralisation and coiling of the marginal band, leading to a platelet shape transition from discoid to spherical mediated by formin-based actin-tubulin connections. When platelets are completely spread, the tubulin coil breaks and microtubules depolymerise (Figure 1.2) (Sadoul, 2015; Cuenca-Zamora et al., 2019).

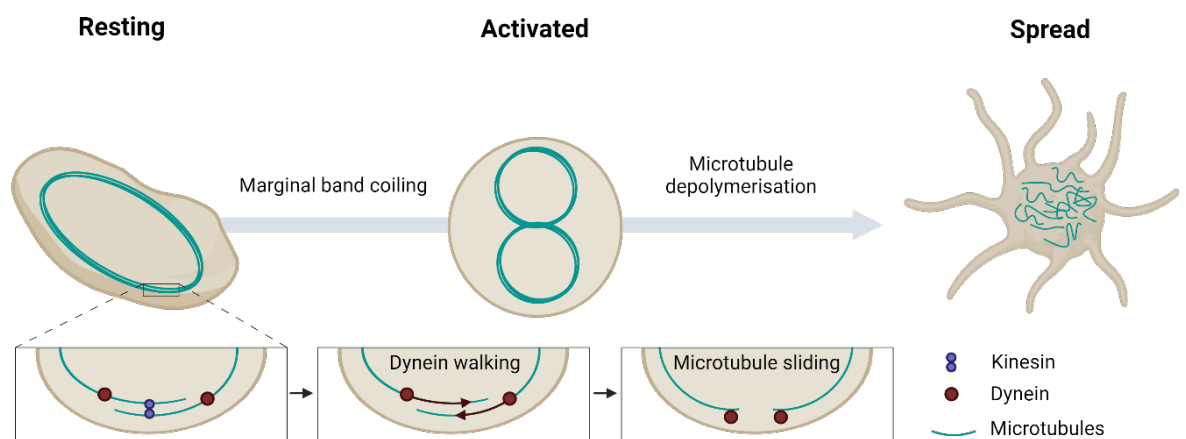


Figure 1.2. Coiling of the marginal band following platelet activation and microtubule depolymerisation. Created in BioRender.com.

1.2.1.3 Myosin

Upon platelet stimulation, actin polymerisation increases downstream integrin α IIb β 3 activation (Bearer et al., 2002). Actin filaments are crucial for the extension of filopodia, which bind to myosin IIA in the cytoplasm and to the fibrin mesh of the clot in the extracellular space. Platelet activation leads to

phosphorylation of the light chains (S19) of myosin IIA (Aburima et al., 2013), which pulls the microfilaments towards the centre of the platelet cytoplasm, initiating clot retraction (G. J. Johnson et al., 2007; Gao et al., 2023).

1.3 Platelet function

1.3.1 Primary haemostasis

Haemostasis is a defense mechanism initiated in response to vascular injury to prevent bleeding. Excessive activation of this system results in the formation of large and unstable clots that could partially or completely obstruct a vessel, causing a thrombotic event. By contrast, an impairment in basal haemostasis would lead to bleeding (Clemetson, 2012).

The haemostatic process can be divided into two stages: primary and secondary haemostasis (Broos et al., 2011). Platelets are essential components in primary haemostasis, which results in the formation of the platelet plug and includes the following phases: platelet adhesion and activation, recruitment and aggregation (Figure 1.3).

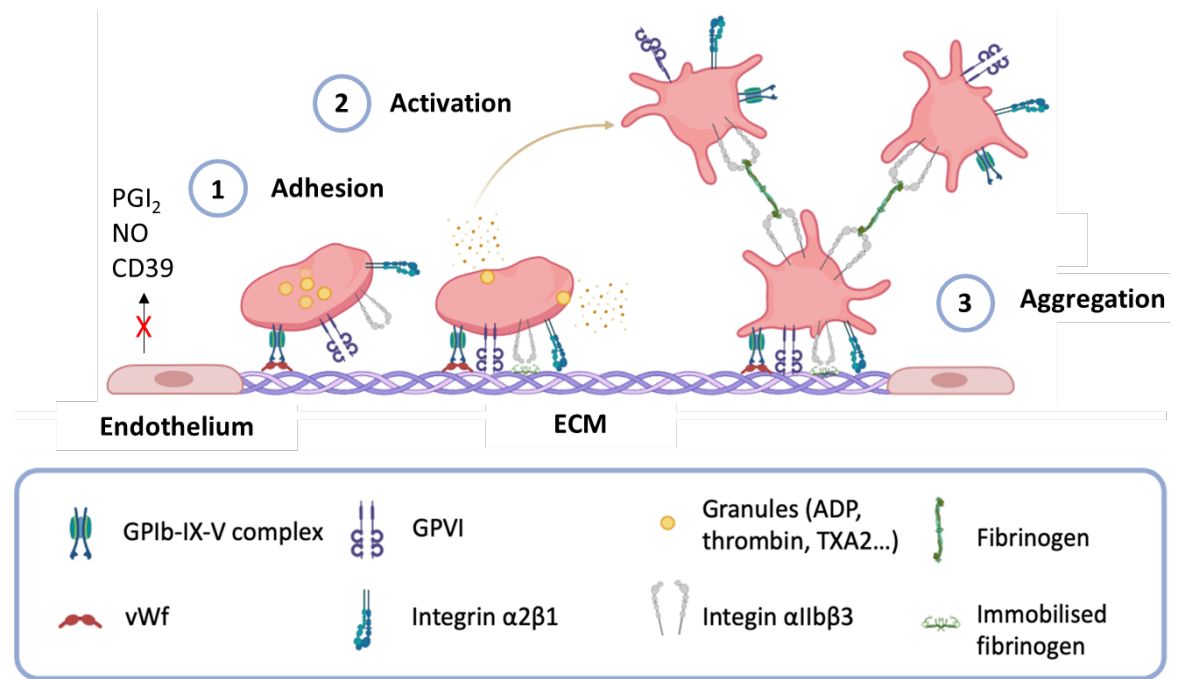


Figure 1.3. Platelets in primary haemostasis. The healthy endothelium releases prostacyclin (PGI_2), nitric oxide (NO) and CD39 to inhibit platelet activation. After vascular injury, primary haemostasis is initiated by the collagen-VWF complex, which promotes platelet initial adhesion. The binding of GPVI and integrin $\alpha 2\beta 1$ to collagen contributes to platelet adhesion and activation. Activated platelets spread and release secondary mediators through degranulation, which activates and recruits other platelets to the injury site. Then, the binding of fibrinogen to the activated integrin $\alpha II\beta 3$ allows platelet-platelet interactions, leading to aggregation and eventually thrombus formation. Created in BioRender.com.

Under physiological conditions, the intact endothelium provides a natural barrier against platelet adhesion. Moreover, inactive endothelial cells suppress platelet activation by releasing molecules that act as inhibitory factors, including prostacyclin (PGI_2), nitric oxide (NO) and CD39, which is an ADP hydrolase expressed on the surface of endothelial cells (Marcus et al., 2001). Upon endothelial damage, the collagen fibres from the extracellular matrix are exposed, allowing the binding of VWF. Platelet binding to immobilised VWF through the GPIb-IX-V complex allows initial transient adhesion (Jackson, 2007). These interactions are stabilised by the interaction of platelets with collagen via integrin $\alpha 2\beta 1$ and GPVI, which triggers platelet activation and integrin $\alpha II\beta 3$ “inside-out” signalling (Surin et al., 2008).

After activation by contact with the components of the extracellular matrix (ECM), several soluble platelet agonists are released into the bloodstream, including adenosine diphosphate (ADP), thromboxane A2 (TXA2) and thrombin. As a result, more platelets are stimulated and migrate to the place of the vascular injury (Robert

Flaumenhaft and Sharda, 2019). “Inside-out” signalling is amplified by secondary feedback. Integrin $\alpha\text{IIb}\beta\text{3}$ binding to fibrinogen leads to platelet aggregation and spreading (Golebiewska and Poole, 2015), allowing the formation of the platelet thrombus on the injury site (Rivera et al., 2009).

Following the generation of the platelet plug, secondary haemostasis begins. The main event of this phase is the coagulation cascade, which results in the conversion of fibrinogen into fibrin, stabilising the thrombus. Activated platelets also play a pivotal role in secondary haemostasis by exposing phosphatidylserine and phosphatidylethanolamine to their surface. This provides a procoagulant platform where prothrombin and the clotting factors V, VII, VIII, FIX and FX can bind (Periyah et al., 2017; S. A. Smith and Morrissey, 2019).

1.3.2 Secondary Haemostasis

Following vascular injury, platelets are activated by the components of the endothelial ECM, such as collagen, VWF and fibronectin (Versteeg et al., 2013), leading to platelet activation, aggregation and thrombus formation. However, a subpopulation of platelets responds to ECM exposure by transforming into procoagulant cells, instead of undergoing integrin $\alpha\text{IIb}\beta\text{3}$ activation. Procoagulant platelets are characterised by caspase activation, proteolytic cleavage of cytoskeletal proteins, surface exposure of anionic phospholipids, membrane contraction, shedding (Schoenwaelder et al., 2009; Battinelli, 2015) and microparticle production (Keuren et al., 2006). Due to flippase action, phosphatidylserine (PS) is only present in the inner layer of the plasma membrane in resting platelets. After platelet activation, the increase in cytosolic calcium caused by phospholipase $\text{C}\gamma$ (PLC γ) and phosphoinositide 3-kinases (PI3K) signalling leads to flippase inactivation and scramblase activation, which translates into high PS surface exposure (Millington-Burgess and Harper, 2022). Redistribution of PS towards the extracellular side of the cytoplasmic membrane is essential for the binding of coagulation complexes, including tenase (factors IXa and VIIIa) and prothrombinase (factors Xa and Va) (Battinelli, 2015), leading to the initiation of the coagulation cascade (Podoplelova et al., 2016), a series of protein cleavage events mediated by different serum serine proteases, many of which are calcium-

dependent. In this process, red blood cells (RBCs) and immune cells are recruited and embedded in a fibrin mesh to allow thrombi growth (Sang et al., 2021).

Coagulation is triggered via the extrinsic pathway when damaged cells expose blood to tissue factor (TF), also called factor (F)IIIa, which is expressed on their surface and present in the subendothelial matrix. TF forms a complex with FVIIa, which activates FX and leads to the common pathway. FXa is essential for FV activation, which facilitates rapid thrombin formation during the initiation of coagulation (Schuijt et al., 2013) (Figure 1.4).

In the intrinsic pathway, FXII is autoactivated into FXIIa after binding to artificial or biologic surfaces, such as high-molecular-weight kininogen (HMWK), collagen or kallikrein. FIIa catalyses the activation of FXI, which activates FX in the presence of FVIII and initiates the common pathway (Grover and Mackman, 2019; Sang et al., 2021) (Figure 1.4).

Although secondary haemostasis can be triggered via two different pathways, this signalling cascade always culminates in the common pathway, which consists of the activation of thrombin (FIIa) from its zymogen, prothrombin (FII). Thrombin catalyses the conversion of soluble fibrinogen (FI) into insoluble fibrin (FIa), which crosslinking by FXIIIa allows the formation of the fibrin mesh in the clot, providing structural stability (Figure 1.4).

To limit the thrombotic response to the injury site and prevent the formation of clots in healthy vessels, negative feedback mechanisms are also involved in secondary haemostasis. Antithrombin (ATIII) is an important SERPIN present in the plasma that forms irreversible complexes with TF and thrombin, which are eventually cleared (Hoffbrand et al., 2016) (Figure 1.4).

Another important member of the anticoagulant system is the Protein C-thrombomodulin (THBD) axis. THBD is a receptor for thrombin present on the surface of endothelial cells (van Hinsbergh, 2012). The binding of thrombin to THBD leads to protein C (PC) activation, which is associated with protein S (PS) on the surface of platelets. This complex inactivates FVa and FVIIIa. In large vessels, the endothelial PC receptor (EPCR) presents the PC to the thrombin-THBD complex, facilitating PC activation (Dahlbäck, 2005) (Figure 1.4).

Finally, tissue factor pathway inhibitor (TFPI), which is present in the plasma, platelets and endothelial cells, deactivates TF by binding to its active site in the presence of the cofactor protein S. Subsequently, TFPI-FXa binds to the TF-FVIIa complex, inhibiting the activation of FX via the extrinsic pathway (Hackeng et al., 2009) (Figure 1.4).

Once the injured vessel is healed, the fibrin in the clot is lysed by plasmin, which is generated by tissue plasminogen activator (tPA) or urokinase (uPA) from plasminogen. This process, known as fibrinolysis, is essential to ensure haemostatic balance (Chapin and Hajjar, 2015) (Figure 1.4).

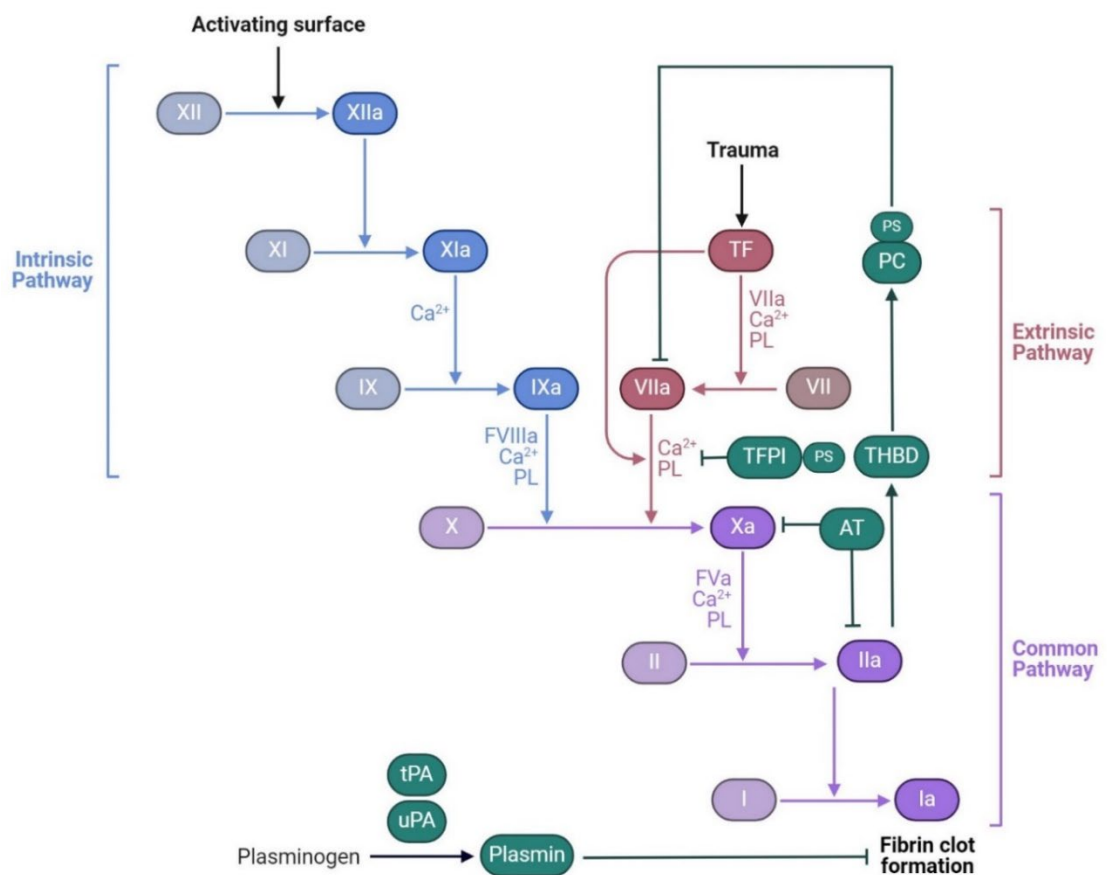


Figure 1.4. Summary of the coagulation cascade enzymatic reactions and negative feedback mechanisms. The coagulation cascade can be initiated via the intrinsic pathway, which requires platelet contact with an activating surface, or the extrinsic pathway, which is triggered by endothelial and subendothelial TF exposure upon vascular trauma. Both of these signalling pathways converge in the production of thrombin (FIIa) and the conversion of fibrinogen (FI) into fibrin (FIa). Fibrin clot formation is limited by negative feedback mechanisms, including the inactivation of TF and thrombin by AT; the binding of thrombin to THBD and the subsequent formation of the PC-PS complex, which blocks FVIIa; the inhibition of TF by TFPI in the presence of PS; and the degradation of fibrin by plasmin, which is created via the enzymatic conversion of plasminogen by tPA and uPA. Created in Biorender.com.

1.4 Platelet signalling

1.4.1 Adhesion receptors

Platelets present unique receptors that mediate their adhesion to the components of the subendothelial matrix upon vascular injury. The most important ones are the glycoprotein Ib-IX complex (GPIb-IX-V), glycoprotein VI (GPVI) and integrins $\alpha 2\beta 1$ (GPIa-IIa) and $\alpha \text{IIb}\beta 3$ (GPIIb-IIIa) (Yip et al., 2005; Hosseini et al., 2019), which signalling would be explained in detail in the following paragraphs.

The GPIb-IX-V complex is formed by four different subunits, namely GPIb α , GPIb β , GPIIX, and GPV. Binding to most of the GPIb-IX-V ligands is mediated by GPIb α (Huizinga et al., 2002; Bendas and Schlesinger, 2022). The main ligand of GPIb-IX-V is VWF (Figure 1.5). However, this receptor can also bind to thrombin, factor XI, factor XII and counter-receptors present in the surface of neutrophils or endothelial cells, such as integrin $\alpha \text{M}\beta 2$ (Mac-1) or P-selectin, respectively (Andrews et al., 2003; R. Li and Emsley, 2013).

In basal conditions, the GPIb α binding sites on VWF are inactive. After an injury on the vessel, circulating VWF binds to the collagen on the ECM. This event triggers a conformational change of VWF, exposing the binding sites and allowing fast and temporary platelet adhesion (Arce et al., 2021). This process activates integrin $\alpha \text{IIb}\beta 3$ (Figure 1.5), leading to stable platelet adhesion, platelet spreading and degranulation. Therefore, GPIb-IX-V is crucial for platelet adhesion under high-shear stress and has a key role in the initiation of arterial thrombus formation (Bendas and Schlesinger, 2022). Moreover, increases in the shear rate can induce VWF conformational change and binding to the complex without ECM exposure, which attributes mechanosensitive properties to this receptor (Ju et al., 2015; Quach and Li, 2020; Y. Zhang et al., 2022).

GPVI is an important collagen receptor in platelets and megakaryocytes, which is part of the immunoglobulin superfamily. It consists of two extracellular immunoglobulin-like domains, which are called D1 and D2, linked by a peptide chain. The D2 domain is connected to the transmembrane domain through a glycosylated peptide chain. GPVI also has a cytoplasmic tail formed by two sequences: a calmodulin (CaM) binding region and a proline-rich motif that

selectively binds to Fyn and Lyn, which are two tyrosine kinases of the Src family (Smethurst et al., 2007; Schlesinger, 2018; Slater et al., 2024).

GPVI can be present in monomeric or dimeric form, but it is always bound to the γ chain of the Fc receptor (FcR γ), as only the GPVI-Fc complex can reach the platelet surface and exert its activity (Pollitt et al., 2013). The FcR γ chain is formed by the covalent bond of two dimers, both containing an Immunoreceptor Tyrosine-based Activation Motif (ITAM) (Moroi and Jung, 2004). ITAMs are characterized by the sequence YxxL/I, which consists of a tyrosine linked to a leucine or isoleucine through a bridge of two amino acids. All ITAMs present two YxxL/I sequences separated by 6 to 12 amino acids (Pollitt et al., 2013).

The main function of GPVI is to initiate platelet activation through its binding to the GPO (Glycine-Proline-Hydroxyproline) repeats of the collagen triple helix (Watson et al., 2001; Smethurst et al., 2007; Surin et al., 2008; Burkhart et al., 2014). However, collagen is not the only endogenous ligand of GPVI, as it also binds to fibronectin, fibrin, laminin and galectin 3 (Pollitt et al., 2013). Regarding its exogenous ligands, GPVI binds to CRP-XL (Collagen-Related Peptide Cross Linked) and the snake venom convulxin. CRP-XL is a synthetic peptide containing 10 repeats of the GPO sequence. Contrary to collagen, CRP-XL is a specific agonist of GPVI (Polanowska-Grabowska et al., 2003).

GPVI binding to one of its ligands leads to the phosphorylation of Fyn and Lyn, which phosphorylates the ITAM motifs of the Fc receptor. Then, Syk binds the ITAM domains and phosphorylates, initiating a signalling cascade that allows the activation of PLC γ 2 (Surin et al., 2008; Pollitt et al., 2013) and protein kinase C (PKC), leading to calcium mobilization, granule secretion and activation of the integrin α 2b β 3, which triggers platelet aggregation (Loyau et al., 2012) (Figure 1.5).

GPVI has gained a lot of attention in the past decade for being a promising new antithrombotic target in cardiovascular disease (Induruwa et al., 2016). Population studies (Nagy et al., 2020) and investigations in animal models (Kato et al., 2003; Massberg et al., 2003; Lockyer et al., 2006; Bender et al., 2011; Matus et al., 2013) have demonstrated that the absence of this receptor significantly reduced thrombotic risk without increasing bleeding events, indicating that it plays a major role in thrombosis but not in haemostasis (Slater et al., 2024).

Integrins are a family of heterodimeric receptors formed by α and β subunits that also have a crucial role in platelet stable adhesion to the ECM. Each subunit includes an extracellular domain with the ligand binding site, a transmembrane domain, and a short cytoplasmic domain (Hynes, 2002). In platelets, $\beta 1$ and $\beta 3$ integrins are responsible for the firm adhesion to the ECM. These receptors are present in a low-affinity state on the membrane of resting platelets. After platelet activation, integrins undergo a conformational change to an intermediate state first and then a high-affinity state to bind their ligands (Nieswandt et al., 2009; Yunfeng Chen et al., 2019).

Three $\beta 1$ integrins are present in the membrane of platelets. The most studied, **$\alpha 2\beta 1$** , is a collagen receptor, while $\alpha 5\beta 1$ and $\alpha 6\beta 1$ bind to fibronectin and laminin, respectively (Nieswandt et al., 2009). Although the interaction between platelets and the ECM collagen is initially mediated by the GPIb-IX-V complex and GPVI, the integrin $\alpha 2\beta 1$ stabilises platelet adhesion to collagen (Nieswandt et al., 2001).

Integrin $\alpha IIb\beta 3$ is the most abundant in platelets and plays a key role in haemostasis. This receptor can bind to different ligands containing an arginine-glycine-aspartic acid (RGD) motif or the KQAGDV sequence, including VWF, thrombospondin, vitronectin, fibronectin, fibrin and, the most important, fibrinogen (Bledzka et al., 2013). Due to the bivalent nature of fibrinogen, two molecules of activated integrin $\alpha IIb\beta 3$ from different platelets can interact with the same fibrinogen molecule, allowing platelet aggregation (Shattil and Newman, 2004; Huang et al., 2019; J. Huang et al., 2019).

The main characteristic that differentiates integrin $\alpha IIb\beta 3$ from other receptors in platelets is the ability to transmit information bidirectionally across the plasma membrane. The series of events that lead to integrin conformational change, binding to fibrinogen and a series of intracellular signalling events that culminate with platelet irreversible aggregation and thrombus growth can be classified into “inside-out” and “outside-in” signalling (Huang et al., 2019) (Figure 1.5).

In basal conditions, the integrin $\alpha IIb\beta 3$ is present on the surface of platelets in an inactive conformation, characterised by a low affinity of the extracellular domain for its ligands. Stimulation with platelet agonists leads to the activation of other surface receptors and the initiation of a cascade of intracellular events that allow

the binding of talin and kindlin to the cytoplasmic tails of integrin $\alpha\text{IIb}\beta\text{3}$, which initiates a conformational change and the exposure of ligand-binding site through the extension of the extracellular domain (Figure 1.5). This transition between the resting state of the integrin to the activated conformation is known as “inside-out” signalling or integrin $\alpha\text{IIb}\beta\text{3}$ activation (Huang et al., 2019; van den Kerkhof et al., 2021).

Fibrinogen binding leads to integrin $\alpha\text{IIb}\beta\text{3}$ clustering and binding of c-Src to the terminal tail of the cytoplasmic domain. Trans-autophosphorylation of proximal c-Src proteins leads to Syk activation and binding to the terminal portion of the β3 tail. Then, SFKs phosphorylate the cytoplasmic tail of the β3 integrin at tyrosine (Y)773 and Y785 (Z. Li et al., 2010), recruiting several intracellular adaptor proteins and enzymes. Phosphorylation of FAK and cleavage of talin and the β3 tail triggers “outside-in” signalling, which consists of a series of enzymatic reactions that allow stable adhesion, actin cytoskeleton coupling to the β3 tail, platelet spreading and clot retraction (Durrant et al., 2017; J. Huang et al., 2019).

1.4.2 G-protein coupled receptors

Platelet activation by contact with extracellular matrix proteins exposed at the site of vascular injury leads to the release of several signalling mediators. Some of these soluble platelet agonists are released via platelet degranulation, such as ADP, ATP, and serotonin; TXA₂ is a lipid that is synthesised and released by activated platelet; and thrombin is generated through activation of the coagulation cascade. The presence of these molecules in the circulation initiates a positive feedback loop that results in thrombi growth through the recruitment of more platelets to the injury site via the interaction with G protein-coupled receptors (GPCRs) (Figure 1.5).

GPCRs are integral membrane proteins formed by several transmembrane (TM) α -helices. These are allosteric receptors, as binding of an agonist at the extracellular site of the receptor (orthosteric site) generates a conformational change that allows coupling of the G-protein at the cytoplasmic side. The versatility of the GPCR function lies in the different G-proteins associated (Offermanns, 2006; Oldham and Hamm, 2008).

G-proteins are heterotrimeric guanine nucleotide-binding proteins and the consequences of GPCR activation depend on the G-protein associated with the receptor. The three subunits that form G-proteins are G α , which carries the binding site for GDP or GTP, G β and G γ . In the resting state of the GPCR, G α is bound to GDP. Activation with a ligand leads to the recruitment of G α and the replacement of GDP for GTP, which dissociates the α subunit from the $\beta\gamma$ complex and induces a different signalling cascade depending on the type of G α subunit associated with the receptor (Weis and Kobilka, 2018). In the following paragraphs, the characteristics of the GPCRs relevant to this project will be explained in detail.

Table 1.1. Different types of G-protein α subunits and their functions.

G α subunit	Effect
Gs	Stimulation of adenylyl cyclase and increased production of cyclic AMP (cAMP)
Gi	Inhibition of adenylyl cyclase and decreased production of cAMP
Gq	Activation of phospholipase C β (PLC- β) and release of the secondary mediators inositol trisphosphate (IP3) and diacylglycerol (DAG)
G12/13	Activation of the Rho Guanine Exchange Factors (GEFs)-Rho pathway

Platelets express three *purinergic receptors* on their surface. **P2Y₁** and **P2Y₁₂** are GPCRs that respond to **ADP** (Figure 1.5), while **P2X₁** is a calcium-permeable ion channel activated by ATP. In platelets, ADP can induce activation in an autocrine and paracrine way via the purinergic receptors or sustained activation of Rap1b. Although stimulation of both P2Y₁ and P2Y₁₂ receptors is required for full platelet aggregation in response to ADP (Jantzen et al., 1999) and the induction of a procoagulant platelet phenotype (Leon et al., 2003), P2Y₁ and P2Y₁₂ are not coupled to the same G-proteins and, therefore, have different effects on platelet response. While P2Y₁ associates with Gq, exerting its function through cytosolic calcium mobilisation via PLC- β activation; P2Y₁₂ couples to Gi, reducing cAMP-dependent protein kinase-mediated (PKA) phosphorylation of vasodilator-stimulated

phosphoprotein (VASP) serine (S)239, which prevents integrin $\alpha\text{IIb}\beta\text{3}$ activation (Brass et al., 2007). Moreover, in the case of P2Y₁₂ the $\beta\gamma$ complex also plays a major role in aggregation, as it binds PLC- β , replicating the effects of Gq (S. Kim and Kunapuli, 2011). In line with these signalling events, studies in murine knock-out (KO) models have demonstrated that initial platelet activation, shape change, granule secretion and unstable platelet aggregation are triggered by P2Y₁ activation, while P2Y₁₂ is more relevant in signal amplification (Fabre et al., 1999; Léon et al., 1999).

Upon activation of the coagulation cascade, circulating prothrombin is converted into **thrombin** on cellular surfaces (Al-Amer, 2022). Apart from cleaving fibrinogen to generate the fibrin mesh of the clot, thrombin contributes to haemostatic plug formation through the stimulation of **protease-activated receptors (PARs)** on the surface of platelets. Activation of human platelets by thrombin is mediated by PAR1 and PAR4 (Figure 1.5), which couple to Gq, G12/G13 and Gi (Offermanns, 2006). Platelet stimulation with thrombin increases the bioavailability of cytoplasmic calcium and induces PLC- β activation downstream Gq signalling, which results in platelet activation, shape change, platelet adhesion, and aggregation. Moreover, G12/13 activates Rho and Gi decreases intracellular cAMP (Rwibasira Rudinga et al., 2018). As a consequence, platelets activate, change their shape and release the content of their granules, such as ADP and P-selectin, promoting platelet aggregation and supporting the growth and stability of the haemostatic plug.

The activation mechanism of PARs is the cleavage of a portion of the N-terminal exodomain by thrombin, which reveals a new amino-terminal sequence that constitutes a tethered ligand (Coughlin, 1999; 2005). The ligand interacts with the second extracellular loop of the receptor, which stimulates GTP binding to the G protein α subunit. PAR1 has a higher affinity for thrombin than PAR4, as the latter only contributes to platelet activation at high ligand concentrations (Brass et al., 1992; Nieman and Schmaier, 2007). This event could be explained by the absence of the hirudin-like sequence in PAR4, which makes the exodomain shorter than PAR1 and difficult thrombin interaction with the receptor (Keularts et al., 2000; Wettschureck et al., 2004; Woulfe, 2005).

To investigate the contribution of the different PARs to the formation of the haemostatic plug, specific agonists for these receptors have been developed (Andersen et al., 1999). The peptide SFLLRN, also known as TRAP-6, allows the specific stimulation of PAR1, while GYPGQV and AYPGKF are selective PAR4 agonists (Coughlin, 1999; J. Yang et al., 2022). Moreover, these synthetic peptides are useful tools to investigate the effects of PAR activation on PRP independently of coagulation since fibrinogen cleavage does not occur.

As mentioned previously, another important soluble platelet agonist is **TXA2**, which is produced from arachidonic acid by the cyclooxygenase (COX) and TXA2 synthase. In platelets and endothelial cells, COX-1 is expressed constitutively and converts arachidonic acid into prostaglandin H₂ (PGH₂) (Pahl, 2008). Upon a vascular injury, PGH₂ is subsequently metabolised by TXA2 synthase into TXA2, which contributes to platelet activation by autocrine and paracrine interaction with the **thromboxane receptor (TP)** (Rand et al., 2005; Gelbenegger and Jilma, 2022). Signal transduction downstream of the TP receptor leads to Gq stimulation of PLC and the consequent increase in cytosolic calcium. This GPCR can also couple G13, activating the RhoGEFs pathway. The importance of TXA2 in platelet activation and aggregation is evidenced by the successful use of aspirin, which inhibits COX-1, in the prevention of arterial thrombotic events (Capra et al., 2014).

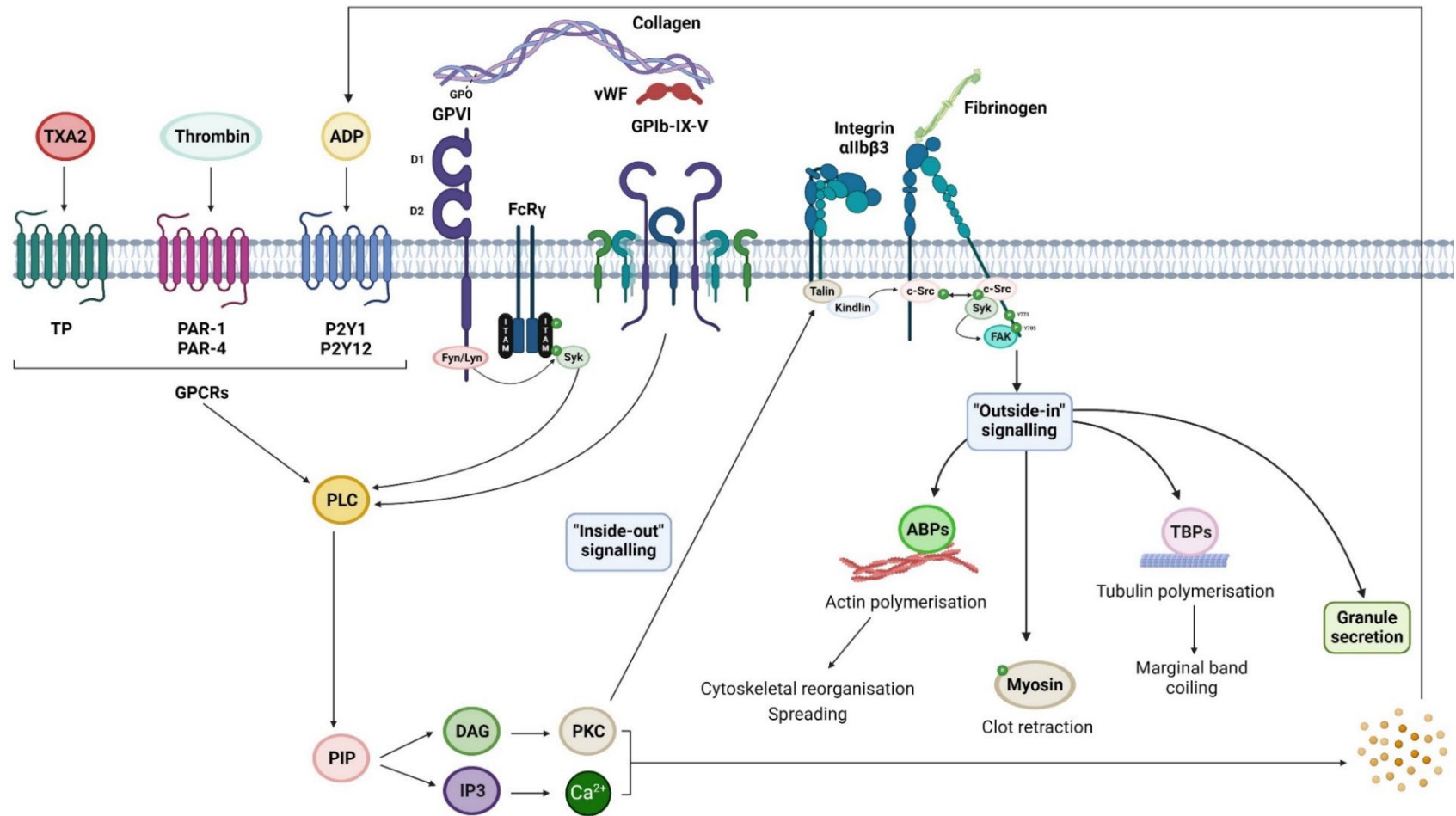


Figure 1.5. Summary of the main signalling pathways in platelets. Activation of GPIIb/IIIa, GPIb-IX-V or GPCRs initiates the phospholipase C (PLC) signalling pathway, which allows the conversion of phosphatidylinositol (4,5)-bisphosphate (PIP) into diacylglycerol (DAG) and inositol triphosphate (IP3). Then, DAG activates the protein kinase C (PKC), leading to “inside-out” signalling and the activation of integrin α IIb β 3, while IP3 causes calcium (Ca^{2+}) mobilisation and granule release. Activated integrin α IIb β 3 binds to fibrinogen, which results in “outside-in” signalling. TP – thromboxane receptor. Created with BioRender.com.

1.5 Vascular endothelial cell structure

The endothelium is a monolayer of endothelial cells that covers the inside of lymphatic and blood vessels. Although the morphology of endothelial cells varies depending on the type of vessel, they are thin and elongated, with 30-50 μm length, 10-30 μm width and 0.1-10 μm thickness. Healthy endothelial cells show a cobblestone shape *in vitro* (Krüger-Genge et al., 2019) when under static conditions, with an elongated appearance when cultured under laminar flow.

The luminal membrane of endothelial cells is in direct contact with the elements of the blood, while the basolateral surface is separated from the surrounding tissues by the ECM, a diverse glycoprotein layer secreted by the endothelial cells (Witjas et al., 2019). The endothelium and the ECM constitute the vascular intima, which sits on top of the smooth muscle cells (SMCs). This introduction will focus on the endothelial cells that cover large arteries, as these are the ones relevant to this project.

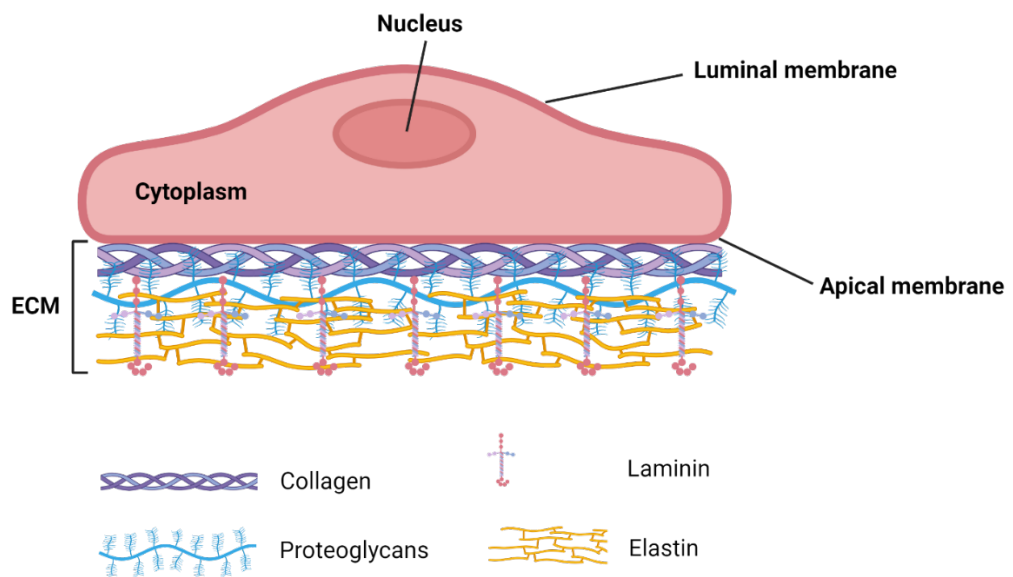


Figure 1.6. The basic structure of endothelial cells and the ECM. The main components of the ECM are collagen, proteoglycans, laminin and elastin. Created in Biorender.com.

1.6 Vascular endothelial cell function

Endothelial cells play a crucial role in the paracrine control of the vascular tone and the selective exchange of fluid, macromolecules, ions and gases between the circulation and the surrounding tissues via the endothelial adherens and tight junctions (Duong and Vestweber, 2020).

Table 1.2. Adhesion molecules involved in the maintenance of endothelial junctions.

Adherens junctions	Nectin-2
	Vascular Endothelial Cell Cadherin (VE-cadherin)
Tight junctions	Endothelial Cell-Selective Adhesion Molecule (ESAM)
	Junctional Adhesion Molecule-A (JAM-A)
	Occludin
	Claudin-5
Platelet Endothelial Cell Adhesion Molecule-1 (PECAM-1)	

The endothelium also expresses surface adhesion molecules and cytokines, such as Tumour Necrosis Factor- α (TNF- α) and interleukin-1 (IL-1) (C. Zhang, 2008), that coordinate the recruitment and extravasation of leukocytes in response to inflammation. The initial capture of leukocytes is dependent on the selectin family and P-selectin glycoprotein ligand 1 (PSGL-1). Endothelial cells express E-selectin (CD62E) and P-selectin (CD62P), while leukocytes and platelets only present L-selectin (CD62L) and P-selectin (CD62P), respectively (da Costa Martins et al., 2007). PSGL-1 is expressed in endothelial cells and leukocytes. Upon endothelial activation, endothelial selectins are exposed and leukocytes bind to them via PSGL-1, initiating the capture and rolling processes. Firm adhesion and spreading of leukocytes on the vessel wall are mediated by the β 1 and β 2 integrin families, vascular cell adhesion molecule 1 (VCAM-1) and intracellular adhesion molecule 1 (ICAM-1) followed by transendothelial migration (TEM), which is coordinated by VE-cadherin, PECAM-1 and CD99 (Zarbock et al., 2011; Rutledge and Muller, 2020).

The endothelium also has a critical role in wound healing, vasculogenesis and angiogenesis. In these processes, endothelial cell survival, migration and proliferation are key and stimulated primarily by Vascular Endothelial Growth Factor-A (VEGF-A) (K. E. Johnson and Wilgus, 2014).

Finally, the rest of this section will be focused on endothelial regulation of haemostasis. The endothelium constitutes a physical barrier against platelet activation and thrombus formation. Moreover, healthy endothelial cells produce different antiplatelet and anticoagulant molecules (Figure 1.7), namely NO, PGI₂ and ectonucleoside triphosphate diphosphohydrolase-1 (E-NTPDase1; CD39), which are essential mechanisms to prevent platelet activation in primary haemostasis. During secondary haemostasis, endothelial cells secrete different inhibitory molecules to limit coagulation, such as TFPI, tPA and uPA, but also PAI-1, which stops plasmin-mediated degradation of fibrin. Endothelial cells also express antithrombotic molecules on their surface, including heparin-like proteoglycans (Hep), which are part of their glycocalyx and act as an ATIII cofactor in the inhibition of FXa and thrombin, as explained in section 1.3.2 (K. Neubauer and B. Zieger, 2022; Katharina Neubauer and Barbara Zieger, 2022).

NO, TXA₂ and PGI₂ are important vasoactive molecules produced by endothelial nitric oxide synthase (eNOS) and cyclooxygenase (COX). While TXA₂ is a vasoconstrictor, NO and PGI₂ generate vasorelaxation by reducing intracellular calcium via an increase in cGMP and cAMP in the vascular smooth muscle cells (J. A. Mitchell et al., 2008).

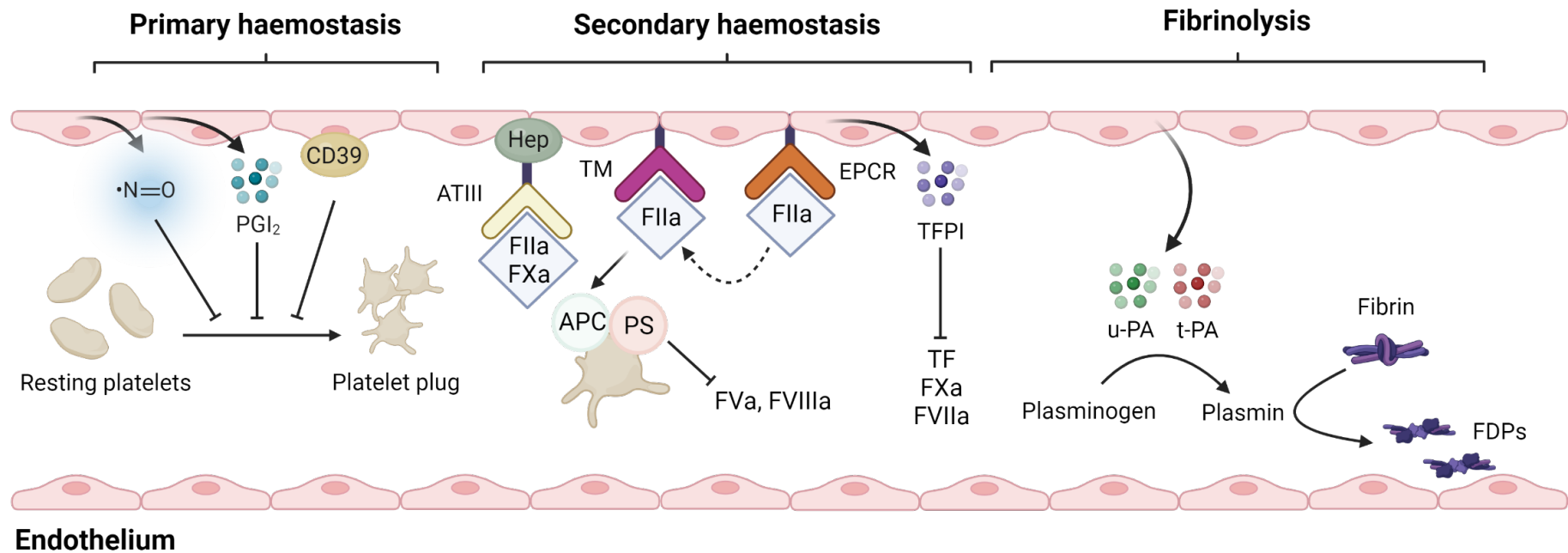


Figure 1.7. Endothelial regulation of haemostasis. The release of NO, PGI₂ and CD39 by healthy endothelial cells prevents platelet activation and adhesion. The molecular mechanisms involved in the negative regulation of coagulation are the irreversible binding and clearance of ATIII to thrombin (FIIa) and FXa; the presentation of FIIa to thrombomodulin by EPCR to generate activated protein C (APC), which complex with PS inhibits FVa and FVIIIa; and the release of TFPI, which binds to FXa and neutralises the TF-FVIIa complex, subsequently inhibiting the activation of FX in the extrinsic pathway. Endothelial cells contribute to fibrinolysis by secreting u-PA and t-PA, which convert plasminogen into plasmin, allowing the metabolization of fibrin into fibrin degradation products (FDPs). Created in BioRender.com.

1.7 Cardiovascular diseases

CVDs are the leading cause of death and disability globally, with an estimated 19.05 million deaths in 2020, which represents an increase of 18.71% from 2010 (Tsao et al., 2023). According to World Health Organisation (WHO) data, up to 85% of these deaths are due to atherothrombotic events that lead to myocardial infarction and ischemic stroke (WHO, 2021). In the following sections, the hallmarks of endothelial dysfunction and how these diseases lead to atherosclerosis will be explained, alongside the importance of antithrombotic drugs for the prevention and treatment of atherothrombotic events.

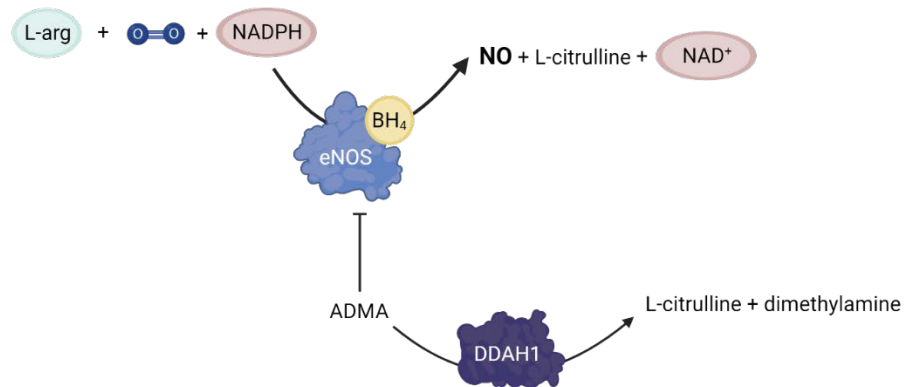
1.7.1 Endothelial dysfunction

The endothelium is an endocrine organ that guarantees the correct functioning of the vascular system by interacting with SMCs, pericytes, platelets and leukocytes through the release of mediators and the expression of surface proteins (M. Li et al., 2018; Wautier and Wautier, 2020). CVD risk factors, such as ageing, smoking, hypercholesterolemia, hypertension or diabetes, increase endothelial production of reactive oxygen species (ROS), which alter transcription and redox signalling pathways. This results in vasoconstriction, a decrease in NO bioavailability, chronic inflammation (Hadi et al., 2005) and a prothrombotic phenotype, leading to endothelial dysfunction. Endothelial dysfunction in lesion-prone areas of the arterial tree is the earliest detectable change that precedes an atherosclerotic plaque (Gimbrone and García-Cardeña, 2016; H. J. Sun et al., 2019; D. D. Lee and Schwarz, 2020).

Endothelial cells contain eNOS, a nicotinamide adenine dinucleotide phosphate (NADP)^H-dependent enzyme that, in the presence of the cofactor tetrahydrobiopterin (BH₄), metabolises L-arginine (L-arg) to NO, L-citrulline and the oxidised form of nicotinamide adenine dinucleotide (NAD⁺). Basal production of NO by the endothelium is required to promote an antithrombotic phenotype in the vascular system, as NO prevents platelet activation, and maintains the vascular tone by inducing vasorelaxation.

Decreased NO vascular levels are a hallmark of endothelial dysfunction and mark the onset of cardiovascular disease. The increase of ROS induced by CVD risk factors causes eNOS uncoupling. In this process, eNOS produces superoxide anion (O_2^-) instead of NO, becoming a source of harmful free radicals that further contribute to oxidative stress (Janaszak-Jasiecka et al., 2023).

Healthy endothelium



Dysfunctional endothelium

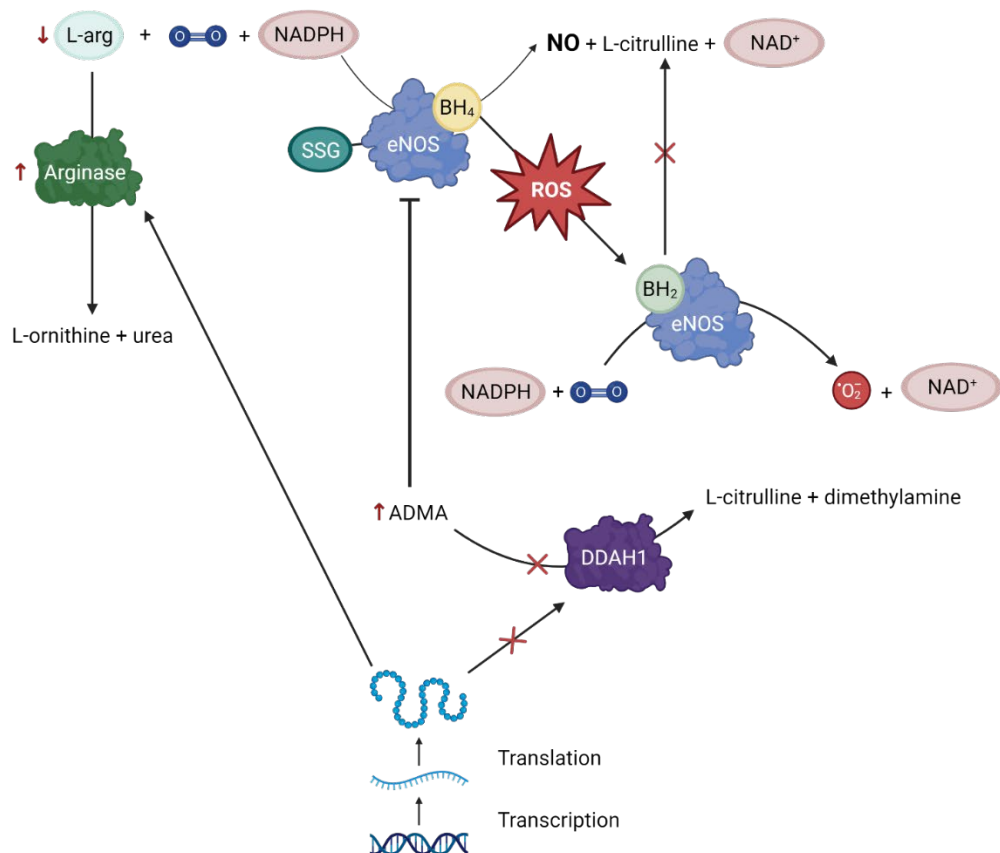


Figure 1.8. Molecular mechanisms of eNOS uncoupling. The three main mechanisms of eNOS uncoupling are BH₄ or L-arginine deficiency, ADMA accumulation and eNOS S-glutathionylation.

Under oxidative stress conditions, excessive superoxide levels oxidize BH₄ to dihydrobiopterin (BH₂) (Bendall et al., 2014), which is catalytically incompetent but can substitute for BH₄ as a coenzyme, preventing the generation of NO while promoting the production of O₂⁻ (Alp and Channon, 2004; Crabtree et al., 2009). Moreover, NO can react with the superoxide to produce peroxynitrites, which subsequently oxidise BH₄. Therefore, a positive loop is created in which eNOS uncoupling and oxidative stress increase progressively (Habib and Ali, 2011; Fujii et al., 2022) (Figure 1.8).

The bioavailability of eNOS substrate is another regulation mechanism of NO production (W. H. Tang et al., 2009). Increased arginase expression or activity, which was linked with inflammation and oxidative stress (Caldwell et al., 2015), reduces L-arginine levels, causing eNOS uncoupling and generating O₂⁻ instead of NO (Kietadisorn et al., 2012) (Figure 1.8).

Moreover, eNOS is inhibited by asymmetric dimethylarginine (ADMA), which is degraded by the enzyme dimethylarginine dimethylaminohydrolase 1 (DDAH1). Evidence in the literature demonstrated that excessive ROS and inflammation downregulate DDAH1 (Xin et al., 2007; Wilcox, 2012), which results in the accumulation of ADMA and a decrease in NO synthesis (K. Y. Lin et al., 2002) (Figure 1.8).

NO production is also regulated by transcriptional and post-translational changes of eNOS (Sessa, 2004). According to the literature, S-glutathionylation (SSG) protects proteins from ROS-induced irreversible oxidation of sulfhydryl groups and consequent degradation (Xiong et al., 2011; Rashdan et al., 2020). However, glutathionylation of eNOS in cysteine (S) residues 689 and 908 leads to conformational changes that result in a decrease in NO production (C. A. Chen et al., 2010) (Figure 1.8).

Transcription of the eNOS gene (NOS3) is altered by hypoxia, thrombin, LPS, interleukins and fluid mechanical forces (Searles, 2006). While laminar flow promotes NO release, the amount of this gas present in arterial regions with turbulent flow, such as arterial branches, is reduced. This explains the increased risk

of atherosclerosis in arterial regions with disturbed laminar flow (Chiu and Chien, 2011).

Depending on the morphological and transcriptional changes that occur in the cells, endothelial dysfunction can be divided into different types. In type I endothelial activation, cells react to acute inflammation caused by an infection or injury by retracting and releasing pre-synthesised proteins, including VWF and P-selectin. This response is usually self-limited and leads to a rapid and complete recovery (Immanuel and Yun, 2023).

Type II endothelial activation can be caused by gram-negative lipopolysaccharides (LPS), damage-associated molecular patterns (DAMPs) or cytokines, including interleukin-6 (IL-6) and TNF- α (Poher and Sessa, 2007). In contrast with type I, during type II endothelial dysfunction the phenotype of endothelial cells can be significantly altered due to the activation of pleiotropic transcription factors, such as nuclear factor- κ B (NF- κ B), which subsequently induce the expression of different inflammatory genes. As a result, surface expression of E-selectin, ICAM-1 and VCAM-1 is increased, besides VWF, TF, IL-1 and IL-8 release, leading to chronic inflammation (X. Wang and He, 2024). Various studies indicated that VCAM-1 could be a novel biomarker for early molecular imaging-based non-invasive detection of atherosclerosis (Kuroda et al., 2001; Troncoso et al., 2021; Kaur et al., 2022), as overexpression of this molecule in the intact endothelium immediately precedes monocyte capture in the nascent atherosclerotic lesions (Gimbrone and García-Cardena, 2016; Thayse et al., 2020).

Following type II endothelial activation, constant stimulation of NF- κ B transcription results in endothelial detachment and fragmentation due to apoptosis and necrosis, which leads to increased vascular permeability, microthrombotic events (Bonaventura et al., 2021; J. Zhang, 2022) and atherogenesis.

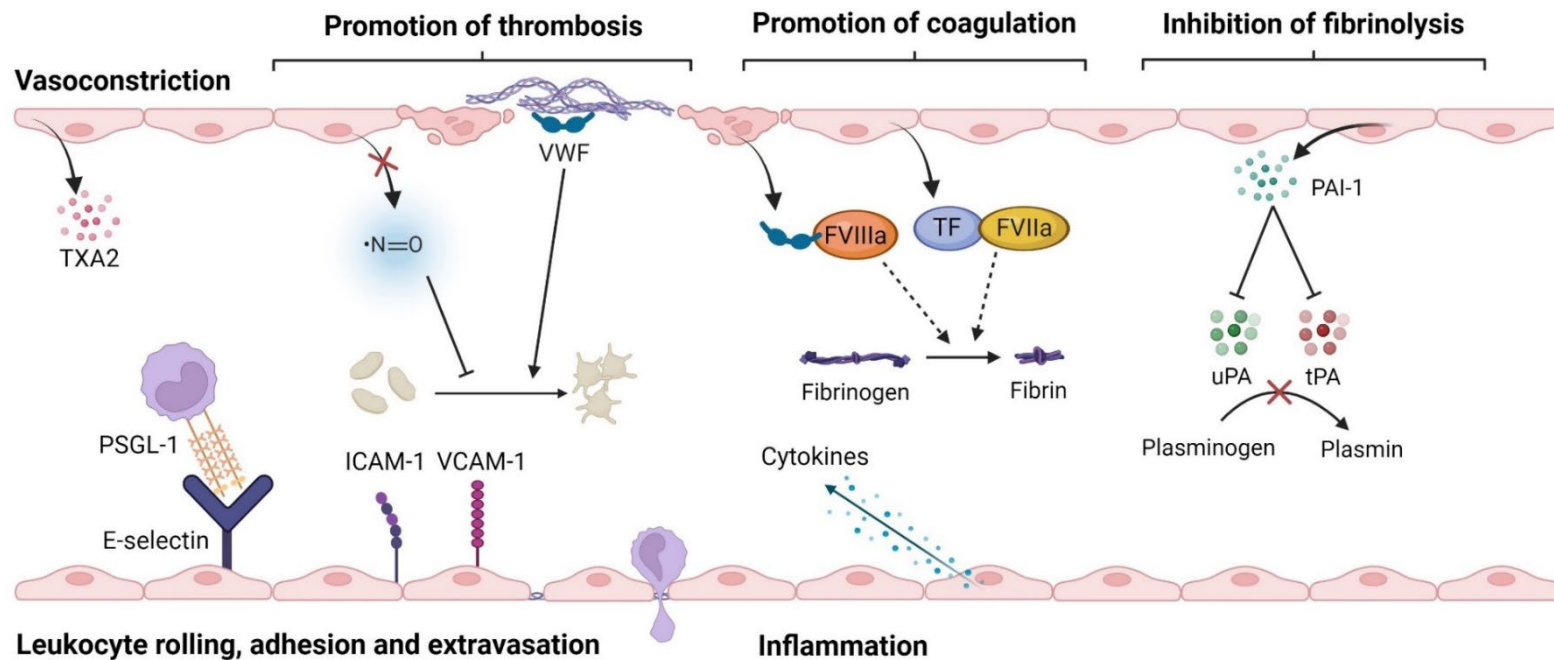


Figure 1.9. Molecular mechanisms involved in endothelial dysfunction. Upon an injury or infection, endothelial cells produce the vasoconstrictor TXA2. In response to inflammation, endothelial cells contract, which increases vascular permeability. Continuous exposure to inflammatory molecules, DAMPS or antigens, such as LPS, increases ROS levels, which reduces NO production. Activation of NF- κ B changes the endothelial transcriptome. Endothelial cells present leukocyte adhesion molecules on their surface, including E-selectin, ICAM-1 and VCAM-1, allowing leukocyte capture, rolling and extravasation. Moreover, dysfunctional endothelial cells express different cytokines, contributing further to the inflammatory cascade. Constant inflammation leads to cell death, causing denudation of the endothelium. Immobilisation of circulating VWF on the exposed ECM allows platelet adhesion and activation via the GPIb-IX-V complex. VWF release from the Weibel-Palade bodies is also increased, which facilitates the action of FVIIIa by acting as a carrier. The release of TF by endothelial cells activates the extrinsic coagulation pathway. Finally, fibrinolysis is inhibited due to an increase in the production of PAI-1, which translates into the inactivation of uPA and tPA. As a consequence, the thrombotic risk in healthy areas of the vessels increases.

1.7.2 Atherosclerosis and atherothrombosis

In arterial branches, curvatures or bifurcations, which are characterised by oscillatory shear stress (Jenkins et al., 2013), exposure of the endothelial cells to cardiovascular disease risk factors, such as hypertension, obesity, diabetes or smoking (Rajendran et al., 2023), increases the production of reactive oxygen species (ROS) in the vessel wall. As a result, different pro-inflammatory signalling pathways are activated, which contributes to a further increase in oxidative stress. Chronic exposure to ROS and inflammatory molecules causes endothelial dysfunction and activation (Batty et al., 2022). Subsequently, NO production is reduced and platelets become activated, adhering to the PSGL-1 of the dysfunctional endothelium via P-selectin (Hamilos et al., 2018; Huilcaman et al., 2022). Adhered platelets release inflammatory molecules, feeding into endothelial dysfunction and recruiting leukocytes, which migrate to the intima of the arteries. Infiltrated monocytes develop into macrophages and accumulate lipids, primarily low-density lipoprotein (LDL), in their cytoplasm, turning into foam cells. Oxidation of LDL by ROS contributes to this process, leading to the formation of the fibrous cap of the atherosclerotic plaque, where other cells such as pericytes and smooth muscle cells can also be found alongside a layer of connective tissue (Alonso-Herranz et al., 2023). Macrophages release matrix metalloproteases, which degrade collagen and the extracellular matrix, weakening the plaque (Braganza and Bennett, 2001). During atherosclerosis progression, immune cells produce cytokines that contribute to local inflammation and plaque growth (Fatkhullina et al., 2016). Eventually, reduction of the blood flow to the tissue surrounding the atherosclerotic plaque and constant inflammation, oxidative stress and lipid intake triggers cell death, which generates the necrotic core (Puylaert et al., 2022).

Atherosclerotic plaques are more predisposed to rupture if they have a high content of lipids, inflammatory cells and metalloproteases, whereas the amount of smooth muscle cells and collagen is low (Braganza and Bennett, 2001). They conserve the endothelial cells, although they are dysfunctional. However, plaques that are prone to erosion have a thicker fibrous cap, a small lipid core and a high content of smooth muscle cells and extracellular matrix. Local endothelial cells are missing (X. Luo et al., 2021). Plaque rupture or erosion leads to the release of the plaque contents into

the bloodstream and exposure of the extracellular matrix, initiating platelet aggregation. This process, called atherothrombosis leads to the formation of a thrombus that can either obstruct the artery or detach from the vascular wall and form an embolus, which can travel to proximal vessels and cause an obstruction (Gawaz et al., 2005; M. Y. Wu et al., 2017) (Figure 1.10).

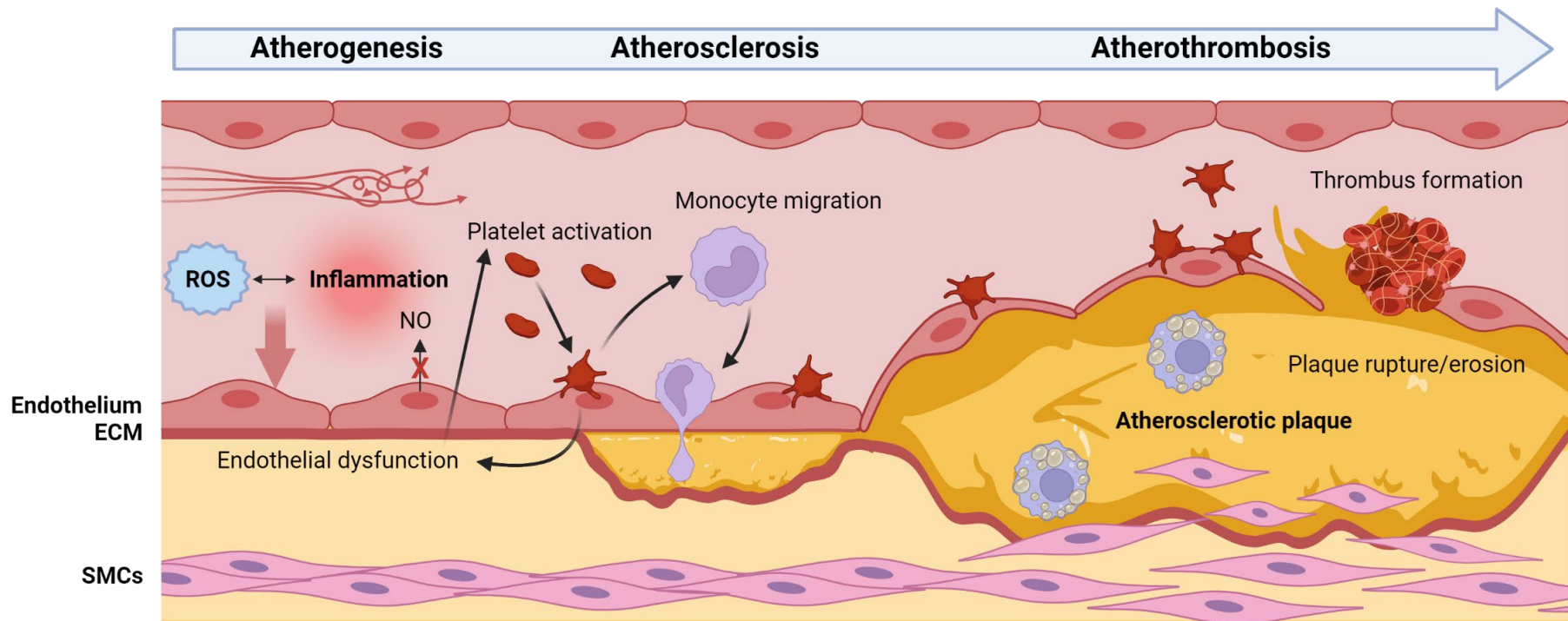


Figure 1.10. Contribution of platelets to atherosclerosis and atherothrombosis. Atherosclerosis usually develops in the areas of the arteries with disturbed flow, such as the branching arterial regions, and is characterized by chronic vascular inflammation and oxidative stress, which leads to endothelial dysfunction. As a consequence, the antithrombotic effects of endothelial cells are impaired. In this prothrombotic scenario, activated platelets adhere to the vascular wall, contributing to the development of an atherosclerotic plaque. Plaque rupture or erosion leads to thrombus formation, which can either cause a total or partial occlusion of the vessel or travel towards arteries nearby. Created in Biorender.com.

1.7.3 Antithrombotic treatments

Antithrombotic agents are fundamental to prevent and treat the thrombotic complications associated with the rupture or erosion of an atherosclerotic plaque (Baaten et al., 2024). These drugs can be classified as antiplatelet agents and anticoagulants. Antiplatelet drugs are indicated in patients with atherosclerotic disease, while anticoagulant drugs are prescribed for patients at high risk of cardioembolic events, such as atrial fibrillation and heart valve disease patients, or venous thromboembolism (VTE). A combination of both types of antithrombotic agents has only been proven beneficial effects in the case of an individual with prosthetic heart valves (Eikelboom and Hirsh, 2007). As this research project is focused on atherothrombotic complications, this section will give an overview of the current antiplatelet treatments available and clinical guidelines (Espinola-Klein, 2022).

Due to the key pathophysiological role of platelets in the formation of arterial thrombi, antiplatelet therapy is essential in the prevention and treatment of thrombotic events in individuals at high risk of CVD, such as coronary artery disease, ischaemic stroke and peripheral artery disease patients (McFadyen et al., 2018). At present, the most prescribed antiplatelet treatments are aspirin and clopidogrel (B. P. L. Chan et al., 2024).

Aspirin is a non-selective non-steroidal anti-inflammatory drug (NSAID) with antiplatelet properties due to the irreversible inhibition of the two isoforms of the cyclooxygenase (COX) enzyme (Hunter et al., 2015) (Figure 1.11). In platelets, COX-1 is present constitutively and converts arachidonic acid into prostaglandin H₂ (PGH₂). Upon platelet activation, PGH₂ is subsequently metabolised by thromboxane synthase into thromboxane A₂ (TXA₂), which contributes to platelet activation by autocrine and paracrine interaction with the thromboxane receptor (TP) (Rand et al., 2005; Gelbenegger and Jilma, 2022). By contrast, COX-2 expression is induced by cytokines to produce prostaglandins involved in inflammation and cancer, such as prostaglandin E₂ (PGE₂) (FitzGerald, 2003). Therefore, low doses of aspirin (75-100 mg) reduce both platelet activation and inflammatory responses (Campbell et al., 2007; Patrono, 2023). However, aspirin increases the risk of

adverse bleeding events. The most common haemorrhagic complication associated with this treatment is gastrointestinal bleeding, as aspirin also inhibits PGE₂ production by the gastric and duodenal mucosa, reducing the protection against gastric acid and pepsin (Gresele, 2013). Due to the lack of improved antiplatelet therapies, aspirin is still a cornerstone in the secondary prevention of myocardial infarction and ischaemic stroke despite these adverse bleeding events (Thachil, 2016). However, different clinical studies have discarded the use of aspirin for primary prevention, as the balance between absolute thrombotic risk reduction and bleeding risk is not advantageous (ATC, 2009; Soodi et al., 2020).

Current European treatment guidelines recommend dual antiplatelet therapy (DAPT), which is the combination of aspirin with a **P2Y₁₂ inhibitor**, over antiplatelet monotherapy for acute short-term treatment and secondary prevention of non-cardioembolic stroke, as the risks of recurrence and bleeding are lower (Wijns et al., 2010; Bhatia et al., 2021). P2Y₁₂ inhibitors, also called ADP antagonists (Angiolillo, 2012), can be classified into thienopyridines, formed by **clopidogrel** and **prasugrel**, and non-thienopyridines, including **elinogrel**, **ticagrelor** and **cangrelor** (Figure 1.11). Thienopyridines are prodrugs whose active metabolite irreversibly blocks P2Y₁₂, while the molecules in the non-thienopyridines group are pharmacologically active and are reversible antagonists. The choice of P2Y₁₂ inhibitor and the treatment duration depends on the clinical setting and an assessment of the ischaemic and bleeding risks for a particular patient (Pradhan et al., 2022).

For ischemic stroke and high-risk transient ischemic attack, the combination of aspirin with clopidogrel is preferred over other P2Y₁₂ inhibitors, as clopidogrel is widely accessible and administered orally (B. P. L. Chan et al., 2024). However, clopidogrel is a prodrug that requires metabolism by cytochrome P450 2C19 (CYP2C19) into the active molecule, which causes a delay in the antiplatelet properties (Franchi and Angiolillo, 2015).

Apart from the slow onset of action, clopidogrel treatment has other important limitations. As the effectiveness of clopidogrel depends on its conversion to the active metabolite by CYP2C19, the concomitant use of drugs that inhibit this enzyme is contraindicated with clopidogrel, as this would considerably reduce the efficiency of the treatment (Damman et al., 2012). Moreover, there is great variability in

patient responses due to polymorphisms in the CYP2C19 gene. Management of clopidogrel therapy is usually problematic for poor metabolizers, who are homozygote for the loss-of-function copies of the CYP2C19 gene (CYP2C19*2 and *3), and ultrarapid metabolizers, who present two increased function alleles (CYP2C19*17). On the one hand, poor metabolisers are resistant to clopidogrel therapy (O'Donoghue and Wiviott, 2006). On the other hand, ultrarapid metabolisers have an increased risk of bleeding events (Dean and Kane, 2012).

In acute coronary syndrome patients irresponsive to clopidogrel, the aspirin-ticagrelor combination may be considered (De Servi et al., 2023). Ticagrelor and its metabolites are pharmacologically active, exhibiting faster and more potent effects than clopidogrel, although it is also administered orally (Klein et al., 2019).

Individuals with a higher risk of myocardial infarction or stroke, such as type II diabetes mellitus (T2DM) (Vaidya et al., 2021) or obese patients (Blokhin and Lentz, 2013), usually have a poor response to antiplatelet therapy (Ajjan et al., 2008; Ardeshtna et al., 2019; Barrachina et al., 2021; Puccini et al., 2023). The prevalence of aspirin resistance in multinational population studies ranges from 5 to 60% (Bishopric, 2013), while clopidogrel resistance is estimated to be between 5 and 44% (Ray, 2014; Giantini et al., 2023; Parsa-kondelaji and Mansouritorghabeh, 2023). Despite DAPT, approximately 10% of patients who suffered a major cardiovascular event still have a substantial risk of recurrence (Gurbel and Tantry, 2010; de Souza Brito and Tricoci, 2013). Evidence in the literature suggests that this residual thrombotic risk might be linked to platelet activation by thrombin. Therefore, **PAR-1 antagonists** were developed to provide additional platelet suppression and overcome the inefficacy observed with clopidogrel and aspirin in high-risk CVD patients (H. Lee and Hamilton, 2012). Although several PAR-1 antagonists have been developed (R. Flaumenhaft and De Ceunynck, 2017), only **vorapaxar** (Figure 1.11) has completed phase 3 clinical trials and is currently used in clinical practice (Moschonas et al., 2015). Vorapaxar is metabolized by CYP3A4 to M20, whose pharmacological activity is equivalent to the original drug (Gurbel and Tantry, 2010).

Results from the randomised double-blind TRAP 2^oP TIMI 50 (Trial to Assess the Effects of SCH 530348 in Preventing Heart Attack and Stroke in Patients with

Atherosclerosis), in which patients under aspirin treatments and with history of ischaemic stroke, myocardial infarction or peripheral artery disease were administered either vorapaxar (40 mg load then 2.5 mg maintenance) or placebo, demonstrated that the individuals that received vorapaxar experienced less primary ischaemic events but did not significantly reduced the end point of death from cardiovascular causes (Tricoci et al., 2012). Moreover, it leads to a 55% increase in moderate or severe bleeding, which contraindicates the use of vorapaxar in patients with a history of transient ischaemic attack or intracranial haemorrhage (Tantry et al., 2020; Virani et al., 2023).

The high rate of gastric bleeding events and inefficacy of aspirin, together with the high interpatient variability linked with clopidogrel therapy and the high risk of adverse bleeding caused by vorapaxar evidence that the development of more efficient and safer antiplatelet treatments is still an unmet clinical need.

Currently, one of the most promising novel antiplatelet therapies is GPVI antagonists (Borst and Gawaz, 2021). Studies in GPVI KO animal models demonstrated that lacking this receptor does not significantly increase the bleeding risk but successfully decreases thrombotic risk (Lockyer et al., 2006). Therefore, GPVI plays a crucial role in thrombosis but not in haemostasis, which makes it the ideal target for a safer antithrombotic treatment (Slater et al., 2024). A clinical trial to test the safety and efficacy of the **anti-GPVI antibody glenzocimab** (Figure 1.11) in the treatment of acute ischaemic stroke revealed that the combination of this antibody with alteplase reduced serious adverse bleeding events and mortality risk (Mazighi et al., 2024).

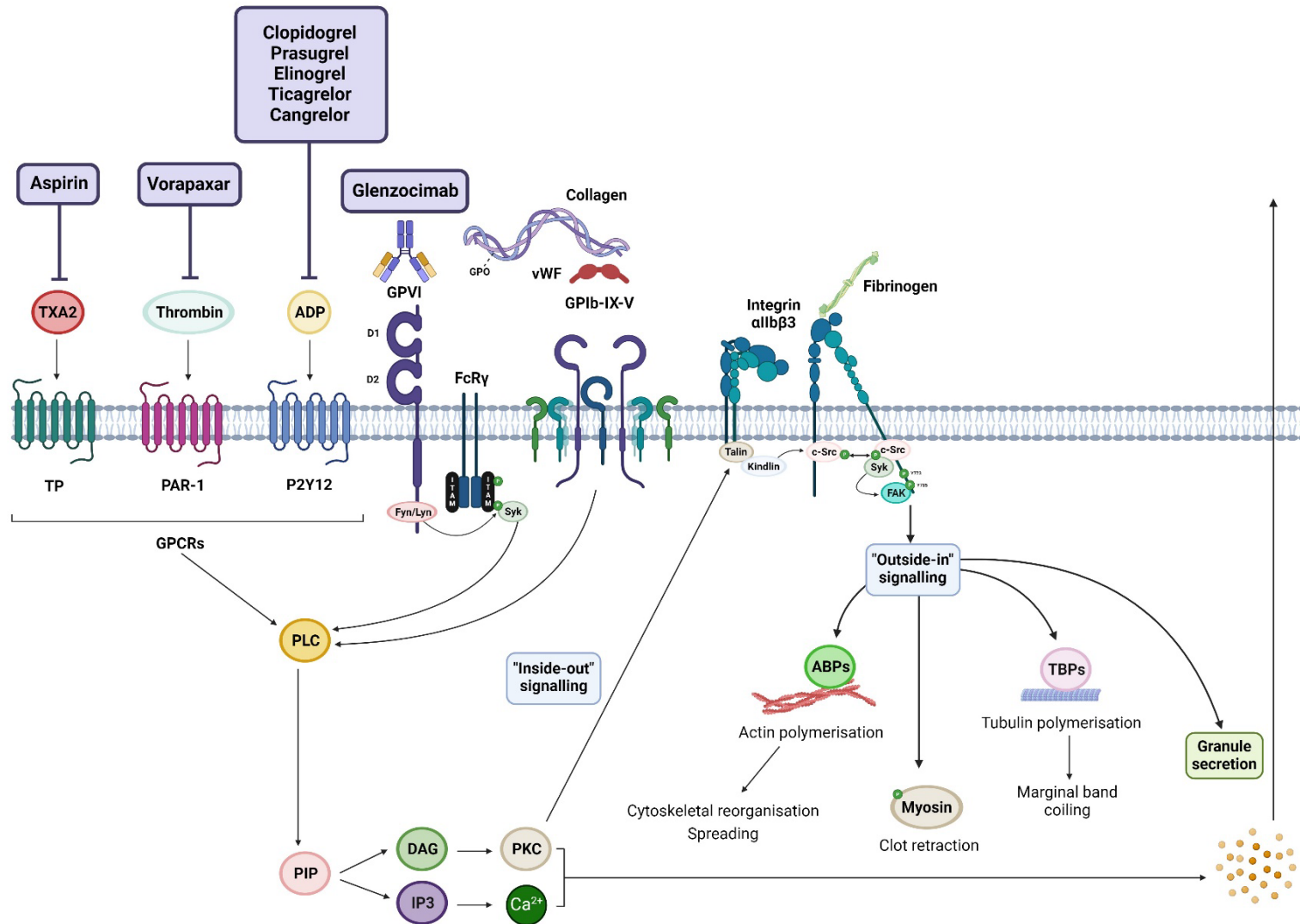


Figure 1.11. Mechanism of action of currently available antiplatelet drugs. Aspirin prevents TXA2 synthesis via irreversible inhibition of COX; Vorapaxar is a PAR-1 antagonist; Clopidogrel, prasugrel, elinogrel, ticagrelor and cangrelor inhibit the P2Y12 ADP receptor and Glanzocimab is an antibody that binds and blocks GPVI, preventing the binding of ligands and GPIIb/IIIa dimerisation. Created in Biorender.com.

1.8 Posttranslational modifications

Following their biosynthesis, proteins can undergo a series of processing events called posttranslational modifications (PTMs). To date, more than 400 different types of PTMs have been described. The mechanism behind these changes in the structure of the proteins is the covalent bonding of the amino acid side chain to a modifying group, such as acetyl, phosphoryl or glycosyl. This biochemical reaction can be enzymatic or non-enzymatic and reversible or irreversible (L. E. Smith and White, 2014).

PTMs are involved in the modulation of transcription and protein dynamics, increasing the functional diversity of the proteome and regulating several biological pathways (Latorre and Moscardó, 2016). In this section, the importance of PTMs in both platelets and nucleated cells will be discussed.

As platelets do not have a nucleus, the study of proteomics has been crucial to understanding how the platelet signalling pathways work and the effects of epigenetic modulators in platelets (Burkhart et al., 2014)

Protein phosphorylation is the most common and well-described PTM in platelets. Phosphorylation and dephosphorylation cycles are regulated by kinases and phosphatases, respectively (Gelens and Saurin, 2018). These enzymes play a crucial role in the signal transduction mechanisms that regulate numerous protein functions, including enzymatic activity, localization and protein interactions with molecules, such as other proteins, lipids or nucleic acids (Engholm-Keller and Larsen, 2013).

Several studies have indicated that glycans play a crucial role in the regulation of the haemostatic system (Wandall et al., 2012). As a result, glycosylation of platelet proteins has been widely studied. Different analyses of the platelet proteome have revealed that it contains 148 N-glycosites (Lewandrowski et al., 2007) and 1123 O-glycosites (King et al., 2017), demonstrating that both types of glycosylation are ubiquitous modifications on platelet proteins. However, the specific role of N and O-glycosylation in the regulation of platelet function is still unknown (Mammadova-Bach et al., 2020).

Other important PTMs in platelets are palmitoylation, ubiquitination and acetylation. Previous studies have demonstrated that chemical inhibition of protein

palmitoylation abrogates platelet aggregation in mice (Sim et al., 2007; Dowal et al., 2011). Regarding ubiquitylation, the ubiquitome of both resting and collagen-related peptide (CRP-XL) treated platelets has been reported. This work demonstrated that there is widespread ubiquitylation of resting platelet proteins and a two-fold increase in ubiquitylated proteins under CRP-XL stimulation (Unsworth et al., 2019).

According to the literature, acetylation of lysine residues is comparable to phosphorylation of tyrosine, serine or threonine residues because both are reversible PTMs that can regulate cellular responses through the modulation of a vast diversity of proteins that are involved in complex signalling pathways (Kouzarides, 2000; Spange et al., 2009). As the complete platelet acetylome has already been described, specific pharmacological modulation of platelet acetylases and deacetylases might be useful to elucidate the role of protein acetylation in platelet function and thrombosis (Aslan et al., 2015).

In nucleated cells, such as endothelial cells, PTM of histones can regulate gene transcription by changing the structure of nucleosomes and modifying the accessibility of the transcriptional machinery to the DNA. Although the most studied histone modification is methylation (Greer and Shi, 2012), it is well known that acetylation (Verdone et al., 2006), phosphorylation (Healy et al., 2012) and ubiquitination (J. Cao and Yan, 2012) also play a crucial role in this process. In contrast with histone methylation (H. T. Lee et al., 2020), histone acetylation usually increases gene expression (Alaskhar Alhamwe et al., 2018).

Epigenetic modification of nucleic acids, proteins and lipids has been observed in the cardiovascular disease phenotype. The study of epigenetic changes from a proteomic approach is focused on PTMs. Therefore, investigating compounds that target PTMs could be a new strategy to improve cardiovascular disease therapy (Zhu et al., 2024).

1.8.1 Lysine acetyltransferases

The enzymes responsible for the acetylation of the ϵ -amino group of protein lysine residues are lysine acetyltransferases (KATs), also called histone acetyltransferases (HATs) (P. Li et al., 2020).

Histones were the first substrates of KATs described. Therefore, these enzymes were only considered gene expression epigenetic regulators for years. It was not until 2009, after the publication of a quantitative proteomic study of the lysine-acetylated residues in human proteins, that the ability of KATs to modulate non-histone proteins was discovered. Previous work has identified 1750 human acetylated proteins and 3600 different acetylation sites by high-resolution mass spectrometry (Choudhary et al., 2009). Consequently, the role of KATs in the regulation of different cell functions has been extensively studied over the last years, implicating lysine acetylation in many cytoplasmatic processes, such as redox metabolism and cell development (Delcuve et al., 2012; X. J. Sun et al., 2015).

According to their subcellular location, human KATs can be divided into types A and B, which, as a general rule, are present in the nucleus and cytoplasm, respectively (X. J. Sun et al., 2015). Type A KATs are usually involved in gene transcription regulation, whereas type B KATs acetylate free histones and cytoplasmatic proteins. However, recent investigations have revealed some exceptions, which are indicated in Table 1.3.

Type A KATs can be further classified into families depending on the homology and acetylation mechanism of the enzymes. This group is formed by the GNAT (Baumgartner et al., 2021), p300/CBP, MYST (Avvakumov and Côté, 2007), basal transcription factors (TAF1 and TIFIIC90) and nuclear or steroid receptor coactivator (NCoA or SRC) families (Menzies et al., 2016; Triscioglio et al., 2018) (Table 1.3).

Only a small number of type B KATs have been identified so far, including KAT1 (Tafrova and Tafrov, 2014) and N-alpha-acetyltransferase 60 (NAA60) (X. Yang et al., 2011) (Table 1.3).

Table 1.3. Classification of KAT in types and families and their subcellular location in human cells. In brackets and grey, are the former names of the different KATs. KAT, lysine acetyltransferase; KDAC, lysine deacetylases; α TAT1, α -tubulin N-acetyltransferase; CBP, CREB-binding protein; CRM1, chromosomal maintenance 1 or exportin 1; NAA60, N- α -acetyltransferase 60; NcoA, nuclear receptor coactivator; Tf, transcription factors.

Type	Family	Members	Subcellular location
A	GNAT	α TAT1 KAT2A (Gnc5) KAT2B (PCAF) KAT9 (ELP3) ATF2	Nucleus
	p300/CBP	KAT3B/KAT3A complex	Cytoplasm Nucleus
	MYST	KAT5 (Tip60)	Nucleus Cytoplasm
		KAT6A (MOZ, RUNXBP2 or MYST3) KAT6B (MOREF, MYST4 or MOZ2) KAT7 (HBO1 or MYST2) KAT8 (MOF or MYST1)	Nucleus
		Basal Tf	KAT4 (TAF1/TBP, TAFII250 or p250) KAT12 (TIFIIC90)
	SRC (NCoA)	KAT13A (SRC1, BHLHE74 or NCoA-1) KAT13C (p600) KAT13B (SCR3/AIB1/ACTR) KAT13D (CLOCK) TIF2 (SRC2, BHLHE75 or NCoA-2) NCoA-3 (BHLHE42)	Nucleus Cytoplasm
B	KAT 1		Cytoplasm
	NAA60 (HAT4)		Cytoplasm

1.8.2 Lysine deacetylases

Protein acetylation homeostasis is maintained by the opposing activities of lysine acetyltransferases (KATs) and lysine deacetylases (KDACs) (Latorre and Moscardó, 2016). KDACs catalyse the removal of acetyl groups from the lysine residues of proteins (Toro et al., 2023).

In human cells, 18 KDACs have been described so far. According to what cofactor is involved in their catalytic mechanism, these enzymes are classified as zinc-dependent histone deacetylases (HDACs) and nicotinamide adenine dinucleotide (NAD⁺)-dependent deacetylases or sirtuins (SIRTs) (Van Dyke, 2014).

HDACs are divided into 4 different classes. Class I includes HDACs 1, 2, 3 and 8. Class IIa comprises HDACs 4, 5, 6, 7 and 9, while class IIb is formed by HDACs 6 and 10. Finally, class IV HDACs, with HDAC11 as the only member. Class III HDACs is the former denomination of SIRTs, including 7 enzymes (SIRT1-7) (Delcuve et al., 2012).

Like KATs, KDACs have an important role in epigenetic regulation of gene expression (de Ruijter et al., 2003) and metabolic processes, such as cellular respiration and redox state (Latorre and Moscardó, 2016). Several specific and non-specific inhibitors and activators for HDACs and SIRTs have been developed recently (Van Dyke, 2014) that can be used to investigate the functions of KDACs in healthy endothelial cells and platelets and their role in CVD.

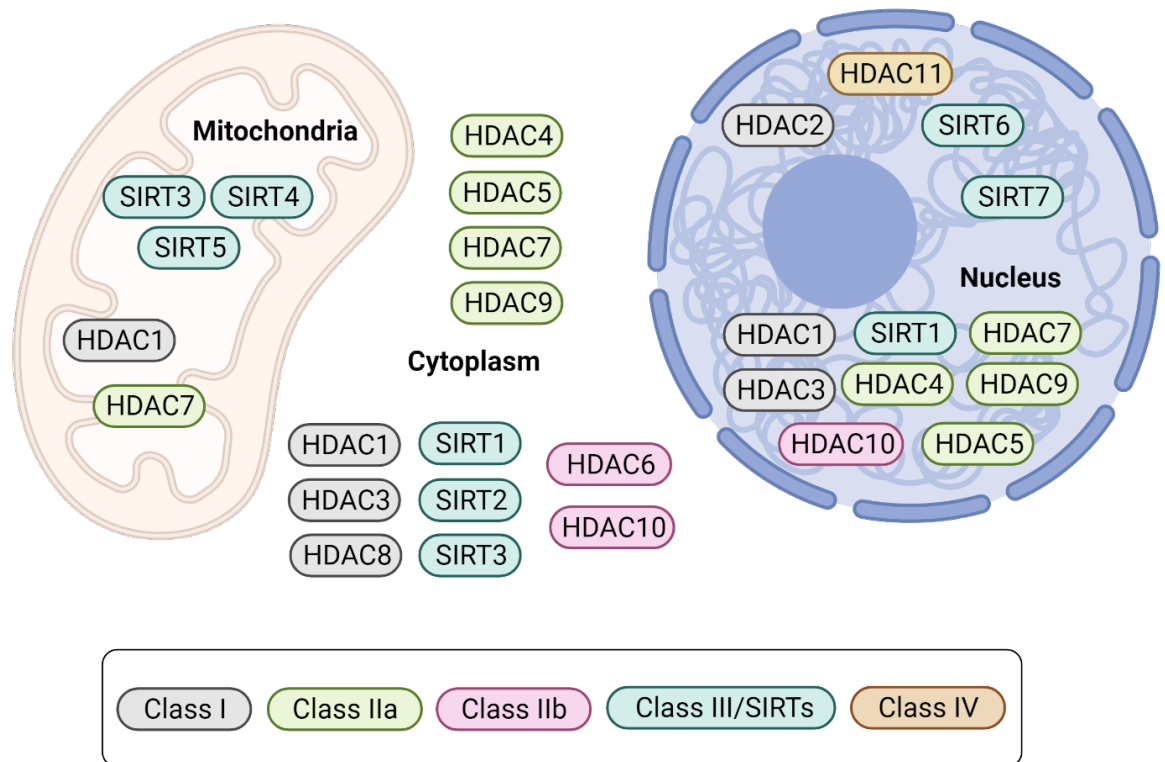


Figure 1.12 Classes and subcellular location KDACs. In terms of cellular location, KDACs are more diverse than KATs. HDACs are mainly located in the nucleus, except class IIb HDACs. Contrarily, SIRT proteins can be found in the cytoplasm, mitochondria or nucleus. These differences in subcellular distribution suggest that HDACs and SIRTs play distinct roles in cell functions. Created in Biorender.com.

1.8.3 Targeting acetylation in atherosclerosis

Acetylation constitutes an important epigenetic and posttranslational modification that regulates gene transcription and protein function, respectively, in health and disease. Several studies have associated disruption of histone and lysine acetylation, which is controlled by lysine acetyltransferases (KATs) and lysine deacetylases (KDACs), with the development of atherosclerosis.

Work by Reddy et al. (2009) in rat SMCs demonstrated that histone H3 acetylation by the KAT p300 is required to induce the expression of inflammatory genes involved in atherogenesis, such as IL-6 (Reddy et al., 2009). Moreover, under inflammatory conditions, HAT1 and p300 induce NOX5 overexpression (Vlad et al., 2019), which has been proven to worsen the prognosis of atherosclerosis in animal models (Petheć et al., 2021).

Regarding the role of protein deacetylation in atherosclerosis, treatment with the class I and II HDAC inhibitor trichostatin A (M. Kim et al., 2019) led to an increased rate of neointimal arterial lesions plus TNF- α and VCAM-1 overexpression in a murine model of atherosclerosis, indicating that deacetylases have a protective role against the inflammatory cascade that drives the formation of atherosclerotic plaques (Choi et al., 2005). In mice on a high-fat diet and with increased proprotein convertase subtilisin/kexin type 9 (PCSK9), HDAC2 overexpression was protective against oxidised LDL injury, reducing the risk of developing endothelial dysfunction and atherosclerosis (Hori et al., 2020). However, the function of HDAC3 in atherosclerosis is controversial. On the one hand, reduction of HDAC3 expression in double KO mice for the apolipoprotein E gene (APOE) leads to an increased rate of atherogenesis and vessel rupture via Akt inhibition (Zampetaki et al., 2010). On the other hand, deacetylation of eNOS by HDAC3 in human umbilical vein endothelial cells (HUVECs) is proatherogenic, reducing NO production (Jung et al., 2010).

The effects of class III HDACs in atherosclerosis have also been investigated. SIRT1 inhibition increased the risk of developing atherosclerotic plaques in double KO mice for the apolipoprotein E gene (APOE). Moreover, different studies have identified that SIRT1 deacetylation of autophagy protein 5 (ATG5) induces autophagy, which reduces necrosis and apoptosis due to oxidised-LDL cytotoxicity (I. H. Lee et al., 2008; Jiang et al., 2016).

Apart from the maintenance of autophagy homeostasis, SIRT1 anti-atherogenic properties might be linked to eNOS activation. Investigations in HUVECs demonstrated that SIRT1-mediated deacetylation of cortactin (Shentu et al., 2016) and eNOS (Mattagajasingh et al., 2007) are atheroprotective, via the regulation of F-actin dynamics and eNOS activation and subcellular location, respectively.

As mentioned in section 1.7.1 activation of NF- κ B is one of the hallmarks of endothelial dysfunction and, therefore, atherogenesis. Studies in different cell types, including U2OS, HEK 293 (H. Yang et al., 2012), hepatocytes (de Gregorio et al., 2020) and neuronal cells (Y. Li et al., 2013), have shown that NF- κ B function is regulated by lysine acetylation, as acetylation of the p65 subunit by p300 initiates transcriptional activity, while deacetylation by SIRT1 leads to inhibition, avoiding the expression of inflammatory genes. Thus, SIRT1 activation has been considered

to prevent the inflammation associated with the development of atherosclerotic plaques (P. Li et al., 2020).

Moreover, SIRT1 and SIRT6 activation has been proven to be beneficial in obesity (Dubois-Deruy et al., 2022) and T2DM, which are risk factors for CVD. Considering that increased acetylation has been linked with atherosclerosis and that there are pharmacological acetylase inhibitors and deacetylase activators available (H. Dai et al., 2018; White et al., 2024), these drugs have been considered a potential novel therapeutic strategy to treat CVD.

1.9 SIRT1 pharmacological modulators

Due to the protective effects of SIRT1 activation or overexpression in animal and *in vitro* models of several pathologies (Milne and Denu, 2008), such as CVDs (Ministrini et al., 2021), Alzheimer (Razick et al., 2023) and vascular calcification in T2DM (Bartoli-Leonard et al., 2019), and the results from genome-wide association studies (GWAS) demonstrating that SIRT1 reduced-function polymorphisms are present in many disease scenarios, including CVDs (Kilic et al., 2014) and obesity (Clark et al., 2012), different selective activators have been developed (Mai et al., 2009; Fiorentino et al., 2022) to be tested in clinical trials. For instance, SRT2104 has been investigated as a new treatment for T2DM (GlaxoSmithKline, 2010), psoriasis (Sirtris, 2011), skeletal muscle atrophy (GlaxoSmithKline, 2011) and ulcerative colitis (Sirtris, 2013). The drugs were well tolerated and, importantly, no adverse bleeding events were reported. A specific SIRT1 inhibitor, EX 527, is also available commercially (Broussy et al., 2020), providing all the necessary pharmacological tools to evaluate the effect of SIRT1 modulation on platelet function (Table 1.4).

Table 1.4. SIRT1-specific modulators.

Activators	Inhibitors
SRT1720	EX 527
SRT1460	
SRT2104	
SRT2379	
SRT2183	
SRT3025	

1.10 Aims and objectives

Current antiplatelet treatments are limited by high interpatient variability, having no effect in some patients while causing adverse bleeding in others. Therefore, developing novel safer and more efficient antithrombotic treatments is a clinical need.

The aim of this project was to assess the potential use of the SIRT1 pharmacological activator SRT1720 to treat and prevent atherosclerosis and the thrombotic complications associated with this disease via the investigation of the effect of this drug on platelets and endothelial cells *in vitro*.

The objectives of this thesis were to:

1. Investigate the impact of SIRT1 activation in platelet reactivity and *in vitro* arterial thrombus formation.
2. Study the specific functions and molecular pathways in which SIRT1 is involved in platelets.
3. Evaluate the effects of SRT1720 in healthy and dysfunctional Human Coronary Artery Endothelial Cells (HCAEC) and the impact on arterial thrombosis using an endothelialised *in vitro* model.
4. Investigate the molecular mechanisms behind the effects of SIRT1 activation in HCAEC function.

Chapter 2. Materials and methods

2.1 Pharmacological modulation of SIRT1

SIRT1 was activated using the widely used specific SIRT1 agonist SRT1720 (Milne et al., 2007; Chauhan et al., 2011; S. J. Mitchell et al., 2014) (10011020, Cayman Chemical, Ann Arbor, Michigan, USA). Stock solutions of this compound (100 mM) were prepared in 100% dimethyl sulfoxide (DMSO; Sigma-Aldrich, Dorset, UK), aliquoted and stored at -20°C. For experiments, SRT1720 was diluted in phosphate-buffered saline (PBS) and DMSO concentration was always 0.1% or lower unless specified.

2.2 Platelet agonists

Table 2.1. Platelet agonists used in experiments and supplier information.

Agonists	Commercial name	Supplier
ADP, Potassium Salt		Merck Life Science Ltd, Dorset, UK
Fibrinogen (from human plasma)		
Collagen I	CHRONO-PAR COLLAGEN	Labmedics, Abingdon, UK
Thrombin	CHRONO-PAR THROMBIN	
CRP-XL		Peptide Protein Research Ltd, Bishops Waltham, UK
TRAP-6 (SFLLRN)		R&D Systems, Abingdon, UK

2.3 Human blood extraction and preparation

2.3.1 Phlebotomy

The study was approved by the Manchester Metropolitan University Ethics Committee (Ethos application 29126) and conducted in accordance with the Declaration of Helsinki. Blood samples were collected from healthy adult donors

aged between 18 and 65 years old following informed consent. Individuals with blood-borne diseases, anaemia, clotting disorders, and those on antiplatelet or anticoagulant therapy 10 days or less before the donation were excluded from the study. Blood samples were taken into 3.2% (v/v) sodium citrate 2.7 or 4.5 mL BD Vacutainer™ tubes (Scientific Laboratory Supplies Ltd, Nottingham, UK), or 3.2% (v/v) sodium citrate 9 mL Vacuette® tubes (Greiner Bio-One, Stonehouse, UK). After collection, the tubes were gently inverted to mix the blood with the anticoagulant and samples and were kept at room temperature (RT) under rocking conditions for a maximum of 4 hours.

2.3.2 Preparation of platelet-rich plasma and washed platelets

Platelet-rich plasma (PRP) was isolated from whole blood by centrifuging the tubes at 100xg for 20 min at RT. PRP was transferred into falcon tubes and used for experiments.

To prepare ADP-sensitive washed platelets, 150 µL acid citrate dextrose (ACD; 29.9 mM trisodium citrate, 113.8 mM glucose, 2.9 mM citric acid, pH 6.4) was added per 1 mL of PRP before centrifugation at 350xg for 20 min. The platelet pellet was then resuspended in 1 mL of Tyrodes-HEPES buffer (134 mM sodium chloride, 2.9 mM potassium chloride, 0.34 mM disodium phosphate, 12 mM sodium bicarbonate, 20 mM HEPES, 1 mM magnesium chloride, pH 7.3) with glucose (5 mM). The platelet count was obtained using an XP-300 blood analysis system (Sysmex Ltd, Milton Keynes, UK) and diluted in Tyrodes-HEPES buffer as required.

2.4 Plate-Based Aggregometry

Light Transmission Aggregometry (LTA) is the gold standard method for assessing platelet function and Plate-Based Aggregometry (PBA) is a high-throughput version of this performed in 96-well plates. These techniques are based on the reduction in turbidity of PRP or washed platelets that occurs when platelets aggregate, which allows the percentage of platelet aggregation to be calculated by measuring the absorbance of these samples. The absorbance of non-stimulated PRP equals null aggregation, while the absorbance of Platelet Poor Plasma (PPP), is considered maximal aggregation (M. V. Chan et al., 2018). Although LTA and PBA are based on

the same principle, PBA allows testing 96 different experimental conditions at the same time. Consequently, PBA experiments were performed in this study as a first approach to investigate the effect of SRT1720 in platelet aggregation.

In a half-area 96-well plate (Greiner Bio-One), PRP was incubated with a range of concentrations of SRT1720 (0.01, 0.03, 0.1, 0.3, 1, 3 and 10 μM) and vehicle control (0.1% DMSO) for 10 and 60 min at 37°C. Platelet agonists were diluted in PBS and different concentrations of collagen (0.1, 0.3, 1, 3 and 10 $\mu\text{g}/\text{mL}$), ADP (0.1, 0.3, 1, 3 and 10 μM) or TRAP-6 (0.1, 0.3, 1, 3 and 10 μM) were added to the plates, which were shaken at 1200 revolutions per minute (rpm) for 5 minutes at 37°C using a BioShake iQ (QINSTRUMENTS GmbH, Jena, Germany).

Absorbance was measured at 450 nm using the GloMax® Explorer Multimode Microplate Reader (Promega, Southampton, UK) and normalised by the absorbance of SRT1720 dissolved in PBS in the same proportions in the absence of PRP. Normalised absorbance data was transformed first into the percentage of light transmission and then the percentage of aggregation was calculated using the following equations:

$$\text{Light transmission (\%)} = 10^{(-\text{sample absorbance})} \times 100$$

$$\text{Aggregation (\%)} = 100 - (\text{sample} - \text{PPP}) \times \left(\frac{100}{\text{PRP} - \text{PPP}} \right)$$

Dose-response curves were constructed and comparisons were made between the percentage aggregation of vehicle-treated samples and the different concentrations of SRT1720.

2.5 Flow cytometry

Flow cytometry experiments were performed using the MACSQuant® Analyzer 10 Flow Cytometer (Miltenyi Biotec Ltd, Bisley, UK). Platelets were gated based on CD42b positive staining and forward and side scatter profiles. Data for 10,000 events in the platelet gate was collected and analysed using version 8.7 of the FlowLogic software. Differences in the median fluorescence intensity (MFI) and the percentage of positive events were analysed.

2.5.1 Platelet activation markers

Flow cytometry was used to examine integrin α IIb β 3 activation and degranulation by detecting the levels of fibrinogen, PAC-1 (integrin activation), P-selectin (α granules), and CD63 (dense granules) present on the surface of platelets.

In the wells of a flat-bottomed 96-well plate (Greiner Bio-One), 5 μ L of PRP were mixed with 6 μ L of PAC-1 or 1 μ L of the other antibodies (Table 2.2), and Tyrodes-HEPES buffer was added until the total volume of the well was 40 μ L. Then, 5 μ L of SRT1720 (10 μ M final) or vehicle (0.1% DMSO final) were added to each well and incubated at 37°C for 10 minutes before platelet activation with 5 μ L of CRP-XL (0.1, 0.5 and 1 μ g/mL final) or TRAP-6 (1, 5 and 10 μ M final) over 20 minutes at RT in the dark. Isotype, unstained and single stain controls were included in all experiments. The contents of each well were diluted with 250 μ L of Tyrodes-HEPES buffer before flow cytometry measurement.

Table 2.2. Antibodies used for testing platelet activation markers using flow cytometry.

	Antibodies	Supplier
Platelet specific marker	APC mouse anti-human CD42b	BD Biosciences, Berkshire, UK
α-granule release	PE-Cy5 mouse anti-human CD62P	
Dense granule release	PE mouse anti-human CD63	
Fibrinogen binding	FITC Mouse Anti-Human PAC-1	
	FITC rabbit anti-human fibrinogen	Agilent, London, UK

2.5.2 Actin polymerisation assay

To assess actin polymerisation, 80 μ L of PRP were treated with 10 μ L of SRT1720 at a final concentration of 10 μ M or vehicle (0.1% DMSO) for 10 minutes at 37°C. Platelets were then activated with 10 μ L of TRAP-6 (10 μ M final) for 5 minutes at RT prior to the addition of 400 μ L of 10% neutral buffered formalin (NBF; Sigma-Aldrich) and incubation for 10 minutes on ice. Fixed platelets were washed by adding 1 mL of PBS to the tubes and centrifuging at 1000xg for 10 minutes at 4°C.

The supernatant was removed, and the wash was repeated. The PBS was then discarded and the pellet was resuspended in 200 μL of ice-cold BD Phosflow™ Perm Buffer III (BD Biosciences). After a 30-minute incubation on ice, another two cold PBS washes were performed as explained previously. The pellet was resuspended in 1 mL of PBS again and the contents of each tube were split into two 500 μL aliquots before centrifugation at 1000xg over 10 minutes at 4°C. The pellet from one of the aliquots was resuspended in 50 μL of a solution containing APC mouse anti-human CD42b antibody (1:50) and Alexa Fluor™ 488 Phalloidin (Thermo Fisher Scientific; 1:750), while the other was resuspended in PBS and constituted the unstained control. Staining was performed over 1 hour at RT before dilution with 200 μL of PBS and flow cytometry analysis.

2.6 Platelet adhesion and spreading assay

96-well plates (Greiner Bio-One) or 15 mm glass coverslips (Sigma-Aldrich) were coated with collagen (10 $\mu\text{g}/\text{mL}$) or fibrinogen (100 $\mu\text{g}/\text{mL}$) for 1 hour at RT or overnight at 4°C. After a PBS wash, blocking was performed with a 1% Bovine Serum Albumin (BSA) in PBS solution for 45 minutes at RT. ADP-sensitive washed platelets were prepared at a concentration of 2×10^7 cells/mL and treated with SRT1720 (10 μM) or vehicle (0.1% DMSO) for 10 minutes at 37°C. The residues of the blocking solution were washed with PBS before the addition of SRT1720-treated platelets, which were allowed to adhere and spread for 45 minutes at 37°C. Platelets were also added to a non-coated well as a negative control for adhesion and spreading (Figure 2.1).

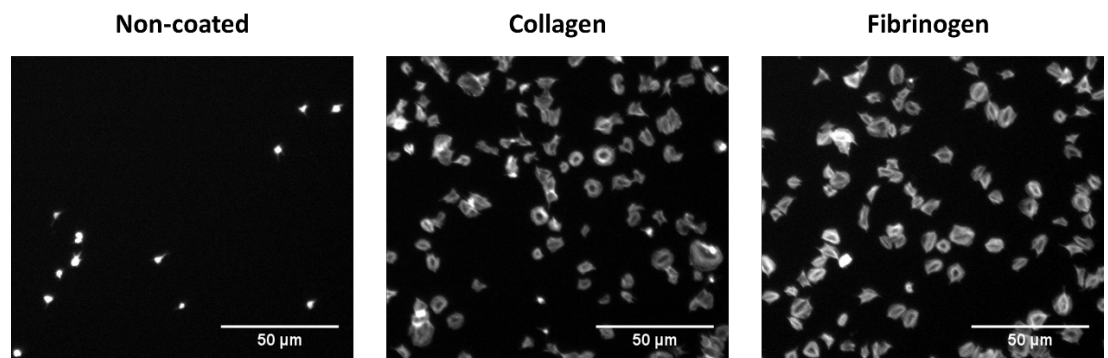


Figure 2.1. Representative images of platelets spread on non-coated wells and wells coated with collagen or fibrinogen. All wells were blocked with 1% BSA-PBS. The non-coated wells were used as a negative control for platelet adhesion and spreading.

Non-adhered platelets were removed by washing with PBS before fixing with 10% NBF (Sigma-Aldrich) for 10 minutes. Samples were then permeabilised with 0.1% Triton X-100-PBS for 5 minutes and F-actin was stained with Alexa Fluor™ 488 Phalloidin (Thermo Fisher Scientific; 1:750 in 1% BSA-PBS). Fluorescent images of adhered platelets in 3 different fields of view were captured with the 20x objective of the CELENA® S Digital Imaging System (Logos Biosystems, Villeneuve d'Ascq, France). A minimum of 100 platelets per field of view were counted and classified. Using ImageJ version 1.53e, automated analysis was performed to quantify the percentage of area coverage. Manual platelet count and platelet morphological classification into the categories explained in Figure 2.1. were also executed on ImageJ. Only representative high-quality images were taken from the mounted coverslip samples using the 63x oil immersion objective of the Thunder Imager Tissue (Leica).

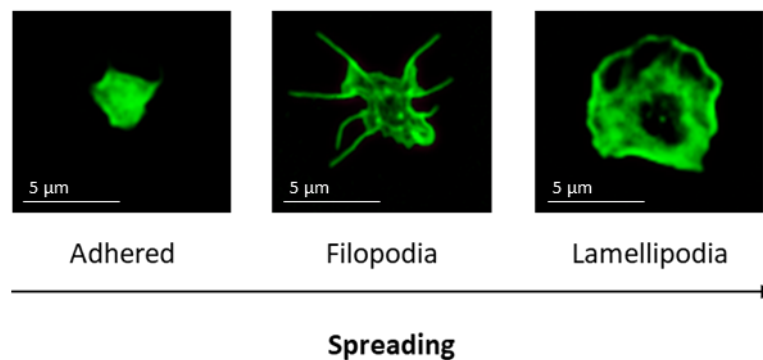


Figure 2.2. Morphological classification of platelets based on the grade of spreading. From the least (left) to the most (right) spread, cells were categorised into 3 groups: adhered, filopodia forming platelets and lamellipodia forming platelets.

2.7 Scanning Electron Microscopy

A cytoskeleton stabilisation buffer was prepared (0.2 M 1,4-piperazinediethanesulfonic acid (PIPES), pH 6.9, 60% glycerol, 10% DMSO, 2 mM MgSO₄, 2 mM ethylene glycol-bis(β-aminoethyl)-N,N,N',N'-tetra acetic Acid (EGTA), 2% Triton X-100, 1 mM phenylmethanesulfonylfluoride fluoride (PMSF), 2 mM sodium orthovanadate, 10 µg/mL leupeptin, 10 µg/mL aprotinin, 1 µg/mL pepstatin A, 2 mM adenosine 5'-triphosphate (ATP)), diluted in PBS (1:2) and supplemented with 2.5% glutaraldehyde.

In a 24-well plate (Greiner Bio-One), 15 mm glass coverslips (Sigma-Aldrich) were coated with 300 μL of poly-L-lysine (Sigma-Aldrich) for 10 min at RT, washed three times with deionised water and dried in the chemical hood. ADP-sensitive washed platelets were prepared at 2×10^7 cells/mL and 540 μL of the cell suspension were treated first with SRT1720 (10 μM) or vehicle (0.1% DMSO) for 10 min at 37°C and then stimulated with TRAP-6 (10 μM) or PBS for 3 min at RT. Samples were centrifuged into coverslips at 1450xg for 5 min and the platelet suspension was carefully removed. The actin fibres were conserved by adding 300 μL of cytoskeleton stabilisation buffer and incubating for 2 min at RT. The buffer was then removed and 300 μL of 2.5% glutaraldehyde in PBS was added to the wells and incubated O/N at 4°C.

The next day, the glutaraldehyde was removed from the wells before washing twice with PBS. Sample dehydration was performed by doing 30-minute washes using different methanol dilutions in deionised water (20%, 40%, 60%, 80%). Finally, samples were washed twice with 100% ethanol and left in the fume hood to dry O/N.

Codes were assigned to the samples to allow blindfolded imaging and mounted on pin stubs. After gold sputtering using the Polaron SEM Coating System (Artisan Technology Group, Champaign, Illinois, USA) images of the samples were obtained by Scanning Electron Microscopy using the Zeiss Crossbeam 350 FIB-SEM microscope (Carl Zeiss Microscopy Limited) and a 20,000x magnification. Platelet area coverage was quantified on ImageJ by contouring cells using the segmented line tool and measuring the area of the selection.

2.8 Investigation of the platelet marginal band

Glass coverslips (Sigma-Aldrich) were placed in a 24-well plate and coated with 0.01% poly-L-lysine (Sigma-Aldrich) for 10 minutes at RT. After three washes with deionised distilled water, coverslips were dried for 2 hours in the fume hood. PRP was diluted to 4×10^7 platelets/mL with Tyrodes-HEPES buffer supplemented with glucose, transferred to 15 mL falcon tubes and incubated with SRT1720 (10 μM) or vehicle (0.1% DMSO) for 10 minutes at 37°C. Platelets were stimulated in solution with TRAP-6 (0.1 μM) for 1 minute. The reaction was stopped by adding the same volume of a 10% NBF-1.32% ACD solution to fix the platelets while avoiding aggregate formation.

Then, 300 μL of the fixed platelets solution were added to the coated coverslips and plates were centrifuged at 200 $\times g$ for 10 minutes, washed with PBS and permeabilised with 0.1% Triton X-100-PBS for 5 min. Samples were washed three times with PBS and blocked with 1% BSA-2% Goat Serum in PBS for 1 hour at RT. Cells were stained with a β -tubulin polyclonal antibody (PA1-41331, Thermo Fisher Scientific; 1:200) for 1 hour at RT. The coverslips were washed with PBS prior to the addition of Invitrogen™ goat anti-rabbit Alexa Fluor™ 647 antibody (A32733, Thermo Fisher Scientific; 1:200) and Invitrogen™ Alexa Fluor™ 488 Phalloidin (P3457, Thermo Fisher Scientific, 1:750) diluted in blocking buffer. Coverslips were then mounted in glass slides using VECTASHIELD® Antifade Mounting Media (2BScientific, Kirtlington, UK). The percentage of platelets with an intact marginal band was calculated by dividing the number of platelets with a circular marginal band (Figure 2.2), which was counted using the ImageJ software, by the total platelet number and multiplying by 100.

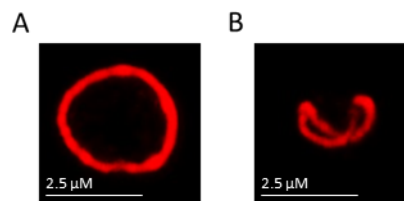


Figure 2.3. Morphological classification of the platelet marginal band. In the resting state, microtubules form a ring-like structure (A), while platelet activation leads to coiling (B).

2.9 Clot retraction

A total of 700 μL of Tyrode's with glucose, 5 μL of red blood cells and 50 μL of SRT1720 (10 μM final) or vehicle (0.1% DMSO) were mixed in a glass tube with 200 μL of PRP. Clotting was initiated by the addition of 50 μL of thrombin at 20 U/mL (1 U/mL final) in Tyrodes-HEPES buffer supplemented with glucose at RT. Tubes were flicked and an end-sealed glass pipette was secured in the centre of the tube. Photographs of the tube were taken at the beginning of the assay and every 10 minutes over 1 hour. ImageJ was used to determine the area occupied by the clot and the percentage of clot retraction was calculated using the fractional area occupied by the clots at 10-min intervals. The area of the vehicle at time 0 for every condition was considered null clot retraction. The weight of the clots in milligrams (mg) was measured at the end of the assay and compared.

2.10 Western Blotting

Lysates generated as explained in sections 2.10.1 and 2.10.2 were heated at 95°C for 5 minutes and loaded in 4-20% or 10% Mini-PROTEAN TGX Stain-Free precast gels (Bio-Rad) or hand-cast gels made with the TGX Stain-Free FastCast 10% Acrylamide Kit (Bio-Rad). Semi-dry or wet-transfer, depending on the size of the target proteins, was performed onto an Immobilon E Polyvinylidene Fluoride (PVDF) membrane (Sigma-Aldrich) with Towbin buffer (25 mM Tris, 192 mM glycine, 20% (v/v) methanol, pH 8.3) using the Trans-Blot SD Semi-Dry Transfer Cell (Bio-Rad) or the Mini Trans-Blot® Cell (Bio-Rad). The membrane was blocked for 1 hour at RT either in 5% skimmed milk in tris-buffered saline (TBS; 10 mM Tris, 150 mM NaCl) supplemented with 0.1% Tween-20 (TBST) or 5% BSA in TBST. The membrane was then incubated with primary antibodies (Table 2.3) overnight at 4°C.

The membrane was washed in TBST for 5 minutes three times and incubated for 1 hour at RT with one of the horseradish peroxidase (HRP)-linked secondary antibodies included in Table 2.3. After three washes of 5 minutes in TBST, the membrane was developed using the Immobilon® Western Chemiluminescent HRP Substrate (Millipore Ltd, Livingston, UK) and imaged with the Odyssey® Fc Imaging System (LI-COR Biosciences Ltd, Cambridge, UK).

Stripping was performed by incubating the membrane in Restore™ Western Blot Stripping Buffer (Sigma-Aldrich) for 15 min at RT. The stripping buffer was then discarded and the membrane was washed twice in TBS for 5 minutes.

Table 2.3. Antibodies used for Western blotting. mAb, monoclonal antibody.

Antibodies	Dilution	Manufacturer
Rabbit anti-SIRT2 mAb 12650	1:1000	Cell Signalling Technology, Leiden, The Netherlands
Rabbit anti-SIRT3 mAb 5490	1:1000	
Rabbit anti-SIRT5 mAb 8782	1:1000	
Rabbit anti-SIRT6 mAb 12486	1:1000	
Rabbit anti-SIRT7 mAb 5360	1:1000	
Rabbit anti-acetylated lysine mAb 9441	1:1000	
Phospho-Myosin Light Chain 2 (Ser19) Antibody 3671	1:1000	
Phospho-FAK (Tyr397) (D20B1) Rabbit mAb 8556	1:1000	

FAK Antibody 3285	1:1000	
Phospho-Cofilin (Ser3) (77G2) Rabbit mAb 3313	1:1000	
Cofilin (D3F9) XP® Rabbit mAb 5175	1:1000	
Mouse anti-β-actin mAb 8226	1:1000	
HRP-linked goat anti-rabbit IgG 7074	1:3000	
HRP-linked horse mAb anti-mouse 7076	1:3000	
Rabbit anti-SIRT1 mAb ab32441	1:1000	
Anti-Integrin beta 3 (phospho Y773) antibody ab38460	1:1000	Abcam, Cambridge, UK
Invitrogen β-Tubulin Polyclonal Antibody PA5-16863	1:1000	Thermo Fisher Scientific

2.10.1 F/G actin ratio

ADP-sensitive washed platelets were prepared at 8×10^8 cells/mL and treated with SRT1720 (10 μ M) or vehicle (0.1% DMSO-PBS) by adding 25 μ L of 10x drug or vehicle to 225 μ L of platelet suspension for 10 min at 37°C. Actin polymerisation was induced by activating platelets with 2.5 μ L of 1 mM TRAP-6 (10 μ M final) for 3 min at RT. An equal volume of cytoskeleton stabilisation buffer, which was prepared following the instructions specified in section 2.7, was added to the 1.5 mL microfuge tubes containing the platelets. The tubes were gently inverted and placed on ice. After centrifugation at 16,000xg for 75 min at 4°C, the supernatant, which contains the soluble components, was transferred to a different tube and mixed with 126 μ L of 5x Laemmli (50% (v/v) glycerol, 2% (w/v) Sodium Dodecyl Sulphate (SDS), 10% (v/v) β-Mercaptoethanol, 0.25% (w/v) Bromophenol Blue, 250 mM Tris-HCl pH 6.8, deionised water to final volume). The pellet, which is formed by filamentous actin and microtubules, was resuspended in 505 μ L of cytoskeleton destabilisation buffer (0.1 M PIPES, pH 6.9, 1 mM MgSO₄, 10 mM CaCl₂) by vortexing and left on ice for 10 min to dissolve completely prior to adding 126 μ L of 5x Laemmli.

Following the general Western Blotting protocol, 10 μ L and 30 μ L of monomeric and polymeric samples, respectively, were loaded in precast 10-well 10% SDS-PAGE gels and run at 60 volts (V) for 30 minutes followed by 100 V for 1 hour. Semi-dry transfer was performed at 10 V over 60 minutes. The membrane was blocked in 5% BSA-TBST for 1 hour at RT before incubation with antibodies against

human β -tubulin or β -actin (Table 2.3) O/N at 4°C. The membranes were washed 3 times with TBST, incubated in HRP-labelled anti-rabbit secondary antibody (Table 2.3) and imaged. Band intensities were quantified using and the F/G actin and MT/T ratios were calculated by dividing the band intensity of the filamentous forms by the band intensity of the monomers of these proteins.

2.10.2 Platelet signalling

ADP-sensitive washed platelets were prepared at 4×10^8 cells/mL and treated with SRT1720 at (10 μ M) or vehicle (0.1% DMSO). In a flat bottom 96-well plate, 90 μ L of the platelet suspensions were added to the wells and incubated at 37°C. After 30 minutes, 10 μ L of TRAP-6 (10 μ M final), CRP-XL (1 μ g/mL final) or PBS were added to the wells and incubated for 30, 90 and 180 seconds at 37°C under static conditions. Platelets were then lysed by adding 25 μ L of 5x Laemmli and stored immediately at -20°C.

Western Blotting was performed using the technique described previously in section 2.10 . Band intensities were quantified using ImageJ and levels of the total protein or β -actin were used to normalise the phosphorylation data.

2.11 Arterial thrombus formation *in vitro* on collagen

Ibidi VI 0.1 μ -slides (Thistle Scientific LTD, Rugby, UK) were used in a high-throughput *in vitro* arterial flow model to measure thrombus formation, enabling six chambers to be assessed at one time. The thrombus formation model was set up (Figure 2.3) using a six-channel syringe pump (World Precision Instruments, Hitchin, UK), syringes of different volumes (Thermo Fisher Scientific), 0.8 mm silicone tubing (RS Components, Corby, UK) and Luer adaptors (RS Components, Corby, UK).

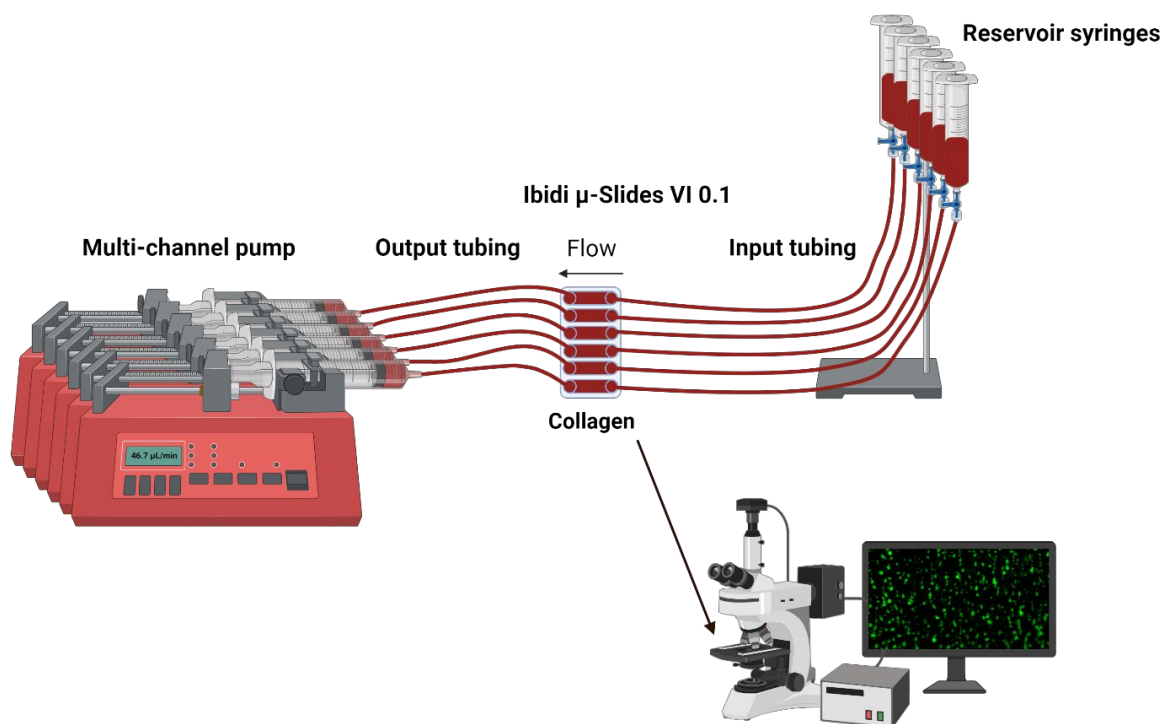


Figure 2.4. Basic operation of the *in vitro* arterial thrombosis model on collagen. Blood was added to the 3 mL reservoir syringes (right) before the activation of the programmable pump, which withdraws the liquid from the slide channels at a shear stress representative of the arterial environment. Blood flowed over the collagen coated Ibidi slides and images of the thrombi were captured in real-time and at the end of the assay. Residual blood and Tyrodes-HEPES buffer were accumulated in the output 20 mL syringes (left) and disposed of according to the health and safety regulations. Created in BioRender.com.

Thrombus formation on collagen was used to evaluate the effect of SRT1720 on platelet function. The slide chambers were coated with collagen (100 $\mu\text{g}/\text{mL}$) for 1 hour at RT. Prior to perfusion, the pump was programmed to withdraw liquid from the channels at an arterial shear rate (15 dyne/cm^2), which translates into a flow of 46.70 $\mu\text{L}/\text{min}$. Platelets were then fluorescently labelled by adding DIOC6 (Sigma-Aldrich) to whole blood at a final concentration of 1 μM and incubating for 15 minutes at RT. Then, 500 μL of stained blood were treated with SRT1720 (10 μL) or vehicle for 10, 30 or 60 minutes at 37°C. Slide chambers were washed with Tyrodes-HEPES buffer supplemented with glucose before perfusing the treated blood for 8 minutes. Thrombus formation was captured on the 488 nm channel using the CELENA® S Digital Imaging System. Endpoint images and live, every 10 seconds, were taken. Images were analysed using the following macro on ImageJ:

```
selectImage("GFP.tif");
```

```

setOption("ScaleConversions", true);

run("8-bit");

run("16-bit");

setOption("ScaleConversions", true);

run("8-bit");

run("8-bit");

run("Auto Threshold", "method=Huang white");

run("Analyze Particles...", "display");

String.copyResults();

run("Measure");

String.copyResults();"

```

Then, the area coverage percentage, the thrombi number and the area of each thrombus (μm^2) were obtained by applying the “measure” and “analyse particles” tools on ImageJ. The average thrombi size was calculated on Microsoft Excel using the area of the individual thrombi.

2.12 HCAEC dysfunction inducers

Table 2.4. Molecules used to induce endothelial dysfunction in HCAEC and suppliers.

Dysfunction factors	Supplier
TNF- α	Thermo Fisher Scientific
PeproTech® recombinant human IL-6	
Lipopolysaccharides from Escherichia coli O111:B4 (LPS)	Sigma-Aldrich
H ₂ O ₂ (Sigma-Aldrich; 100 μM)	

2.13 HCAEC culture

Cell culture was performed in class II safety cabinets under sterile conditions. Primary Human Coronary Artery Endothelial Cells (HCAEC, C-12221) were acquired from Promocell (Heidelberg, Germany) and cultured using the Endothelial Cell Growth Medium MV 2 Kit (C-22121, Promocell), which is constituted by Endothelial Cell Growth Medium MV2 (C-22022) with 5% (v/v) foetal calf serum (FCS), recombinant human (rH) epidermal growth factor (5 ng/mL), rH basic fibroblast growth factor (10 ng/mL), insulin-like growth factor (20 ng/mL), vascular endothelial growth factor (VEGF) 165 (0.5 ng/mL), ascorbic acid (1 µg/mL) and hydrocortisone (0.2 µg/mL). The media was also supplemented with 1% Penicillin-Streptomycin (Sigma-Aldrich).

HCAECs were grown in T-75 cell culture flasks, Nunc™ plates or glass circle coverslips (Thermo Fisher Scientific Inc., Cambridge, UK) in a 5% CO₂ incubator at 37°C. Media changes were performed every 48 hours.

Once confluent, the media was removed from the flask and cells were washed with pre-warmed Dulbecco's Phosphate Buffered Saline (DPBS; Lonza, Visp, Switzerland). Then, 4 mL of pre-warmed Trypsin-Ethylenediaminetetraacetic acid (EDTA; Lonza) were added to the T-75 flask and incubated for 3 minutes at 37°C to allow cell detachment. Trypsin was neutralised by adding 8 mL of pre-warmed HCAEC media. The cell suspension was transferred into a 15 mL falcon tube (Fisher Scientific, Loughborough, UK) and centrifuged at 300xg for 5 minutes at RT. The pellet was resuspended in 1 mL of media and the number of cells was counted using the TC20 Automated Cell Counter (Bio-Rad Laboratories Ltd, Watford, UK). HCAECs were seeded at 1.3×10^4 cells/cm² in flasks, plates and coverslips, while the seeding density in the Ibidi VI 0.1 µ-slides (Thistle Scientific, Glasgow, UK) was 3.6×10^4 cells/cm², unless stated otherwise. HCAECs were used for experiments at passage 3-7.

For cryopreservation, cells were isolated following the protocol above but the pellet was resuspended in 90% (v/v) foetal bovine serum (FBS; Lonza) supplemented with 10% (v/v) DMSO at 1×10^6 cells/mL. The cell suspension was aliquoted into 1.2 mL cryopreservation vials (1 mL/vial) and placed in a CoolCell™ LX Cell Freezing Vial

Container (Fisher Scientific) at -80°C for at least 24 hours before long-term storage in liquid nitrogen.

2.14 HCAEC immunofluorescence

2.14.1 SIRT1 expression

HCAEC were cultured in 15 mm glass coverslips (Sigma-Aldrich) until confluent and treated with PeproTech® recombinant human TNF- α (10 ng/mL) or vehicle (0.1% DMSO) for 20 minutes and 1 hour. Cells were washed with PBS, fixed with 10% NBF and permeabilised with 0.1% Triton X-100-PBS. Samples were then blocked with 1% BSA-PBS for 1 hour and incubated with an antibody against SIRT1 (ab12193, Abcam; 1:200) or IgG control (I-1000-5, 2BScientific) for 1 hour. After three PBS washes, samples were stained with Thermo Scientific™ DAPI (Fisher Scientific; 100 ng/mL), Invitrogen™ Rhodamine phalloidin (Thermo Fisher Scientific; 1:750) and Invitrogen™ Alexa Fluor™ 488 Goat anti-Rabbit IgG (A-11008, Thermo Fisher Scientific; 1:200). Images were taken with the 40x oil immersion objective of the STELLARIS 5 confocal microscope (Leica Microsystems Ltd, Milton Keynes, UK). Three representative images of each experimental condition were captured. SIRT1 expression was quantified by measuring the mean fluorescence intensity in the 488 nm channel and normalising by the nuclei count.

2.14.2 Actin staining

HCAEC were cultured in 96-well plates until confluent and treated with SRT1720 (10 μ M) for 24 hours at 37°C. After a PBS wash, HCAEC were fixed with 10% NBF for 10 minutes, permeabilised for 5 minutes with 0.1% Triton X-100-PBS and then blocked over 1 hour with 1% BSA-PBS. To visualise the outline of the cells, F-actin was stained with Invitrogen™ Rhodamine phalloidin (Thermo Fisher Scientific; 1:750). DAPI (Sigma-Aldrich; 100 ng/mL) was used to stain the nuclei. Disruptions in the cellular morphology and size were assessed.

2.14.3 NF- κ B subcellular location and actin polymerisation

HCAEC were seeded in a 96-well plate at 1×10^4 cells/well. When confluent, cells were incubated with TNF- α (Thermo Fisher Scientific; 10 ng/mL) for 20 minutes at 37°C before treatment with a range of concentrations of SRT1720 (0.1, 0.3, 1, 3 and 10 μ M) or vehicle (0.1% DMSO) for 4 hours. Following a PBS wash, HCAEC were fixed with 10% NBF for 10 minutes, permeabilised with 0.1% Triton X-100-PBS for 5 minutes and blocked with 1% BSA-PBS for 1 hour. Samples were then incubated with a rabbit anti-NF- κ B antibody (ab12193, Cell Signalling Technology; 1:200) for 1 hour at RT. Nuclei were stained with DAPI (Fisher Scientific; 100 ng/mL), F-actin was stained with Invitrogen™ Rhodamine phalloidin (Thermo Fisher Scientific; 1:750) and Invitrogen™ Alexa Fluor™ 488 Goat anti-Rabbit IgG (Thermo Fisher Scientific, A-11008; 1:200) was used for visualization of NF- κ B. A minimum of three images per condition were taken using the 20x objective of the CELENA® S microscope (Logos Biosystems). Masks of the nucleus were created based on the DAPI staining. The MFI in the 488 nm channel in the nuclear area and the total area of the cells were quantified on ImageJ using the following macro:

```
"selectImage("DAPI.tif");  
  
run("Enhance Contrast...", "saturated=0.35");  
  
setOption("BlackBackground", false);  
  
run("Convert to Mask");  
  
run("Fill Holes");  
  
run("Remove Outliers...", "radius=2 threshold=50 which=Bright");  
  
run("Despeckle");  
  
run("Analyze Particles...", " show=[Overlay Masks] add composite");  
  
selectImage("GFP.tif");  
  
makeRectangle(375, 503, 37, 64);  
  
run("Subtract Background...", "rolling=50");
```

```

run("From ROI Manager");

roiManager("Measure");

run("Remove Overlay");

run("Measure");"

```

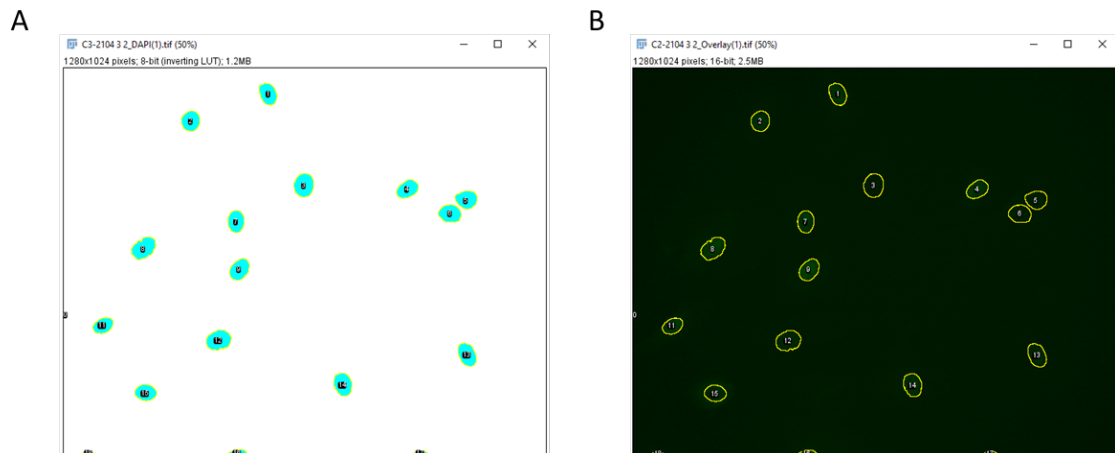


Figure 2.5. Example of nuclear NF- κ B analysis on ImageJ. Masks of the nucleus were created on the DAPI images (A) and overlaid on the GFP images (B) to measure NF- κ B presence in the nucleus.

The nuclear-total MFI ratio was calculated, compared between conditions and presented as the ratio normalised to the vehicle healthy control. To measure differences in actin polymerisation, MFI was quantified at 555 nm, normalised to the nuclei count and compared.

2.14.4 Evaluation of HCAEC eNOS levels post-thrombosis model

After performing the arterial thrombus formation model, the HCAEC were fixed in the Ibidi 0.1 VI μ -slides using 10% NBF. After one PBS wash, cells were permeabilised and blocked using 0.1% Triton X-100 in 5% goat serum (GS)-PBS for 1 hour at RT. Samples were washed once with PBS prior to a 1-hour incubation at RT with an anti-eNOS antibody (ab252439, Abcam; 1:100) diluted in 5% GS-PBS. Fluorescent staining was performed by incubating the cells in a solution of 5% GS-PBS containing DAPI (Fisher Scientific; 100 ng/mL), DIOC6 (Sigma-Aldrich; 1 μ M) and Invitrogen™ goat anti-rabbit Alexa Fluor™ 647 antibody (A32733, Thermo Fisher Scientific; 1:300). A minimum of three images per field of view were captured for each experimental condition using the 40x

objective of the STELLARIS 5 confocal microscope (Leica Microsystems Ltd). Total eNOS expression was obtained by quantifying the MFI at 647 nm, normalising it to the nuclei count and comparing it between conditions.

2.15 MTS assay

HCAEC were seeded in a 96-well plate at 1×10^4 cells/well and cultured O/N. The next day cells were treated with different concentrations of SRT1720 (0.1, 0.3, 1, 3 and 10 μ M). Vehicle (0.1% DMSO) was used as a negative control and 0.1% SDS was used as a positive control of cell death. All conditions were tested in duplicate and incubated for 24, 48 and 72 hours. Following the kit recommendations, 3-(4,5-dimethylthiazol-2-yl)-5-(3-carboxymethoxy phenyl)-2-(4-sulfophenyl)-2H-tetrazolium (MTS) reagent (Abcam) was added to the plate and incubated for 2 hours at 37°C. Absorbance at 490 nm was measured in the GloMax® Explorer Multimode Microplate Reader (Promega). The average absorbance (Abs) of the vehicle wells was considered 100% of cell viability. The cell viability percentage of the other wells was calculated using the following equation:

$$\text{Cell viability (\%)} = \frac{\text{Abs treated HCAEC}}{\text{Abs vehicle HCAEC}} \times 100$$

2.16 Cell migration assay

Using sterile forceps, Ibidi 2-well cell culture silicone inserts (Thistle Scientific) were placed in a 24-well plate (Sarstedt, Nümbrecht, Germany) and 70 μ L of a 3×10^5 cells/mL HCAEC suspension were seeded into each well. The next day, the inserts were removed and the cells were treated with SRT1720 (0.3, 1 and 3 μ M) or vehicle (0.1% DMSO) diluted in complete endothelial media using reverse pipetting. The plate was anchored into the PHI HoloMonitor® M4 System vessel holder (Thistle Scientific) and the standard lids were replaced with sterile HoloLids™ (Thistle Scientific), avoiding the creation of bubbles. The Wound Healing application was selected on the HoloMonitor® App Suite 3.5 software and the capture areas were designated to allow the visualisation of the gap. Cell motility in the gap area was monitored by capturing images in a minimum of six positions per well every 10 minutes over 20 hours. Images were analysed using the HoloMonitor® App Suite 3.5 software to obtain the cell-covered area (%) and

the gap width (mm). The gap closure (%) was calculated by dividing the gap width after 10 and 20 hours of incubation by the initial gap width and multiplying by 100. To quantify how SRT1720 affected the kinetics of HCAEC motility, the cell-covered area (%) at every timepoint of the assay was represented and the Area Under the Curve (AUC) was calculated for each condition.

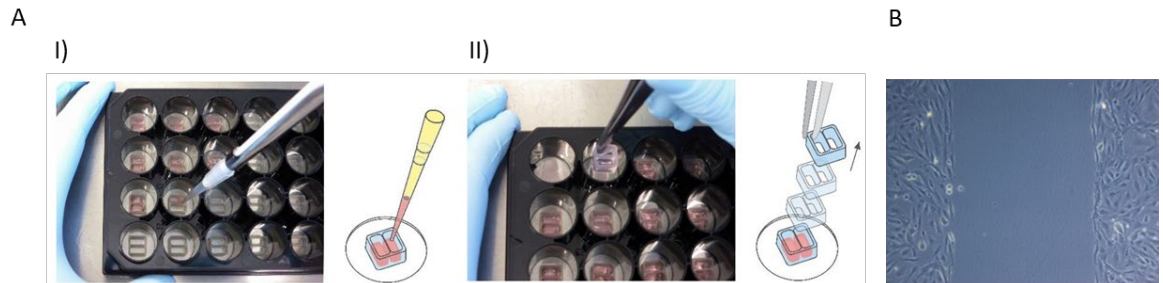


Figure 2.6. Seeding HCAEC for the scratch assay. HCAEC were grown O/N on Ibidi 2-well cell culture inserts (AI), which were then removed (AII), leaving a space between the cells. Representative images of the gap (B) were acquired using the 10x objective of the ZEISS Primovert inverted microscope (Carl Zeiss Microscopy Limited).

2.17 Endothelial permeability assay

To evaluate the impact of SIRT1 activation on the permeability of a HCAEC monolayer, the *In Vitro* 24-Well Vascular Permeability Assay kit from Millipore (ECM644) was used. Collagen-coated porous cell culture inserts were hydrated by incubating them with 250 μ L of endothelial growth media for 15 minutes at RT. Then, 200 μ L of media were removed from the inserts and replaced with 200 μ L of a 1×10^6 cells/mL HCAEC suspension. The receiver plate was filled with 500 μ L of media before incubating for 72 hours in a 37°C/5% CO₂ tissue culture incubator. The media was then removed from both the inserts and the receiver plates without disturbing the cell monolayer. Using sterile forceps, the inserts were transferred to a new receiver plate. The HCAEC monolayer was treated with 200 μ L of SRT1720 (1 μ M) or vehicle (0.1% DMSO) in the presence or absence of TNF- α (1 μ g/mL) or LPS (1 μ g/mL) and 500 μ L of the same solution were added to the receiver tray. After 24 hours, inserts were transferred to a fresh receiver plate. The receiver tray was filled with 500 μ L of fresh serum-free endothelial media and 200 μ L of a FITC-dextran solution were added to the inserts. The plate was incubated for 2 hours in the dark and then 150 μ L of media from the inserts and the receiver tray were transferred into a black-bottomed 96-well plate. Fluorescence was

measured at 488 nm in the GloMax® Explorer Multimode Microplate Reader (Promega). The FITC fluorescent signal in the media from the receiver tray is directly proportional to the permeability of the HCAEC monolayer, as healthy confluent cells would prevent the exchange of dextran between the two compartments. The fluorescence of FITC-dextran of the receiver tray was normalised by the fluorescence of the insert media using Microsoft Excel and compared between conditions.

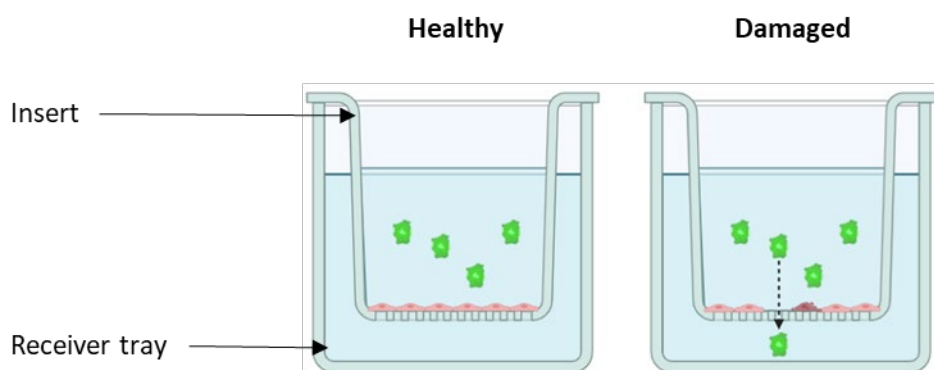


Figure 2.7. Principle of the endothelial permeability assay. FITC-dextran would only be present in the receiver tray if the permeability of the HCAEC monolayer is increased as a result of endothelial dysfunction. Created in BioRender com.

2.18 Endothelialised arterial thrombus formation *in vitro*

HCAEC were grown on the Ibidi chamber slides for at least 48 hours (Figure 2.7). Media changes were performed every day. Once the cells were forming a confluent monolayer, they were incubated O/N with SRT1720 (1 μ M) or vehicle (0.1% DMSO) in the presence of LPS (100 ng/mL) or PBS. On the day of the assay, untreated blood was stained with DIOC6 and a new Ibidi slide was coated with collagen following the indications mentioned in section 2.11. Every channel of the collagen slide was then connected to the slide containing the HCAEC using serial connectors of the μ -slides (Ibidi) (Figure 2.8 and Figure 2.9). After a wash with Tyrodes-HEPES-glucose, stained blood was run on the model as described in section 2.11, flowing first through the HCAEC-containing channels and then through the collagen-coated chambers. At the end of the assay, pictures of the thrombi formed on both slides were taken using the 488 nm channel of the CELENA® S Digital Imaging System (Logos Biosystems). In the collagen slides, the area coverage percentage, thrombi number and thrombi size were compared

between conditions using ImageJ thresholding, as previously described in section 2.11 . However, to evaluate these parameters on the HCAEC the Trainable Weka Segmentation v3.3.4 from ImageJ (Figure 2.10) was used.

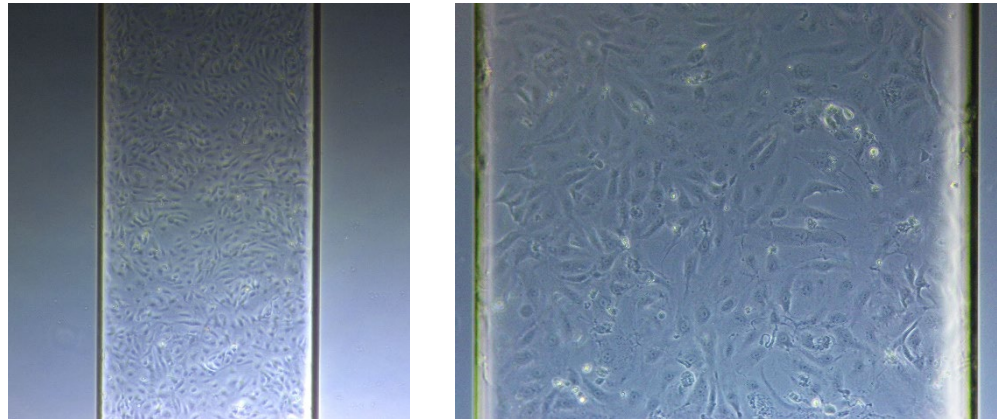


Figure 2.8. Representative image of a confluent HCAEC monolayer in the Ibidi VI 0.1 μ -slides. Images were taken with the 20x (left) and 10x (right) objectives of the ZEISS Primovert inverted microscope (Carl Zeiss Microscopy Limited, Cambridge, UK).

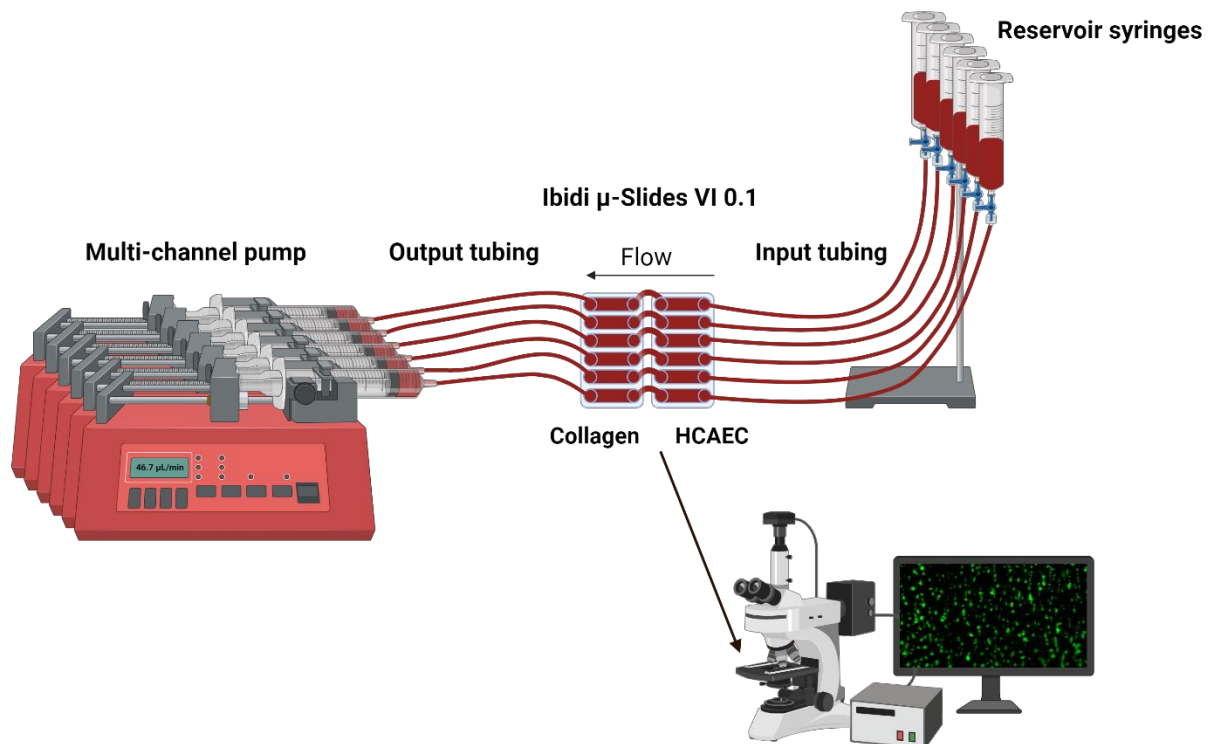


Figure 2.9. Endothelialised thrombus formation model set up. Reservoir syringes on the right, two connected Ibidi slides coated with HCAEC and collagen, respectively, on the microscope in the middle, and the multi-syringe pump on the left. Created in BioRender.com



Figure 2.10. Picture of the endothelialised arterial thrombus formation model setting.

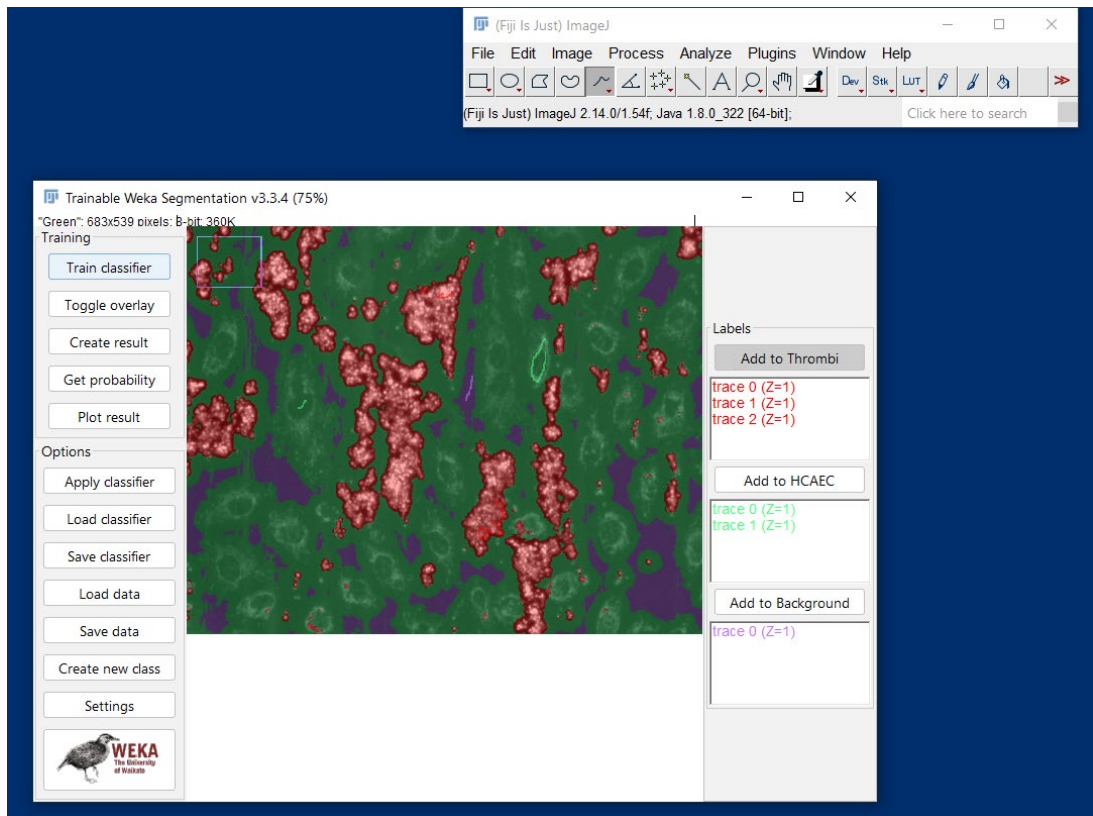


Figure 2.11. Example of Weka trainable segmentation. Using an 8-bit image, the Weka segmentation tool from ImageJ was trained to differentiate the thrombi (red) from the HCAEC (green) and background (purple) using a reference image. The classifier was then saved and applied to the rest of the images of that dataset.

2.19 Quantitative reverse transcription polymerase chain reaction

2.19.1 Treatments, extraction and purification

HCAEC were grown in 12-well plates and serum-starved O/N prior to treatment for 24 h with different inflammatory mediators, including IL-6 (50 ng/mL), LPS (100 ng/mL), TNF- α (10 ng/mL), and H₂O₂ (100 μ M), or PBS control. RNA was extracted and purified using the Norgen BioTek Total RNA Purification Plus Kit (Geneflow, Lichfield, UK). Following the instructions from the manufacturer, the media was removed and, after a PBS wash, 300 μ L of RT Buffer were added to each well. The lysates were stored at -80°C.

During the purification process, lysates were thawed on ice and centrifuged through genomic DNA (gDNA) removal columns at 14,000xg for 1 minute. The flow through was collected and vortexed with 180 μ L of 96-100% ethanol. The mix was centrifuged through RNA retention columns at 3,500xg for 1 minute. Following 3 washing steps using 400 μ L of wash solution A supplemented with ethanol, the columns were dried by spinning at 3,500xg over 2 minutes and reassembled into an elution tube. Pure RNA was collected by adding 50 μ L of elution buffer and centrifuging at 200xg for 2 minutes, followed by 14,000xg for 1 minute. The purified RNA was stored at -80°C.

2.19.2 Reverse transcription

Purified RNA was quantified using a Nanodrop One Spectrophotometer (Thermo Fisher Scientific) and diluted with Invitrogen ultrapure DNase/RNase-free water (Thermo Fisher Scientific). Complementary DNA (cDNA) was obtained using the Qiagen QuantiTect Reverse Transcription Kit (Qiagen, Manchester, UK). First, a DNA removal step was performed by mixing 12 μ L of a 200 ng RNA solution with 2 μ L of gDNA wipeout buffer and incubating at 42°C for 2 minutes on the Blue Ray Thermal Cycler (Scientific Laboratory Supplies). The reverse transcriptase, primer mix and buffer provided in the kit were added to the RNA solution following the instructions in the protocol sheet. RNA was then reverse transcribed to

complementary DNA (cDNA) using the Blue Ray Thermal Cycler. Samples were incubated at 25°C for 3 minutes for primer annealing, followed by 45°C for 10 minutes to allow DNA polymerisation and 85°C for 5 minutes to inactivate the reverse transcriptase. The cDNA (10 ng/μL) was then stored at -20°C.

2.19.3 Real-time quantitative Polymerase Chain Reaction (RT-qPCR)

The Qiagen QuantiTect SYBR Green PCR Kit was used to perform PCR experiments. In a 96-well PCR plate (Scientific Laboratory Supplies), 1 μL of cDNA (10 ng/mL), 5 μL SYBR green, 1 μL of forward primer (200 μM), 1 μL of reverse primer (200 μM) and 2 μL of DNase/RNase-free water per reaction were mixed. Primers used for qPCR reactions are detailed in Table 2.5. The plate was centrifuged and placed in a CFX Connect Real-Time PCR Thermocycler (Bio-Rad). Samples were incubated at 95°C for 5 minutes, before the initiation of 40 cycles consisting of 20 seconds at 95°C, 20 seconds at 62°C and 25 seconds at 72°C. Following successful amplification of the gene of interest, cycle threshold (Ct) values were normalised to the housekeeper genes (GAPDH and RPLPO) and analysed using the delta-delta Ct (Livak and Schmittgen, 2001) method, in which the Ct values for the housekeeper technical replicates were averaged before calculation of the geometric mean of both housekeepers. The Ct values of the technical replicates for the gene of interest were then averaged and delta Ct (ΔCt) was calculated using the following equation:

$$\Delta Ct = Ct (\text{gene of interest}) - Ct (\text{housekeeping gene})$$

The delta-delta Ct value (ΔΔCt) was obtained by subtracting the vehicle ΔCt value from the treated ΔCt value:

$$\Delta\Delta Ct = \Delta Ct (\text{treated sample}) - \Delta Ct (\text{vehicle sample})$$

Finally, the mRNA fold expression was calculated using $2^{-\Delta\Delta Ct}$.

2.19.4 Primer design and sequences

Genes were searched on the Ensembl genome browser 112. As the objective of the project was to measure the effect of SIRT1 activation in the general regulation of gene expression, rather than one specific transcript, two exons common to all

protein-coding transcripts were selected. The sequence of the RefSeq transcript was browsed on NCBI nucleotide and primers for that sequence were designed using Primer-BLAST. The range of the primers must include a minimum of 2 exons. Regarding the primer parameters, the PCR product size was between 90 and 250 base pairs (bp). The primer melting temperatures (T_m) were minimum 62°C, optimal 65°C and maximum 68°C. The primer pair had to be separated by at least one intron on the corresponding genomic DNA and the intron length range was between 100 and 10,000 bp. Specificity checking of the primer pairs was performed using the human (9606) RefSeq mRNA database. Primers had at least 4 total mismatches to unintended targets, including at least 3 mismatches within the last 5 bps at the 3' end. Targets with 6 or more mismatches to the primer were ignored. Two primer pairs were selected based on the T_m (difference between forward and reverse lower than 5°C) and the GC content (35–80%). Dry primers were ordered to Sigma-Aldrich in a tube format and reconstituted in Tris-EDTA (TE) buffer upon arrival at 200 μ M.

Table 2.5. Primers used for RT-qPCR. F = forward, R = reverse.

Protein	Gene	Primer direction	Primer sequence
DDAH1		F	ACGAGGTGCTGAAATCTTGGCT
		R	ATTGCGATCAGGTTAGGCCAG
CD39	ENTPD1	F	ACACATCCATGTGCCATCACA
		R	GGTGCCTTCCTCTGGATGCACT
GAPDH		F	CGGATTTGGTCGTATTGGGCG
		R	GTCTTCACCACCATGGAGAAGGC
eNOS	NOS3	F	TCGGCCGGAACAGCACAAGA
		R	AAAGGCGCAGAAGTGGGGGT
COX1	PTGS1	F	ACGCACAGGAGCCTGCACTC
		R	GGTCAAGGCCGAAGCGGACA
COX2	PTGS2	F	CTGGGCCATGGGGTGGACTT
		R	CCTGCCCCACAGCAAACCGT
SIRT1		F	AATTGTTCGAGGATCTGTGCCA
		R	GGACTCCAAGGCCACGGATAG
RPLPO		F	GCAGCAGATCCGCATGTCCC
		R	TCCCCGGATATGAGGCAG
THBD		F	CAACACACAGGGTGGCTTCG
		R	GGCTGGACAGGCAGTCTGGT
VCAM-1		F	GAACCCAAACAAAGGCAGAGTACG
		R	TGCTTCTTCCAGCCTGGTTAATTC
VWF		F	TCATCCACGGCCCGATGCAG
		R	TGGTCCCCCTGTGTCACGGT

2.19.5 Primer efficiencies

A standard curve was generated by diluting HCAEC cDNA in ultrapure DNase/RNase-free water (Thermo Fisher Scientific) 1:2 (0.625, 1.25, 2.5, 5 and 10 ng/ μ L) or 1:10 (0.001, 0.01, 0.1, 1 and 10 ng/ μ L) depending on the level of expression of the gene of interest. A qPCR reaction using the concentrations of the standard curve was performed as described in section 2.19.3. To obtain the primer efficiencies using Microsoft Excel, the Ct values from the repeats were averaged and the common logarithm (log) of the concentrations of cDNA used in ng/ μ L were calculated. A regression line was represented using the log (x) and the average Ct (y) values and the slope of the line was obtained. Primer efficiencies were calculated using the following equation:

$$\text{Efficiency (\%)} = \left(\frac{-1}{10^{\text{slope}} - 1} \right) \times 100$$

Only primers with efficiencies between 90-110% were used in experiments (Rodríguez et al., 2015). The efficiencies for each primer used in this project can be consulted in the Appendix.

2.20 Statistical Analysis

All experiments were performed using a minimum of three different blood donors or HCAEC batches. Statistical analysis was performed using Microsoft Excel and GraphPad Prism 10 (GraphPad, California, USA). Normal distribution of data was confirmed using a Shapiro-Wilk test and, therefore, parametric tests were used throughout. Depending on the number of data sets, the statistical significance of the differences was analysed by paired t-test, One-way analysis of variances (One-way ANOVA) or Two-way ANOVA followed by Tukey correction. In the case of data that do not follow a normal distribution or when comparing percentages or arbitrary units, the appropriate non-parametric tests were used. Numerical data was presented as mean \pm standard error of the mean (SEM). $P \leq 0.05$ was considered statistically significant. Where normalised data was shown, statistics were always performed before normalisation.

Chapter 3. SIRT1 activation reduces platelet reactivity and thrombus formation *in vitro*

3.1 Introduction

Antiplatelet therapy is crucial for treating and preventing cardiovascular events. Aspirin and clopidogrel are currently the most prescribed antiplatelet drugs (Harper, 2019). However, patients offer varied responses to these treatments. Some individuals have an increased risk of severe bleeding events (Hankey and Eikelboom, 2006; Wallentin et al., 2009), while 25% and 15.40% of patients are estimated to be resistant to aspirin and clopidogrel, respectively (Mega and Simon, 2015). Therefore, the development of more effective and safer antiplatelet drugs is still an unmet clinical need.

Because platelets do not have a nucleus, the study of proteomics and post-translational modifications (PTMs) has been crucial to understanding how platelet signalling pathways work (Burkhart et al., 2014). As mentioned in Chapter 1, acetylation of lysine residues is an abundant and reversible PTM that plays a key role in the complex signal transduction mechanisms that regulate numerous protein functions in both resting and activated platelets (Kouzarides, 2000; Spange et al., 2009). As the complete platelet acetylome has already been described, specific pharmacological modulation of platelet acetylases and deacetylases might be useful to elucidate the role of protein acetylation in platelet function and develop novel antithrombotic treatments (Aslan et al., 2015). An example of the importance of investigating compounds that target acetylation to regulate platelet activation is the inhibition of cyclooxygenase-1 (COX-1) by Aspirin through covalent acetylation of S530, which results in a steric blockade of the active site of this enzyme (Ornelas et al., 2017). By irreversibly inhibiting COX-1, Aspirin prevents Thromboxane A₂ production in platelets, which is one of the key mediators in the expansion of platelet response and aggregation (Scridon, 2022). Although aspirin-induced acetylation is not mediated by an enzyme, it illustrates the possibility of using the modulation of protein acetylation levels in platelets as a novel antiplatelet strategy (Vane and Botting, 2003; Latorre and Moscardó, 2016).

Platelet acetylation and deacetylation cycles are regulated by KATs and KDACs, which are explained in detail in Chapter 1. Previous studies have demonstrated that the KAT p300 (Aslan et al., 2015) and different KDACs, such as HDAC6 (K. Sadoul et al., 2012) and SIRT2 (Moscardó et al., 2015), are involved in the regulation of platelet function. SIRT1 is a member of the KDAC family, along with the other SIRTs and HDACs (Van Dyke, 2014). It has been shown that SIRT1 plasma and metabolic tissue levels are reduced in individuals at a high risk of myocardial infarction or ischaemic stroke, such as type II diabetes mellitus (T2DM) patients (Bartoli-Leonard et al., 2021) and patients suffering from obesity (Pardo and Boriek, 2020), who usually are poor responders to antiplatelet therapy (Paven et al., 2020; Puccini et al., 2023).

Studies in mice have demonstrated that pharmacological and genetic inhibition of SIRT1 accelerated thrombus formation *in vivo* in a photochemical injury model (Breitenstein et al., 2011). Moreover, SIRT1-specific inhibition with EX 527 induced platelet apoptosis (Kumari et al., 2015), which indicates that SIRT1 downregulation or pharmacological inhibition not only increases thrombotic risk but also has a detrimental effect on platelet health.

To date, the role of SIRT1 in human platelet aggregation has not been investigated using selective SIRT1 agonists. In 2016, Kim et al. demonstrated that platelets treated with resveratrol, which is a non-specific SIRT1 activator (Kulkarni and Cantó, 2015), had a decreased response to arachidonic acid (Y. H. Kim et al., 2016). However, Resveratrol can activate many other protein targets that play a key role in platelet function, such as AMP-activated protein kinase (AMPK) (Randriamboavonjy et al., 2010) or oestrogen receptors (Kobylka et al., 2022). Therefore, it is uncertain whether the decrease in platelet aggregation observed with resveratrol is SIRT1-mediated. Evaluating the effect of specific SIRT1 agonists on human platelet function is required to determine whether SIRT1 activation directly reduces platelet activation and aggregation, and therefore whether pharmacological activators of SIRT1 may offer a novel therapeutic approach to antiplatelet treatment.

3.2 Hypothesis, chapter aim and objectives

The aim of this chapter was to investigate whether activation of SIRT1, using the selective agonist SRT1720, negatively regulates platelet function and may therefore represent a novel antiplatelet approach in the prevention of myocardial infarction and ischaemic stroke.

Considering previous investigations, we hypothesise that SIRT1 activation negatively regulates platelet function. To test this hypothesis, the following objectives were addressed:

1. Demonstrate that SIRT1 is present in human platelets.
2. Determine whether SIRT1 activation alters platelet aggregation mediated by different platelet agonists.
3. Assess whether SIRT1 activation alters “inside-out” signalling through the investigation of the effect of SRT1720 on integrin $\alpha\text{IIb}\beta\text{3}$ activation.
4. Investigate the effect of SRT1720 activation on degranulation during platelet stimulation.
5. Determine the effect of SIRT1 activation on platelet thrombus formation and stability under arterial flow conditions.

3.3 Results

3.3.1 All SIRT proteins are present in human platelets

Although this study is focused on SIRT1, investigating the presence of all sirtuins (SIRT1-7) in human platelets provides an insight into the relevance of this protein family in platelet function. Therefore, the expression of all SIRTs was examined in human-washed platelets from three different donors (D1-D3) by Western Blotting.

SIRT1 was found as a doublet at 82 and 130 kDa, which correspond to SIRT1 and O-glycosylated SIRT1 (O-GlcNAc-SIRT1), respectively (Han et al., 2017) (Figure 3.1A). Both isoforms 1 (43 kDa) and 2 (39 kDa) of SIRT2 were present in human platelets (Uniprot, 2022) (Figure 3.1B). SIRT3 (Figure 3.1C), SIRT4 (Figure 3.1D), SIRT5 (Figure 3.1E), SIRT6 (Figure 3.1F) and SIRT7 (Figure 3.1G) were also identified in human-washed platelet lysates.

The existence of all the proteins of the SIRT family in platelets indicates that these enzymes may have a role in platelet signalling and, therefore, the regulation of platelet function.

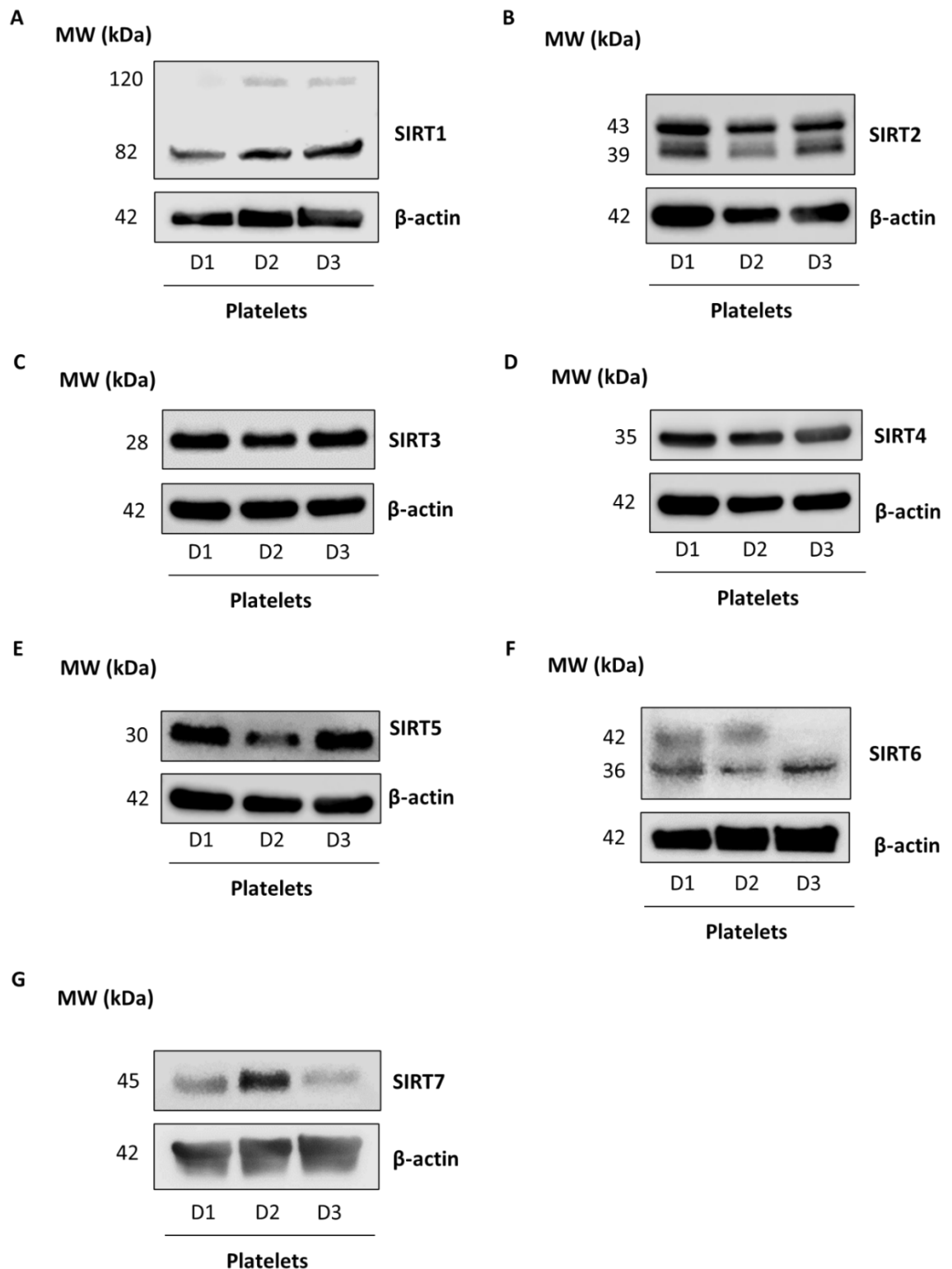


Figure 3.1. All proteins from the SIRT family were detected in human platelets by Western Blotting. Washed platelet lysates from 3 different donors (D1-D3) were immunoblotted with antibodies against SIRT1-7. Protein detection was performed using an HRP-labelled antibody and chemiluminescence. In the case of SIRT1, two bands were observed: one at 82 kDa and the other at 120 kDa, corresponding to SIRT1 and O-GlcNAc-SIRT1, respectively (A). The presence of SIRT2 isoform 1 (43 kDa) and isoform 2 (39 kDa) (B), SIRT3 (C), SIRT4 (D), SIRT5 (E), SIRT6 (F) and SIRT7 (G) were also confirmed in human platelets. MW=molecular weight.

3.3.2 SIRT1 activation reduces platelet aggregation

To investigate the role of SIRT1 in the regulation of platelet aggregation, the effect of the specific SIRT1 activator SRT1720 was tested by PBA. PRP was incubated for 10 or 60 minutes with increasing concentrations of SRT1720 (0.01, 0.03, 0.1, 0.3, 1, 3 and 10 μ M) or vehicle (0.1% DMSO). Platelet aggregation was induced with a range of concentrations of TRAP-6 (0.1, 0.3, 1, 3 and 10 μ M) (Figure 3.2), collagen (0.1, 0.3, 1, 3 and 10 μ g/mL) (Figure 3.3), and ADP (0.1, 0.3, 1, 3 and 10 μ M) (Figure 3.4).

Pre-incubation with SRT1720 at 10 μ M attenuated platelet aggregation in response to all agonists but with different kinetics. The percentage of aggregation in the SRT1720-treated samples was compared to vehicle control at the concentrations of the platelet agonists in the slope of the dose-response curve. In the case of TRAP-6-mediated platelet aggregation, attenuation is only observed when using TRAP-6 at 3 μ M and after 10 minutes, as it is offset after 60 minutes (Figure 3.2). On the contrary, differences in collagen (0.3 μ M) (Figure 3.3) and ADP (1 μ M) (Figure 3.4) induced aggregation were observed after a 60-minute treatment with SRT1720, but not after 10 minutes. These findings suggest that SIRT1 has a protective role in platelet aggregation and allowed us to select 10 μ M as the working concentration of SRT1720 to perform experiments in platelets.

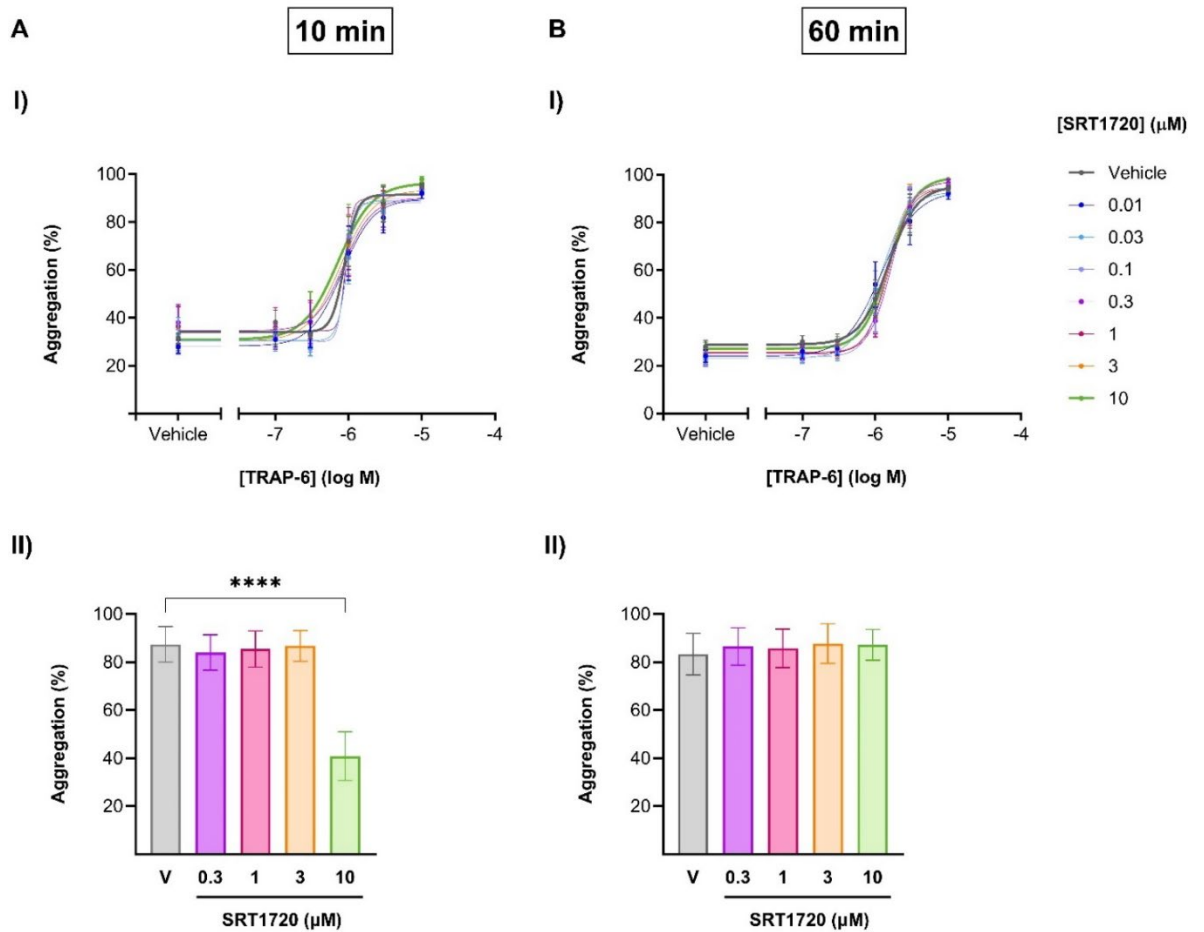


Figure 3.2. SIRT1 activation reduces platelet aggregation in response to TRAP-6. PRP was incubated with different concentrations of SRT1720 (0.01 - 10 μM) or vehicle (V, 0.1% DMSO) for 10 (A) and 60 (B) minutes. Then, platelet aggregation was induced with TRAP-6 (0.1 - 10 μM). Absorbance was measured at 450 nm and the aggregation percentage was calculated. Dose-response curves were constructed (I) and aggregation stimulated by 3 μM TRAP-6 was compared (II) using One-Way ANOVA. Data represent mean \pm SEM. **** $p < 0.0001$. N=6.

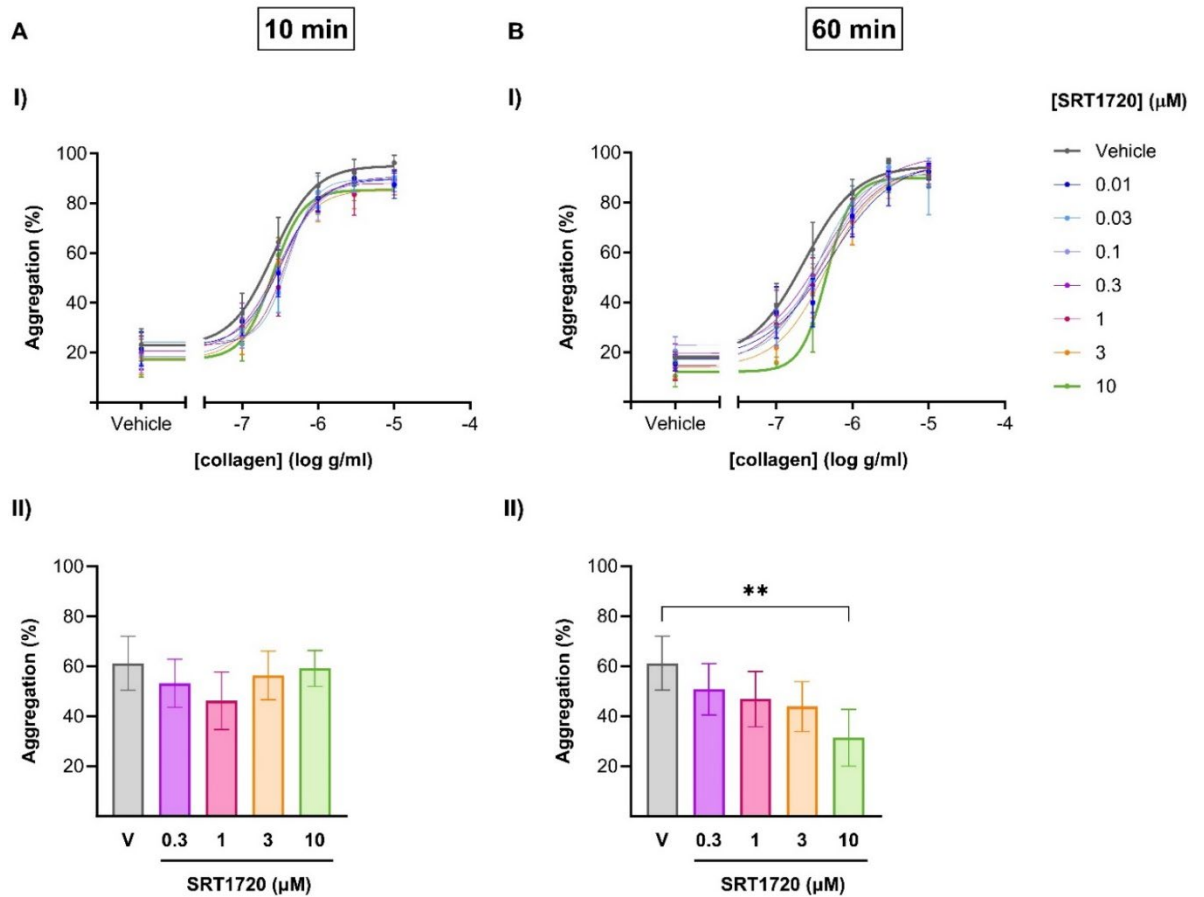


Figure 3.3. SIRT1 activation reduces platelet aggregation in response to collagen. PRP was incubated with different concentrations of SRT1720 (0.01 - 10 μM) or vehicle (V, 0.1% DMSO) for 10 (A) and 60 (B) minutes. Then, platelet aggregation was induced with collagen (0.1 - 10 $\mu\text{g/mL}$). Absorbance was measured at 450 nm and the aggregation percentage was calculated. Dose-response curves were constructed (I) and aggregation stimulated by 0.3 $\mu\text{g/mL}$ of collagen was compared (II) using One-Way ANOVA. Data represent mean \pm SEM. ** $p < 0.01$. N=6.

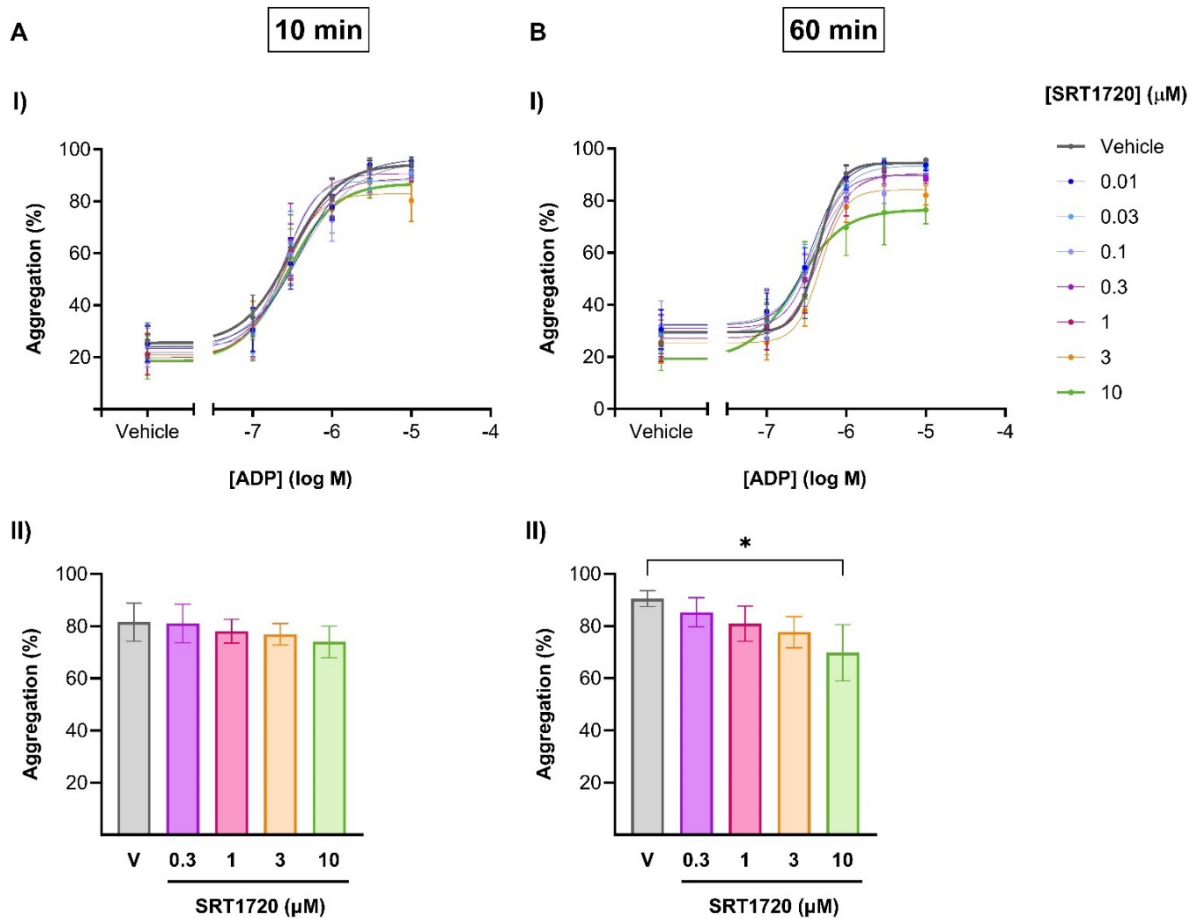


Figure 3.4. SIRT1 activation reduces ADP-induced platelet aggregation. PRP was incubated with different concentrations of SRT1720 (0.01 - 10 μM) or vehicle (V, 0.1% DMSO) for 10 (A) and 60 min (B). Then, platelet aggregation was induced with ADP (0.1 - 10 μM). Absorbance was measured at 450 nm and the aggregation percentage was calculated. Dose-response curves were constructed (I) and aggregation stimulated by 1 μM ADP was compared (II) using One-Way ANOVA. Data represent mean ± SEM. * $p < 0.05$. N=6.

3.3.3 SRT1720 reduces integrin α IIb β 3 activation

Platelet aggregation is dependent on the binding of the integrin α IIb β 3 to its functionally bivalent ligands fibrinogen and von Willebrand factor, which allows interaction between activated platelets, leading to aggregation (Golebiewska and Poole, 2015). As SIRT1 activation attenuated platelet aggregation to multiple platelet agonists, the effect of SRT1720 in integrin activation was tested using flow cytometry.

PRP was treated with SRT1720 (10 μ M) in the presence of FITC-labelled anti-fibrinogen (Fg) or FITC-labelled PAC-1 antibody, which recognises the open conformation of integrin α IIb β 3, for 10 min at 37°C. Then, platelets were activated using increasing concentrations of CRP-XL (0.1, 0.5 and 1 μ g/mL) or TRAP-6 (1, 5, 10 μ M). Samples were incubated in the dark for 20 min and the percentage of positive platelets and MFI were measured using flow cytometry.

SIRT1 activation significantly decreased the percentage of platelets that bound fibrinogen in response to CRP-XL at 0.1 and 0.5 μ g/mL (Figure 3.5A) and TRAP-6 at 5 and 10 μ M (Figure 3.5B). Moreover, SRT1720 reduced the amount of fibrinogen bound per platelet, which was represented by a decrease in MFI in response to all concentrations of CRP-XL (Figure 3.5C) and the highest concentrations of TRAP-6 tested (5 and 10 μ M) (Figure 3.5D), indicating that SRT1720 reduces α IIb β 3 activation and the ability of the integrin to bind its ligand fibrinogen.

In support of the findings with fibrinogen, SIRT1 activation also inhibited PAC-1 binding to platelets, reducing approximately by half both the percentage of positive events (Figure 3.6B) when platelets were stimulated with TRAP-6 (5 and 10 μ M), and the MFI (Figure 3.6D) when platelets were activated with TRAP-6 (10 μ M). A decrease in the number of platelets bound to FITC anti-PAC-1 was observed in response to CRP-XL too, which is represented by a significant reduction in the percentage of positive platelets with CRP-XL (0.1 μ M) (Figure 3.6A) but not in the MFI (Figure 3.6C), indicating that SIRT1 activation reduced the number of platelets that present active α IIb β 3 molecules on its surface, while the median amount of active α IIb β 3 molecules per platelet does not vary.

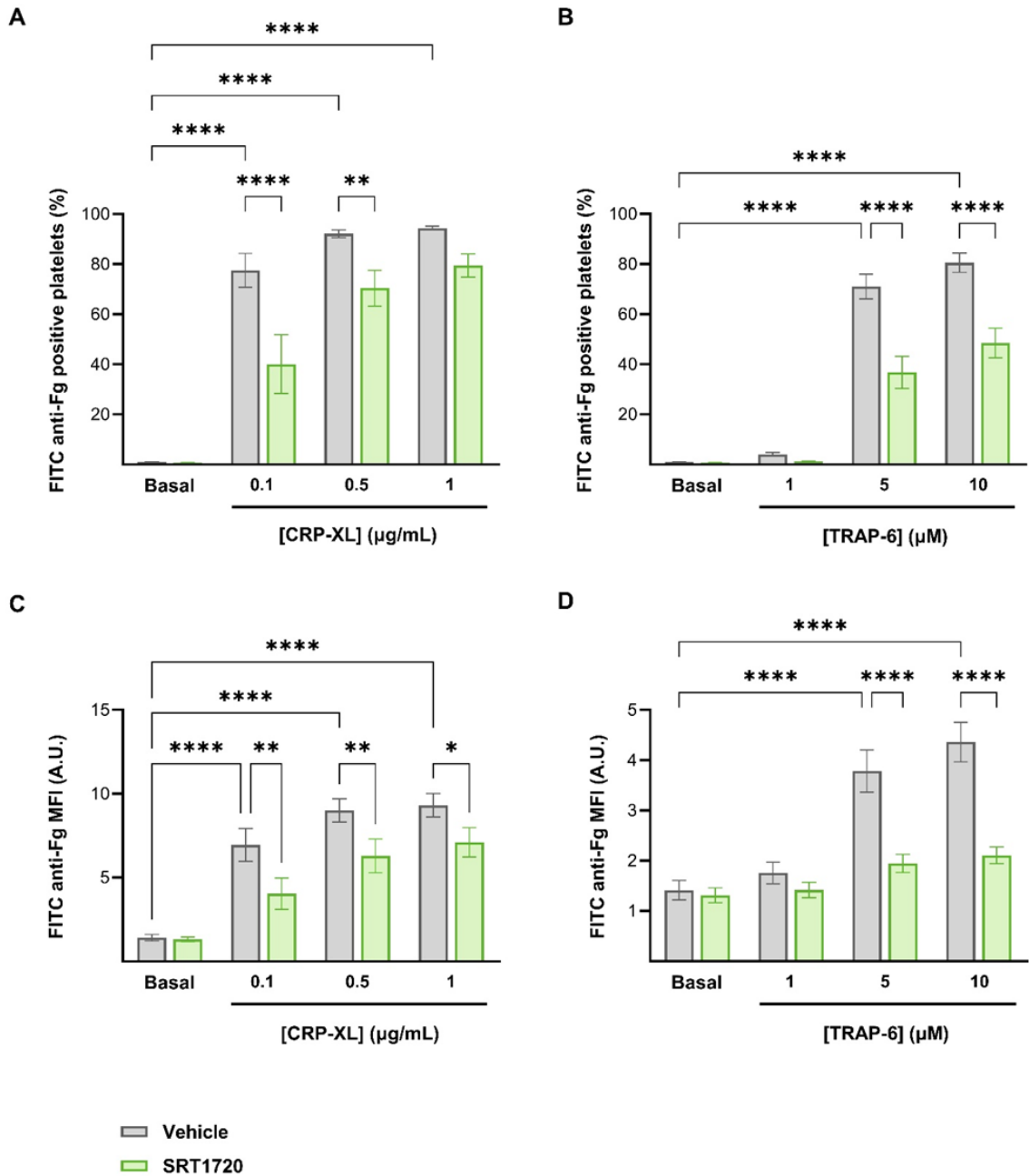


Figure 3.5. SRT1720 inhibits fibrinogen binding to platelets. PRP was incubated with SRT1720 (10 µM) or vehicle (0.1% DMSO) for 10 min at 37°C and platelet activation induced with different concentrations of CRP-XL (A, C) and TRAP-6 (B, D) for 20 min at RT in the presence of FITC anti-fibrinogen. Fibrinogen binding was quantified using flow cytometry. Data is represented as the percentage of FITC anti-fibrinogen positive platelets (A, B) and MFI (C, D). The platelet gate was established based on size and CD42 positive staining. Data was analysed using the FlowLogic software and compared using the Friedman test. Data represent mean ± SEM. *p<0.05, **p<0.01, ****p<0.0001 N=6. Fg = fibrinogen.

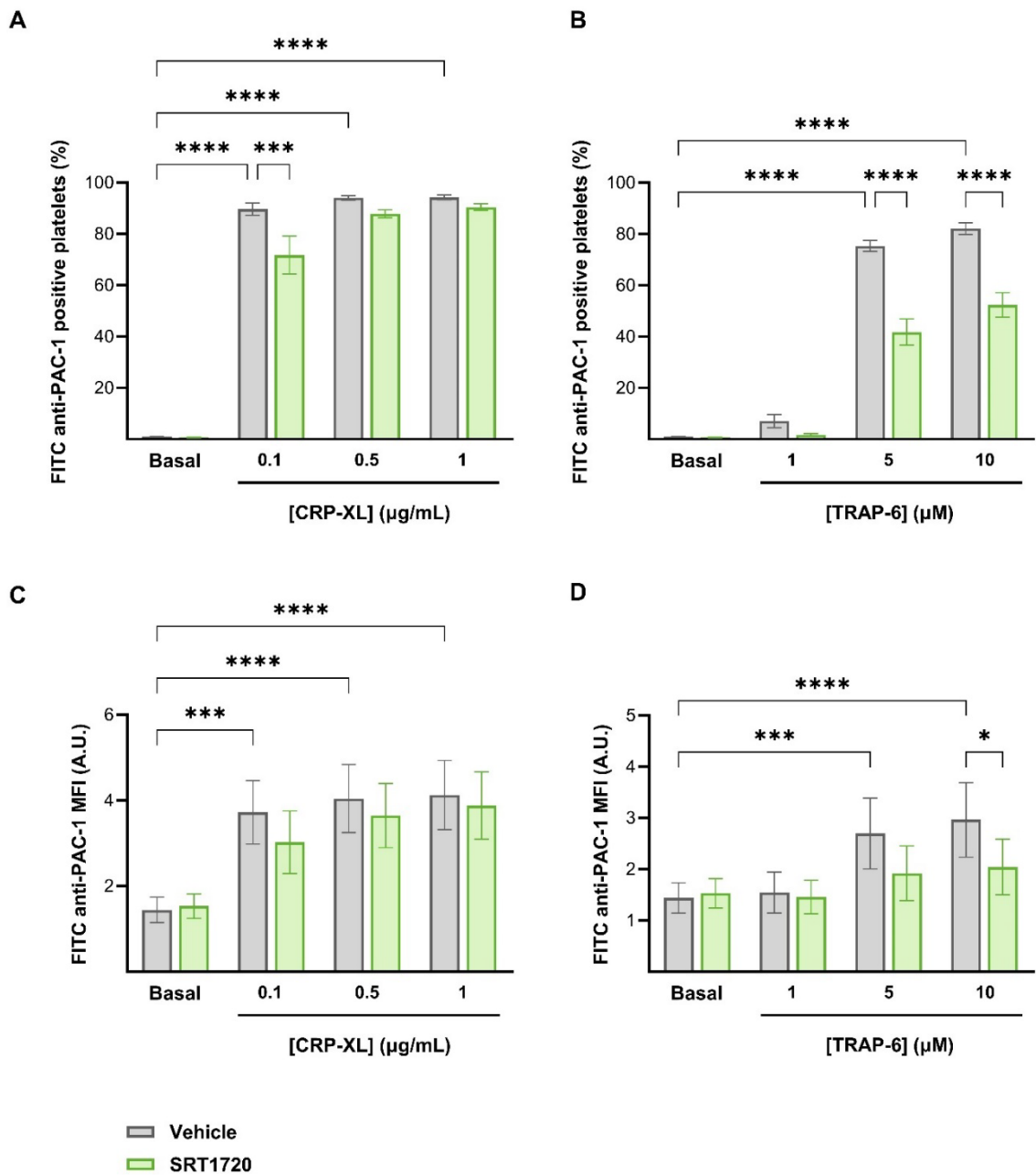


Figure 3.6. SRT1720 inhibits platelet integrin $\alpha 2\text{b}\beta 3$ activation. PRP was incubated with SRT1720 (10 μM) or vehicle (0.1% DMSO) for 10 min at 37°C and platelet activation was induced with different concentrations of CRP-XL (A, C) and TRAP-6 (B, D) for 20 min at RT in the presence of FITC anti-PAC-1. PAC-1 binding to the active conformation of the integrin $\alpha\text{IIb}\beta 3$ was quantified using flow cytometry. Data is represented as the percentage of FITC anti-PAC-1 positive platelets (A, B) and MFI (C, D). The platelet gate was established based on size and CD42 positive staining. Data was analysed using the FlowLogic software and using the Friedman test. Data represent mean \pm SEM. * $p < 0.05$, *** $p < 0.001$, **** $p < 0.0001$. N=6.

3.3.4 SRT1720 reduces dense granule release but does not affect α -granule secretion

Platelet stimulation leads to the release of both α and dense granules from platelets, which contributes to the activation of integrin $\alpha\text{IIb}\beta\text{3}$ (Golebiewska and Poole, 2015). Alpha granules also represent an important internal pool of integrin $\alpha\text{IIb}\beta\text{3}$, which gets translocated to the surface upon secretion (Janus-Bell and Mangin, 2023). Due to the decrease observed in fibrinogen and PAC-1 binding with SRT1720, the effect of SIRT1 activation in platelet granule release was evaluated.

SRT1720 (10 μM) or vehicle (0.1% DMSO) were added to PRP and incubated for 10 minutes at 37°C. Platelets were activated with different concentrations of CRP-XL (0.1, 0.5 and 1 $\mu\text{g}/\text{mL}$) or TRAP-6 (1, 5, 10 μM) in the presence of PE anti-CD63 and PE-Cy5 anti-CD62P to measure dense and alpha granule secretion, respectively. After 20 minutes of antibody incubation, the percentage of positive events and MFI were obtained using flow cytometry.

SRT1720 did not affect the number of dense granules released per platelet, which is represented by no changes in MFI, independently of the platelet agonist used (Figure 3.7C and Figure 3.7D). SIRT1 activation decreased the percentage of platelets that release dense granules when these are stimulated with CRP-XL 0.1 and 0.5 $\mu\text{g}/\text{mL}$ (Figure 3.7A), but no effects were observed with higher concentrations of CRP-XL (A) or TRAP-6 (Figure 3.7B).

In contrast to the observations made with dense granule secretion, no significant changes in the percentage of platelets exposing surface CD62P (percentage of positive events) (Figure 3.8A and Figure 3.8B), or average CD62P surface levels, represented by the MFI (Figure 3.8C and Figure 3.8D), were observed in PRP treated with SRT1720 versus vehicle control.

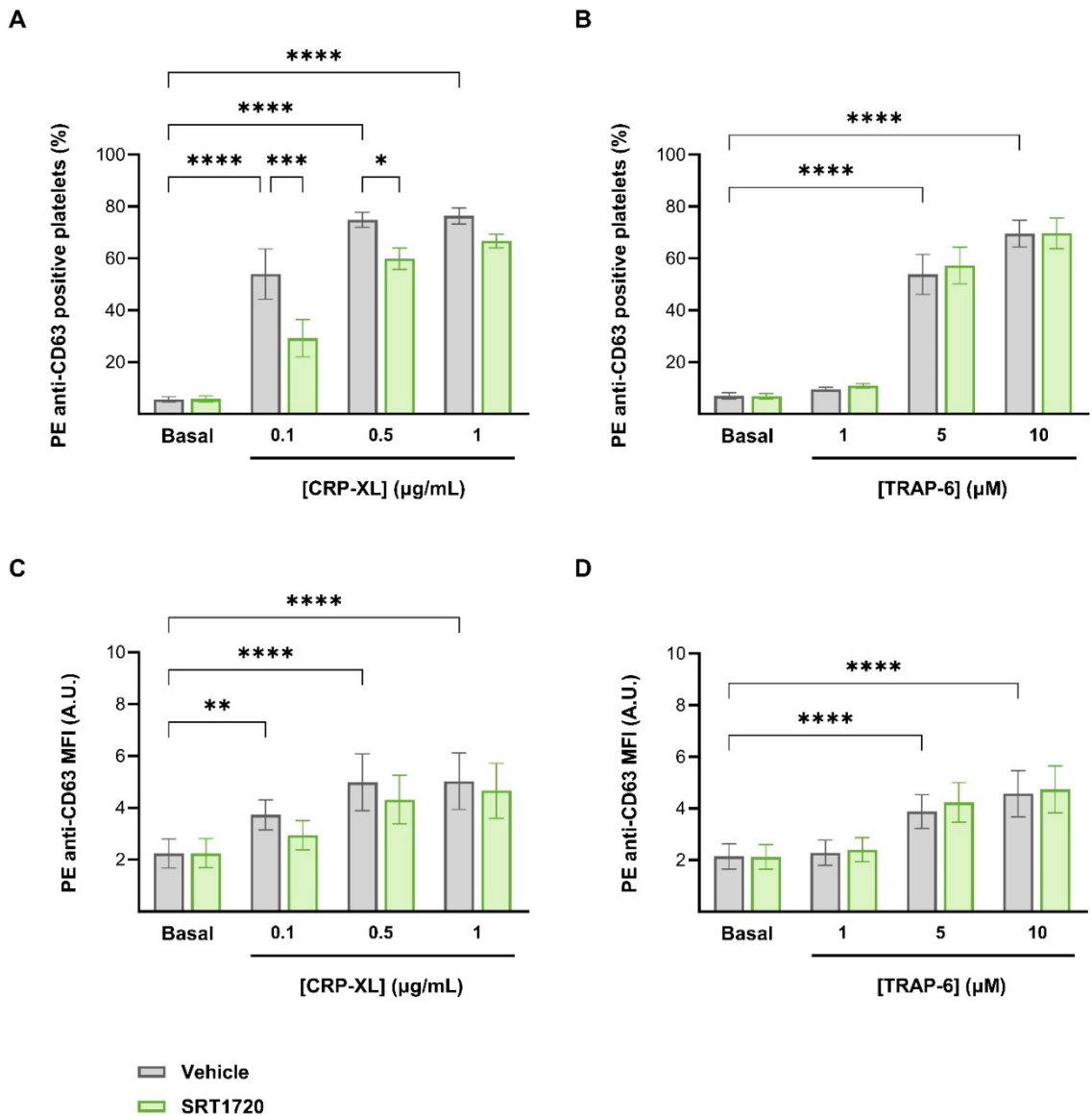


Figure 3.7. SRT1720 reduced the number of platelets that release dense granules in response to CRP-XL. PRP was treated with SRT1720 (10 μM) or vehicle (0.1% DMSO) for 10 min at 37°C prior to platelet stimulation with different concentrations of CRP-XL (A, C) and TRAP-6 (B, D) for 20 min at RT in the presence of a PE-CD63 antibody. Dense granule secretion was determined by measuring CD63 surface levels in platelets using flow cytometry. The platelet gate was established based on size and CD42 positive staining. Data was analysed using the FlowLogic software and compared using the Friedman test. Data presented as mean \pm SEM. * $p < 0.05$, ** $p < 0.01$, *** $p < 0.001$, **** $p < 0.0001$. N=6.

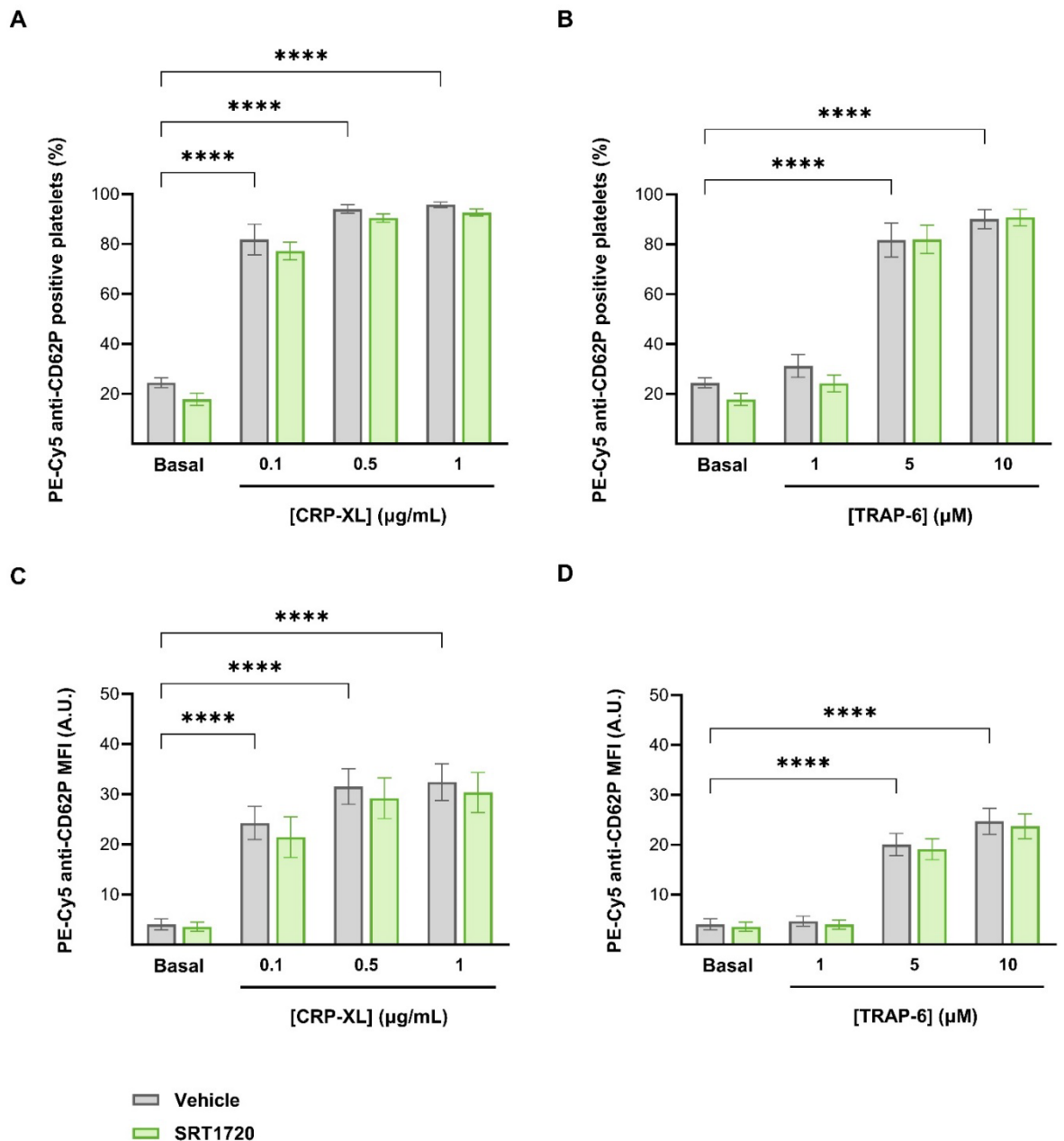


Figure 3.8. P-selectin exposure, a marker for platelet α -granule release, remained unaffected after SIRT1 activation. PRP was treated with SRT1720 (10 μ M) or vehicle (0.1% DMSO) for 10 min at 37°C prior to platelet stimulation with different concentrations of CRP-XL (A, C) and TRAP-6 (B, D) for 20 min at RT in the presence of a PE-Cy5-CD62P antibody. α -granule secretion was determined by measuring CD62P surface levels in platelets using flow cytometry. The platelet gate was established based on size and CD42 positive staining. Data was analysed using the FlowLogic software and compared using the Friedman test. Data is presented as mean \pm SEM. ****p<0.0001. N=7

3.3.5 SIRT1 activation reduces thrombus formation *in vitro*

Previous experiments demonstrated that SRT1720 decreases platelet reactivity through a reduction in collagen-induced aggregation and the inhibition of the integrin $\alpha\text{IIb}\beta\text{3}$. Collagen receptors, such as integrin $\alpha\text{2}\beta\text{1}$ and GPVI, and the fibrinogen receptor integrin $\alpha\text{IIb}\beta\text{3}$ are key for platelet adhesion at the injury site (Durrant et al., 2017). Therefore, investigating the effect of SIRT1 activation on thrombus formation and stability was required. To identify whether SIRT1 activation could have an impact on this process, we used an *in vitro* arterial thrombosis model in which whole blood was incubated with SRT1720 (10 μM) or vehicle for 10, 30 and 60 min. Then, treated blood was flowed over a collagen I-coated Ibidi VI 0.1 $\mu\text{-slide}$ for 8 min at an arterial shear rate and the thrombi number (Figure 3.9A), thrombi size (Figure 3.9B) and percentage of area occupied by the thrombi (Figure 3.9C) were quantified. For analysis of thrombus formation over time, images were also taken every 10 seconds and the area coverage percentage was quantified on ImageJ to assess thrombus stability (Figure 3.9D).

Although the differences observed in thrombi number and size were found to not be statistically significant (Figure 3.9A, Figure 3.9B), SIRT1 pharmacological activation of whole blood with SRT1720 led to a decrease in the thrombi area coverage percentage on collagen after 10 and 30-minutes of pre-incubation (Figure 3.9C). Conversely, after 60 min this effect is offset, observing no significant changes between SRT1720-treated blood and vehicle control (Figure 3.9C). Real-time monitorisation of thrombus formation revealed that, even though thrombi area coverage is decreased after treating blood with SRT1720 for 10 and 30 min, thrombus formation is similar to vehicle over the first half of the assay in the samples preincubated with SRT1720 for 10 min; while in the case of the 30 min SRT1720-treated samples thrombus formation is decreased from the start of the assay (Figure 3.9D). The compensation mechanism through which thrombus formation returns to basal after 60 min with SRT1720 (Figure 3.9A, Figure 3.9B, Figure 3.9C, Figure 3.9D) is still unknown.

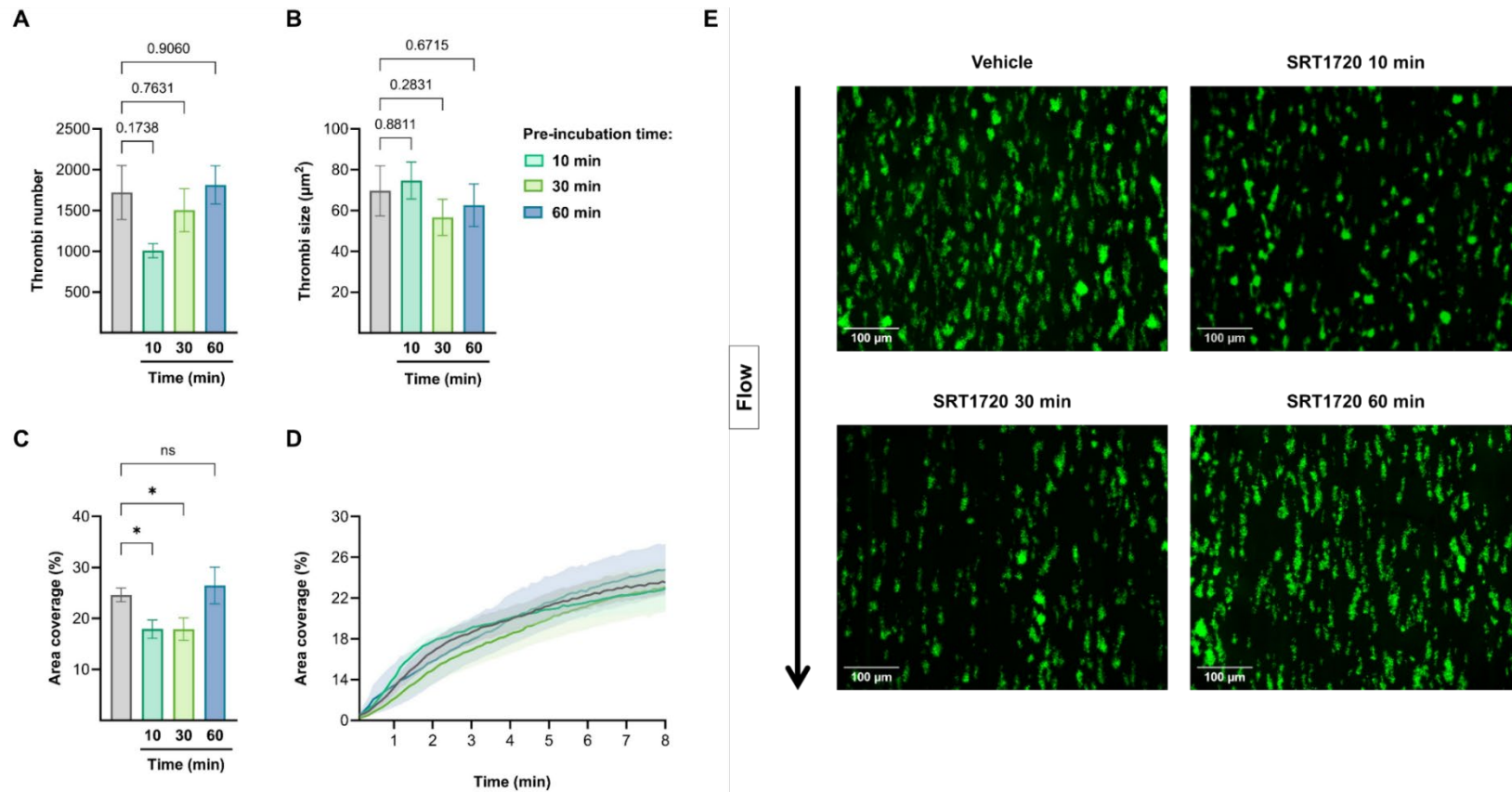


Figure 3.9. SIRT1 activation inhibits thrombus formation on collagen-coated slides after 10 and 30 min of treatment, recovering after 60 min. Whole blood was incubated with SRT1720 (10 µM) or vehicle (0.1% DMSO) for 10, 30 and 60 min, and exposed to collagen at an arterial shear rate (15 dynes/cm²) for 8 min. Images of DIOC-6-labelled platelets were taken every 10 seconds using the CELENA[®] S Logos Biosystems microscope. Area coverage of vehicle and SRT1720-treated samples were quantified using the Image J software at the different time points (D) and the average thrombi size, thrombi number and area coverage were compared at the end of the assay by One-way ANOVA (A, B, C). Data represent mean ± SEM. *p<0.05. Representative images shown (E). N=6 (A, B, C) and N=3 (D).

3.4 Discussion

The aim of the experiments presented in this chapter was to confirm the presence of SIRT1 in human platelets and investigate whether SIRT1 activators had the potential to act as novel antiplatelet agents by reducing platelet activation in response to standard platelet agonists. Results from this study demonstrated that SIRT1 is present in platelets and that its activation with SRT1720 attenuates platelet aggregation. Flow cytometry studies of platelet degranulation revealed that SIRT1 activation has no effect on platelet α -granules release but reduced dense granule secretion in response to the selective GPVI ligand CRP-XL (Smethurst et al., 2007). As aggregation to ADP, collagen and TRAP-6 were all impeded by SIRT1 activation, it suggested a common mechanism was involved. Therefore, the impact of SRT1720 activation on the conformational change of integrin α IIb β 3 was explored. Our findings show that the levels of integrin α IIb β 3 in the high-affinity state are considerably reduced under SIRT1 activation in both CRP-XL and TRAP-6 activated platelets, suggesting that SRT1720 is involved in the regulation of “inside-out” signalling. However, SIRT1 does not appear to be involved in the upregulation of surface expression of integrin α IIb β 3 since alpha granule secretion was not reduced by SIRT1 activation. *In vitro* thrombus formation assays demonstrated that SRT1720 significantly reduced the thrombi area coverage on type I collagen under arterial shear conditions. Although not statistically significant, there was a trend towards reduced thrombi number, rather than reduced thrombus size, indicating that SIRT1 activation affects platelet adhesion rather than thrombus amplification.

To date, seven sirtuins (SIRT1-7) and 23 isoforms have been identified in different human cell types. Our findings show that all SIRTs are present in human platelets, which suggests that this family of deacetylases may have a role in these cells. Deacetylase activity varies between the different isoforms (X. Zhang et al., 2021). As this project is focused on the role of SIRT1 in platelets, only SIRT1 isoforms will be discussed in this section.

Western Blotting analysis of protein expression shows two bands for SIRT1 in platelets: one at 120 kDa and the other in the 80 kDa region. Cleavage of SIRT1 by cathepsin B, which is present in platelets (Burkhart et al., 2012), produces a 75 kDa inactive product (Oppenheimer et al., 2012). However, it cannot correspond to the

smaller size band, as the antibody recognition site is in the fragment that is cleaved and degraded. According to the literature, the 120 kDa-band corresponds to O-glycosylated SIRT1 (O-GlcNAc-SIRT1) (Han et al., 2017), whereas the other band is the isoform 1 of SIRT1 (82 kDa) (Uniprot, 2022). SIRT1 isoform 1 is enzymatically active, but its glycosylation (120 kDa) leads to a three-fold increase in deacetylase activity (Han et al., 2017). Our findings demonstrate the presence of both active forms of SIRT1 in platelets and showed inter-donor variation in the expression of SIRT1 isoform 1 and O-GlcNAc-SIRT1, as donor 1 (D1) had reduced expression of SIRT1 compared to the others and lacked O-GlcNAc-SIRT1. This experiment illustrates the opportunity of targeting SIRT1 with pharmacological modulators in individuals with lower SIRT1 expression to recover basal activity.

Although the subcellular location of SIRT1 has not been described in megakaryocytes or platelets, SIRT1 is predominantly located in the nucleus in other cell types (W. Bai and Zhang, 2016). However, studies in HEK293T (Nasrin et al., 2009) and epithelial cells (Yanagisawa et al., 2018), indicate that this enzyme can shuttle from the nucleus to the cytoplasm and vice versa in response to stimuli, demonstrating the presence of SIRT1 and other nuclear sirtuins in the cytosol.

During thrombopoiesis, platelets are produced from the cytoplasm of megakaryocytes, whereas the nucleus is exuded and phagocytosed (Machlus and Italiano, 2013), raising a question regarding the origin of SIRT1 in platelets. However, the presence of numerous nuclear proteins has been previously demonstrated in platelets (Unsworth et al., 2018). One of the mechanisms through which megakaryocytes can pass nuclear proteins into platelets is shuttling from the nucleus to the cytoplasm before nuclear extrusion (X. Fu et al., 2018). Also, platelets contain translation machinery and different forms of RNA. As a result, platelets can produce proteins despite lacking genomic DNA (Weyrich et al., 2009), which is another explanation for the presence of nuclear proteins, including SIRT1, in platelets.

Once the presence of SIRT1 was confirmed, platelet aggregation experiments were performed to elucidate the effect of SIRT1 activation on this process. Treatment of platelets with SRT1720 caused a decrease in the percentage aggregation after stimulation with subthreshold concentrations of collagen, TRAP-6 and ADP. In the

case of collagen and ADP-activated platelets, a dose-dependent response to SRT1720 can be observed after 60 minutes of incubation; while treatment with SRT1720 10 μ M for 10 minutes induced a sharp reduction of platelet aggregation in response to TRAP-6, which was compensated after 60 minutes. A potential explanation for this phenomenon could be that SRT1720 might reduce platelet aggregation via different pathways when the activation is triggered by collagen or ADP versus TRAP-6. However, these differences could also be attributed to the activation of KATs via PAR-1, which counteracts SRT1720 deacetylation.

The decrease observed in the dose-response curve performed with ADP should be interpreted with caution, as a decrease in platelet aggregation was only observed when using SRT1720 at 10 μ M. Ideally, another dose-response curve using higher concentrations of SRT1720 should have been performed and will be considered as future work.

Although this is the first study to investigate the effect of SIRT1-specific activation in platelets, previous reports have explored the impact of non-selective SIRT1 activators, such as resveratrol (Kulkarni and Cantó, 2015), in platelet function. A study from Marumo et al. (2020) revealed that resveratrol at 12.5 μ M decreases platelet aggregation in response to thrombin, which correlates with the decrease observed with SRT1720 in response to the PAR-1 agonist TRAP-6 (Gremmel et al., 2010; Marumo et al., 2020). Also in line with our findings, Jang et al. demonstrated that 1 μ M resveratrol reduces collagen-induced platelet stimulation by 50% through a decrease in ROS production that prevents SHP-2 oxidative inactivation, impairing the signalling downstream GPVI (Jang et al., 2015). Moreover, similar to the results obtained in our platelet aggregation assays, Stef et al. (2006) evaluated the effect of resveratrol at 10 μ M on platelet aggregatory response in aspirin-resistant patients and concluded that this drug produced a slight decrease in ADP-induced aggregation, while collagen mediated aggregation was considerably reduced (Stef et al., 2006). Although the alignment of the effects of resveratrol in platelet aggregation reported in the literature with the outcomes of our study is encouraging, this must be interpreted with caution, as resveratrol targets other proteins, such as AMPK (Kulkarni and Cantó, 2015). However, Randriamboavonjy et al. (2010) reported that it is AMPK inhibition which reduces platelet aggregation in response to thrombin

(Randriamboavonjy et al., 2010), while resveratrol activates AMPK. Furthermore, research by Lan et al. (2017) demonstrated that resveratrol activation of AMPK only happens when using high concentrations of resveratrol (50-100 μ M) and is dependent on the presence of functional LKB1, which might explain the variability in the results between different cell types (Lan et al., 2017). As there is no evidence that the predominantly nuclear protein LKB1 (Sebbagh et al., 2011) is present in platelets (Burkhart et al., 2012), the concentrations of resveratrol used in the studies mentioned are below 50 μ M and considering that it was AMPK inhibition and not activation which provided protection against platelet aggregation, it is probable that resveratrol exerted its effects on platelet aggregation via SIRT1 activation, rather than AMPK.

Recent studies have demonstrated that KAT and KDAC enzymes, which maintain acetylation homeostasis, are important regulators of platelet aggregation (Latorre and Moscardó, 2016). Both increasing protein acetylation by inhibiting the HDAC (Bishton et al., 2013) family and decreasing acetylation via inhibition of p300 (Aslan et al., 2015) leads to impaired GPVI aggregatory response, which highlights the importance of maintaining a balance in platelet acetylation levels. As SIRT1 is reduced in many pathologies related to cardiovascular diseases, such as obesity (Pardo and Boriek, 2020) or type II diabetes (Bartoli-Leonard et al., 2021), administering a SIRT1 activator to these patients would replace the natural protection offered by this enzyme via restoring basal acetylation levels.

In contrast to our results with the SIRT1 activator, a study by Moscardó et al. indicated that SIRT2 inhibition leads to a decrease in platelet aggregation in response to collagen, thrombin and U46619, while no significant changes were observed when inhibiting SIRT1. The effects of SIRT1 inhibition were associated with acetylation of Akt, which prevented its phosphorylation (Moscardó et al., 2015). However, research by Liu et al. (2023) revealed that thrombin-induced platelet aggregation was increased in platelets from SIRT6 KO mice and that treatment with a selective SIRT6 agonist decreases aggregation by 50% in WT mouse platelets, which indicates that SIRT6 negatively regulates platelet function (Y. Liu et al., 2023). These studies have demonstrated that the different SIRT isoforms have distinct roles in platelet function, with SIRT2 appearing to positively regulate platelet activation while SIRT6, like SIRT1,

reduce platelet reactivity. Therefore, further investigation of the mechanism behind the individual effects of the seven SIRT isoforms is required.

To determine whether SRT1720 was affecting platelet activation and have a better understanding of the signalling pathways involved, flow cytometry experiments to assess surface levels of a series of platelet activation markers were performed.

Overall, our findings demonstrate that treatment with SRT1720 reduces integrin $\alpha\text{IIb}\beta\text{3}$ activation, as both PAC-1 and fibrinogen binding were reduced. The fact that the percentage of positive platelets and MFI are decreased by SRT1720 indicates that SIRT1 activation increases the threshold for platelet activation via integrin $\alpha\text{IIb}\beta\text{3}$ and that less of these receptors are activated, respectively (He and Chen, 2019).

Considering that the PAC-1 percentage of parent and MFI in response to CRP-XL and TRAP-6 does not vary considerably between the different concentrations of the platelet agonists in the vehicle conditions, it is possible that platelets were activated to their maximum even with the lowest concentrations tested and, therefore, SIRT1 activation might not overcome such a stimulation. These would explain the mild protection observed when measuring PAC-1 binding versus the inhibition of fibrinogen binding detected.

In line with our findings using CRP-XL as a platelet agonist, results by Jang et al. (2015) demonstrate that resveratrol inhibits integrin $\alpha\text{IIb}\beta\text{3}$ activation in platelets stimulated with convulxin (Jang et al., 2015), which is a GPVI agonist (Horii et al., 2009). Pterostilbene and 3,4',5-tetramethoxy-trans-stilbene (TMS) are resveratrol analogues with the ability to activate SIRT1 (Cheng et al., 2016; C. Zhou et al., 2022), among other proteins. Platelet incubation with pterostilbene reduces integrin $\alpha\text{IIb}\beta\text{3}$ "inside-out" signalling through a decrease in PAC-1 binding induced by collagen (Huang et al., 2021), which correlates with our flow cytometry results. However, as mentioned previously in this discussion, the results obtained with non-selective SIRT1 activators should be interpreted with caution, as they might not be mediated by this deacetylase but by other of the many targets of these drugs (Kulkarni and Cantó, 2015; Kosuru et al., 2016), emphasising the value of using a specific SIRT1 activator in our assays. For instance, in contrast to our findings with SRT1720, TMS treatment had no effect on PAR-1 mediated integrin $\alpha\text{IIb}\beta\text{3}$ activation but reduced PAC-1

binding in response to PAR-4 stimulation, which might be due to a weaker activation of SIRT1 by TMS (Chiang et al., 2022).

Consistent with our results, a study from Aslan et al. (2015) identified that decreasing acetylation levels via specific p300 inhibition reduces platelet integrin α IIb β 3 activation in response to CRP-XL (Aslan et al., 2015), which was deduced from a decrease in both fibrinogen and PAC-1 binding.

There are not many publications addressing the role of acetylation in platelet granule release. In contrast to our findings, resveratrol inhibited α -granule release in platelets activated with convulxin. However, this effect might be mediated by another target of resveratrol in platelets, such as the inhibition PI3K/Akt axis, which plays an important role in platelet activation (Guidetti et al., 2015; Kulkarni and Cantó, 2015). Moreover, Moscardó et al. (2015) revealed that SIRT2 inhibition reduces dense granule secretion in response to both collagen and thrombin (Moscardó et al., 2015) and Liu et al. (2023) demonstrated that SIRT6 activation reduces α -granule release (Y. Liu et al., 2023), which again suggests that the different SIRTs are not involved in the same signalling pathways in platelets and perform diverse functions.

Interestingly, SRT1720 only decreased the percentage of platelets that release dense granules when activation is induced with CRP-XL, but not TRAP-6. Some key players in PAR and GPVI differential regulation of dense granule secretion in platelets have already been identified. Protein kinase C- δ (PKC- δ) activation in platelets positively regulates PAR-mediated dense granule secretion and negatively regulates GPVI-mediated dense granule release. A study from Chari et al. (2009) demonstrated that activation of the SFK Lyn causes phosphorylation and association of PKC- δ and SHIP-1, preventing dense-granule secretion upon GPVI stimulation (Chari et al., 2009). Work by Huang et al. (2021) demonstrated that pterostilbene inhibits collagen-induced Lyn phosphorylation (Huang et al., 2021), which results in decreased platelet adhesion to collagen, in line with our thrombus formation findings. Therefore, the mechanism behind the differential regulation of dense and α -granules release in SRT1720-treated platelets might be the prevention of Lyn phosphorylation. However, this is only a hypothesis and further investigation using a specific SIRT1 activator is needed to elucidate the signalling behind this event.

Lyn, along with other SFKs, mediates integrin-dependent “outside-in” signalling in platelets (Durrant et al., 2017). Moreover, as activation of integrin $\alpha\text{IIb}\beta\text{3}$ with its endogenous ambivalent ligand fibrinogen is essential for platelet-platelet interactions (Springer et al., 2008), a disruption in this signalling pathway would explain the decrease in aggregation observed.

In line with our thrombus formation results, Breitenstein et al. (2011) reported that SIRT1 inhibition with splitomicin increases thrombus formation caused by photochemical injury in a carotid artery thrombosis mouse model, which was associated with an increase in tissue factor activity (Breitenstein et al., 2011). Also consistent with our findings, an investigation by Liu et al. (2023) explored the effect of SIRT6 pharmacological activation in a ferric chloride-induced arterial thrombosis mouse model, concluding that SIRT6 activation prolonged the time to thrombotic occlusion and, therefore, thrombus formation (Y. Liu et al., 2023). However, these studies were performed *in vivo* and, due to the systemic nature of the treatments, the contribution of the endothelium and the extracellular matrix to the thrombus formation process should also be considered. In the case of the study by Breitenstein et al. (2011), platelet function was not investigated in blood from these mice and, therefore, the decrease in thrombus formation cannot be attributed to a reduction in platelet reactivity. Conversely, Liu et al. (2023) demonstrated that platelet reactivity was reduced in the presence of the SIRT6 selective activator by performing several platelet function assays, such as aggregation, spreading and clot retraction. Moreover, one of the limitations of the study by Breitenstein et al. (2011) is the use of splitomicin, as this drug inhibits both SIRT1 and SIRT2, which suggests that these effects could be mediated by any of these enzymes (Park et al., 2019).

Previous *in vitro* studies have reported the protective effects of resveratrol against thrombus formation on collagen I under arterial flow (Jang et al., 2015; Michno et al., 2022), which also supports the outcome of our research.

Moreover, Aslan et al. (2015) demonstrated that pharmacological inhibition of the KAT p300 also reduced arterial thrombus formation on collagen (Aslan et al., 2015). Previous reports have demonstrated that p300 becomes phosphorylated and activated by SFKs upon platelet stimulation with GPVI. As a result, lysine acetyltransferase enzymatic activity is increased in CRP-XL-activated platelets, which

supports the idea that activation of deacetylases, such as SIRT1, could prevent platelet activation downstream GPVI. Overall, the effects associated with p300 inhibition in platelets correlate with the results obtained in this study after SIRT1 activation: reduced platelet aggregation, decreased integrin $\alpha\text{IIb}\beta\text{3}$ activation and impaired arterial thrombus formation on collagen *in vitro* (Aslan et al., 2015). In other cell types, it has been demonstrated that SIRT1 represses p300 through deacetylation of the lysine residues 1020/1024 (Bouras et al., 2005). Therefore, the effects observed when treating platelets with SRT1720 could be a result of SIRT1-mediated inhibition of p300.

The impact of SRT1720 on the acetylated residues of relevant targets, such as p300, was not investigated due to the lack of antibodies targeting lysine-acetylated proteins, which constitutes a limitation of this study. Further research using immunoprecipitation or mass spectral analysis of acetylated proteins is required to understand the implications of SIRT1 activation in platelet “inside-out” signalling.

This chapter shows the importance of SIRT1-mediated deacetylation in the regulation of platelet function via the modification of platelet “inside-out” signalling and the consequent reduction of integrin $\alpha\text{IIb}\beta\text{3}$ activity, opening the possibility of using selective SIRT1 activators, such as SRT1720, as novel antiplatelet agents. Further investigation of the mechanism behind the protective effects of SIRT1 activation against platelet aggregation and thrombus formation using platelet static adhesion and spreading assays was required and will be explained in the next chapter. Moreover, thrombus formation and stabilisation are dependent on integrin $\alpha\text{IIb}\beta\text{3}$ “outside-in” signalling and the consequent cytoskeletal rearrangement that allows the synthesis of actin fibres and the formation of filopodia and lamellipodia. Considering the reduction in thrombus formation observed with SRT1720, the role of SIRT1 activation in integrin $\alpha\text{IIb}\beta\text{3}$ “outside-in” signalling and platelet cytoskeletal dynamics will be explored in the following chapter.

Chapter 4. SIRT1 activation disrupts actin cytoskeleton dynamics, decreasing platelet spreading and clot retraction

4.1 Introduction

In the previous chapter, it was demonstrated that SIRT1 activation by treating platelets with SRT1720 leads to a decrease in integrin $\alpha\text{IIb}\beta\text{3}$ activation, suggesting that this deacetylase might affect platelet “outside-in” signalling. Although there is no evidence of the presence of lysine-acetylated residues in integrin $\alpha\text{IIb}\beta\text{3}$, recent studies have linked acetylation of integrin β1 with increased activation (Vega et al., 2020), which indicates that acetylation might be a novel regulation mechanism of integrin conformational change and activation. Some of the proteins involved in the regulation of “outside-in” signalling are targets for KATs and KDACs, such as Focal Adhesion Kinase (FAK), Integrin Linked Kinase (ILK), Ras-related C3 botulinum toxin substrate 1 (Rac1) and Ras GTPase-activating protein 3 (Rasa3) (Aslan et al., 2015; Durrant et al., 2017; Huang et al., 2019). For instance, a study by Lee et al. (2018) demonstrated that epithelial cell migration is inhibited by a decrease in FAK acetylation (Lee et al., 2018).

Integrin $\alpha\text{IIb}\beta\text{3}$ activation and β3 subunit phosphorylation initiate a cascade of intracellular signalling events (Phillips et al., 2001) in which posttranslational modification of different cooperating proteins drive stable platelet adhesion, irreversible aggregation, cytoskeletal reorganisation, spreading, clot retraction and stable thrombus formation (Durrant et al., 2017; Huang et al., 2019).

The platelet cytoskeleton is a key element in clot retraction. Upon integrin $\alpha\text{IIb}\beta\text{3}$ activation, the light chain of myosin IIA phosphorylates and binds to the platelet cytoskeleton (Tucker et al., 2012; George et al., 2021), which coordinates actin filaments, microtubules and myosin to exert the forces that generate the contraction of the fibrin matrix (Shin et al., 2017), leading to a decrease in the volume of the clot. This process is essential for the stabilisation of the clot and wound healing (Nurden, 2023)

Although the different components that comprise the platelet cytoskeleton are explained in detail in section 1.2.1, the importance of microfilament and microtubule turnover in platelet shape change during activation should be highlighted.

In platelets, actin exists in a dynamic balance between the monomeric or globular form (G-actin) and the polymeric or F-actin. Actin filament turnover, also called actin polymerisation, depends on several ABPs and is key for the emission of platelet filopodia and lamellipodia (Romero et al., 2020). Some of these ABPs maintain the discoid shape of circulating platelets by interacting with actin monomers and inhibiting filament formation, such as cofilin, or through the binding and stabilisation of actin filaments, like VASP or cortactin (Weaver et al., 2001). Other ABPs drive reorganisation through the disassembly of old filaments, such as gelsolin, and the polymerisation of new ones, like Arp2/3 (Bearer et al., 2002; Bender and Palankar, 2021; De Silva et al., 2022). Recent studies revealed that posttranslational modifications, namely acetylation, are essential for the regulation of actin cytoskeleton reorganisation (Casey et al., 2020; MacTaggart and Kashina, 2021). For instance, it has been demonstrated that N-terminal actin acetylation regulates cell motility, filament turnover and the formation of filopodia and lamellipodia (Aksnes et al., 2018; Drazic et al., 2018; Chin et al., 2022). Six lysine acetylation sites have been identified in the platelet β -actin molecule. Cortactin, cofilin, Arp2/3 and gelsolin are also heavily acetylated in platelets. A study from Aslan et al. (2015) demonstrated that lysine acetylation of these ABPs is p300-mediated and that pharmacological inhibition of this KAT leads to a decrease in F-actin production and spreading (Aslan et al., 2015). Moreover, in other cell types SIRT1 (Zhang et al., 2009), SIRT2, HDAC6 (Zhang et al., 2007) and HDAC8 (Li et al., 2014) have been identified as key regulators of cell migration by modulating cortactin acetylation. This evidence shows that actin cytoskeleton dynamics are largely regulated by lysine acetylation and illustrates the importance of investigating the role of SIRT1 in platelet spreading and actin reorganisation.

Microtubule dynamics are also crucial to allow rapid platelet shape change during activation. In resting platelets α and β -tubulin form a ring under the cellular membrane called marginal band, which structure and function were explained in more depth in section 1.2.1.2. Under platelet stimulation, microtubule

rearrangement leads to marginal band coiling and centralisation, which allows the transition from the discoid shape of resting platelets to the spherical shape of activated ones, followed by quick depolymerisation (Cuenca-Zamora et al., 2019). Similarly to ABPs, MBPs are a large group of proteins that control microtubule assembly and stability. It has been demonstrated in different cell models, including platelets, that lysine acetylation of tubulin is crucial for the regulation of microtubule dynamics through the modulation of the binding of microtubules to dynein and kinesin-1, which are the most important MBPs (Alper et al., 2014; Casey et al., 2020; MacTaggart and Kashina, 2021). Previous studies linked platelet marginal band coiling after activation to the deacetylation of α -tubulin in lysine 40 by HDAC6 (Sadoul et al., 2012) and SIRT2 (Moscardó et al., 2015), while this tubulin site is acetylated in resting platelets by α TAT1 (Ribba et al., 2021). However, the role of SIRT1-mediated deacetylation in platelet microtubule rearrangement has yet to be elucidated.

Considering the significant impact of acetylation and deacetylation cycles in the regulation of the platelet cytoskeleton, the role of SIRT1 in cytoskeletal-mediated platelet functions, such as platelet spreading, microfilament turnover, microtubule reorganisation and marginal band coiling will be explored in the following chapter. Due to the importance of acetylation as a regulatory mechanism of platelet cytoskeletal function and the key role of filopodia in fibrin mesh contraction, it is necessary to evaluate the effect of KDACs, such as SIRT1, in clot retraction. Moreover, the signalling pathways behind these effects will be investigated using Western Blotting.

4.2 Hypothesis, chapter aim and objectives

Considering the dramatic decrease in thrombus formation under flow reported in section 3.3.5 and the evidence in the literature highlighting the importance of lysine acetyl transfer in platelet cytoskeleton rearrangement (K. Sadoul et al., 2012; Aslan et al., 2015), we hypothesised that SIRT1 might be involved not only in the regulation of integrin $\alpha\text{IIb}\beta\text{3}$ activation but also in the cascade of signalling events that trigger platelet stable adhesion, cytoskeletal reorganisation, spreading and clot retraction during integrin $\alpha\text{IIb}\beta\text{3}$ “outside-in” signalling.

The aim of this chapter is to understand whether SIRT1 activation using the selective agonist SRT1720 alters integrin $\alpha\text{IIb}\beta\text{3}$ -dependent functions, including platelet spreading and clot retraction, and whether this is entirely mediated through a decrease in integrin $\alpha\text{IIb}\beta\text{3}$ activity or if SIRT1 activation is also altering cytoskeletal rearrangement. To answer this research question, the following objectives were pursued:

1. Explore the effect of SIRT1 activation with SRT1720 on platelet adhesion and spreading on collagen and fibrinogen.
2. Investigate the impact of SIRT1 activation on the platelet cytoskeleton by evaluating platelet morphology using Scanning Electron Microscopy and assessing the effect of SRT1720 in microfilament and microtubule dynamics.
3. Evaluate whether SRT1720 alters clot retraction.
4. Explore the role of SIRT1 in integrin $\alpha\text{IIb}\beta\text{3}$ “outside-in” signalling and cytoskeletal reorganisation pathways.

4.3 Results

4.3.1 SRT720 inhibits platelet adhesion and spreading in static conditions

As explained in section 3.3.5, SIRT1 activation reduced *in vitro* thrombus formation under arterial flow. To have a better understanding of the mechanism behind this, the effect of SIRT1-mediated deacetylation on the ability of platelets to adhere and spread on collagen I and fibrinogen was investigated.

Washed platelets were treated with SRT1720 (10 μ M) or vehicle for 10 minutes and left to adhere and spread on 96-well plates or coverslips coated with collagen (10 μ g/mL) or fibrinogen (100 μ g/mL) for 45 min at 37°C. The SIRT1 agonist SRT1720 decreased platelet adhesion to collagen (Figure 4.1A) and fibrinogen (Figure 4.2A). Moreover, SIRT1 activation reduced the ability of platelets to form lamellipodia on both collagen (Figure 4.1B) and fibrinogen (Figure 4.2B) with an increased proportion of platelets in the earlier adhered and filopodia stages observed. As a result, SRT1720 significantly reduced the mean platelet area (Figure 4.1C, Figure 4.2C) and the platelet area coverage percentage (Figure 4.1D, Figure 4.2D) after exposure to collagen or fibrinogen.

These findings indicate that SIRT1 activation decreases platelet adhesion to extracellular matrix proteins, such as collagen I, and impairs integrin α IIb β 3-mediated adhesion, supporting the reduction in platelet aggregation and fibrinogen binding discussed in Chapter 3. Moreover, platelet lamellipodia formation was decreased by SRT1720 on both collagen and fibrinogen, which suggests that SIRT1 activation is not only targeting integrin α IIb β 3 but also might have an effect on the reorganisation of the platelet cytoskeleton.

Collagen

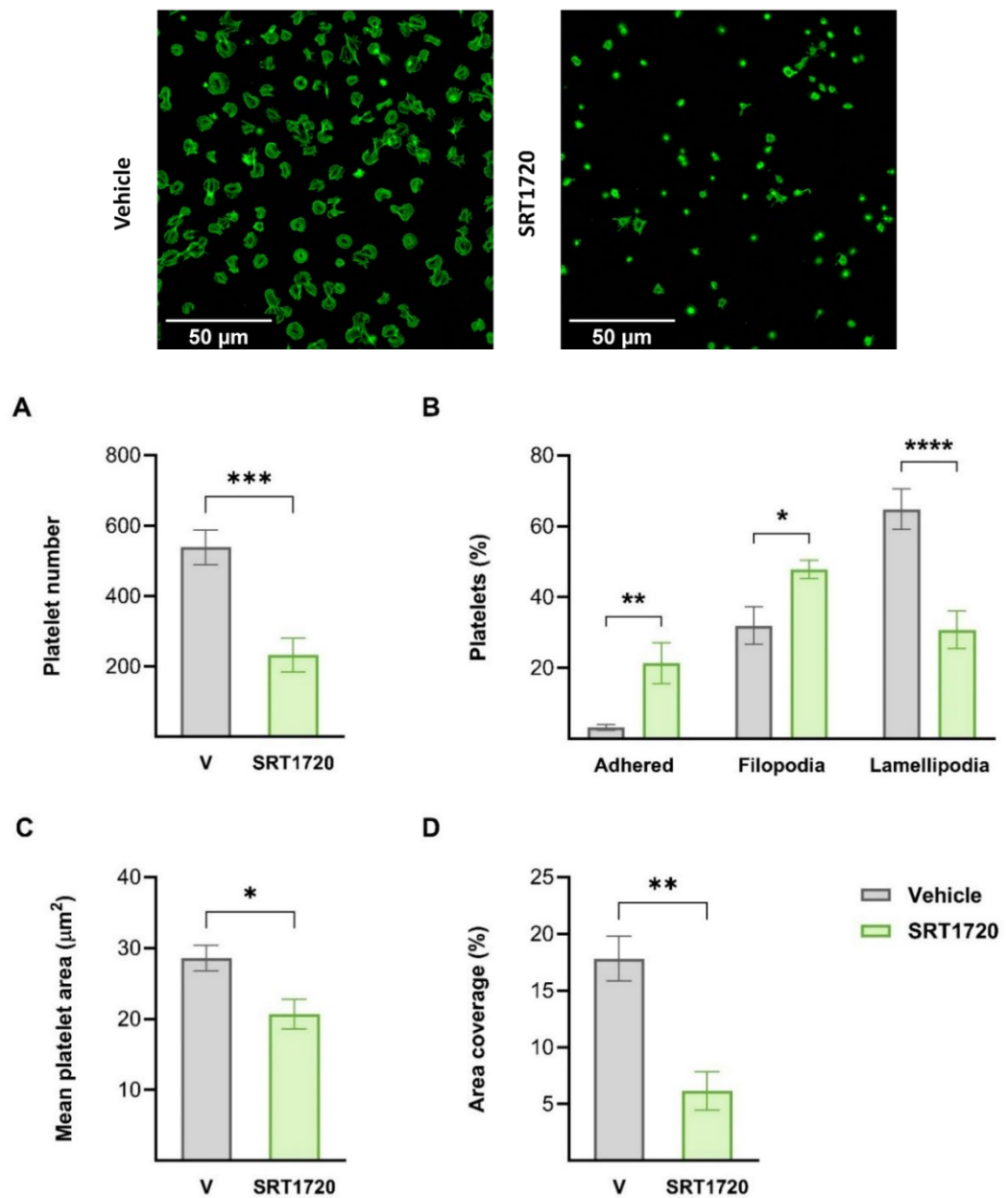


Figure 4.1. SIRT1 activation inhibits platelet spreading and adhesion on collagen. ADP-sensitive platelets were incubated with SRT1720 (10 μM) or vehicle (V, 0.1% DMSO) for 10 min and exposed to collagen (10 $\mu\text{g}/\text{mL}$) for 45 min at 37°C. Platelets were labelled with Alexa 488-phalloidin. Images of adherent platelets for analysis were captured using the 20x objective on the CELENA® S Logos Biosystems microscope. Representative images taken on the 63x oil immersion lens of the Thunder microscope are shown. The image J software was used to morphologically classify platelets depending on the formation of filopodia or lamellipodia (B) and calculate the number of adhered platelets per field of view (A), the mean platelet area (C) and the percentage area covered by platelets (D). Statistical differences were assessed by t-test (A, C, D) and Repeated Measures Two-Way ANOVA (B). Scale bar is 50 μm . Data represent mean \pm SEM. * $p < 0.05$, ** $p < 0.01$, *** $p < 0.001$, **** $p < 0.0001$. N=6.

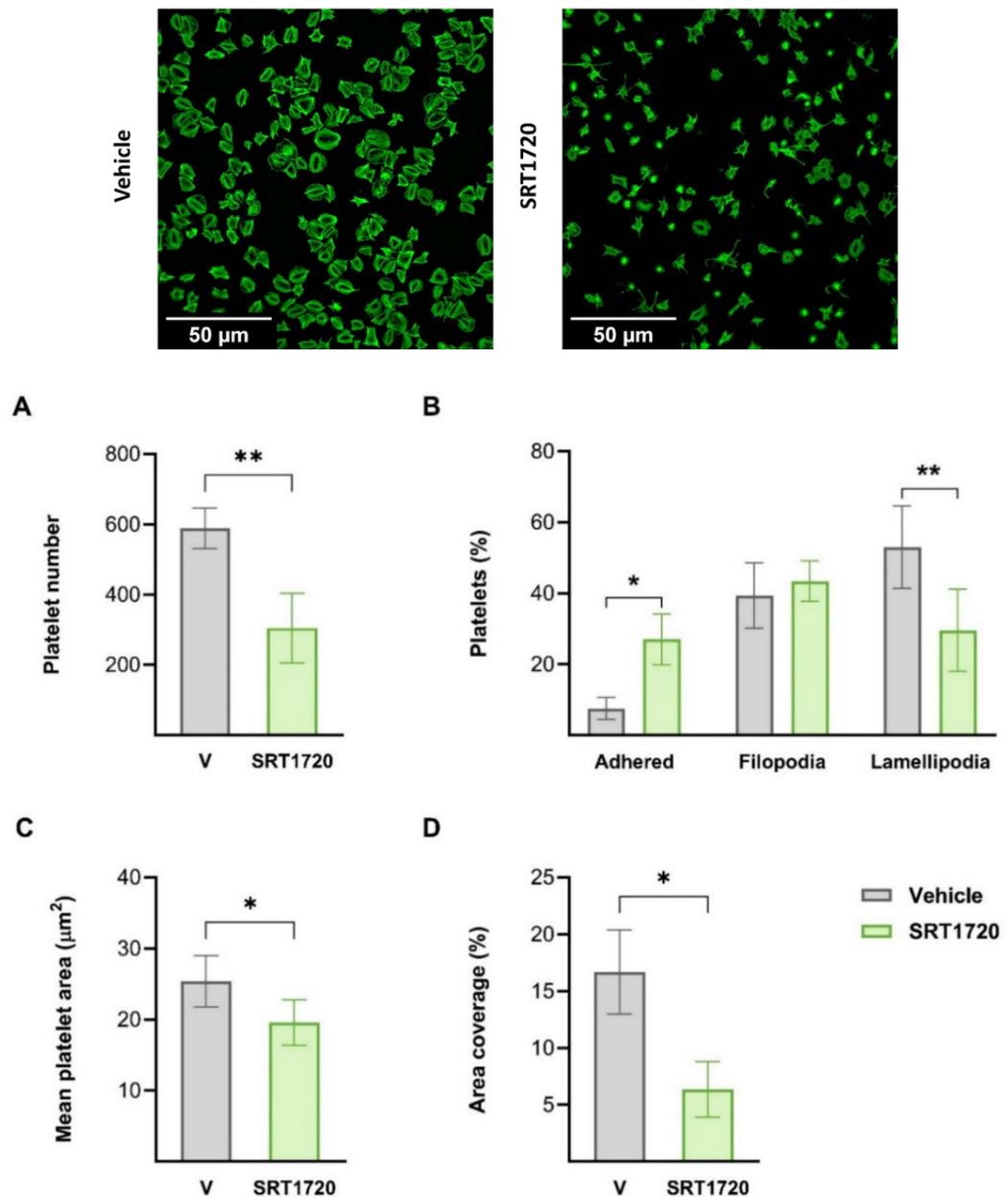


Figure 4.2. SIRT1 activation inhibits platelet spreading and adhesion on fibrinogen. ADP-sensitive platelets were incubated with SRT1720 (10 µM) or vehicle (V, 0.1% DMSO) for 10 min and exposed to fibrinogen (100 µg/mL) for 45 min at 37°C. Platelets were labelled with Alexa 488-phalloidin. Images of adherent platelets for analysis were captured using the 20x objective on the CELENA® S Logos Biosystems microscope. Representative images taken on the 63x oil immersion lens of the Thunder microscope are shown. The image J software was used to morphologically classify platelets depending on the formation of filopodia or lamellipodia (B) and calculate the number of adhered platelets per field of view (A), the mean platelet area (C) and the percentage area covered by platelets (D). Statistical differences were assessed by t-test (A, C, D) and RM Two-Way ANOVA (B). Scale bar is 50 µm. Data represent mean ± SEM. *p<0.05, **p<0.01. N=5.

4.3.2 SRT1720 disrupts the platelet cytoskeleton

SRT1720 treatment dramatically reduces platelet adhesion and spreading in response to both collagen and fibrinogen. However, it was unclear whether this effect is entirely mediated by the decrease in integrin $\alpha\text{IIb}\beta\text{3}$ activation observed in section 3.3.3 or whether SIRT1 is involved in the regulation of platelet cytoskeletal dynamics. Therefore, Scanning Electron Microscopy was performed to determine if SIRT1 activation was affecting the organisation of the cytoskeleton of human platelets.

Cells were preincubated with SRT1720 (10 μM) and stimulated with TRAP-6 (10 μM). Platelets were centrifuged into glass coverslips and the structure was conserved by adding a cytoskeleton stabilisation buffer. After fixation, dehydration, mounting and gold sputtering, images of the samples were obtained by Scanning Electron Microscopy using the Zeiss Crossbeam 350 FIB-SEM microscope and a 20,000x magnification.

As expected, representative pictures show an increase in the average platelet area triggered by TRAP-6 (Figure 4.3A) and demonstrate that SIRT1 activation reduces the average platelet size by preventing the formation of lamellipodia in both basal (Figure 4.1A) and activated platelets (Figure 4.3B), which supports the hypothesis that SIRT1-mediated deacetylation has a key role in platelet cytoskeletal remodelling.

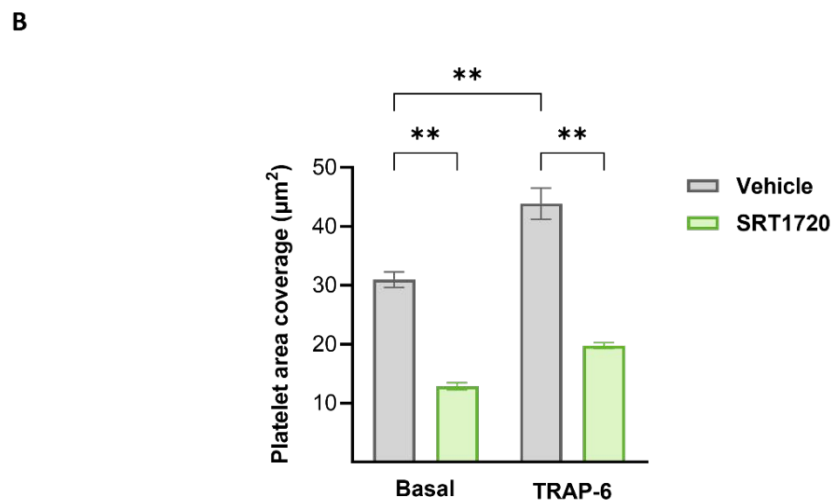
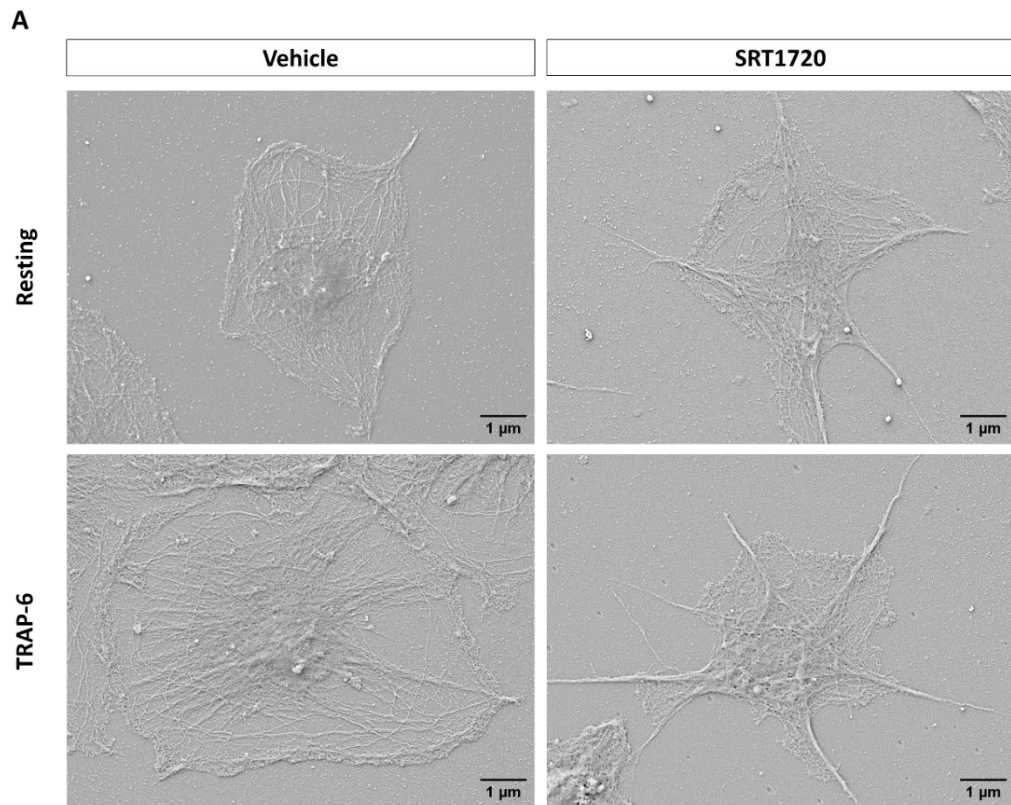


Figure 4.3. SRT1720 altered the platelet cytoskeleton. Platelets were treated with SRT1720 (10 μ M) or vehicle (0.1% DMSO) for 10 min followed by a 3-min incubation with TRAP-6 (10 μ M) or PBS (0.1%) and span down into poly-L-lysine-coated coverslips at 1450xg for 5 min. Adhered platelets were treated with cytoskeleton stabilisation buffer to conserve the structure of microfilaments and microtubules. Samples were fixed, dehydrated, and dried before mounting them on a stub and coating them with gold. Scanning Electron Microscopy was performed, and pictures of the platelet cytoskeleton were taken using the Zeiss Crossbeam 350 FIB-SEM microscope and a 20,000x magnification. SIRT1 activation disrupted the platelet cytoskeleton, as shown in the representative images (A), and significantly reduced platelet area coverage in both basal and TRAP-6 activated platelets (B). Platelet area coverage was quantified on ImageJ. Statistical differences were assessed by One-way ANOVA (B). Scale bar is 1 μ m. Data represent mean \pm SEM. ** p <0.01. N=2.

4.3.3 SIRT1 activation reduces the F-actin pool in activated platelets

In platelets, the extension of filopodia and lamellipodia relies on actin polymerisation. As mentioned in section 4.1, the continuous equilibrium between globular and filamentous actin is regulated by ABPs (Bearer et al., 2002) and p300-mediated acetylation of these proteins increases microfilament levels in platelets (Aslan et al., 2015). Prior research demonstrated that SIRT1 inhibits p300 acetylase activity, operating as its counterpart in the regulation of different cellular processes (Bouras et al., 2005). Considering that SIRT1 activation altered platelet shape and cytoskeletal structure, the effect of SRT1720 in platelet F-actin levels was evaluated using flow cytometry (Figure 4.4A, Figure 4.4B, Figure 4.4C) and F/G actin ratio determined using Western Blotting (Figure 4.4D, Figure 4.4E).

PRP (Figure 4.4A, Figure 4.4B, Figure 4.4C) or ADP-sensitive platelets (Figure 4.4D, Figure 4.4E) were treated with SRT1720 (10 μ M) or vehicle for 10 minutes and F-actin formation was induced by activating platelets with TRAP-6 (10 μ M). For flow cytometry, PRP samples were fixed in solution and stained with Alexa488-phalloidin, and the percentage of parent and MFI were measured (Figure 4.4A, Figure 4.4B, Figure 4.4C). For analysis of the F/G actin ratio, washed platelets were lysed using a cytoskeleton stabilisation buffer. Lysates were centrifuged to separate the globular or monomeric fraction from the polymeric or filamentous component. The impact of SRT1720 in the ratio of these fractions was assessed by Western Blotting (Figure 4.4D, Figure 4.4E).

Both experimental approaches demonstrated that SIRT1 activation significantly reduced F-actin levels in stimulated platelets, which shows that SIRT1 is involved in platelet actin cytoskeletal dynamics and explains the decrease in platelet lamellipodia formation observed in the spreading assay discussed in section 4.3.1 and the abnormalities in the platelet cytoskeleton detected in the SEM experiment in section 4.3.2

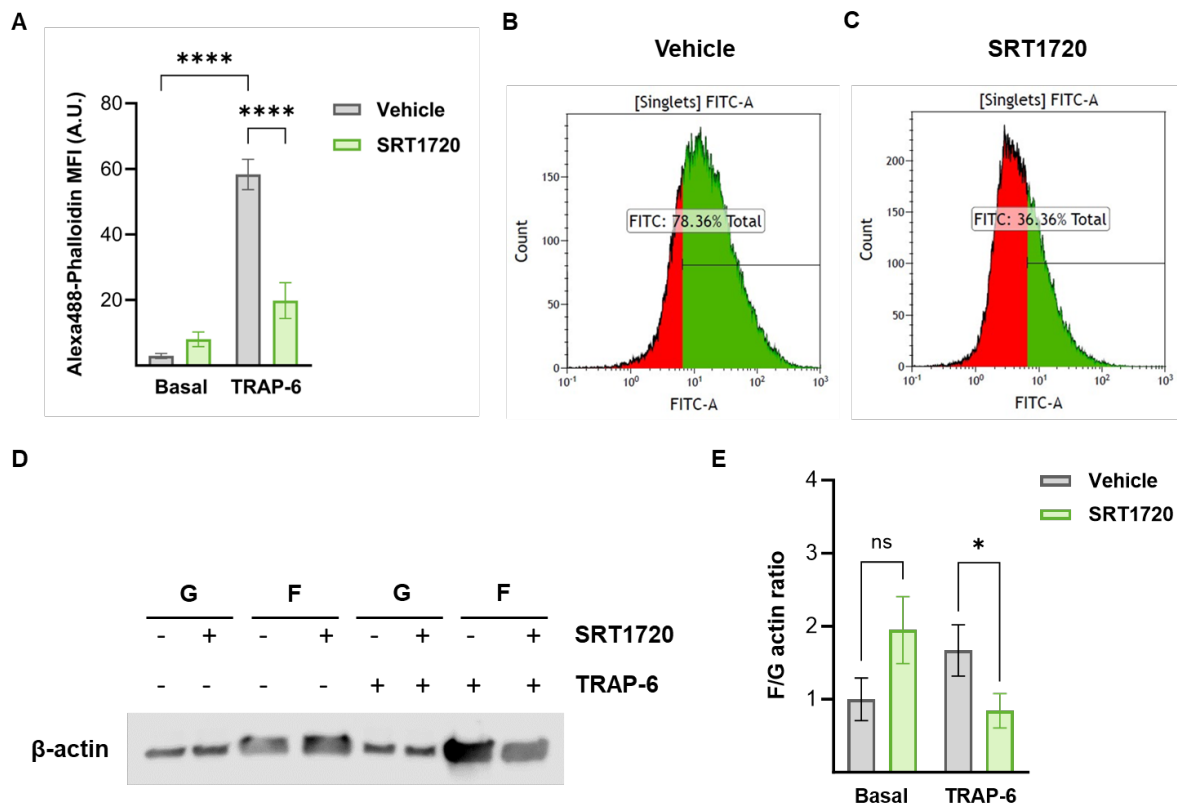


Figure 4.4. Measurement of filamentous actin levels revealed that SIRT1 activation decreases platelet actin polymerisation upon stimulation with TRAP-6. PRP (A, B, C) or ADP-sensitive platelets (D, E) were treated with SRT1720 (10 μ M) or vehicle (0.1% DMSO) for 10 minutes. Actin polymerization was induced by activating platelets with TRAP-6 (10 μ M) for 3 min. F-actin levels were detected using flow cytometry by staining fixed platelets with Alexa488-phalloidin (A, B, C) or generating lysates of the globular (G) and filamentous (F) components of the cytoskeleton to detect β -actin using western blotting (D, E). Flow cytometry (B, C) and Western Blotting (D) results showed a decrease in F-actin levels in SRT1720-treated platelets versus vehicle control (A, E). Differences in MFI (A) and the F/G actin ratio (E) were measured using FlowLogic and ImageJ, respectively, and analysed by One-way ANOVA. Only statistically significant differences are shown. Data represent mean \pm SEM. **** $p < 0.0001$. N=5. G=globular actin; F=filamentous actin.

4.3.4 SIRT1 activation has no effect on platelet microtubule reorganisation

According to our previous experiments, SIRT1 activation alters the reorganisation of actin filaments. Considering that there is evidence in the literature that associates platelet stimulation and shape change with α -tubulin deacetylation (Cuenca-Zamora et al., 2019; Robaux et al., 2023) by HDAC6 (Sadoul et al., 2012) and SIRT2 (Moscardó et al., 2015), it was necessary to investigate whether SIRT1 activation could affect the rearrangement of the platelet microtubules and the tubulin ring in addition to F-actin polymerisation.

While platelet activation results in stable F-actin formation, tubulin polymerisation occurs after platelet stimulation and is associated with microtubule coiling and platelet spherical shape, followed by quick depolymerisation during platelet spreading (Cuenca-Zamora et al., 2019). Microtubule formation was tested in ADP-sensitive washed platelets preincubated with SRT1720 (10 μ M) or vehicle for 10 minutes and stimulated with TRAP-6 (10 μ M). Platelets were lysed with cytoskeleton stabilisation buffer and centrifuged to separate the globular tubulin from the microtubules. Samples were tested by Western Blotting.

No statistically significant changes were observed in the microtubule: tubulin ratio after treatment with SRT1720 either in basal or in TRAP-6-activated platelets, indicating that SIRT1 does not control tubulin polymerisation (Figure 4.5).

To fully understand the role of SIRT1 in platelet tubulin dynamics, it was necessary to assess the impact of SRT1720 not only on tubulin polymerisation but also on marginal band coiling, as this event depends on dynein and kinesin-1, which have different lysine acetylation sites (Aslan et al., 2015).

The effect of SIRT1 activation in microtubule turnover was assessed by treating PRP with SRT1720 (10 μ M) for 10 minutes and triggering marginal band coiling by adding TRAP-6 at a final concentration of 0.1 μ M for 1 minute. Platelets were fixed in suspension and spun down into coverslips. The actin cytoskeleton was stained with Alexa488-Phalloidin and the tubulin ring with a β -tubulin antibody and an Alexa647-anti rabbit secondary antibody. Images were taken using the STELLARIS 5 confocal microscope. The number of platelets with an intact marginal band was quantified using Image J and compared between SRT1720 and control samples.

SRT1720 had no significant effect either in the resting shape of the tubulin ring (Figure 4.6A) or the extension of the microtubule marginal band of activated platelets (Figure 4.6B), which suggests that, contrarily to SIRT2, SIRT1-mediated deacetylation has no major role in tubulin reorganisation in platelets.

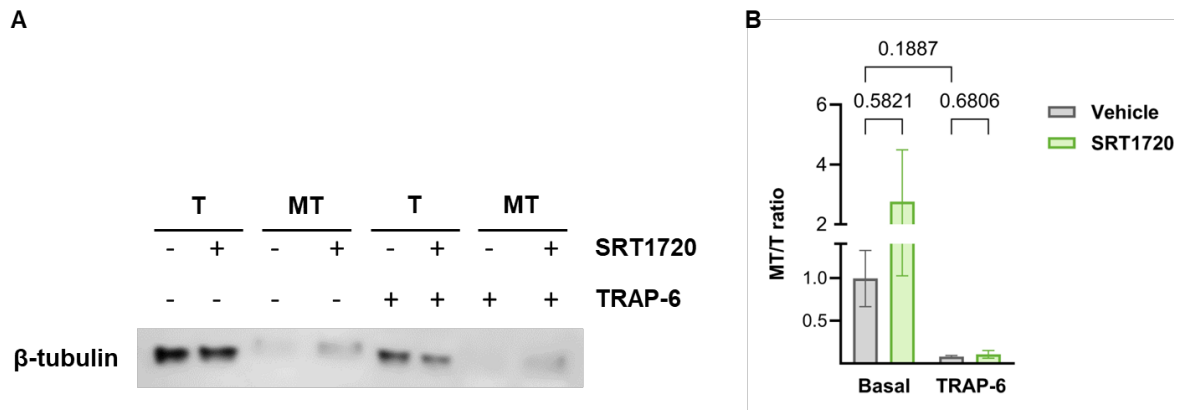


Figure 4.5. SIRT1 activation with SRT1720 does not alter platelet microtubule formation. ADP-sensitive platelets were treated with SRT1720 (10 μ M) or vehicle (0.1% DMSO) for 10 minutes. Tubulin polymerization was induced by activating platelets with TRAP-6 (10 μ M) for 3 min. Polymerised tubulin levels were tested by generating lysates using a cytoskeleton stabilisation buffer and separating using centrifugation the soluble tubulin (T) from the insoluble microtubules (MT). Evaluation of the ratio of globular and polymerised tubulin was performed by Western Blotting. Differences in the MT/T ratio were measured on ImageJ and analysed by One-way ANOVA, revealing that SRT1720 did not affect tubulin polymerisation in platelets. Only statistically significant differences were shown. Data represent mean \pm SEM. N=5. T= β -tubulin; MT=microtubules.

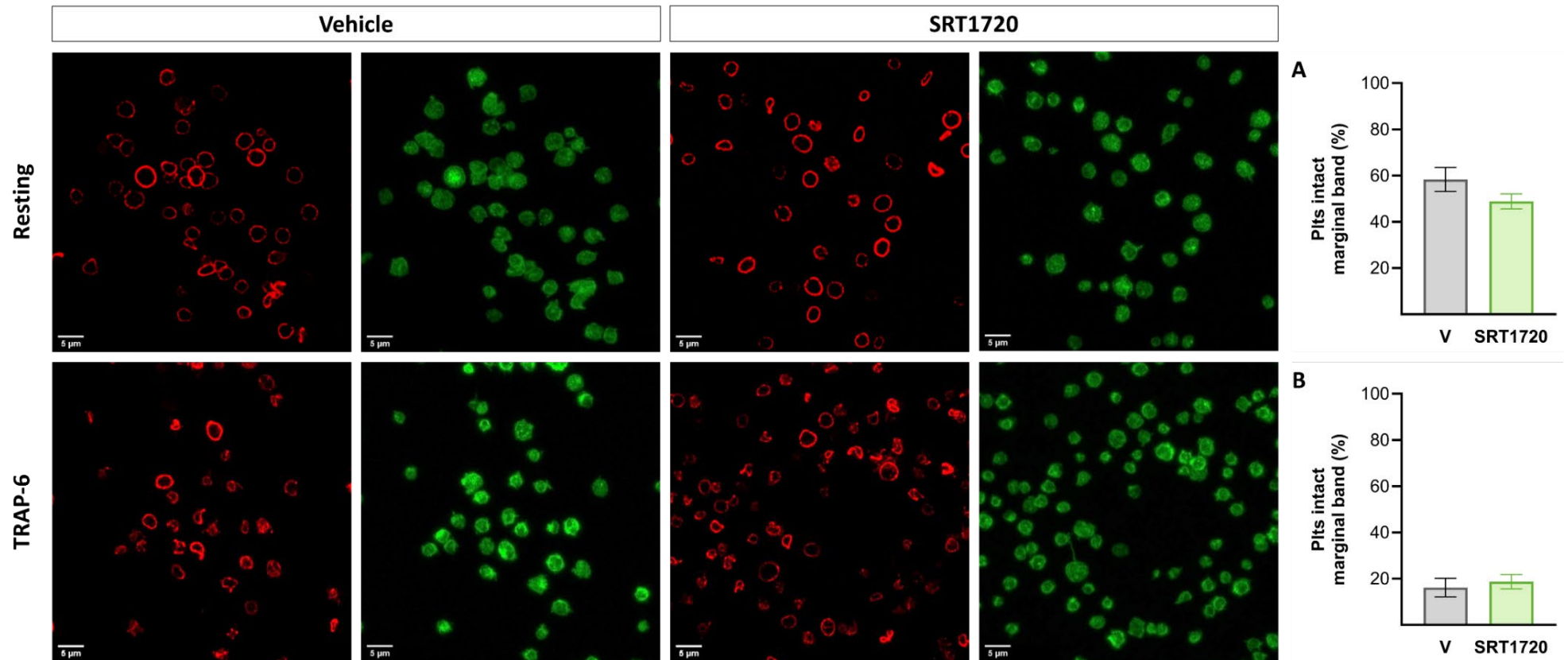


Figure 4.6. The platelet marginal band remains unaffected after SIRT1 activation. PRP was incubated for 10 min with SRT1720 (10 μ M) or vehicle (V, 0.1% DMSO) before platelet activation with TRAP-6 (0.1 μ M) for 3 min. Platelets were fixed in suspension and added to poly-L-Lysine coated coverslips. Platelet cytoskeleton was stained using Alexa488-conjugated phalloidin for F-actin (green) and Alexa647-conjugated anti- β -tubulin antibody for visualisation of the marginal band (red). Images were taken in the 100x oil immersion objective of the STELLARIS confocal microscope. Platelets with an intact marginal band were counted using ImageJ and differences were analysed by One-way ANOVA. Data represent mean \pm SEM. N=6.

4.3.5 SIRT1 activation attenuates the late stage of platelet clot retraction

According to the results presented in Chapter 3, SRT1720 reduced integrin $\alpha\text{IIb}\beta\text{3}$ activation, which appears to lead to a reduction in “outside-in” signalling, as demonstrated in this chapter. These findings were validated by the reduction in lamellipodia caused by SRT1720 when platelets were spread on fibrinogen. As explained in section 4.1, the production of filamentous actin is initiated by integrin $\alpha\text{IIb}\beta\text{3}$ “outside-in” signalling and is crucial for platelet cytoskeletal rearrangement, which leads to spreading and clot retraction (Tucker et al., 2012; Hartwig, 2013). Due to the reduction in platelet integrin $\alpha\text{IIb}\beta\text{3}$ function, lamellipodia extension and F-actin production linked with SIRT1 activation, the effect of SRT1720 in clot retraction was investigated.

In the clot retraction assay, Tyrodes, red blood cells and PRP are mixed and placed in glass tubes. Thrombin was added to the tubes at 1 U/mL final concentration and the formation and contraction of the clot was monitored for 60 min, taking pictures every 10 minutes. Preincubation of PRP with SRT1720 (10 μM) increased the area occupied by the clot in the tube (Figure 4.7A) and the clot weight (Figure 4.7B) compared to the vehicle after a 60-minute treatment with thrombin, suggesting SIRT1 pharmacological activation decreases the late stage of clot retraction, which corresponds to the contraction of the fibrin mesh by the actomyosin cytoskeleton (Jansen and Hartmann, 2021).

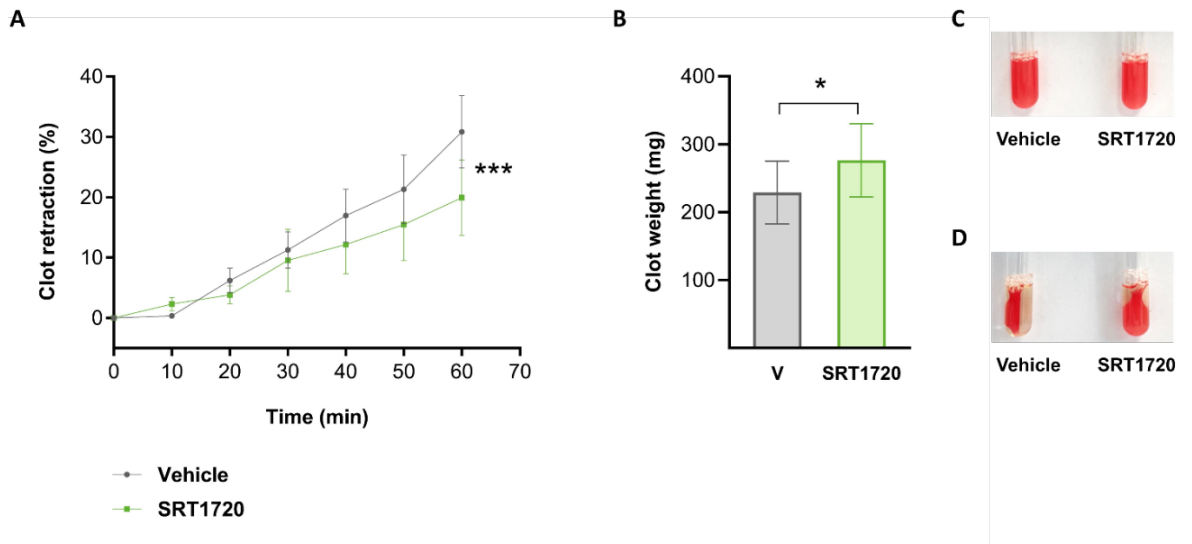


Figure 4.7. SIRT1 pharmacological activation with SRT1720 inhibits the late stage of clot retraction. PRP and RBC diluted in Tyrode's with glucose were treated with SRT1720 (10 μ M) or vehicle (V, 0.1% DMSO) for 10 minutes at 37°C. Platelet aggregation was induced with thrombin (1 U/mL) and clot retraction was monitored for 1 hour at 37°C. The percentage of clot retraction was calculated using the fractional area occupied by the clots at 10-min intervals (A) using RM Two-way ANOVA. The weight of the clots after 60 min was compared by Paired t-test (B). Representative images of the clots at the beginning (C) and the end (D) of the assay are shown. Data represent mean \pm SEM. * p <0.05, ** p <0.01. N=6.

4.3.6 The role of SIRT1 in platelet signalling

To understand the mechanism underlying the effects of SIRT1 activation on platelet “outside-in” signalling, cytoskeletal reorganisation and clot retraction, human washed platelets were treated with SRT1720 (10 μ M) or vehicle for 30 minutes and stimulated with CRP-XL (1 μ g/mL) or TRAP-6 (10 μ M) for 30, 90 and 180 seconds in static conditions. Different signalling pathways involved in integrin α IIb β 3 activation and cytoskeletal rearrangement were tested by Western Blotting.

4.3.6.1 Exploring the effect of SIRT1 activation in “outside-in” signalling

Although there are different players in the transduction of integrin α IIb β 3 signalling, this process is always linked to the phosphorylation of Y773 in the β 3 tail (Huang et al., 2019). Upon platelet binding to fibrinogen, a cascade of signalling events induces the phosphorylation of Y773, which is represented by two bands when protein lysates are evaluated by immunoblotting (120 and 140 kDa) (Tsai et al., 2021). In Chapter 3, it was demonstrated that SIRT1 reduces integrin α IIb β 3 activation, even though the mechanism behind this event is yet unknown. To elucidate whether SIRT1 has an impact on integrin signal transduction and, therefore, “outside-in” signalling, Y773- β 3 phosphorylation levels were evaluated in this study.

As expected the Y773 residue of the integrin α IIb β 3 was phosphorylated after activating platelets with TRAP-6 or CRP-XL but SRT1720 had no effect (Figure 4.8), which indicates that the decrease in platelet spreading, actin polymerisation and clot retraction observed in the presence of the SIRT1 activator is either due to the decrease in of integrin α IIb β 3 activity mentioned in Chapter 3 or the modulation of any of the effectors downstream this receptor.

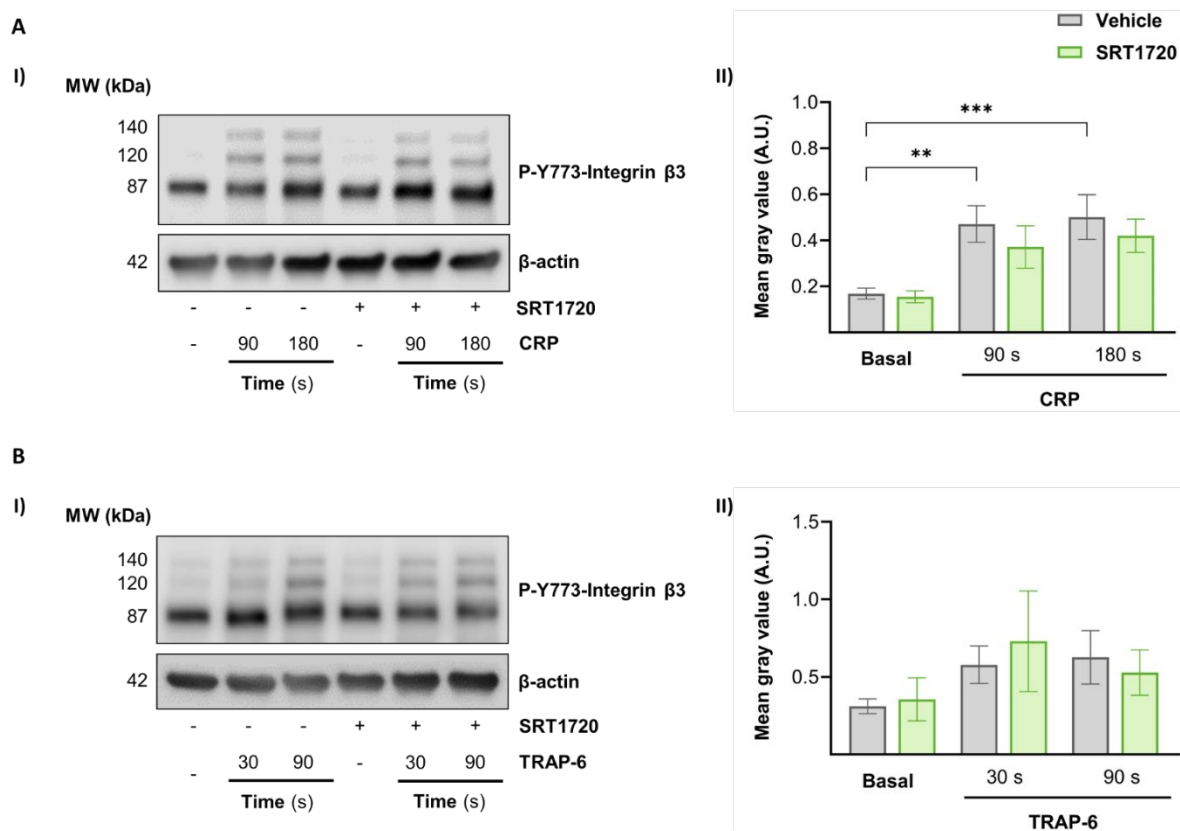


Figure 4.8. SRT1720 causes no significant changes in the phosphorylation of the integrin α IIb β 3 tail. Human washed platelets were pretreated for 30 min with or without SRT1720 (10 μ M) and activated with CRP-XL (1 μ g/mL) for 90 and 180 seconds or TRAP-6 (10 μ M) for 30 and 90 seconds. Platelets were lysed in SDS Laemmli sample buffer and Western Blotting was performed using an antibody against Y773 in the integrin α 2b β 3 tail. Actin was used to confirm equal loading. Representative blots and quantified data are shown. Levels of phosphorylation were quantified and expressed as a ratio of the vehicle control (0.1% DMSO). Differences were analysed by One-way ANOVA. Data represent mean \pm SEM. ** p <0.01 *** p <0.001. N=4.

4.3.6.2 SIRT1 signalling in clot retraction

Myosin and actin filaments are the key platelet components for generating the fibrin mesh contraction that drives clot retraction (Tucker et al., 2012). This process is dependent on integrin $\alpha\text{IIb}\beta\text{3}$ signalling and driven by the contractile force exerted by the platelet actomyosin cytoskeleton. The phosphorylation of S19 in the myosin light chain 2 (MLC2) causes a conformational change that allows myosin to bind to microfilaments and initiates clot retraction (Hartwig, 2013). Several kinases are involved in this event (Egot et al., 2013), which activity might be affected by acetylation. Previous experiments explained in section 4.3.5 indicate that SIRT1 activation reduces clot retraction. To elucidate whether this is a consequence of the SIRT1-mediated decrease in integrin $\alpha\text{IIb}\beta\text{3}$ function and actin polymerisation or whether there is a direct effect on myosin, the phosphorylation levels of MLC2 were investigated using Western Blotting.

SRT1720 and vehicle-treated platelets in the presence or absence of CRP-XL and TRAP-6 were lysed and tested by Western Blotting. Quantification of S19-MLC2 phosphorylation revealed a significant increase in myosin phosphorylation in the vehicle samples when platelets were activated with CRP-XL (Figure 4.9A) and TRAP-6 (Figure 4.9B) after 180 and 90 seconds, respectively. However, no changes were observed between the SRT1720-treated samples and vehicle control independently of the platelet agonist used and the incubation time, suggesting that the decrease in clot retraction observed after SIRT1 activation is probably a result of the reduction in $\alpha\text{IIb}\beta\text{3}$ “inside-out” signalling and F-actin production.

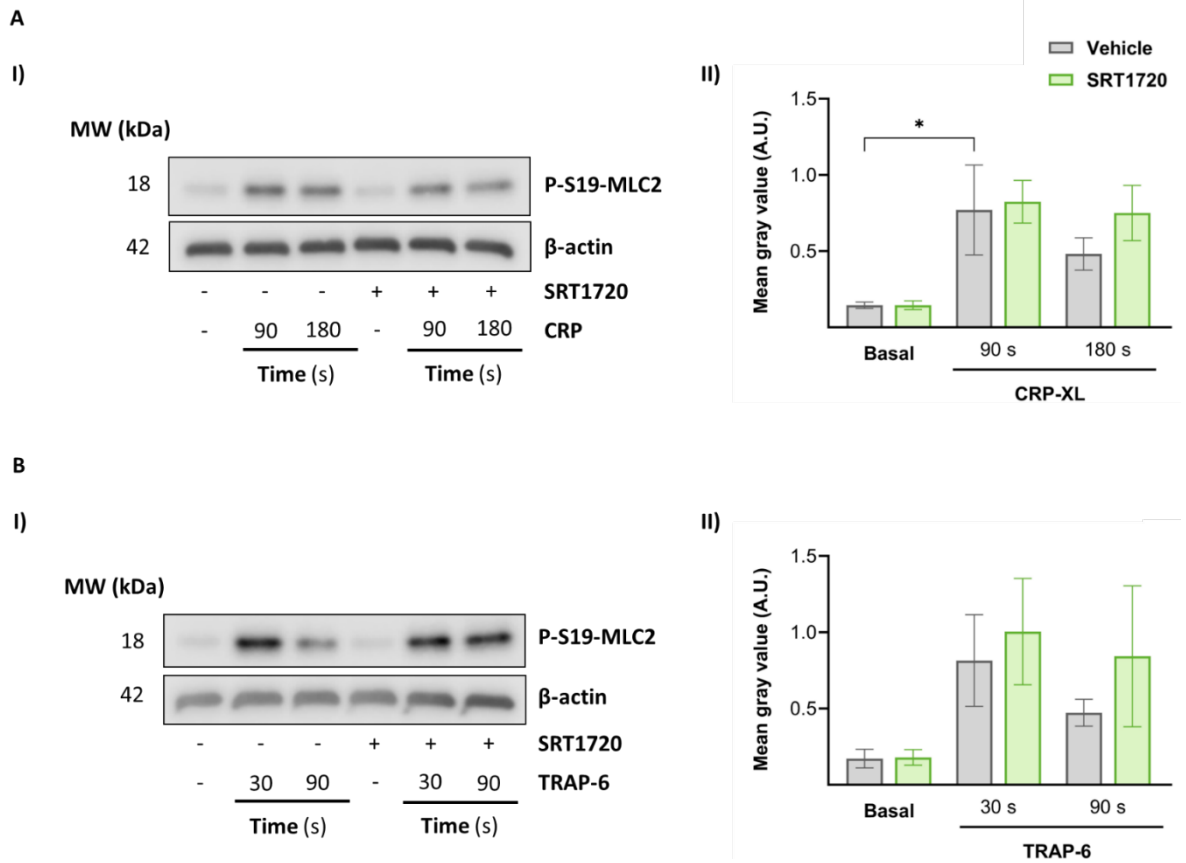


Figure 4.9. SIRT1 activation had no effect on platelet MLC2 phosphorylation. Human washed platelets were pretreated for 30 min with or without SRT1720 (10 μ M) and activated with CRP-XL (1 μ g/mL) for 90 and 180 seconds or TRAP-6 (10 μ M) for 30 and 90 seconds. Platelets were lysed in SDS Laemmli sample buffer and Western Blotting was performed using an antibody against S19-MLC2. β -actin was used as a loading control. Representative blots (I) and quantified data (II) are shown. Levels of phosphorylation were quantified and expressed as a ratio of the vehicle control (0.1% DMSO). Differences were analysed by One-way ANOVA. Data represent mean \pm SEM ** p <0.01 *** p <0.001. N=4.

4.3.6.3 SIRT1 in the signalling involved in actin reorganisation during spreading

FAK autophosphorylation on Y397 is associated with platelet activation downstream of the integrin $\alpha\text{IIb}\beta\text{3}$ (Hitchcock et al., 2008) and is crucial for early adhesion signalling (Hartwig, 2013; D. W. Zhou et al., 2021). Previous studies indicate that FAK mediates actin cytoskeleton rearrangement and platelet spreading (Izaguirre et al., 2001). According to the platelet acetylome (Aslan et al., 2015), FAK is acetylated in platelets, suggesting that SIRT1 could potentially regulate FAK autophosphorylation via deacetylation. As SRT1720 reduced platelet spreading, the effect of SIRT1 activation on FAK phosphorylation was investigated.

Platelets were treated with SRT1720 or vehicle, stimulated with CRP-XL and TRAP-6, lysed and tested by Western Blotting. Quantification of Y397-FAK phosphorylation revealed a significant increase in FAK autophosphorylation in the vehicle samples when platelets were activated with CRP-XL (Figure 4.10A) and TRAP-6 (Figure 4.10B) after 180 and 90 seconds, respectively. However, no changes were observed between the SRT1720-treated samples and vehicle control independently of the platelet agonist used and the incubation time, indicating that SIRT1 does not regulate platelet spreading through the modulation of FAK autophosphorylation.

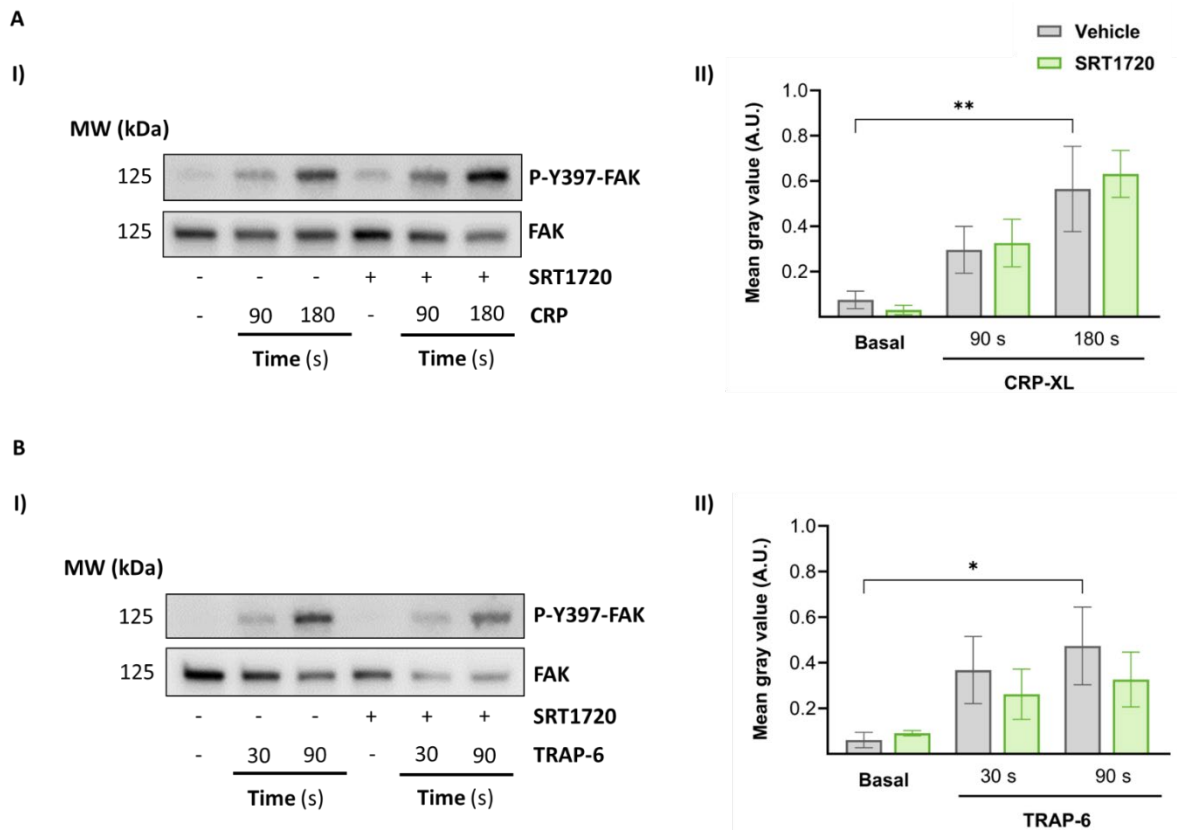


Figure 4.10. SIRT1 activation had no effect on platelet FAK autophosphorylation. Human washed platelets were pretreated for 30 min with or without SRT1720 (10 μ M) and activated with CRP-XL (1 μ g/mL) for 90 and 180 seconds or TRAP-6 (10 μ M) for 30 and 90 seconds. Platelets were lysed in SDS Laemmli sample buffer and Western Blotting was performed using an antibody against Y397-FAK. Total FAK was used as a loading control. Representative blots (I) and quantified data (II) are shown. Levels of phosphorylation were quantified and expressed as a ratio of the vehicle control (0.1% DMSO). Differences were analysed by One-way ANOVA. Data represent mean \pm SEM. ** $p < 0.01$ *** $p < 0.001$. N=4.

4.3.6.4 Investigating the effect of SIRT1 activation in actin polymerisation signalling

As explained in section 4.1 , cofilin-1 is a crucial ABP in the regulation of platelet microfilament turnover (Dasgupta and Thiagarajan, 2020). The binding of cofilin to actin filaments induces severing, releasing actin monomers from the fibres (Hartwig, 2013). In resting platelets, cofilin S3 is phosphorylated and, therefore, inactive. Upon “outside-in” signalling, cofilin is dephosphorylated and activated, accelerating actin polymerisation (Falet et al., 2005). Considering that SIRT1 activation reduced platelet F-actin production, we hypothesised that SIRT1 activation could reduce actin filament turnover through an increase in cofilin phosphorylation by the deacetylation of an intermediary protein, probably a kinase. The role of SIRT1 in cofilin activation was investigated by measuring the phosphorylation levels of cofilin S3 in SRT1720 and vehicle-treated platelet lysates in the presence or absence of CRP-XL and TRAP-6 by Western Blotting.

Quantification of S3-cofilin phosphorylation revealed no changes between the samples incubated with SRT1720 versus vehicle control regardless of the platelet agonist used and the incubation time (Figure 4.11). Vehicle-treated platelets activated with CRP-XL (Figure 4.10A) and TRAP-6 (Figure 4.10B) were used as positive controls for cofilin dephosphorylation. These findings indicate that SRT1720 does not prevent cofilin activation and that SIRT1 is modulating actin filament production through other mechanisms.

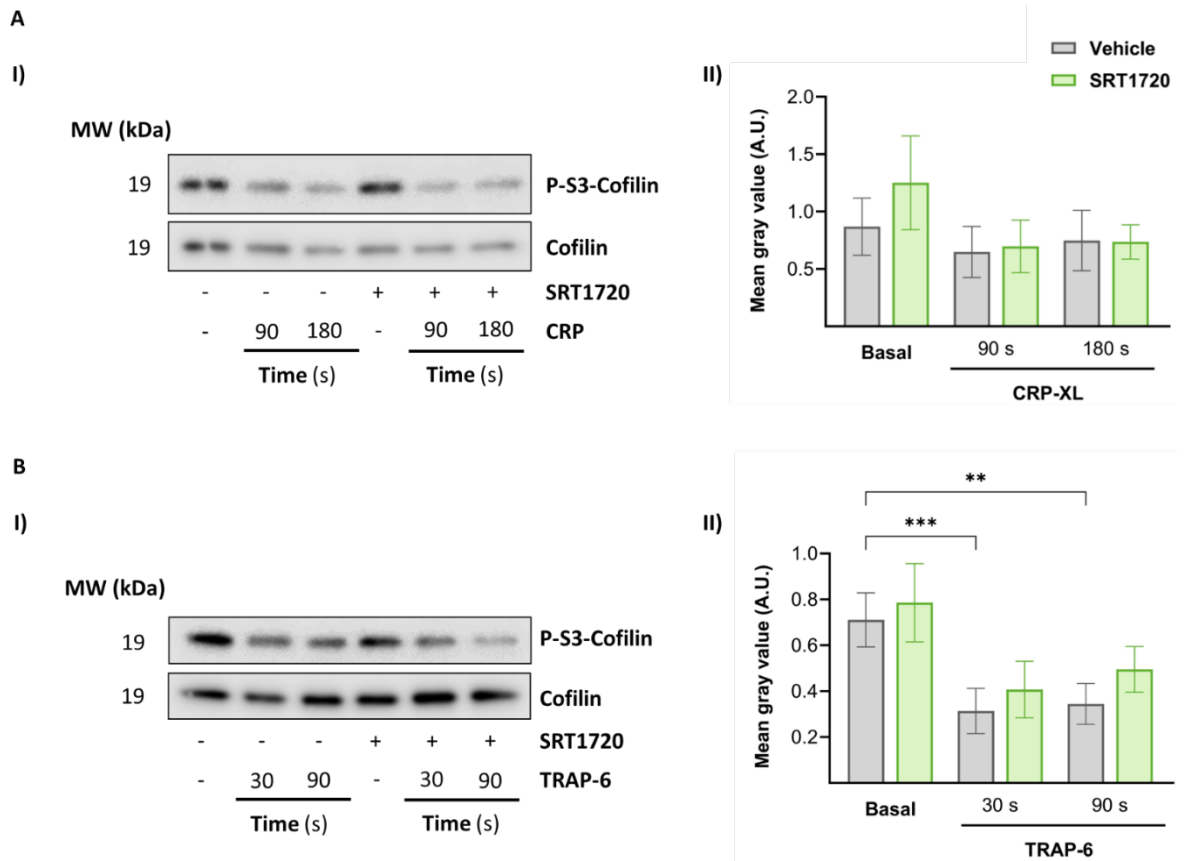


Figure 4.11. SIRT1 activation did not affect cofilin-1 phosphorylation levels in platelets. Human washed platelets were pretreated for 30 min with or without SRT1720 (10 μ M) and activated with CRP-XL (1 μ g/mL) for 90 and 180 seconds or TRAP-6 (10 μ M) for 30 and 90 seconds. Platelets were lysed in SDS Laemmli sample buffer and Western Blotting was performed using an antibody against S3 in cofilin-1. Total cofilin was used as a loading control. Representative blots (I) and quantified data (II) are shown. Levels of phosphorylation were quantified and expressed as a ratio of the vehicle control (0.1% DMSO). Differences were analysed by One-way ANOVA. Data represent mean \pm SEM. ** $p < 0.01$ *** $p < 0.001$. N=4.

4.4 Discussion

The results presented in this chapter demonstrate that SIRT1 is a key player in the regulation of platelet actin cytoskeletal rearrangements which leads to alterations in integrin activation, stable platelet adhesion, cytoskeletal rearrangements and platelet spreading and clot retraction. SIRT1 activation reduced platelet adhesion and spreading in static conditions on both collagen and fibrinogen, which correlates with the decrease in collagen-induced thrombus formation *in vitro* and the reduction in integrin $\alpha\text{IIb}\beta\text{3}$ activation reported in Chapter 3. SEM images of the platelet cytoskeleton show a disruption in microfilament reorganisation in both resting and activated platelets in the presence of SRT1720, preventing the formation of lamellipodia after TRAP-6 stimulation. Flow cytometry and Western Blotting experiments demonstrated that SIRT1 activation reduces platelet F-actin production, while microtubule formation and marginal band coiling remained unaffected. Due to the reduction observed in integrin $\alpha\text{IIb}\beta\text{3}$ activation and platelet spreading, the impact of SIRT1 activation in clot retraction was also studied. Our results show that SRT1720 decreased the later stages of clot retraction. Finally, to investigate the mechanism by which SIRT1 altered integrin $\alpha\text{IIb}\beta\text{3}$ activity and cytoskeletal rearrangement, related signalling events in platelets were explored by Western Blotting. The phosphorylation status of key cytoskeletal regulators, including Y773- β3 , S3-cofilin-1, Y397-FAK and S19-MLC2, were analysed in resting and activated platelets following SIRT1 activation. While the phosphorylation levels of all proteins tested changed upon platelet agonist stimulation, the presence of the SIRT1 activator SRT1720 had no effect. Therefore, the mechanism behind SIRT1 effects is yet to be elucidated.

As explained in section 3.1, this is the first study to evaluate the impact of SIRT1 selective activators on platelet function. However, the effect of resveratrol (Kulkarni and Cantó, 2015) quercetin (Hung et al., 2015; Jakaria et al., 2019) and pterostilbene (Cheng et al., 2016; Yanan Chen et al., 2021), which activate SIRT1 in addition to other proteins, have been previously tested in platelets. In line with our results, Michno et al. (2022) revealed that static adhesion to collagen was reduced by 85% in platelets treated with resveratrol compared to vehicle control (Michno et al., 2022) and Navarro-Nunez et al. (2010) showed that quercetin prevents platelet adhesion to

collagen and fibrinogen via the inhibition of SFKs (Navarro-Núñez et al., 2010). Pterostilbene not only reduced platelet adhesion to fibrinogen, supporting the decrease in “outside-in” signalling presented in this chapter, but also impaired spreading (Huang et al., 2021). A note of caution is due here, as the drugs mentioned target many other proteins that have been shown to regulate these processes in platelets, such as AMPK (Randriamboavonjy et al., 2010; Kim et al., 2018; Ren et al., 2018) and the PI3K/Akt axis (Guidetti et al., 2015; Kulkarni and Cantó, 2015; Zubčić et al., 2020; Tong et al., 2021).

Several reports have shown that SIRT1 regulates cytoskeletal rearrangements and cell migration in other cell types. It has previously been demonstrated that SIRT1 controls cell migration via the regulation of F-actin production in human umbilical vein endothelial cells (HUVECs) (Qin et al., 2019) and through the deacetylation of cortactin in podocytes (Motonishi et al., 2015), corneal epithelial cells (Lin et al., 2022) and myoblasts (N. Iwahara et al., 2022; Naotoshi Iwahara et al., 2022). However, in these nucleated cell lines, SIRT1 activation was associated with increased cell mobility and lamellipodia formation, while the effects observed in our spreading experiments are the opposite. As mentioned in section 4.1, SIRT1 can shuttle between the nucleus and the cytoplasm depending on stimuli (Yanagisawa et al., 2018). When this enzyme is located in the nucleus, it can regulate mRNA expression through epigenetics or by deacetylating several transcription factors, such as p53, NF- κ B and p300 (Yang et al., 2022). Whether observations made in nucleated cell types are driven by SIRT1-mediated changes in gene expression or non-genomic regulation is unclear. If SIRT1 is present in the cytoplasm, it will regulate different signalling pathways by modulating the activity of other proteins through deacetylation. In a previous study by Yang et al. (2019), wild-type (WT) SIRT1 and nuclear localisation signals (NLSs) mutated SIRT1 were overexpressed in ovarian carcinoma cells. Genetical alteration of the NLSs prevents the enzyme from travelling into the nucleus, abolishing SIRT1-mediated transcriptional effects. The cells that overexpressed WT SIRT1 presented an increased motility, while cell migration was considerably decreased in those that overexpressed NLS mutated SIRT1 compared to control (Yang et al., 2019). This is complementary to our observations that SIRT1 activation decreases platelet spreading. Platelets are a useful cell model to assess the

cytoplasmatic 'non-genomic' effect of proteins, as they lack a nucleus. Taken together, these studies demonstrate that SIRT1 modulates cell migration and spreading via different mechanisms depending on its subcellular location.

The importance of acetylation as a regulatory mechanism of platelet spreading and microfilament turnover has been highlighted in prior studies. Consistent with the results of our static spreading and actin polymerisation assays, Aslan et al. (2015) reported that pharmacological inhibition of the KAT p300, which reduces protein acetylation levels, leads to a decrease in F-actin and impaired platelet spreading on collagen and fibrinogen (Aslan et al., 2015). As mentioned in section 3.4, it has been demonstrated that SIRT1 regulates p300 function in other cell types (Bouras et al., 2005). Therefore, the effects observed in platelet spreading after SIRT1 activation could potentially be mediated through the inhibition of p300.

Other deacetylases, such as SIRT6 and HDAC6, have been directly associated with changes in platelet morphology. In murine platelets, activation of SIRT6 with UBCS039 dramatically reduced static platelet spreading on fibrinogen (Y. Liu et al., 2023) in the same way that SRT1720 decreased human platelet lamellipodia extension in our experiments. Work from Sadoul et al. revealed that murine HDAC6 KO platelets spread faster than WT, which again links lysine acetylation with enhanced filopodia and lamellipodia formation (Sadoul et al., 2012). These results support our research outcome, as we have associated a reduction in lysine acetylation via SIRT1 activation with a decrease in platelet spreading. In the future, performing a time course for 90 minutes might be useful to determine whether spreading is slowed down by SIRT1 activation or whether lamellipodia formation is frustrated permanently.

Regarding the impact of deacetylation in platelet microtubule rearrangement, the effect of HDAC6 in platelet tubulin homeostasis has also been investigated by Sadoul et al. (2012). The results from this study show that α -tubulin is acetylated in resting platelets, quickly deacetylated after contact with fibrinogen or collagen, which corresponds to the coiling and centralisation of the marginal band, and re-acetylated in spread platelets, when tubulin depolymerises (Cuenca-Zamora et al., 2019; Casey et al., 2020). They also demonstrated that deacetylation of tubulin after platelet activation is performed by HDAC6, as microtubules are hyperacetylated in murine

HDAC6 KO platelets (Sadoul et al., 2012). In other cell types, SIRT2 was proved to be a key player in the regulation of tubulin acetylation and, therefore, microfilament dynamics (North et al., 2003; Skoge et al., 2014). However, SIRT2 deacetylation of tubulin was not sufficient to compensate for the absence of HDAC6 in the KO models (K. Sadoul et al., 2012). Moreover, Moscardó et al. (2015) reported that tubulin K40 acetylation levels remained unaffected after SIRT1 and SIRT2 pharmacological inhibition (Moscardó et al., 2015), which supports the lack of effect on tubulin polymerization-depolymerisation cycles and marginal band coiling observed in our experiments with SRT1720-treated platelets. The data provided in this chapter along with the evidence in the literature show that platelet microfilament reorganisation is not affected by SIRT1 or SIRT2 modulation, as this process is primarily mediated by HDAC6.

The process of clot retraction is dependent on both integrin α IIb β 3 signalling and cytoskeletal rearrangements. Prior reports have identified that pterostilbene impairs this process through the modulation of integrin α IIb β 3 “outside-in” signalling, specifically inhibiting β 3, Src and FAK phosphorylation. However, whether these effects are SIRT1-mediated is yet unknown. In addition, similar to the effects observed with the SIRT1 activator in human platelets, SIRT6 pharmacological activation in murine platelets reduced clot retraction (Y. Liu et al., 2023), suggesting that the members of the SIRT family might be important regulators of fibrin clot contraction and, therefore, the use of SIRT1 activators could be a novel therapeutic approach to reduce the density of the clot and enhance the delivery of fibrinolytic drugs (Henderson et al., 2018).

To investigate the mechanism by which SIRT1 activation alters platelet function, the effect of this deacetylase in platelet signalling was explored in this chapter. We have demonstrated that SRT1720 reduced platelet spreading and clot retraction, which are dependent upon “outside-in” signalling. Phosphorylation of Y773 in the β 3 tail is a hallmark of integrin α IIb β 3 signal transduction after activation through fibrinogen binding. Therefore, evaluating the Y773 β 3 phosphorylation levels would indicate whether SIRT1 affects the ability of integrin α IIb β 3 to signal. The lack of changes in β 3 phosphorylation in the SRT1720 samples indicates that the decrease in integrin α IIb β 3 activation associated with SIRT1 activation in Chapter 3 is caused by the effect

on microfilament dynamics, as it has been reported previously with other disruptors of the actin cytoskeleton, such as jasplakinolide and cytochalasin D (Kriek et al., 2022).

Since platelet adhesion and spreading were impaired independently of the use of collagen or fibrinogen as an adhesive surface, the impact of SIRT1 activation was tested in FAK autophosphorylation, which is a crucial step in early platelet adhesion signalling and occurs downstream GPVI and integrin α IIb β 3 activation (Guidetti et al., 2019). Evidence in the literature indicates that pterostilbene reduces integrin β 3 and FAK phosphorylation, which contributed to the rationale behind the investigation of the effect of SRT1720 on these targets (Huang et al., 2021). In contrast to this study by Huang et al. (2021), no alteration in β 3 or FAK phosphorylation was observed following treatment with SRT1720. Our results, therefore, indicate that the decrease in β 3 and FAK phosphorylation reported by Huang et al. (2021) is not mediated by SIRT1 but by other targets of pterostilbene.

To investigate the signalling events behind the decrease in F-actin caused by SIRT1 activation, S3 cofilin phosphorylation was evaluated, as this is required for the release of actin monomers from the microfilaments (Falet et al., 2005; Hartwig, 2013) and it is the most abundant ABP in platelets (Dasgupta and Thiagarajan, 2020). After the initiation of “outside-in” signalling, different kinases, such as LIM-kinase (LIMK) dephosphorylate and activate cofilin, accelerating actin polymerisation (Pandey et al., 2006). We hypothesised that SIRT1 could potentially deacetylate one of these intermediate kinases, affecting cofilin phosphorylation. The results from our research demonstrated that SIRT1 activation does not affect cofilin phosphorylation levels. However, a potential crosstalk between SIRT1 and cofilin cannot be discarded, as cofilin is acetylated in platelets (Aslan et al., 2015) and the regulation of the function of this protein by deacetylation has not been investigated previously. Further work involving the coimmunoprecipitation of SIRT1 and cofilin and the detection of acetylated residues is needed to elucidate whether SIRT1 modulates cofilin's ability to bind to microfilaments and initiate severing.

As explained in section 4.1, actin, cortactin, cofilin, Arp2/3 and gelsolin contain several lysine-acetylated residues in platelets. Aslan et al. (2015) showed that pharmacological inhibition of the SIRT1 counterpart p300 leads to a decrease in F-

actin production and spreading through a reduction in actin, filamin and cortactin acetylation levels (Aslan et al., 2015). Given that the decrease in platelet spreading linked to SIRT1 activation was also mediated by a reduction in F-actin, we hypothesised that SIRT1 was altering microfilament homeostasis either through deacetylation of β -actin or an ABP, which potentially disrupts its interaction. However, one of the main limitations of this study is the lack of anti-acetyl lysine antibodies against these targets. Additional research is needed to understand whether SIRT1 interacts with p300 or any of the mentioned ABPs via coimmunoprecipitation of SIRT1 with these proteins and assessment of lysine acetylation levels.

Although the evidence in the literature demonstrates that SIRT1 modulates p300 (Bouras et al., 2005) and cortactin (Motonishi et al., 2015; N. Iwahara et al., 2022; Y. Lin et al., 2022) function via deacetylation in other cell types and that these two proteins are key in the regulation of platelet actin cytoskeletal dynamics (Aslan et al., 2015), no high-quality antibodies against the acetylated forms of these enzymes have been commercialised. Therefore, more time-consuming and costly alternatives must be used to evaluate the effect of SRT1720 on the acetylation level of these targets, such as high-resolution mass spectrometry (Schilling et al., 2019) or immunoprecipitation of the potential SIRT1 targets and detection of the lysine-acetylated residues using a pan-acetylation antibody (Horita et al., 2018). Considering that no SIRT1 targets have been identified in platelets so far using a Western Blotting approach, performing these techniques will be evaluated in the future to elucidate the mechanism behind the numerous effects in platelet function observed in this research project.

Finally, we have demonstrated that the attenuation observed in the late stage of clot retraction under SIRT1 activation is due to the effects of this enzyme in platelet spreading rather than the modulation of myosin II phosphorylation.

In chapters 3 and 4, the role of SIRT1 in platelet function and signalling was explored in depth, indicating that SIRT1 activation reduces platelet aggregation and *in vitro* thrombus formation through the disruption of actin cytoskeletal dynamics, although the signalling molecules involved in these events have not been discovered yet. However, the main objective of this project is to study the effect of SIRT1 in

haemostasis and thrombus formation from a holistic approach, in which the key components of the vascular system are considered. Therefore, in the next chapter, the impact of SIRT1 activation on endothelial function will be described.

Chapter 5. Protective effects of SIRT1 on endothelial function

5.1 Introduction

Inflammation, which could be caused by an infection, a mechanical injury or constant exposure to free radicals (Cimmino et al., 2023), induces endothelial dysfunction and is recognised as the major driver of atherosclerosis (Libby, 2021; Kong et al., 2022). Endothelial dysfunction is defined as impaired endothelial-dependent vasorelaxation in response to stimuli, such as hypoxia or shear stress (Lüscher and Corti, 2004). The hallmarks of endothelial dysfunction are oxidative stress, increased cell senescence, enhanced transcription of proinflammatory genes via NF- κ B activation and reduced NO levels (Kitada et al., 2016; Bettioli et al., 2023).

NO is a soluble vasodilatory molecule that prevents thrombus formation through the inhibition of platelet activation and adhesion to the endothelium (Russo et al., 2023). In endothelial cells, NO is produced by eNOS (Cylwik et al., 2005; Förstermann and Sessa, 2012). The lack of NO production in the presence of abundant substrate could be caused by ROS-induced eNOS uncoupling (Janaszak-Jasiecka et al., 2023), a reduction of eNOS expression or a decrease in eNOS activity via posttranslational modifications, such as acetylation (Heiss and Dirsch, 2014).

As explained in section 1.6, the endothelium is a key regulator of haemostasis and thrombosis. The reduction in NO bioavailability and the secretion of proinflammatory cytokines characteristic of endothelial dysfunction enhance platelet adhesion, coagulation and leukocyte recruitment, contributing to the development of atherosclerosis and increasing the thrombotic risk (Y. Shao et al., 2020; K. Neubauer and B. Zieger, 2022).

SIRT1 is present in all elements of the vasculature, including the endothelium (Man et al., 2019). Different studies have identified that SIRT1 has vasculoprotective properties through the reduction of endothelial inflammation and oxidative stress (Csiszar et al., 2008; Kao et al., 2010; S. H. Chan et al., 2017). SIRT1 can shuttle

between the nucleus and the cytoplasm (Tanno et al., 2007) and performs different functions depending on its subcellular location.

In the nucleus, SIRT1 regulates the function of transcription factors and causes epigenetic changes through deacetylation. SIRT1 prevents NF- κ B activation through the deacetylation of Lys310 in the p65 subunit (Wu et al., 2022), which inhibits the expression of proatherogenic and prothrombotic genes, such as TNF- α (McKellar et al., 2009), IL-6 (Gager et al., 2020), COX-2 (Burleigh et al., 2002) and thrombomodulin (Mussbacher et al., 2019).

Most of the protective effects of SIRT1 against oxidative stress are thought to be mediated by the deacetylation and activation of the forkhead box O class (FOXO) transcription factors, namely FOXO3 (Maiese, 2021), which increases the expression of catalase and manganese-superoxide dismutase (Zhao and Liu, 2021). Several studies also reported that SIRT1 increases the production of nuclear factor erythroid 2-related factor 2 (Nrf2), a transcription factor that modulates the expression of other anti-oxidant enzymes (Patel et al., 2022). Therefore, SIRT1 activation could be a novel strategy to combat the ROS-induced endothelial dysfunction that leads to atherosclerosis and thromboinflammation.

Moreover, the mutual regulation of SIRT1 and eNOS via a positive feedback loop has been reported in the literature. One of the possible mechanisms through which SIRT1 controls NO production in endothelial cells is the induction of eNOS expression. Research by Wallerath et al. (2002) revealed that treating HUVECs with resveratrol leads to an increase in eNOS mRNA levels (Wallerath et al., 2002). In line with this study, Xia et al. (2013) demonstrated that knocking down SIRT1 prevented the upregulation of eNOS mRNA and protein by resveratrol in HUVECs. These studies indicate that SIRT1 activation is one of the potential mechanisms by which resveratrol exerts protective effects against endothelial dysfunction (Ning Xia et al., 2013). Considering this evidence, SIRT1 would not only prevent eNOS uncoupling through a reduction of oxidative stress but also directly increase NO production via upregulation of eNOS.

Regarding the effects of SIRT1 in the cytoplasm, work from Bai et al. (2016) demonstrated that SIRT1 prevents endothelial senescence via deacetylation of Liver

kinase B1 (LKB1), which induces its proteasomal degradation (Kitada et al., 2016; Presneau et al., 2017). Studies using a murine SIRT1 knock down model, associated reduced SIRT1 levels with an accumulation of LKB1 and adverse arterial remodelling (B. Bai et al., 2016). Also, investigations by Luo et al. (2019) demonstrated that SIRT1 pharmacological activation with SRT1720 in a murine model of hypoxia enhanced autophagy through AMPK activation, increasing cell survival (G. Luo et al., 2019). These investigations indicate that SIRT1 prevents endothelial damage associated with ageing, which is also a major risk factor for the development of atherosclerosis, through a decrease in senescence and the maintenance of homeostatic levels of autophagy (Ministrini et al., 2021).

Apart from the increase in eNOS protein expression already mentioned in this section, SIRT1 activation can also increase NO production through activation of eNOS via deacetylation at Lys496 and Lys506 in the cytoplasm of HUVECs (Mattagajasingh et al., 2007).

Moreover, different *in vitro* and *in vivo* studies have associated SIRT1 downregulation with an increase in vascular permeability through a reduction in tight junction (TJ) proteins. Data by Stamatovic et al. (2019) demonstrated that decreasing SIRT1 expression in brain microvascular endothelial cells (BMEC) using silencing RNA (siRNA) increases barrier permeability through a decrease in claudin-5 protein expression (Stamatovic et al., 2019). SIRT1 downregulation in HUVECs also caused an increase in the permeability of the cell monolayer, while activation of SIRT1 with SRT1720 prevented LPS-induced hyperpermeability and recovered VE-cadherin expression and distribution (W. et al., 2017).

In brain endothelial cells specific SIRT1 KO mice, vascular permeability was considerably increased. SIRT1 pharmacological activation with SRT1720 reduced the permeability of the mouse brain endothelial layer and rescued the protein levels of claudin-5 (Stamatovic et al., 2019). Moreover, Cuiping et al. (2019) evaluated the role of SIRT1 in an acute lung injury (ALI) mouse model based on intratracheal administration of LPS. In line with the work by Stamatovic et al. (2019), claudin-5 expression was decreased, alongside TJ proteins 1 and 2, and treatment with SRT1720 rescued both lung permeability and all TJ proteins expression (Cuiping et al., 2019). Considering the promising effects of SIRT1 activation or overexpression in the

homeostasis of monolayers formed by other endothelial cell types, the role of SIRT1 in the permeability of the arterial endothelium should be investigated.

Consistently with the results in platelets presented in Chapter 4 of this thesis, a study by Ruijie et al. (2019) demonstrated that SIRT1 has a crucial role in the regulation of F-actin levels in HUVECs, affecting cell migration (Ruijie et al., 2019). SIRT1 regulation of actin polymerisation was also observed in other cell nucleated cell types, such as myocytes (Naotoshi et al., 2022), corneal epithelial cells (Y. Lin et al., 2022) and podocytes (Motonishi et al., 2015).

All these investigations demonstrate that SIRT1 plays a key role in endothelial function. However, the impact of SIRT1 activation on the antithrombotic properties of the arterial endothelium in the context of inflammation has not been investigated yet. Two recent studies have evaluated the antithrombotic effects of the P2Y12 receptor blocker prasugrel and aspirin eugenol ester (AEE) beyond their antiplatelet activity (Shen et al., 2019; Gomaa et al., 2021). Prasugrel recovered SIRT1 expression in rat hippocampus after ischaemia-reperfusion injury (Gomaa et al., 2021) and AEE prevented the decrease in SIRT1 levels in platelets associated with thrombin stimulation. Although the mechanism is still unknown, this effect might be due to a reduction in SIRT1 degradation (Shen et al., 2019). In line with this evidence, prasugrel and AEE might reduce thrombotic risk by upregulating SIRT1 in the cells and tissues surrounding a thrombotic event, apart from a reduction in platelet aggregation through traditional and well-known mechanisms. Even though the mentioned studies were not performed in endothelial cells, these findings suggest that SIRT1 is important in controlling thrombus formation and that SIRT1 activators may represent a promising new source of anti-thrombotic therapies. Therefore, SIRT1 could potentially be a novel target to treat and prevent endothelial thromboinflammation through a plethora of nuclear and cytoplasmatic effects.

5.2 Hypothesis, chapter aim and objectives

Considering the number of reports in the literature supporting that SIRT1 could prevent endothelial dysfunction through deacetylation of several substrates on a nuclear and cytoplasmatic level, we hypothesised that SIRT1 activation could maintain a healthy endothelial phenotype in the presence of inflammatory stimuli, reducing the risk thrombosis.

The aim of this chapter is to elucidate the effect of SIRT1 activation on the function of endothelial cells in the presence and absence of inflammatory stimuli. To investigate this, the selective SIRT1 agonist SRT1720 was used, together with commercially available HCAEC. The following objectives were addressed:

1. Demonstrate the presence of SIRT1 in HCAEC.
2. Assess the toxicity of SRT1720 in HCAEC.
3. Determine the effect of SIRT1 activation on a variety of HCAEC functions, including NF- κ B nuclear translocation, cell migration, and cell permeability.
4. Establish a reproducible inflammatory response in HCAEC, using inflammatory mediators relevant to the study of atherothrombosis.
5. Assess whether SIRT1 activation provides endothelial-dependent protection against thrombus formation using a novel endothelialised *in vitro* model of thrombosis.
6. Determine the transcriptional effects of SRT1720 on key endothelial regulators of thrombosis and haemostasis in HCAECs

5.3 Results

5.3.1 SIRT1 is present in HCAEC

Before investigating the effects of SIRT1 activation on endothelial cell function, it was first necessary to confirm the expression of this enzyme in endothelial cells and determine whether this changes under inflammatory conditions. HCAEC were selected as a model of the arterial endothelium and SIRT1 protein expression was evaluated using microscopy in healthy and TNF- α -treated cells.

HCAEC were treated with TNF- α (10 ng/mL) or vehicle (0.1% PBS) for 20 and 60 minutes. Samples were fixed, incubated with a primary antibody against SIRT1 and stained with an Alexa488 secondary antibody, rhodamine-phalloidin and DAPI. Images were taken in the STELLARIS 5 confocal microscope using the 40x oil immersion objective.

The presence of SIRT1 in HCAEC was demonstrated (Figure 5.1A). Comparison of Alexa488 fluorescence intensity between conditions showed that acute inflammation induced with TNF- α for 20 and 60 minutes did not change SIRT1 protein expression levels significantly (Figure 5.1B). In line with the literature, these results suggest that the reduced SIRT1 expression observed in the serum and vascular smooth muscle cells of patients at high risk of cardiovascular disease is a result of chronic inflammation (Gorenne et al., 2013; Kitada and Koya, 2013) and, therefore, our *in vitro* model of endothelial inflammatory damage should evaluate SIRT1 effects using longer treatments with TNF- α and other damage molecules.

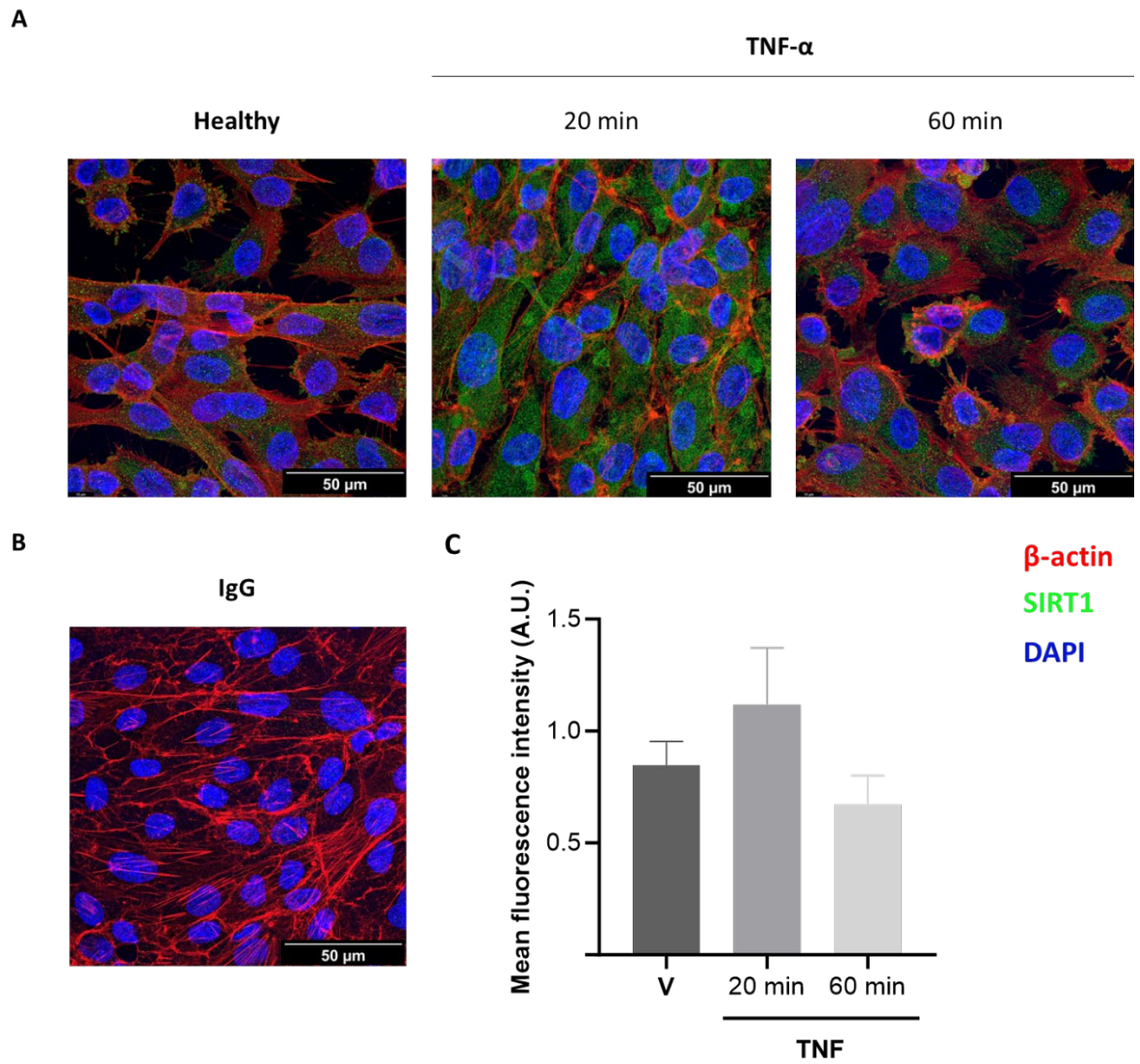


Figure 5.1. SIRT1 is present in HCAEC, but its expression does not significantly change with an acute TNF- α treatment. HCAEC were treated with TNF- α (10 ng/mL) or vehicle (V, 0.1% PBS) for 20 and 60 minutes (A). Samples were fixed, incubated with a primary antibody against SIRT1 and stained with an Alexa488 secondary antibody, rhodamine-phalloidin and DAPI. An IgG control was included in the assay (B). Images were taken in the STELLARIS 5 confocal microscope using the 40x oil immersion objective. SIRT1 mean fluorescence intensity was quantified with the ImageJ software and changes in the expression of this enzyme were compared between conditions by One-Way ANOVA (C). Data represent mean \pm SEM. N=3.

5.3.2 The effect of SRT1720 on HCAEC viability

The results explained in the previous section demonstrated that acute treatments with TNF- α do not affect SIRT1 expression. To investigate whether longer treatments with inflammatory stimuli impact endothelial function, in the presence and absence of SRT1720, the toxicity of SRT1720 on HCAECs had to be evaluated first. In other cell types, such as cardiomyocytes (G. Luo et al., 2019) or chondrocytes (Sacitharan et al., 2020), autophagy has been reported as one of the effects of SRT1720. To test whether long treatments with this drug could affect HCAEC phenotype or viability, cells were treated with SRT1720 at 10 μ M, which is the concentration used in our previous experiments with platelets, for 24 hours. After fixing and staining the cells with Rhodamine Phalloidin and DAPI, images taken with the 20x objective of the STELLARIS 5 confocal microscope showed changes in cell morphology, a reduction in cell size and the presence of more gaps in the cell monolayer under SRT1720 10 μ M treatment (Figure 5.2AII) versus vehicle control (Figure 5.2AI).

Considering these observations, the viability of HCAEC treated with different doses of SRT1720 (0.1, 0.3, 1, 3 and 10 μ M) was evaluated using an MTS assay. Cells were incubated with the SIRT1 activator for 24 (Figure 5.2BI), 48 (Figure 5.2BII) and 72 (Figure 5.2BIII) hours. Following the manufacturer's instructions, MTS reagent was added to the cells and incubated for 2 hours. Absorbance was measured at 490 nm and the percentage of cell viability was calculated considering the absorbance of the vehicle as the 100% viability, confirming that SRT1720 at 10 μ M reduces HCAEC viability.

The results of these experiments demonstrate that nucleated primary cells are more sensitive to SRT1720 than platelets and indicate that lower doses of this drug should be used in our experiments with HCAEC. Therefore, functional experiments were performed to elucidate which concentration of SRT1720 should be used to evaluate the role of SIRT1 in endothelial function without triggering autophagy, which is explained in detail in the following section.

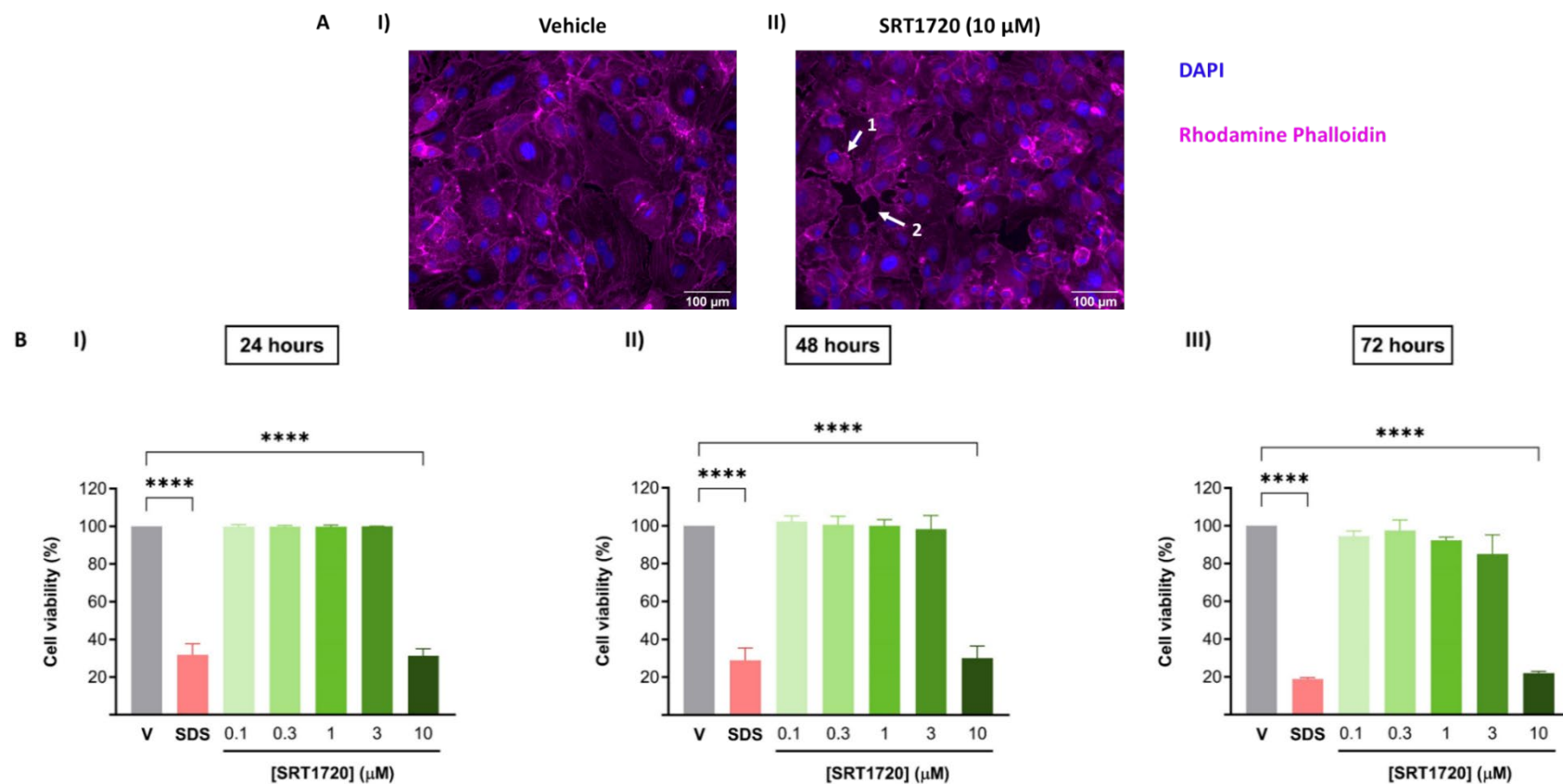


Figure 5.2. SRT1720 10 μ M decreases HCAEC viability. HCAEC were treated with SRT1720 10 μ M for 24 hours, fixed and stained with DAPI and Rhodamine Phalloidin. Samples were imaged using the 20x objective of the STELLARIS 5 Confocal microscope. Representative images are shown (A). In Figure AII, it can be observed that SRT1720 10 μ M reduced the size of the cells (1) and led to gaps in the cell monolayer (2), indicating that high concentrations of this drug could affect cell viability. To test this, HCAEC were incubated with different concentrations of SRT1720 (0.1 - 10 μ M) or vehicle (V, 0.1% DMSO). After 24 (A), 48 (B) or 72 hours (C) of treatment, an MTS assay was performed. SDS at 0.1% was used as a cell death positive control. According to the kit recommendations, MTS reagent was added to every condition and incubated for 2 hours at 37°C. Absorbance at 490 nm was measured. The absorbance of the vehicle was considered 100% of cell viability. Conditions were measured in duplicate. Data represent mean \pm SEM. ****p<0.0001. N=3.

5.3.3 The role of SIRT1 in endothelial cell function

In the following section, the impact of SIRT1 activation will be explored in HCAEC by assessing the effect of SRT1720 in different functional assays.

5.3.3.1 The effect of SRT1720 on NF- κ B nuclear translocation induced by TNF- α

As explained in the introduction to this chapter, SIRT1 inhibits NF- κ B activation and nuclear translocation during inflammation via deacetylation of the p65 subunit (Yeung et al., 2004). Before evaluating the effects of SIRT1 on the endothelial function and transcriptome, a range of doses of SRT1720 were tested in an NF- κ B subcellular location assay to assess which concentration should be used in the next experiments.

HCAEC were cultured in a 96-well plate and NF- κ B nuclear translocation was induced by incubating them with TNF- α (10 ng/mL) for 20 minutes. Then, SRT1720 (0.1, 0.3, 1, 3 and 10 μ M) or vehicle (0.1% DMSO) were added to the plate. After 4 hours, samples were fixed and incubated with an NF- κ B primary antibody for 1 hour. Nuclei were stained with DAPI and an Alexa 488 labelled secondary antibody was used for visualization of NF- κ B. Images were taken with the 20x objective of the CELENA[®] S Logos Biosystems microscope. The MFI in the green channel in the nuclear area and the total MFI were quantified using ImageJ. The nuclear and total MFI ratio was normalised to the vehicle healthy control (Figure 5.3AI) and compared between conditions (Figure 5.3AII) using One-Way ANOVA (Figure 5.3B).

As expected, TNF- α increased the amount of NF- κ B in the nucleus of HCAEC (B). However, after adding SRT1720 to the media 4 hours post-TNF- α treatment, NF- κ B did not return to the cytoplasm (Figure 5.3B), suggesting that SIRT1 mainly prevents the entrance of this transcription factor into the nucleus via deacetylation, rather than inactivating it in the nucleus and inducing its translocation back to the cytoplasm.

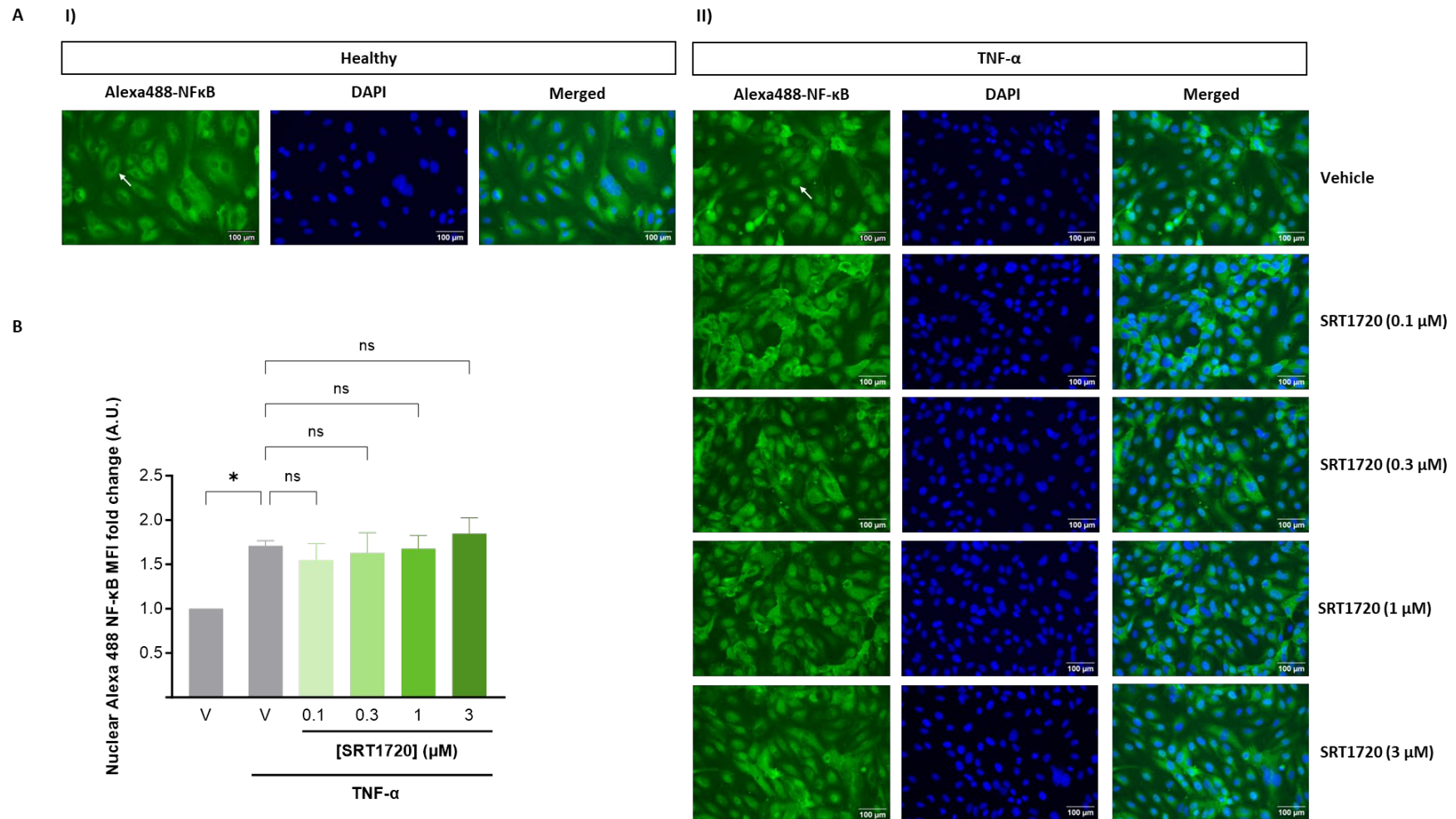


Figure 5.3. SIRT1 activation for 4 hours failed to prevent NF- κ B nuclear translocation. HCAEC were cultured in a 96-well plate and dysfunction was induced with TNF- α (10 ng/mL) for 20 min. SRT1720 (0.1 – 3 μ M) or vehicle (0.1% DMSO) were added to the wells for 4 h. HCAEC were fixed, permeabilised and incubated with an NF- κ B primary antibody. Nuclei were stained with DAPI and NF- κ B was labelled using an Alexa 488 secondary antibody. Images were taken with the 20x objective of the CELENA[®] S microscope. Using ImageJ, masks of the nuclei were created and the median green fluorescence intensity in that area was quantified to measure NF- κ B nuclear presence. Differences were compared by One-Way ANOVA. Data represent mean \pm SEM. * p <0.05. N=3.

5.3.3.2 High concentrations of SRT1720 decrease HCAEC migration

Previous studies have demonstrated that SIRT1 plays a key role in cell migration, reducing the invasive potential of cancer cells (B. L. Tang, 2010) and, as shown in Chapter 3 and Chapter 4 of this report, platelet adhesion and spreading. In a physiological context, endothelial migration is important to allow angiogenesis and vessel reparation upon an injury (Jerka et al., 2024). Recent investigations have shown that dysregulation of actin and tubulin dynamics leads to reduced collective endothelial migration, altering wound healing. Considering that SRT1720 disrupted actin cytoskeleton dynamics in platelets, the effect of this SIRT1 activator was evaluated in HCAEC using a cell migration assay.

HCAEC were cultured in 2-well Ibidi silicone inserts in a clear-bottomed 24-well plate until confluent. Then, the inserts were removed to create a gap and cells were treated with SRT1720 at 0.3, 1 and 3 μM or vehicle (0.1% DMSO). Cell migration was assessed by taking pictures every 10 minutes over 20 hours using the 20x objective of the HoloMonitor Live Cell Imaging System (Figure 5.4C). The percentage of the area covered by the cells at every time point (Figure 5.4AI) and the percentage of gap closure in the middle of the assay (Figure 5.4BI) and at the end (Figure 5.4BII) were measured using the Wound-Healing analysis of the HoloMonitor App Suite cell imaging software. The Area Under the Curve (AUC) was calculated from the percentage of area coverage using the ImageJ software.

Only a high dose of SRT1720 (3 μM) produced a significant decrease in HCAEC migration, represented by a reduction in the area under the curve (Figure 5.4AII) and the gap closure percentage after both 10 (Figure 5.4BI) and 20 hours (Figure 5.4BII). These results indicate that SIRT1 might be involved in the regulation of the HCAEC cytoskeleton, as the viability of the cells is not affected when using SRT1720 3 μM but the motility is dramatically reduced.

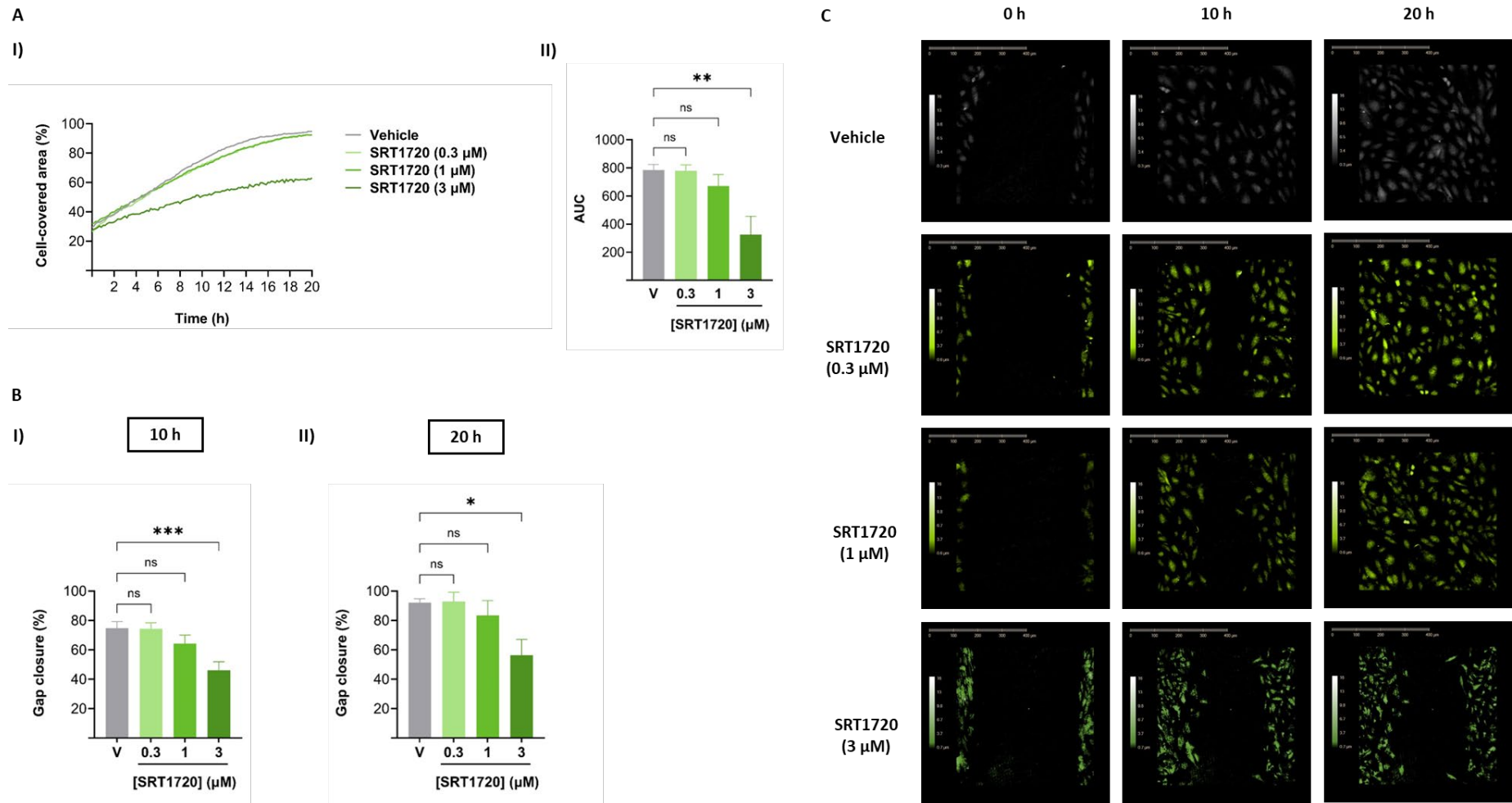


Figure 5.4. SRT1720 reduced HCAEC migration in a dose-dependent way but only significantly at 3 μM. Cells were cultured in Ibdid 2-well inserts in a clear-bottomed 24-well plate until confluency. On the day of the assay, the inserts were removed and media supplemented with SRT1720 (0.3, 1 or 3 μM) or vehicle (0.1% DMSO) was added. Cell migration was monitored for 20 hours by taking images every 10 minutes using the 20x objective of the HoloMonitor Live Cell Imaging System. Images were analysed using the HoloMonitor App Suite cell imaging software (AI, BI, BII) and ImageJ (AII). Representative images of the gap after 10 and 20 hours are shown (C). Data represent mean ± SEM. * $p < 0.05$, ** $p < 0.01$, *** $p < 0.001$. N=5.

5.3.3.3 SIRT1-mediated decrease of HCAEC migration is independent of actin polymerisation

Due to the reduction in F-actin levels in SRT1720-treated platelets reported in section 4.3.3 , it was hypothesised that the decrease observed in HCAEC migration could be caused by a disruption in actin polymerisation.

As HCAEC are adherent cells, changes in filamentous actin were tested using microscopy. In platelets, actin polymerisation was only prevented in the presence of an inducer of F-actin production, such as TRAP-6, but not in non-activated platelets. Therefore, HCAEC were cultured in a 96-well plate, treated with different concentrations of SRT1720 (0.1, 0.3, 1 and 3 μ M) or vehicle (0.1% DMSO) and dysfunction was induced with TNF- α (10 ng/mL) for 24 hours, as Koukouritaki et al. (1999) demonstrated that this cytokine increases F-actin levels in glomerular endothelial cells (Koukouritaki et al., 1999). A vehicle condition without TNF- α was also included in the assay as a negative control, to test whether F-actin is increased in the TNF- α condition versus vehicle control. Cells were fixed and stained with DAPI and rhodamine phalloidin. Images were taken with the 10x objective of the CELENA[®] S Logos Biosystems microscope (Figure 5.5A). Rhodamine mean fluorescence was quantified on ImageJ and normalised by the nuclei count (Figure 5.5B).

No significant changes in F-actin levels were observed neither in the vehicle-treated HCAEC in the presence of TNF- α nor the SRT1720-treated HCAEC. Therefore, it can be concluded that TNF- α failed to induce F-actin production and that, in line with the results in platelets, SRT1720 does not disrupt actin polymerisation when actin polymerisation is not increased.

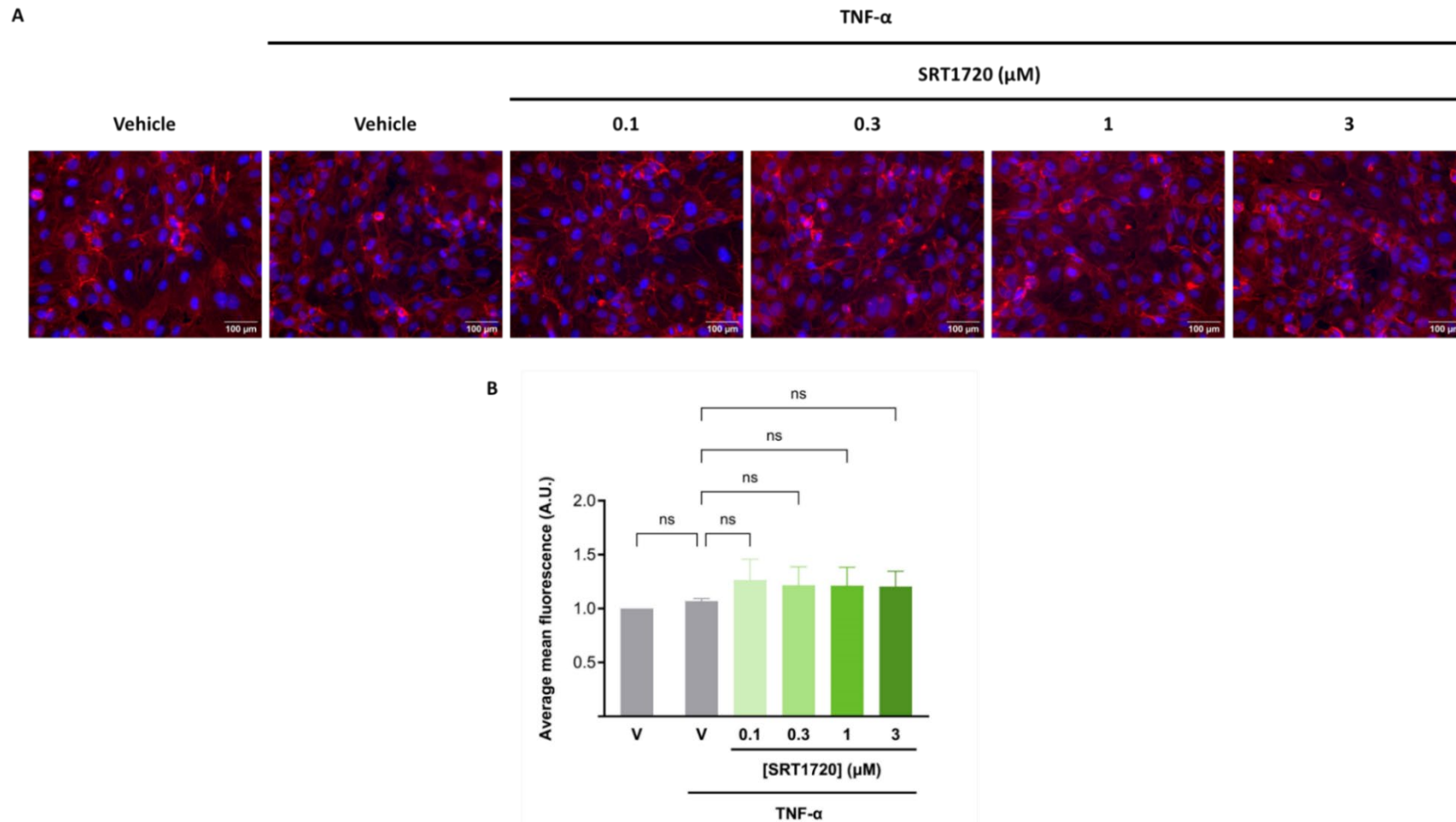


Figure 5.5. SRT1720 does not alter actin polymerisation in HCAEC. Cells were treated with a range of SRT1720 concentrations (0.1 – 3 μ M) or vehicle (V, 0.1% DMSO) and endothelial dysfunction was induced with TNF- α (10 ng/mL). A healthy vehicle control was also included in the assay. Samples were stained with DAPI and rhodamine phalloidin and pictures were taken in the 10x objective of the CELENA[®] S microscope. Representative images are shown (A). The number of nuclei and the rhodamine mean fluorescence were quantified using ImageJ. The fluorescent signal was normalised by the nuclei count (B). No changes in actin polymerisation were observed between HCAEC treated with SRT1720 and vehicle conditions. Data represent mean \pm SEM. N=3.

5.3.3.4 SRT1720 reduces LPS-induced HCAEC permeability

Vascular permeability, which is increased in inflammatory diseases such as atherosclerosis (Botts et al., 2021), is regulated by the interplay of endothelial tight junctions and the cytoskeleton, as these determine the morphology and motility of the endothelial cells (Aghajanian et al., 2008). Considering that incubating HCAEC with SRT1720 caused a decrease in cell migration, it was necessary to evaluate whether this SIRT1 activator could have an effect on the permeability of a confluent monolayer of HCAEC.

HCAEC permeability was evaluated using an *in vitro* vascular permeability assay commercialised by Merck. Cells were cultured for 72 hours in inserts that contain a membrane which allows the exchange of FITC dextran between the media in the inserts and the media in a well of a 96-well plate. HCAEC were treated with SRT1720 (1 μ M) or vehicle (0.1% DMSO) in the presence or absence of TNF- α (1 μ g/mL) or LPS (1 μ g/mL) for 24 hours. FITC dextran was added to the plate following the kit instructions and the FITC fluorescence of the inserts and the plate was measured in the GloMax microplate reader. The FITC fluorescent signal in the plate is directly proportional to the grade of permeability of the HCAEC monolayer, as healthy confluent cells would prevent the exchange of dextran between the two compartments.

TNF- α at 1 μ g/mL caused no significant changes in cell permeability (Figure 5.6A), while LPS increased the permeability of the HCAEC layer by 50% (Figure 5.6B). SRT1720 at 1 μ M, which did not significantly affect HCAEC migration (Figure 5.4), prevented LPS damage of the cell sheet, which was represented by a decrease in cell permeability (Figure 5.6B).

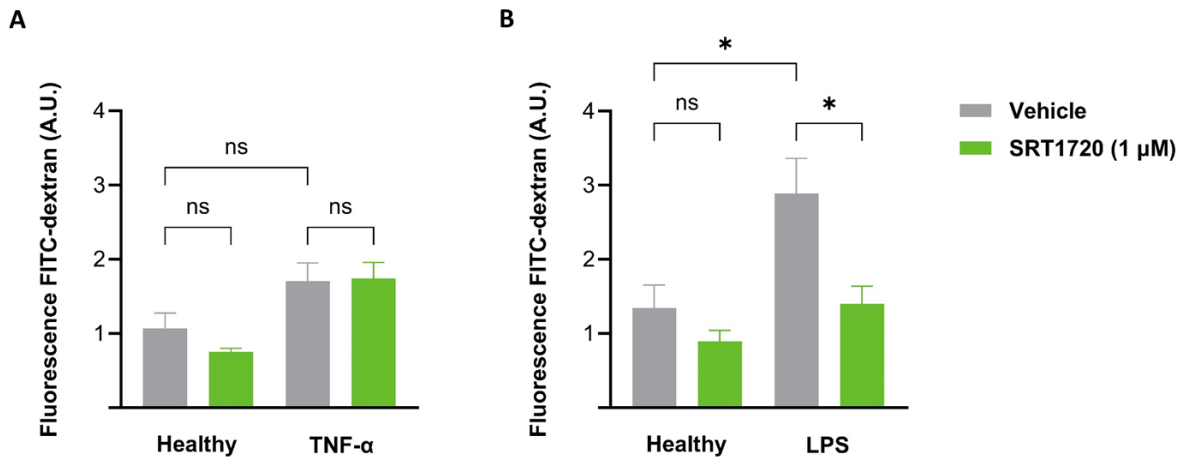


Figure 5.6. SRT1720 protected HCAEC from LPS damage by reducing the permeability of the cell monolayer. HCAEC were seeded in 96-well inserts until confluency and treated with SRT1720 (1 μM) with and without TNF-α at 1 μg/mL (A) or LPS at 1 μg/mL (B) for 24 hours. FITC-dextran was added to the inserts according to the indications of the *in vitro* vascular permeability kit from Merck and incubated for 2 hours. The FITC fluorescence of the media in the inserts and the bottom well was measured in the GloMax microplate reader and compared between conditions by One-Way ANOVA. N=4.

5.3.3.5 Testing different inflammatory mediators to establish a robust and reproducible inflammatory response in HCAEC

To determine whether SIRT1 activation can be protective against endothelial dysfunction in atherosclerosis, it was necessary to develop a model of inflammation in HCAECs that resulted in robust and reproducible activation of endothelial cells. Therefore, the impact of four different disease-relevant dysfunction inducers on HCAEC gene expression was evaluated.

HCAEC were serum starved O/N and treated with IL-6 (50 ng/mL), LPS (100 ng/mL), TNF-α (10 ng/mL), H₂O₂ (100 μM) or PBS for 24 hours. After a PBS wash, RNA lysates were prepared, from which cDNA was generated. Using RT-qPCR, the mRNA expression of SIRT1 (Figure 5.7A); endothelial activation markers, such as VCAM1 (Figure 5.7B) and PTGS2 (Figure 5.7C); and NOS3 (Figure 5.7D), which reduction is characteristic of endothelial dysfunction, was evaluated. GAPDH and RPLPO were used as housekeeper genes.

Although there is growing evidence in the literature of SIRT1 downregulation in inflammation (Yang et al., 2022), none of the inflammatory mediators tested

reduced SIRT1 mRNA levels (Figure 5.7A). The expression of VCAM-1, a marker for atherogenesis (Pickett et al., 2023), was only increased by LPS (Figure 5.7B). Moreover, PTGS2 mRNA levels, which are an indicator of inflammation (Soehnlein and Libby, 2021), remained unaffected following treatment with all of the molecules tested (Figure 5.7C). Regarding the expression of eNOS, only IL-6 and LPS reduced it significantly (Figure 5.7D), which indicated that endothelial dysfunction was evoked and a prothrombotic phenotype was acquired (C. Heiss et al., 2015). Despite the lack of effect on SIRT1 expression, LPS was the only compound that induced the transcription of VCAM while reducing NOS3 mRNA levels, which are key characteristics of the dysfunctional endothelium in the development and progression of cardiovascular disease. Therefore, the effect of SIRT1 activation on endothelial health was evaluated using LPS-induced inflammation in subsequent experiments.

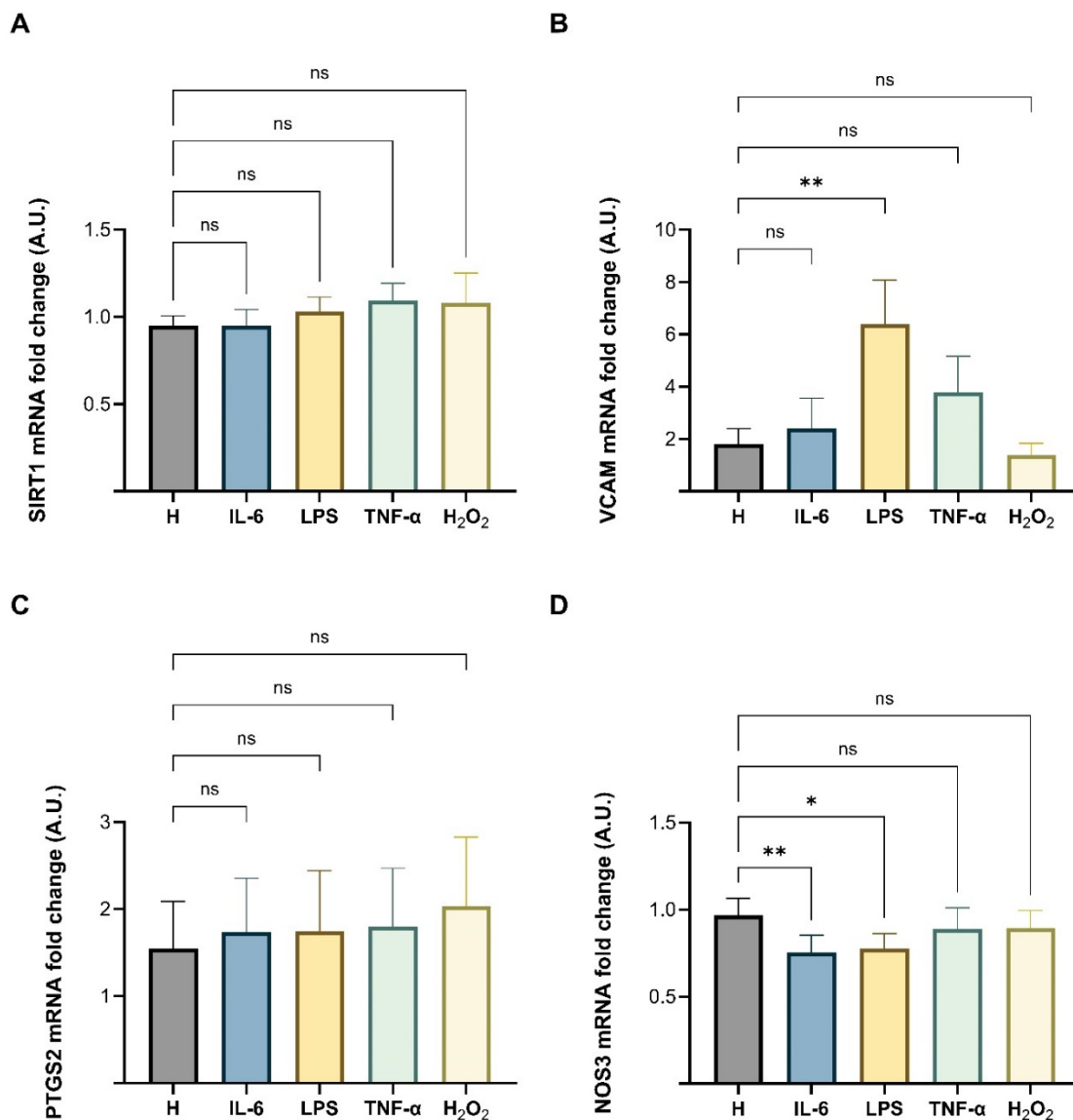


Figure 5.7. LPS increased VCAM and reduced NOS3 mRNA levels. HCAEC were grown in a 12-well plate and serum-starved O/N. Then, treatment with different endothelial dysfunction inducers, including IL-6 (50 ng/mL), LPS (100 ng/mL), TNF- α (10 ng/mL), H₂O₂ (100 μ M), or 0.1% PBS (H), was performed for 24 hours. After a PBS wash, RNA was extracted and purified. cDNA was obtained and qPCR was performed to test the expression of SIRT1 (A), VCAM (B), PTGS2 (C) and NOS3 (D). GAPDH and RPLPO were used as housekeeper genes. The mRNA fold change was calculated using the $\Delta\Delta$ Ct method using the average vehicle Δ Ct of the biological replicates as a control. Data was obtained from three technical replicates. Data represent mean \pm SEM. * p <0.05, ** p <0.01. N=4.

5.3.4 The impact of SIRT1 activation on endothelial regulation of thrombus formation *in vitro*

5.3.4.1 SIRT1 activation prevents thrombus formation on a HCAEC monolayer

Previous experiments have demonstrated that SIRT1 has an important role in the regulation of endothelial function and that activation of this enzyme promotes vascular integrity by decreasing endothelial permeability. To determine whether SIRT1 activation could also promote the antithrombotic capacity of healthy and LPS-treated endothelial cells, a novel endothelialised *in vitro* thrombosis model was utilised.

HCAEC were cultured in Ibidi μ -Slides VI 0.1 until confluent and treated with SRT1720 (1 μ M) or vehicle (0.1% DMSO) in the presence and absence of LPS (100 ng/mL) for 24 hours. Using the *in vitro* arterial thrombus formation model described in section 2.18, untreated blood stained with DIOC6 was flowed first over the HCAEC monolayer and then over a collagen-coated slide. Images of the thrombi formed on the cells (Figure 5.8A) and the collagen slide (Figure 5.8B) were captured with the 10x objective of the CELENA[®] S Logos Biosystems microscope. Using the Weka Trainable Segmentation on ImageJ, the thrombi size, number and area coverage were quantified in both slides.

As expected, the area covered by the thrombi was bigger in the LPS-treated HCAEC than in the healthy cells. However, there was no difference in the thrombi area coverage on collagen after flowing the blood over the LPS-treated cells compared to vehicle control.

Despite no significant differences were observed in thrombus formation on collagen when HCAECs were treated with SRT1720 (Figure 5.8B), SIRT1 activation reduced the area covered by thrombi on LPS-stimulated HCAEC (Figure 5.8AIII). Both thrombi size (Figure 5.8AI) and number (Figure 5.8AII) were decreased by SRT1720 in LPS-treated HCAEC versus vehicle control, although these changes are not statistically significant individually. These results demonstrate that SIRT1 activation protects the arterial endothelial cells from inflammatory damage *in vitro*, indicating that SIRT1 activators could be used as novel therapeutics to

enhance the performance of current antiplatelet treatments by promoting a healthy endothelial phenotype.

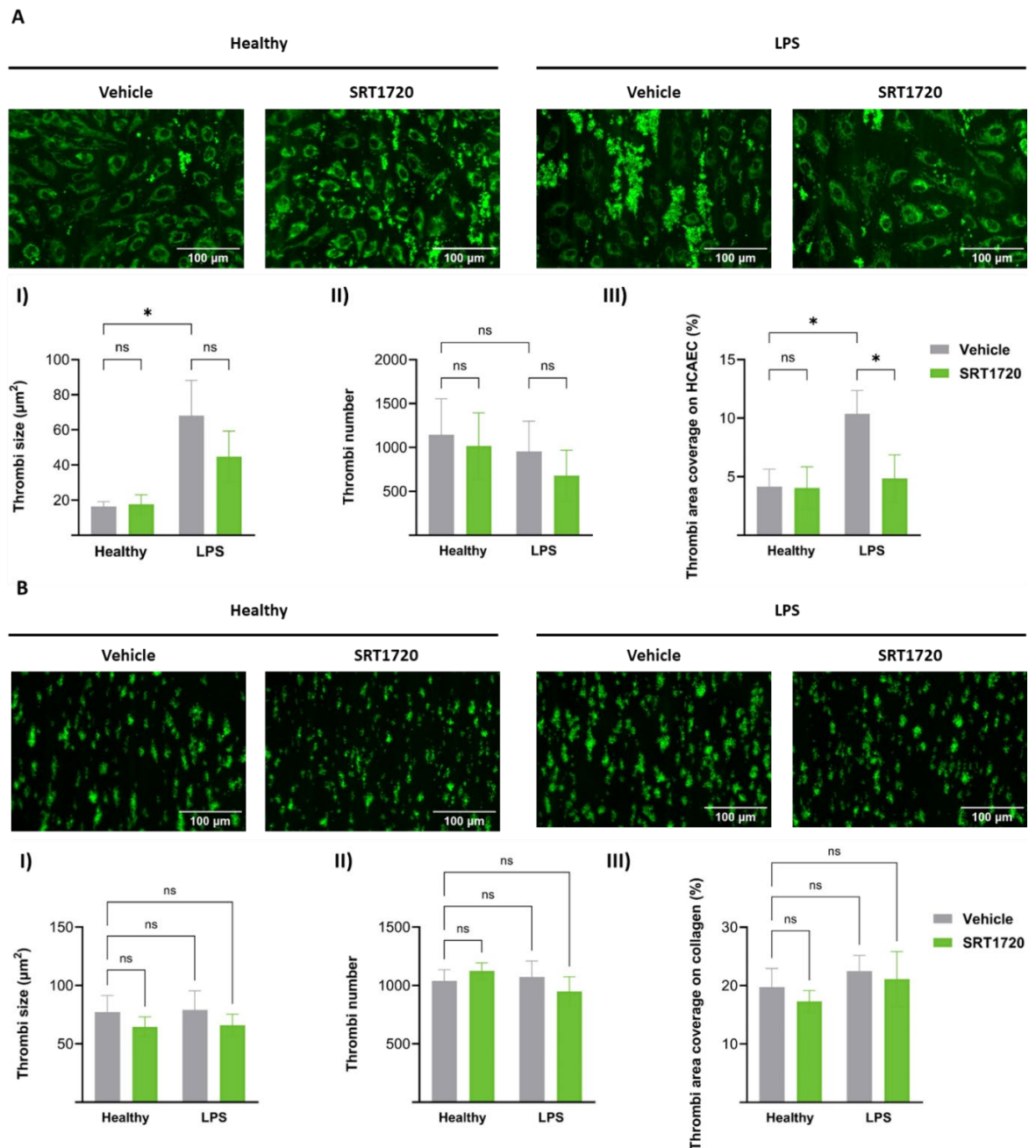


Figure 5.8. Treatment of HCAEC with SRT1720 significantly reduced thrombus formation induced by LPS on the cells, but not on collagen. HCAEC were cultured in Ibidi μ -Slides VI 0.1 until confluent then treated with LPS (100 ng/mL) in the presence of SRT1720 (1 μ M) or vehicle (0.1% DMSO) for 24 hours. Using an *in vitro* thrombus formation model, untreated DIOC6-stained human blood was flowed first over the cell monolayer (A) and then over a collagen-coated slide (B), representative images of the different channels are shown. Images were taken in the 10x objective of the CELENA[®] S Logos Biosystems microscope. Thrombi size (I), number (II) and area coverage (III) were quantified in both slides using the Weka Trainable Segmentation on ImageJ and compared by One-Way ANOVA. Data represent mean \pm SEM. * $p < 0.05$. N=4.

5.3.4.2 SIRT1 activation does not alter eNOS expression in endothelial cells exposed to arterial blood flow

In the previous section, the ability of SRT1720 to promote an antithrombotic phenotype on HCAEC was demonstrated. Therefore, investigating the mechanism behind the protection against inflammatory damage provided by SIRT1 activation was necessary.

A previous study in mice identified that endothelial-specific overexpression of SIRT1 leads to an increase in eNOS protein levels (Zhang et al., 2008). Moreover, post-transcriptional gene silencing of SIRT1 in HUVECs increases eNOS acetylation on lysines 496 and 506, reducing its enzymatic activity (Mattagajasingh et al., 2007). Considering this evidence, the effect of SIRT1 activation on eNOS protein expression was investigated in the HCAEC samples exposed to arterial blood flow *in vitro*.

As explained in section 5.3.4.1, HCAEC were seeded in Ibidi μ -Slides VI 0.1 until confluent and treated with SRT1720 (1 μ M) or vehicle (0.1% DMSO) in the presence and absence of LPS (100 ng/mL). After 24 hours of treatment, blood from donors was stained with DIOC6 and flowed over the HCAEC monolayer using the *in vitro* arterial thrombus formation model explained in section 2.10. HCAEC were then fixed, permeabilised, incubated with an anti-eNOS antibody and stained with DAPI and an Alexa647 labelled secondary antibody. Images of the cells were taken using the 40x oil immersion objective of the STELLARIS 5 Confocal microscope (Figure 5.9.A). The expression of eNOS was evaluated through the quantification of the magenta fluorescent signal using ImageJ, which was normalised by the nuclei count. As expected, LPS treatment significantly decreased eNOS protein levels in HCAEC. However, treatment with SRT1720 failed to recover eNOS levels in the presence of LPS-induced inflammation (Figure 5.9.B), which indicates that in these experimental conditions, the protection against thrombus formation provided via SIRT1 activation must be mediated by another mechanism.

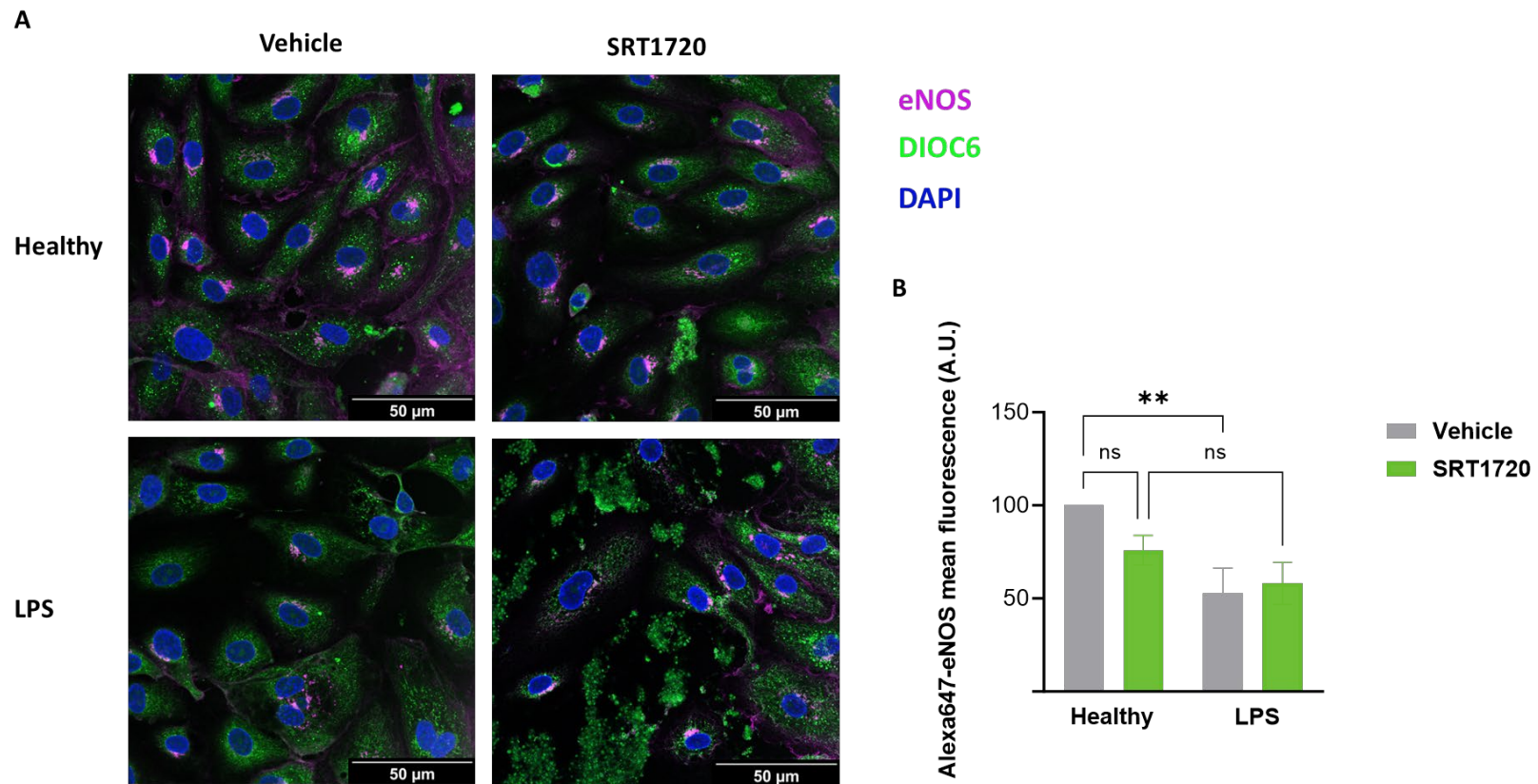


Figure 5.9. SIRT1 pharmacological activation with SRT1720 did not recover eNOS levels after LPS damage in HCAEC. HCAEC were cultured in Ibidi μ -Slides VI 0.1 until confluent and damaged with LPS (100 ng/mL) in the presence of SRT1720 (1 μ M) or vehicle (0.1% DMSO) for 24 hours. Using an *in vitro* thrombus formation model, untreated DIOC6-stained human blood was flowed over the cell monolayer. Samples were fixed, incubated with an eNOS antibody and stained with DAPI and an Alexa647 secondary antibody. Images were taken in the 40x objective of the STELLARIS 5 Confocal microscope. The magenta mean fluorescence intensity was quantified using ImageJ, normalised by the nuclei number and used as a measurement of eNOS expression. Differences between conditions were compared by One-Way ANOVA. Data represent mean \pm SEM. * p <0.05. N=4.

5.3.5 Transcriptional effects of SIRT1 in arterial endothelial cells

5.3.5.1 SIRT1 activation in the expression of endothelial regulators of haemostasis

In section 5.3.3.5, it was demonstrated that incubating HCAEC with LPS (100 ng/mL) for 24 hours under serum-starved conditions is an efficient way of inducing a prothrombotic phenotype on the cells, mimicking the endothelium of an atherosclerotic vessel.

The results from the NF- κ B nuclear translocation experiments performed in section 5.3.3.1 demonstrated that SIRT1 pharmacological activation does not induce NF- κ B migration from the nucleus to the cytoplasm after an inflammatory response and, therefore, did not show which concentration of SRT1720 should be used in the evaluation of gene expression changes. As SRT1720 0.3 and 1 μ M did not disrupt the motility of HCAEC and 1 μ M reduced both the permeability and thrombogenicity of an endothelial layer damaged with LPS, these concentrations were selected for gene expression studies.

HCAEC were serum starved O/N and treated with SRT1720 or vehicle (0.1% DMSO) in the presence or absence of LPS (100 ng/mL) for 24 hours. After a PBS wash, RNA lysates were prepared, from which cDNA was generated. Using RT-qPCR with GAPDH and RPLPO as housekeeper genes, the mRNA expression of a panel of endothelial regulators of haemostasis was tested. The division of these results into different groups was based on the specific role that these genes play in the primary haemostasis process and will be described in the following sections.

5.3.5.1.1 Endothelial-derived platelet inhibitors

The healthy endothelium plays an important antithrombotic role, expressing and releasing several negative regulators of platelet function, including endothelial CD39 (Kanthi et al., 2014), NO and PGI₂ (J. A. Mitchell et al., 2008). In the development of atherosclerosis, abnormalities in the secretion of these inhibitory mediators contribute to vasoconstriction and increased binding and

activation of platelets and leukocytes, leading to vascular remodelling (Pepin and Gupta, 2024). The loss of these regulatory mechanisms also results in exacerbated thrombus growth. To investigate whether SIRT1 activation alters the antithrombotic capacity of the endothelium, the mRNA levels of proteins involved in these pathways were assessed in healthy and LPS-treated HCAEC, in the presence and absence of SRT1720.

ENTPD1 encodes for the enzyme CD39, which converts ATP and the platelet activator ADP into the vasodilator AMP (Bastid et al., 2013). Therefore, increased CD39 expression would prevent ATP-mediated platelet activation. As the effect of SIRT1 activation in CD39 expression was not investigated before, HCAEC were treated with SRT1720 and ENTDP1 mRNA levels were tested. No differences were observed in the SRT1720 conditions versus vehicle (Figure 5.10A), indicating that the protective effects observed in the thrombosis model were not mediated by a reduction in ADP.

Transcription of the NOS3 gene leads to the generation of eNOS, which allows NO production (Tenopoulou and Doulias, 2020). Several studies in other endothelial cell types have identified that SIRT1 regulates endothelial haemostasis by increasing eNOS activity (Mattagajasingh et al., 2007) and expression (Wallerath et al., 2002; Zhang et al., 2008; Ning Xia et al., 2013). Although quantification of eNOS protein levels in confocal images of HCAEC exposed to arterial blood flow showed no significant differences between vehicle and SRT1720 (Figure 5.9), RT-qPCR experiments demonstrated that SIRT1 activation with SRT1720 (1 μ M) significantly increases eNOS mRNA expression in healthy HCAEC (Figure 5.10BI), which suggests that longer treatment with SRT1720 could increase eNOS protein levels.

To cover all possible mechanisms that could lead to an increase in NO, the expression of dimethylarginine dimethylaminohydrolase 1 (DDAH1) was also tested. Asymmetric dimethylarginine (ADMA) inhibits eNOS by competing with its substrate L-arginine, which impairs NO production and leads to endothelial dysfunction. DDAH1 degrades ADMA, recovering NO levels (Liu et al., 2013). SRT1720 at 1 μ M increased DDAH1 expression in LPS-damaged HCAEC (Figure 5.10BII), indicating that SIRT1 activation is involved in the regulation of NO

metabolism and, therefore, its activation could recover NO levels in the atherothrombotic endothelium.

Moreover, the effect of SIRT1 activation was explored in the arachidonic acid pathway, as the prostanoids produced play an important role in both inflammation and platelet function regulation (Wang et al., 2021). The enzymes COX-1 and COX-2 play a key role in this signalling pathway.

On the one hand, inflammatory stimuli induce the expression and activity of COX-2, increasing the production of PGE₂ and causing vasodilation, inflammation and angiogenesis (Soehnlein and Libby, 2021). Work by Zhang et al. (2010) revealed that SIRT1 overexpression in murine macrophages decreases COX-2 mRNA and protein expression (R. Zhang et al., 2010). Thus, PTGS2 transcription was evaluated.

On the other hand, COX-1 is responsible for thromboxane A₂ (TXA₂) production, a potent vasoconstrictor molecule that induces platelet activation (Eckenstaler et al., 2022), and PGI₂, which is a significant platelet inhibitor (Toniolo et al., 2013). As changes in COX-2 mRNA levels could lead to compensatory changes in COX-1 expression, the impact of SRT1720 was also tested in PTGS1 transcription. However, no changes in the mRNA levels of any of these targets were observed under SIRT1 activation (Figure 5.10C, Figure 5.10D), demonstrating that this signalling pathway was not involved in the decrease of arterial thrombus formation observed in the *in vitro* model.

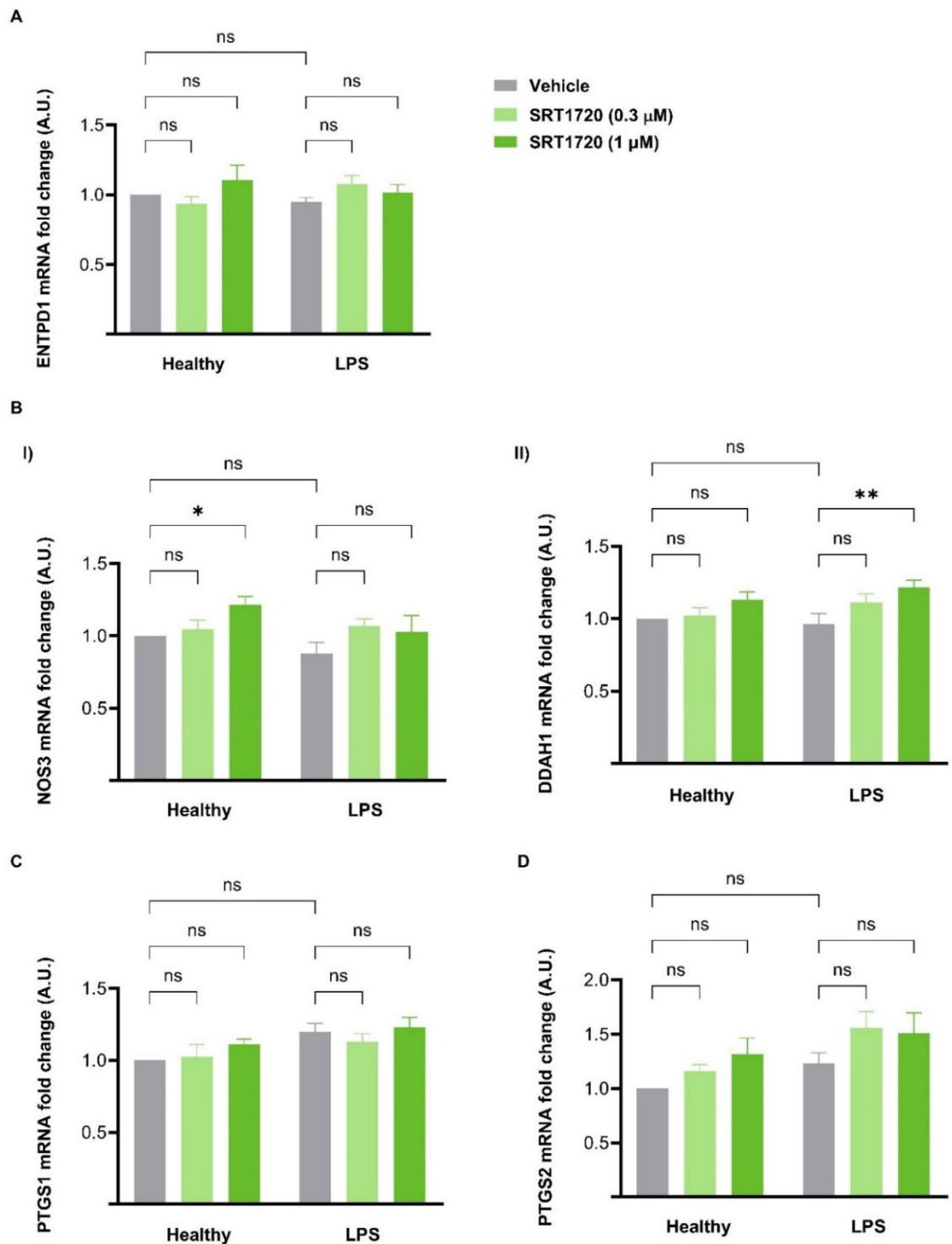


Figure 5.10. SIRT1 contributes to endothelial health through an increase in NOS3 and DDAH1 mRNA expression. HCAEC were grown in a 12-well plate and serum-starved O/N. Cells were treated with SRT1720 (0.3 and 1 μ M) with and without LPS (100 ng/mL) for 24 hours. RNA was extracted, purified and reverse-transcribed into cDNA. qPCR was performed to assess the expression of the genes ENTDP1 (A), NOS3 (BI), DDAH1 (BII), PTGS1 (C) and PTGS2 (D). GAPDH and RPLPO were used as housekeeper genes. mRNA fold change was calculated using the $\Delta\Delta$ Ct method using the average vehicle Δ Ct of the biological replicates as a control. Data was obtained from three technical replicates. Data represent mean \pm SEM. * p <0.05, ** p <0.01. N=5.

5.3.5.1.2 Regulation of platelet adhesion

Upon an injury or inflammation, endothelial Weibel-Palade bodies are secreted, allowing the exposure of the adhesive glycoprotein VWF on the surface of the endothelial cells. Platelet binding to VWF leads to adhesion and activation. Considering that VWF also plays an important role in coagulation, as it acts as a carrier for FVIII, an increase in endothelial VWF expression is considered a risk factor for thrombotic complications in atherosclerosis (Wang et al., 2018). A previous study by Wu et al. (2019) associated an increase in VWF secretion with a reduction in the Sirt1/FoxO1 pathway in HUVECs treated with oxidised LDL (Q. Wu et al., 2019). Therefore, the effect of SRT1720 in the expression of the gene that encodes this protein was evaluated by RT-qPCR in LPS-treated and healthy HCAEC. The results obtained demonstrated that SIRT1 activation does not modulate VWF mRNA expression in these cells (Figure 5.11), suggesting that there are other mechanisms behind the decrease in thrombus formation observed in the arterial thrombosis *in vitro* model (Figure 5.9).

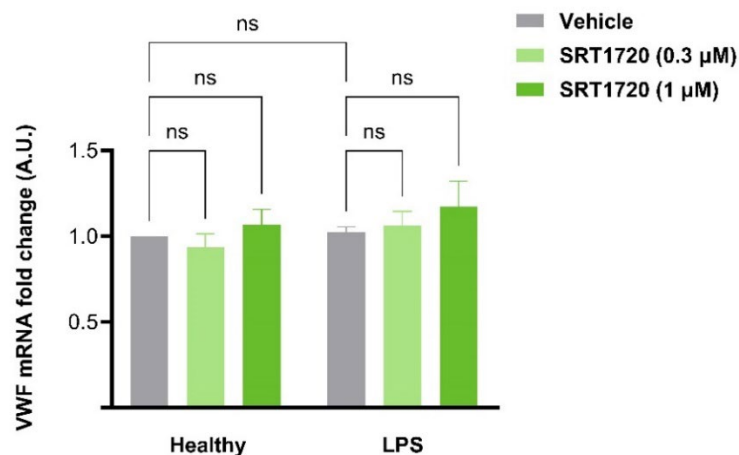


Figure 5.11. SRT1720 does not affect VWF expression in static HCAEC. HCAEC were cultured in a 12-well plate and serum-starved O/N. Cells were treated with SRT1720 (0.3 and 1 μM) in the presence and absence of LPS (100 ng/mL) for 24 hours. RNA was extracted, purified and reverse-transcribed into cDNA. qPCR was performed to assess the expression of the VWF. GAPDH and RPLPO were used as housekeeper genes. mRNA fold change was calculated using the $\Delta\Delta C_t$ method using the average vehicle ΔC_t of the biological replicates as a control. Data was obtained from three technical replicates. Data represent mean \pm SEM. * $p < 0.05$, ** $p < 0.01$. N=5.

5.3.5.1.3 Control of coagulation

As explained in the introduction for this chapter, thrombomodulin (THBD) is a receptor expressed in the surface of endothelial cells with anticoagulant properties, as it reduces the levels of circulating thrombin and generates activated protein C, which degrades factors Va and VIIIa by proteolysis. Investigations by Wu et al. (2012) demonstrated that SIRT1 overexpression through *in vivo* gene delivery prevented lung coagulation via inhibition of THBD downregulation in mice exposed to fine particulate matter (PM_{2.5}) (Z. Wu et al., 2012). Evaluation of THBD mRNA levels in HCAEC revealed that SRT1720 (1 μ M) increases THBD expression in the presence and absence of LPS (Figure 5.12), which constitutes one of the inhibitory mechanisms triggered by SIRT1 activation that led to a decrease in thrombus formation in our flow experiments *in vitro*.

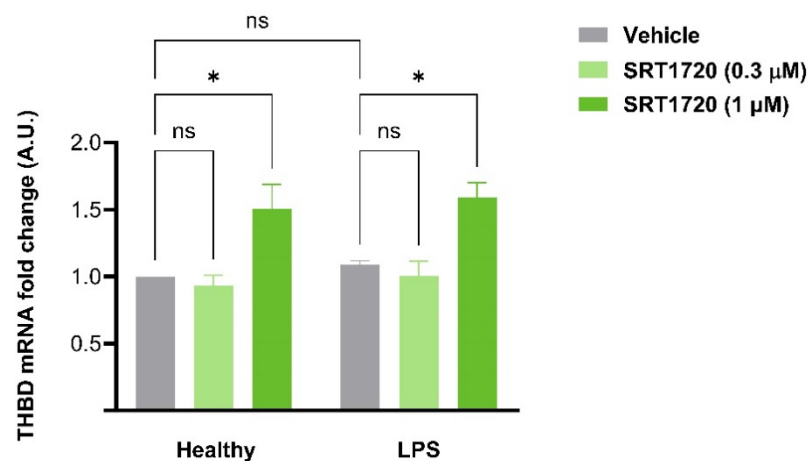


Figure 5.12. SIRT1 activation increases thrombomodulin (THBD) mRNA expression. Cells were treated with SRT1720 (0.3 and 1 μ M) in the presence and absence of LPS (100 ng/mL) for 24 hours. RNA was extracted, purified and reverse-transcribed into cDNA. qPCR was performed to assess the expression of thrombomodulin (THBD). GAPDH and RPLPO were used as housekeeper genes. mRNA fold change was calculated using the $\Delta\Delta$ Ct method using the average vehicle Δ Ct of the biological replicates as a control. Data was obtained from three technical replicates. Data represent mean \pm SEM. *p<0.05, **p<0.01. N=3.

5.4 Discussion

In this chapter, it was demonstrated that SIRT1 is present in HCAECs and that activation of this enzyme with SRT1720 is not toxic when using a 3 μ M dose or lower. Using fluorescence microscopy, it was shown that the SIRT1 activator SRT1720 cannot reverse TNF- α -induced NF- κ B nuclear translocation. SRT1720 3 μ M, which is a high but non-toxic concentration, impaired HCAEC migration in a gap closure assay. Although the mechanism is unknown, evaluation of F-actin levels using a microscopy assay in the presence of TNF- α revealed no changes in this parameter. Using a FITC-dextran permeability assay, it was discovered that SIRT1 activation plays an essential role in the maintenance of a healthy endothelial phenotype by preventing the increase in the permeability of a HCAEC monolayer after treatment with LPS (1000 ng/mL).

Having identified the protective role of SIRT1 against LPS-induced hyperpermeability, the effect of a panel of endothelial dysfunction inducers was tested in HCAEC to create an inflammation cell model *in vitro* to assess the role of SIRT1 in the context of atherosclerosis and thromboinflammation. LPS (100 ng/mL) was selected as the best molecule to induce HCAEC dysfunction because it was the only one that effectively increased VCAM-1 expression while downregulating NOS3 mRNA levels. Therefore, LPS was used to induce a prothrombotic phenotype on HCAEC and the effect of SIRT1 activation on thrombosis was tested *in vitro* using an endothelialised arterial flow model. This experiment demonstrated that, although there was no reduction in thrombus formation on collagen after the blood flowed over an SRT1720-treated HCAEC layer, the area covered by the thrombi was significantly reduced on the cells treated with the SIRT1 activator in the presence of LPS versus the vehicle control.

Considering the promising results obtained in the *in vitro* flow model, the effect of SIRT1 activation on the mRNA expression of endothelial regulators of haemostasis in healthy and dysfunctional HCAEC was evaluated using RT-qPCR. SRT1720 1 μ M significantly induced NOS3 expression only in healthy HCAEC, while it was unable to recover NOS3 mRNA expression after LPS treatment. However, DDAH1 mRNA levels were increased by SRT1720 compared to vehicle control in the presence of LPS, which indicates that SIRT1 activation prevents eNOS inhibition by ADMA rather than

increasing its expression in these conditions. Moreover, SIRT1 activation increased THBD mRNA expression in the presence and absence of LPS, which explains why SRT1720 significantly decreased thrombus formation over the LPS-treated HCAEC monolayer but not on the collagen channels.

SIRT1 protein expression has been confirmed in different endothelial cell types, such as HUVEC (Zhang et al., 2008; Santini et al., 2019; Q. Li et al., 2023), human brain microvascular endothelial cells (Zhang et al., 2019; X. Sun and Liu, 2022) and rat aortic endothelial cells (Mattagajasingh et al., 2007), but this is the first study that demonstrates the presence of this deacetylase in HCAEC. A study by Kao et al. (2010) revealed that SIRT1 was downregulated on an mRNA level in endothelial cells extracted from atherosclerotic human coronary arteries compared to those isolated from healthy portions of the artery (Kao et al., 2010), which suggests that SIRT1 might have a protective role in this disease. Work from McKellar et al. (2009) demonstrated that treatment of endothelial progenitor cells with TNF- α (20 ng/mL), which is one of the key cytokines that induce endothelial dysfunction and triggers inflammation in atherosclerosis (McKellar et al., 2009), reduced SIRT1 expression after 24 hours. SIRT1 downregulation by TNF- α was also observed in other nucleated cell types, such as renal inner medullary collecting duct cells (Q. Lin et al., 2017). Contrary to these findings, evaluation of SIRT1 protein levels in HCAEC after acute treatment with TNF- α revealed no changes. However, in these experiments, the effect of TNF- α in SIRT1 expression was only assessed by incubating HCAEC with this cytokine for 20 and 60 minutes, while the results from other reports were produced by treating for 24 hours. After 20 minutes with TNF- α , SIRT1 levels increased, although this was not statistically significant. As only 3 different HCAEC batches were used in this experiment, G-power calculation should have been performed to ensure it was not underpowered.

Regarding the results obtained from the MTS assay, it was interesting that SRT1720 10 μ M, which was the concentration used in all our platelet studies with no cytotoxic effects, was decreasing HCAEC viability by more than 50%, on a similar level to the SDS cell death control. This could be explained by the fact that most of the experiments to assess the role of SIRT1 in platelets were performed in PRP, which implies a certain binding percentage of the drug to plasma proteins, decreasing

bioavailability. The mechanism of death was not explored, as we were only interested in identifying which concentrations of SRT1720 could be safely used in future assays with HCAEC. However, it has been reported that SRT1720 induces autophagy in mouse cardiomyocytes (G. Luo et al., 2019). Therefore the increased cell death observed in the MTS might be caused by a disruption in autophagic homeostasis.

The NF- κ B nuclear translocation assay is based on the observation that, upon inflammatory stimuli, such as TNF- α or LPS, the transcription factor NF- κ B is acetylated and released from its cytoplasmic inhibitors, which induces its migration to the nucleus and initiates the expression of proinflammatory genes (T. Liu et al., 2017). Previous studies in other cell types have demonstrated that SIRT1 deacetylation of the lysine 310 of the p65 subunit inhibited NF- κ B transcriptional activity (Yeung et al., 2004), enhanced RelA/p65 degradation (Rothgiesser et al., 2010; X. D. Yang et al., 2010) and promoted the association of p65 with the cytoplasmic inhibitor I κ B- α , reducing the levels of nuclear NF- κ B (Y. Dai et al., 2005; de Gregorio et al., 2020). The objective of this experiment was to identify which concentrations of SRT1720 could return NF- κ B to the cytoplasm of HCAEC after a TNF- α treatment. Based on the results obtained, SIRT1 activation for 4 hours could not reverse NF- κ B nuclear translocation once this factor had already migrated into the nucleus, indicating that either a longer exposure with SRT1720 is necessary or that the deacetylation of NF- κ B by SIRT1 occurs in the cytoplasm in HCAEC, preventing its nuclear translocation. Future work would involve a time course with SRT1720 and microscopy or immunoprecipitation experiments to evaluate the interaction of SIRT1 and NF- κ B in the cytoplasm and the nucleus.

Considering that the NF- κ B nuclear translocation experiment did not offer any insights regarding which concentration of SRT1720 should be used in future assays, it was necessary to perform other functional experiments with HCAEC to answer this research question. Due to the number of articles that indicate that SIRT1 is a key regulator of migration in different nucleated cell types (Qiang et al., 2017; T. Yang et al., 2019; Wang et al., 2021; Y. Lin et al., 2022) and the impact of SRT1720 in platelet spreading, which was discussed in chapters 3 and 4, a HCAEC migration assay was performed with different concentrations of the SIRT1 activator. It must be noted that this was not a scratch assay, as the gap was created by seeding HCAEC in special

inserts, providing a consistent, more reproducible gap between cells, rather than by performing a scratch injury in the cell monolayer. Therefore, this model cannot be used to evaluate wound healing, but cell motility.

High but non-toxic concentrations of SRT1720 (3 μ M) significantly decreased HCAEC migration. Despite being clear that SIRT1 is involved in the regulation of cell motility, whether activation of this enzyme enhances or prevents migration is still controversial and seems to be dependent on the cell type. For instance, work by Dong et al. (2018) demonstrated that SIRT1 overexpression in different gastric cancer cell lines suppressed cell migration in wound healing and transwell assays (Dong et al., 2018). On the contrary, specific SIRT1 deletion on the mouse epidermis leads to a decrease in wound healing time *in vivo* (Qiang et al., 2017). Investigations by Yang et al. (2019) on ovarian carcinoma cells demonstrated that overexpression of SIRT1 increased cell motility, while upregulation of a mutant form of SIRT1 that cannot translocate into the nucleus leads to reduced cell migration, indicating that SIRT1 has different roles in the regulation of cell motility depending on its subcellular localization. Considering that SIRT1 activation reduced HCAEC migration, it is probable that SIRT1 is mainly present in the cytoplasm of healthy HCAEC, although this was not investigated further. A previous study by Yanagisawa et al. (2018) has linked inflammatory stimuli with the migration of SIRT1 from the cytoplasm into the nucleus of human bronchial epithelial cells (Yanagisawa et al., 2018). Therefore, although SRT1720 treatment leads to a reduction in healthy HCAEC motility, future work would involve the evaluation of the effect of this drug in the migration of dysfunctional HCAEC, as SIRT1 activation might have a different effect under inflammatory conditions.

The mechanism behind the reduction of HCAEC migration caused by SIRT1 activation is still unclear, but quantification of F-actin levels using microscopy images discarded that there were any alterations in actin polymerisation. However, this assay has three main limitations. First, TNF- α failed to induce actin polymerisation as stated in the literature (Koukouritaki et al., 1999) and could not be used as a positive control. Second, the effect of SRT1720 was not assessed in healthy HCAEC as in the migration assay, but in TNF- α -treated HCAECs only. Third, quantification of F-actin using microscopy is not as sensitive as flow cytometry or Western Blotting, which were

used in the evaluation of the effect of SRT1720 on platelet F-actin levels. Therefore, there might be subtle changes that cannot be detected using this technique. Future work would involve evaluating the effect of SRT1720 in healthy HCAEC F-actin levels and exploring other mechanisms that could be behind the alteration of cell motility caused by SRT1720, such as the deacetylation of cortactin, which has been previously reported as a substrate of SIRT1 (Shentu et al., 2016; N. Iwahara et al., 2022; Y. Lin et al., 2022) with a crucial role in cytoskeletal reorganisation and cell migration (Cosen-Binker and Kapus, 2006; Schnoor et al., 2018).

Although inhibiting cell motility might be interesting in the context of inflammation-driven vascular remodelling during the development of atherosclerosis (Intengan and Schiffrin, 2001), it could also have a detrimental effect on wound healing (Velnar and Gradisnik, 2018) and basal angiogenesis (Lamallice et al., 2007). Therefore, the concentrations of SRT1720 selected for the following experiments are 0.3 and 1 μ M.

In atherosclerotic vessels, endothelial permeability is increased due to a disruption in endothelial junction organisation, leading to the accumulation of LDL and the transmigration of monocytes into the arterial intima (Chistiakov et al., 2015; T. Silva et al., 2020). Therefore, protecting the integrity of the endothelium is key to stopping the progression of atherosclerosis (Claesson-Welsh et al., 2021). In line with the evidence in the literature on blood-brain barrier models (T. Chen et al., 2018; Stamatovic et al., 2019; Y. Zhang et al., 2019), the results of this study demonstrate that SIRT1 activation prevents LPS-induced hyperpermeability in a HCAEC monolayer *in vitro*. Moreover, previous investigations determined that SIRT1 knockdown or inhibition with EX527 in human microvascular endothelial cells exposed to LPS leads to an increase in endothelial permeability (Stark et al., 2022), which further supports the results of our study. The representative pictures taken from the inserts show changes in the cellular distribution of VE-cadherin between the LPS-treated and the healthy HCAEC, with more presence of this protein in the cell-to-cell contacts in the latter. Moreover, incubation with SRT1720 also seems to maintain VE-cadherin on the edges of the cells, which supports the results from the permeability assay (Vestweber, 2008). However, quantification of VE-cadherin protein levels of subcellular location was not possible, as only representative pictures of one repeat

were taken. Further work would be required to elucidate the specific mechanism behind these observations.

Similarly to the actin polymerisation assay, TNF- α failed to produce a statistically significant increase in endothelial permeability, suggesting that the cells were not responding to this treatment as expected. This might be explained by the cell type used, as micro vessels are more susceptible to permeability than larger arteries such as the coronary arteries. Optimisation of this assay by testing different concentrations of TNF- α or different time points would be necessary.

Due to the lack of hyperpermeability observed in HCAEC treated with TNF- α , it was necessary to explore the response of HCAEC to different endothelial dysfunction factors involved in the development of atherosclerosis. Although it is well known that TNF- α (C. W. Kim et al., 2021) and IL-6 (Feng et al., 2022) are key in the perpetuation of vascular inflammation and the development of an atherosclerotic plaque, these cytokines had no significant impact on HCAEC transcriptome under the experimental conditions tested, except for the reduction produced in NOS3 expression by IL-6. The effects of H₂O₂ on the HCAEC mRNA profile were also tested due to the demonstrated antioxidant properties of SIRT1 activation (H. Li, 2014) and the important role of ROS in endothelial dysfunction mechanisms, such as eNOS uncoupling and the transcription of proinflammatory genes via HIF-1 α activation (Batty et al., 2022). However, no statistically significant changes in the transcription levels of genes involved in endothelial dysfunction, such as NOS3 and VCAM, were observed in our RT-qPCR experiments.

An increasing body of scientific evidence has proven that low serum levels of LPS in subclinical infections induce chronic inflammation responses that increase atherosclerotic risk (Carnevale et al., 2018; Sieve et al., 2018; Violi et al., 2023). A clinical study by Kiechl et al. (2001) investigated changes in carotid atherosclerosis in a cohort of 826 white men and women with chronic bacterial infections. In patients without atherosclerosis at the beginning of the study, chronic infection was responsible for approximately 40% of the new atherosclerosis cases (Kiechl et al., 2001; Gorabi et al., 2022). The hyperpermeability produced by LPS in our vascular permeability assay plus the changes in VCAM and NOS3 mRNA levels observed in the RT-qPCR experiments using RNA from HCAEC incubated with LPS indicate that this

molecule successfully induces endothelial dysfunction in HCAEC, constituting a robust and consistent model of endothelial inflammation.

The source of the resistance of HCAEC to TNF- α and IL-6 has yet to be elucidated but could be related to batch or passage variability, as these are primary cells from 50 to 70-year-old males. Despite this issue, HCAECs are still the most disease-relevant cell model to investigate the role of SIRT1 in the arterial endothelium and the use of LPS as an endothelial dysfunction inducer allowed the creation of an *in vitro* endothelial model of inflammation to study the effects of SRT1720 in the dysfunctional arterial endothelium.

Thrombi area coverage was increased on a HCAEC monolayer damaged with LPS, which further supports the use of this dysfunction factor to study the effect of SIRT1 activation in the thrombotic complications associated with the rupture or erosion of an atherosclerotic plaque. Moreover, the decrease in thrombi area coverage caused by SRT1720 on LPS-treated cells is consistent with the results from a previous study by Carrizo et al. (2022), in which mutant mice at high cardiovascular risk were treated with the SIRT1 activator ISIDE11, reducing thrombus formation on femoral artery lesions via the increase of eNOS expression and the consequent improvement of endothelial vasorelaxation (Carrizo et al., 2022). Considering this information, the presence of eNOS was assessed in the HCAEC monolayer after performing the thrombus formation assay. Contrary to the findings by Carrizo et al. (2022), specific activation with SRT1720 did not increase eNOS protein levels in our HCAEC *in vitro* model. A simple explanation for these mechanistic differences is that, in the investigations by Carrizo et al. (2022), the SIRT1 activator was administered systemically to mice in which endothelial dysfunction was not induced by LPS treatment. Therefore, many other cells that signal with the endothelium will be exposed to the SIRT1 activator, potentially changing the endothelial phenotype, and the mechanism behind the endothelial dysfunction is different to our *in vitro* model.

None of the parameters used to measure thrombus formation were increased in the collagen channel after flowing the blood over the LPS-treated HCAEC in the presence or absence of SRT1720. This indicates that LPS is increasing the thrombi area coverage, especially thrombi size, by promoting an antithrombotic phenotype on the surface of endothelial cells rather than decreasing the release of soluble platelet

inhibitors, such as prostacyclin or NO (Fredenburgh and Weitz, 2018). Investigation of the effect of SRT1720 on the mRNA expression of different endothelial regulators of haemostasis demonstrated that, as expected, SIRT1 activation did not change the expression of PTGS1 or PTGS2. In line with our microscopy experiments in which eNOS protein levels were evaluated in HCAEC after the thrombosis *in vitro* model, SRT1720 failed to recover NOS3 mRNA levels in LPS-treated HCAEC. However, SRT1720 (1 μ M) did increase NOS3 transcription on healthy HCAEC, indicating that SIRT1 activation promotes an antithrombotic phenotype in the endothelium, which would be interesting from a prevention point of view. Moreover, evaluation of DDAH1 mRNA levels revealed an increase in the transcription of this gene under SRT1720 treatment in dysfunctional HCAEC, which suggests that, even though SIRT1 activation could not increase NOS3 expression in the LPS-treated HCAEC, NO bioavailability might be higher due to the increased degradation of ADMA by DDAH1. In this scenario, one possible explanation for the lack of prevention of thrombus formation on the collagen slides by SRT1720 in our arterial flow model would be that a longer treatment with the SIRT1 activator might be necessary for this increase in DDAH1 mRNA to translate into an increase in protein expression, and therefore, exert an effect.

A previous study in mice acutely exposed to ambient fine particulate matter demonstrated that SIRT1 overexpression prevents THBD downregulation in murine lung endothelial cells (Z. Wu et al., 2012). Consistently with the results from this study by Wu et al. (2012), SRT1720 (1 μ M) increased THBD mRNA levels in both healthy and LPS-treated HCAEC. This upregulation of THBD expression offers a molecular mechanism to explain the reduction observed in thrombus formation on the HCAEC channel in our *in vitro* thrombosis model.

Work from Breitenstein et al. (2010) demonstrated that treatment of human aortic endothelial cells with sirtinol, which is a SIRT1 and SIRT2 inhibitor (Petroněk et al., 2023), enhanced tissue factor overexpression induced by TNF- α (Breitenstein et al., 2011). Therefore, the reduction of TF expression could be another potential mechanism through which SIRT1 activation prevents thrombus formation. Future work would involve evaluating TF expression in SRT1720-treated dysfunctional HCAECs to elucidate whether this effect is mediated by SIRT1 or SIRT2.

One of the limitations of the qPCR experiments performed in this chapter is that LPS failed to change the expression of some of the genes evaluated in a statistically significant way when this condition was used as a positive control. This was associated with a high variability between the baseline expression of different HCAEC batches. The conditions of the treatment and dose of LPS were standardised and consistent with the endothelial permeability and thrombus formation assays. Changes in expression can be faster or slower depending on which gene is evaluated (Co et al., 2017), which complicates the generation of RNA lysates at the peak of expression of all the genes in our panel. Moreover, the ability of LPS to induce endothelial dysfunction was demonstrated in previous functional and transcriptional experiments explained in this chapter.

In conclusion, selective pharmacological activation of SIRT1 with SRT1720 not only reduces platelet reactivity but also decreases thrombotic risk in an LPS *in vitro* model by upregulating DDAH1 and THBD expression in arterial endothelial cells. These findings suggest that SIRT1 activators could be a potential novel therapy for the prevention of endothelial dysfunction in cardiovascular patients while reducing the risk of atherothrombotic events.

Chapter 6. General discussion

6.1 Key findings

Due to the antioxidant (Singh et al., 2018) and antiaging (Ministrini et al., 2021) effects of SIRT1, the role of this enzyme in many physiological and pathological conditions was investigated (Mohar and Malik, 2012). In the past decade, several studies identified that modulation of SIRT1 activity and expression has important implications for cardiovascular diseases (L. Ma and Li, 2015; Winnik et al., 2015; Costantino et al., 2023; R. Zhou et al., 2024). However, the role of this deacetylase in human haemostasis was completely unknown. The objective of this project was to investigate the effect of SIRT1 pharmacological activation with SRT1720 in thrombosis and haemostasis using a multicellular approach, by assessing the effects of the SIRT1 agonists in both human platelets and HCAECs. In the following sections, the main findings of this project will be summarised.

6.1.1 SIRT1 is a key regulator of platelet function

Understanding the mechanisms underlying platelet activation and aggregation is essential for developing effective strategies to prevent and treat thrombosis (Tomaiuolo et al., 2017). A previous study has demonstrated that treatment of human platelets with resveratrol inhibits Toll-like receptor 4 (TLR4)-mediated inflammatory responses in platelets activated with oxidised LDL (J. Sun et al., 2018). However, whether this protective effect is mediated by SIRT1 or other resveratrol targets, which were detailed in section 3.4, remains unclear. Moreover, work by Kim et al. (2016) revealed that treatment with resveratrol and recombinant SIRT1 decreases platelet-activating factor receptor (PAF-R) expression via proteasomal and lysosomal degradation in mouse platelets, reducing platelet aggregation *in vitro* and pulmonary thrombosis *in vivo* (Y. H. Kim et al., 2016). Despite the lack of specificity of resveratrol, these investigations raised questions about the role of SIRT1 in basal platelet function and whether activating SIRT1 would contribute positively to the treatment of thrombosis and atherosclerosis, which were investigated in this study. Before the development of this project, no studies using specific SIRT1 activators were performed and the mechanisms behind SIRT1

modulation of platelet activity were unknown. Using platelets from healthy donors in the presence and absence of different platelet agonists, the results from Chapter 3 and Chapter 4 of this thesis identified that SIRT1 is an important regulator of human platelet function. The findings presented in Chapter 3 revealed that SIRT1 controls integrin $\alpha\text{IIb}\beta\text{3}$ binding to substrates (Figure 3.5 and Figure 3.6), affecting “outside-in” signalling. In Chapter 4, it was demonstrated that SIRT1 is involved in platelet cytoskeletal rearrangement (Figure 4.3) via the regulation of the F-actin pool (Figure 4.4). The selective SIRT1 agonist SRT1720 reduced platelet reactivity, polymerised actin levels, spreading and clot retraction, which suggests that SIRT1 activation could be a novel therapeutic strategy to reduce platelet hyperreactivity in a variety of disease scenarios, including atherosclerosis.

6.1.2 SIRT1 activation has antithrombotic effects in platelets and endothelial cells, reducing *in vitro* thrombus formation

A study by Breitenstein et al. (2001) demonstrated that mice treated with splitomicin, a global SIRT inhibitor (Bedalov et al., 2001), had enhanced arterial thrombosis in a photochemical injury model, which was associated with an increased tissue factor activity in the carotid vessel wall. Moreover, evaluation of tissue factor mRNA levels in SIRT1 knockdown human aortic endothelial cells showed a decrease in the expression of this gene, consistent with the results of the *in vivo* experiments (Breitenstein et al., 2011). Prior to the development of this thesis, the findings of Breitenstein et al. (2011) were the only evidence of the protective role of SIRT1 against thrombosis and it was still unknown whether this beneficial effect was mediated by a decrease in platelet activity or a healthier endothelium. This project revealed that activating SIRT1 reduces *in vitro* thrombus formation in a platelet and endothelial-like manner using a novel *in vitro* arterial thrombosis model which allows the assessment of thrombus formation on either adhesive surfaces, such as collagen or fibrinogen, or endothelial cells (Drysdale et al., 2024). SRT1720 reduced thrombus formation on collagen I, as expected from the decrease in platelet activation observed in Chapters 3 and 4, but also diminished thrombi area on LPS-treated HCAEC, which indicates that SIRT1 contributes to the correct functioning of the endothelium in haemostasis.

The protection against *in vitro* thrombus formation on collagen was represented by a statistically significant decrease in thrombi area in SRT1720-treated platelets, which was presented in Figure 3.9C. This effect was attributed to the decrease in platelet adhesion and spreading observed in section 4.3.1 (Figure 4.1), as there was a decrease in thrombi number (Figure 3.9A) but not in thrombi size (Figure 3.9B).

In the case of the endothelialised model, it was interesting that the reduction in thrombus formation was observed in the LPS-treated HCAEC but not downstream on the collagen channels (Figure 5.8), which indicates that the protective mechanism triggered by SIRT1 activation is probably an increase in the surface expression of antithrombotic molecules and not the release of soluble agents by the endothelial cells. In section 5.3.5, a panel of endothelial regulators of haemostasis was investigated to identify which pathways were involved in the beneficial effects of SIRT1 in HCAECs. As expected, the mRNA expression of the soluble mediator VWF (Figure 5.11) was not affected. The mRNA levels of ENTPD1 (Figure 5.10A), PTGS1 (Figure 5.10C) and PTGS2 (Figure 5.10D) were also assessed, showing no differences between the SRT1720-treated HCAECs and vehicle control. Therefore, it is unlikely that the effects observed in the thrombosis model were caused by changes in ATP/ADP metabolism or prostanoid production. When evaluating the expression of NO regulators, it was identified that SRT1720 increases NOS3 mRNA but only in the healthy HCAECs (Figure 5.10BI), while DDAH1 expression was increased upon SIRT1 activation in HCAECs only when LPS dysfunction was induced (Figure 5.10BII). However, these differences will probably not have an impact on NO levels, as only a slight upregulation of these two genes was observed when using SRT1720 in the conditions described (section 2.19.1), which is reinforced by the lack of changes in eNOS protein expression in Figure 5.9. However, to robustly evaluate the role of released molecules in SIRT1 function it would be necessary to assess the levels of soluble mediators, including NO, ADP, ATP, VWF, TxA2 and PGI₂, or their degradation products in the media that was in contact with the endothelial cells using techniques such as the Griess assay (Tsikas, 2007), ELISA (Tabatabaei and Ahmed, 2022) or bioluminescence (F. Shao et al., 2023).

Evaluation of THBD mRNA expression revealed an overexpression associated with SIRT1 activation, which is consistent across healthy and LPS-treated HCAEC (Figure

5.12). Therefore, the reduction in thrombus formation on LPS-treated HCAEC observed in section 5.3.4.1 was attributed, at least in part, to THBD upregulation. These findings are supported by the results of Wu et al. (2012), which demonstrated that particulate matter exposure leads to a higher downregulation of THBD expression in the lung of SIRT1 KO mice than in the WT (Z. Wu et al., 2012).

Due to limited time, it was not possible to assess the effect of global SIRT1 activation in the endothelialised model by treating both platelets and HCAECs with SRT1720. However, this experiment would be key to understanding whether the antithrombotic effect would be enhanced and is part of the future directions for this project.

6.1.3 SIRT1 prevents LPS-induced endothelial dysfunction by reducing HCAEC permeability

As explained in section 1.7.1, the increase in endothelial permeability induced by inflammation and oxidative stress is one of the hallmarks of atherogenesis, together with the expression of prothrombotic molecules, cytokine production and NO reduction (Sitia et al., 2010). Due to the antioxidant effects attributed to endothelial SIRT1 (Weijin Zhang et al., 2017), it was necessary to evaluate whether selective activation of this enzyme would prevent hyperpermeability associated with endothelial dysfunction. This is the first study that evaluates whether SIRT1 pharmacological activation with SRT1720 can prevent hyperpermeability in a relevant cell model for atherosclerosis, showing beneficial effects in HCAECs (Figure 5.6). These findings are supported by investigations by Zhang et al. (2017) in a venous cell model, which demonstrated that treatment with the same SIRT1 agonist is also protective against endothelial barrier dysfunction induced by LPS (W. Zhang et al., 2017) .

Although the mechanism behind this protective effect is yet to be discovered, work by Zhang et al. (2017) in HUVECs indicates it could potentially be mediated by an increase in activity and expression of superoxide dismutase 2 (SOD2) and a reduction in NADPH oxidase 4 expression, which caused a decrease in oxidative stress (W. Zhang et al., 2017). Moreover, a study by Fu et al. (2019) in primary human pulmonary microvascular endothelial cells treated with LPS demonstrated

that SIRT1 protects from hyperpermeability possibly via the activation of the RhoA/ROCK pathway (C. Fu et al., 2019). Future work involves investigating the molecular signalling linked with SIRT1 protection of endothelial hyperpermeability in HCAECs.

6.1.4 SIRT1 activation did not compensate for the downregulation in eNOS protein and mRNA expression caused by LPS in HCAEC

Apart from increased permeability, the reduction of NO levels is another key pathological mechanism of endothelial dysfunction that triggers atherogenesis (Cyr et al., 2020). Previous studies have associated an increase in SIRT1 activity or expression with higher NO levels in endothelial cells (Wallerath et al., 2002; Ning Xia et al., 2013). In this project, the effect of SIRT1 activation with SRT1720 in eNOS protein (section 5.3.4.2) and mRNA expression (section 5.3.5.1.1) was evaluated for the first time in both healthy and LPS-treated HCAECs. Although eNOS mRNA levels were significantly increased by SRT1720 in healthy HCAECs, no differences were observed either in eNOS protein (Figure 5.9) or mRNA expression (Figure 5.10BI) in LPS-treated cells after SIRT1 activation.

In a study by Csiszar et al. (2008), HCAECs were treated with resveratrol, leading to an increase in eNOS expression. To determine whether this event was SIRT1 dependent, a SIRT1 knockdown model was performed with the same cells and treatment with resveratrol was reproduced, showing that eNOS expression does not occur upon SIRT1 downregulation and indicating that SIRT1 positively regulates eNOS expression in HCAEC (Csiszar et al., 2008). These results support the increase in eNOS mRNA levels observed in healthy HCAEC upon SRT1720 treatment (Figure 5.10BI). A possible explanation for the lack of upregulation in LPS-treated HCAECs is that the dose of the SIRT1 agonist or the incubation time is not enough to compensate for the dysfunction caused by the specific dose of LPS used (100 ng/mL).

As explained in detail in section 1.7.1, reduction of eNOS expression is not the only mechanism involved in the decrease in NO bioavailability in endothelial dysfunction. The fact that only changes in eNOS protein and mRNA levels were investigated in this project as a representation of endothelial dysfunction mediated by NO

reduction constitutes a limitation and creates the opportunity to further explore eNOS uncoupling in the future. Using rat aortic rings *ex vivo*, Mattagajasingh et al. (2007) demonstrated that SIRT1 overexpression promotes NO production via the deacetylation of eNOS, which increases its activity (Mattagajasingh et al., 2007). To elucidate whether SIRT1 activation has a net positive impact on NO levels in HCAECs, a NO colorimetric assay could be performed. Moreover, as changes in eNOS expression were discarded in LPS-treated HCAEC (Figure 5.9 and Figure 5.10BI) but an increase in DDAH1 was observed (Figure 5.10BII) under the experimental conditions tested, eNOS expression may remain unchanged while its activity is increased. To evaluate this, a nitric oxide synthase activity assay could be performed.

6.1.5 SIRT1 regulates platelet spreading and HCAEC migration

Several investigations have demonstrated that SIRT1 plays a key role in cytoskeletal rearrangements, which was explained in detail in the discussion of Chapter 4 (section 4.4). According to the evidence in the literature, the molecular mechanism behind this event is the regulation of actin polymerisation due to the deacetylation of cortactin (Motonishi et al., 2015; Min et al., 2018). However, it has also been observed that SIRT1 activation can have different effects on cell migration depending on the cell type. For instance, in scratch assays, SIRT1 deletion in retinal endothelial cells led to an inhibition of migration (Y. Lin et al., 2018), while it promoted the migration of gastric cancer cells (Dong et al., 2018).

A previous study by Yang et al. (2019) in ovarian carcinoma cells demonstrated that global overexpression of SIRT1 increased cell motility. However, when only cytoplasmatic SIRT1 was upregulated, the effects were the opposite, causing a reduction in cell migration (T. Yang et al., 2019). These findings indicate that SIRT1 activation translates into different cellular events depending on the subcellular location of the enzyme. Therefore, the controversy in the results in the literature regarding the effect of SIRT1 on cell migration (Motonishi et al., 2015; Qin et al., 2019; N. Iwahara et al., 2022; Y. Lin et al., 2022) could be associated with the subcellular location of the enzyme in different cell types, as the transcriptional and cytoplasmatic effects of SIRT1 might have antagonistic effects in cell migration.

Before the development of this project, the effect of SIRT1 activation in cytoskeletal dynamics had only been investigated in nucleated cells. The findings collected in this thesis demonstrate that SIRT1 decreases platelet spreading, which is represented by a smaller platelet size and about 50% reduction in lamellipodia formation in SRT1720-treated platelets upon contact with either collagen (Figure 4.1) or fibrinogen (Figure 4.2). Platelets are a great model to unravel the cytoplasmic effects of SIRT1, as they lack a nucleus. In this cellular model, we have identified that SIRT1 activation regulates cytoskeletal rearrangements via a decrease in F-actin levels (Figure 4.4). However, the specific target which deacetylation leads to this effect, probably an ABP, has yet to be identified. As mentioned previously, cortactin is a target of SIRT1 in other cell types (Motonishi et al., 2015; Min et al., 2018). Thus, the deacetylation of cortactin by SIRT1 should have been investigated as a potential mechanism in platelets in this project. However, only one anti-acetyl cortactin antibody is commercially available and many technical difficulties were faced in showing acetylation changes using Western Blotting, although the expression of cortactin was demonstrated in platelets previously. Moreover, the time and budget available for this project made not possible to perform mass spectrometry or immunoprecipitation to evaluate changes in acetylated cortactin, which constitutes a limitation. Performing these experiments will be considered in the future.

The role of SIRT1 activation in HCAEC migration was tested for the first time in this study, revealing that low doses of SRT1720 (0.3 and 1 μ M) have no effect, while a higher but non-toxic dose (3 μ M) significantly reduces HCAEC migration. Considering that activation of cytoplasmic SIRT1 has been associated with a decrease in the migration of ovarian carcinoma cells, we hypothesise that higher doses of SRT1720 allow higher cytoplasmic SIRT1 activation, leading to a reduction in cell motility.

Since F-actin homeostasis was altered by SIRT1 activation in several cell types, including platelets, this parameter was also evaluated in SRT1720-treated HCAECs (section 5.3.3.3). In contrast to our findings in platelets, polymerised actin levels in TNF- α treated HCAECs remained unchanged upon treatment with different doses of SRT1720, including 3 μ M (Figure 5.5). The main limitation of this experiment is

that the effect of SRT1720 was not tested in the absence of TNF- α and this condition should be included in the future. Due to limited time, it was not possible to investigate any other signalling pathways, but some major regulators of endothelial cytoskeletal rearrangement independent of the actin cytoskeleton that could potentially be SIRT1 targets and, therefore, could be considered in future investigations, are tubulin and myosin (Mu et al., 2020). Changes in the expression of adhesion molecules would also explain the decrease in cell motility observed in our microscopy experiments (Bogatcheva and Verin, 2008).

6.1.6 SIRT1 activators as novel antithrombotics

Currently, there is a clinical need for safer and more efficient antithrombotic treatments due to the high interpatient variability in the effect of available drugs. Some patients suffer adverse bleeding events, while others are resistant to antithrombotic therapies and suffer recurrent thrombotic events (Kluft et al., 2017; Krishnan et al., 2023). In section 3.3.2 of this thesis, an attenuation of platelet aggregation in response to different agonists, including TRAP-6 (Figure 3.2), collagen (Figure 3.3) and ADP (Figure 3.4), was observed upon treatment with SRT1720 (Figure 6.1). These findings indicate that SIRT1 activation would not completely inhibit platelet aggregation but decrease hyperreactivity, which supports the idea that using negative regulators of platelet function would entangle a lower risk of haemorrhages (Stefanini and Bergmeier, 2018). Moreover, no adverse bleeding events were reported in the clinical trials with the selective SIRT1 agonist SRT2104 (GlaxoSmithKline, 2010; 2011; Sirtris, 2011; 2013), which suggests that SIRT1 activation could be a safe alternative to current antithrombotics.

Investigation of the molecular events involved in the effects of SRT1720 in platelet function revealed that both integrin α IIb β 3 “outside-in” signalling (section 3.3.3) and the amount of filamentous actin (section 4.3.3) are decreased by SIRT1 activation (Figure 6.1). The use of other integrin α IIb β 3 inhibitors, such as abciximab and eptifibatide, is limited in clinical practice due to haemorrhagic side effects (van den Kerkhof et al., 2021). In contrast, SIRT1 activation in platelets only caused a mild reduction of aggregation and thrombus formation *in vitro*. Considering these observations, we hypothesise that SIRT1 activation might only decrease the avidity

of integrin for fibrinogen rather than completely block substrate binding via conformational changes or might trigger compensatory mechanisms that preserve basal platelet activity (Huang et al., 2019).

Considering that the interactions between platelets and the dysfunctional endothelium contribute to the development of atherosclerotic plaques (M. D. Wu et al., 2017), the reduction in platelet adhesion caused by SRT1720 would not only stop the progression of atherosclerotic lesions but also prevent future atherothrombotic events. Similar to the effect in platelet spreading, SIRT1 activation decreased platelet adhesion in both static (Figure 4.1A and Figure 4.2A) and arterial flow (Figure 3.9A) conditions rather than abolish it, which again suggests that SIRT1 agonists reduce platelet activity without compromising basal platelet function.

Due to the mild effects of SIRT1 activation in platelet activity, SIRT1 agonists could be considered to potentiate the effect of existing antithrombotic treatments in resistant patients. In a previous study by Stef et al. (2006), PRP from individuals resistant to aspirin was treated with resveratrol and platelet aggregatory response to collagen was evaluated using LTA, demonstrating that this drug further reduced platelet aggregation (Stef et al., 2006). Whether this effect is mediated by SIRT1 or other resveratrol targets is uncertain. Therefore, an interesting experiment to perform in the future would be to isolate PRP from aspirin-resistant patients and treat it with a selective SIRT1 activator, such as SRT1720, or vehicle to test platelet aggregatory response via LTA or PBA.

Evidence in the literature suggests that targeting the platelet cytoskeleton constitutes an attractive novel antithrombotic strategy (Shin et al., 2017; Antonipillai et al., 2018). A recent study by Robaux et al. (2023) identified that platelets from coronary artery disease patients on DAPT are characterised by increased tubulin acetylation compared to platelets from non-treated patients from the ACCTHEROMA (prospective evaluation of acetyl-CoA carboxylase phosphorylation state in platelets as a marker of atherothrombotic coronary and extra-coronary artery disease) study (Kautbally et al., 2019; Robaux et al., 2023). Since tubulin acetylation is a hallmark of the phenotype of resting platelets, demonstrating that SIRT1 activation did not significantly alter the platelet tubulin

cytoskeleton (Figure 4.5 and Figure 4.6) is crucial to evaluate whether SIRT1 activators could be considered to improve the efficacy of DAPT. Future work will involve studying α -tubulin acetylation levels in platelets treated with SRT1720 over time to demonstrate that microfilament acetylation is sustained.

Having identified that SRT1720 reduces the emission of pseudopodia during platelet activation by decreasing the F-actin pool (Figure 6.1), the potential use of selective SIRT1 agonists in the context of thrombolysis could also be considered. Current fibrinolytic drugs, including tissue plasminogen activator, streptokinase, and urokinase, effectively dissolve the fibrin mesh (Rashedi et al., 2024). The issue is the delivery of these agents to the core of the occlusive thrombi (W. Cao et al., 2024). SIRT1 activators would disrupt platelet actin fibres and reduce clot retraction, which would make the thrombi less dense and increase the bioavailability of thrombolytic drugs on the inside of the thrombi (Henderson et al., 2018). Therefore, SIRT1 agonists could enhance thrombolytic therapy while reducing platelet reactivity, which would decrease the risk of secondary recurrence in myocardial infarction and ischaemic stroke patients. This would allow us to achieve thrombolysis with a lower dose of fibrinolytic agents, reducing the risk of haemorrhagic and embolization secondary events (Kluft et al., 2017). Moreover, the therapeutic window would be shorter, which would reduce the wait time in case surgery was required.

Due to the haemorrhagic complications associated with pharmacological inhibition of platelet function (Godier et al., 2020) and the crucial role of the endothelium in preventing platelet adhesion and thrombus formation (K. Neubauer and B. Zieger, 2022), targeting endothelial cells with antioxidant or anti-inflammatory drugs to prevent endothelial dysfunction is one of the safest antiatherogenic strategies under investigation (Carnemolla et al., 2010; Radenković et al., 2013). It is currently well known that SIRT1 is protective against oxidative stress via several transcriptional, mitochondrial and cytoplasmic mechanisms (H. Li, 2014). A previous study by Xia et al. (2010) has identified that treatment of ApoE-KO mice with resveratrol elevates BH₄ synthesis, which prevents eNOS uncoupling, maintaining NO synthesis and avoiding superoxide production (N. Xia et al., 2010). The findings in Chapter 5 of this thesis demonstrate that SRT1720 increases eNOS (Figure 5.10BI) and DDAH1 (Figure 5.10BII) transcription in healthy and LPS-treated

HCAEC, respectively. However, the impact of SIRT1 selective activation on ROS levels or BH4 production was not evaluated. Therefore, assessing these parameters in dysfunctional endothelial cells would be an interesting experiment to perform in the future.

The increase in vascular permeability associated with endothelial dysfunction is a key pathological event in atherogenesis, as the disruption of the endothelial barrier promotes the accumulation of lipids, namely oxidised LDL, and neutrophils into the intima (Mundi et al., 2018). Excessive oedema caused by an increase in endothelial permeability is one of the main pathological features of ischaemia-reperfusion injury (Kumar et al., 2009). Our study demonstrated that SIRT1 selective activation prevents hyperpermeability in HCAECs treated with LPS (Figure 5.6 and Figure 6.1). Therefore, SIRT1 activation could be beneficial in atherosclerosis as both a prevention and treatment strategy since it would slow down the development of atherosclerotic plaques while reducing the detrimental consequences on the endothelium after plaque rupture. Moreover, considering the results in platelets from chapters 3 and 4, activating SIRT1 in the context of an atherothrombotic event would not only reduce the time of occlusion, as it might contribute to the effect of fibrinolytic agents, but also reduce the impact of ischaemia reperfusion injury, which would potentially make this treatment ideal as an adjunctive therapy post-myocardial infarction or ischaemic stroke.

The results from Chapter 5 of this thesis demonstrate that SIRT1 activation would promote an antithrombotic phenotype during LPS-induced inflammation, as the area occupied by the thrombi in the HCAEC channel is smaller in the SRT1720-treated cells than in the vehicle control cells (Figure 5.8A). Further investigation determined that this effect could be mediated, at least in part, by an increase in THBD mRNA expression in the HCAECs, which explains why thrombus formation in the collagen channels remains unaffected upon SIRT1 activation (Figure 5.8B and Figure 6.1). Therefore, SIRT1 agonists should be investigated as a dual antithrombotic therapy that targets both platelets and the endothelium to prevent platelet hyperactivation and promote endothelial homeostasis.

Vascular remodelling and neovascularisation of atherosclerotic plaques are crucial for plaque growth and destabilisation (Camaré et al., 2017). These two processes

are highly dependent on endothelial cell motility and migration (Michaelis, 2014; Edgar et al., 2022; Du et al., 2024). Experiments in animal models demonstrated that the use of antiangiogenic agents reduces atherosclerotic lesions (Winter et al., 2006; Ahmed et al., 2009). However, some of these drugs were tested in clinical trials as anti-carcinogens showing cardiovascular side effects. For instance, treatment with VEGF receptor tyrosine kinase inhibitors, such as Pazopanib, has been associated with the development of hypertension (Katsi et al., 2014) and QT interval prolongation (Vaklavas et al., 2010; Maurea et al., 2016; Justice et al., 2018). In this study, it was demonstrated that SIRT1 activation causes a reduction in healthy HCAEC migration, offering a potential alternative to VEGFR antagonists. The effect of SRT1720 in HCAEC migration seems to be dose-dependent, but only 3 μ M offered a statistically significant reduction (Figure 5.4). Testing HCAEC migration in the presence of an endothelial dysfunction factor, such as LPS would be required in the future to mimic the inflammation characteristic of atherosclerotic areas. Also, performing a G-Power calculation and increasing the sample size, if necessary, would be ideal to ensure that this experiment is not underpowered. Moreover, assessing the effect of SIRT1 activators in angiogenesis *in vitro* using HCAECs would be an interesting experiment to perform in the future to complement these findings.

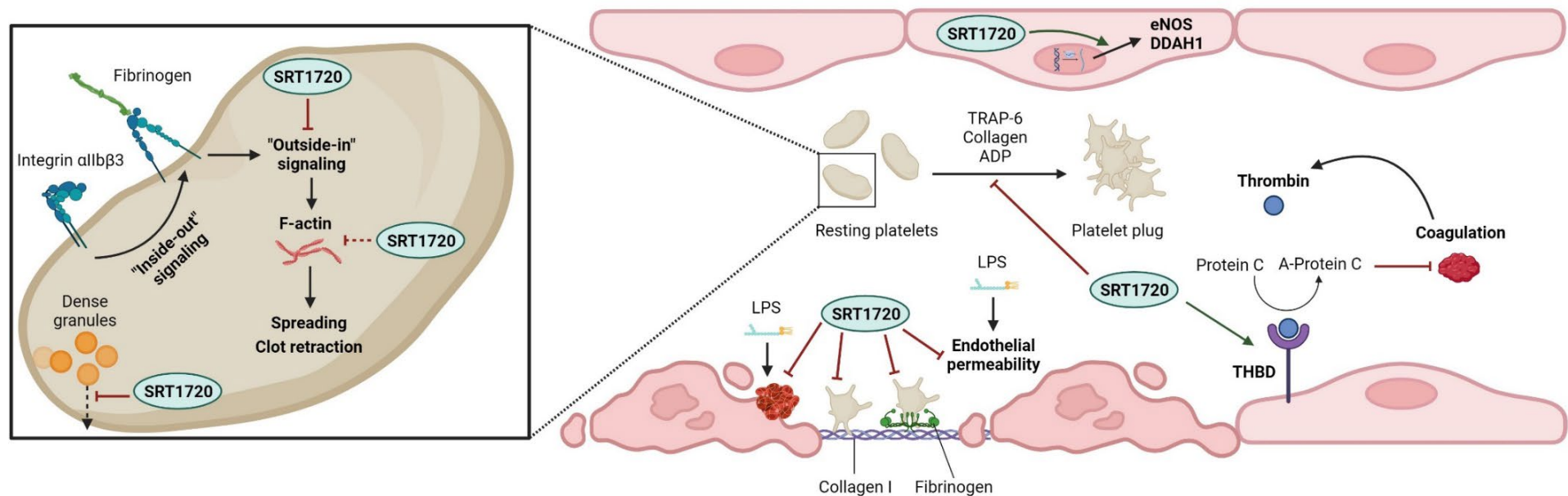


Figure 6.1. Summary of the effects of specific SIRT1 activation with SRT1720 in platelets and endothelial cells. In platelets, SRT1720 (10 μ M) attenuated platelet aggregation in response to TRAP-6, collagen and ADP. SIRT1 activation also reduced dense granule release upon CRP-XL stimulation and decreased fibrinogen binding to the integrin α IIb β 3. Moreover, SRT1720 reduced F-actin levels, although whether this is a consequence of the decrease in integrin “outside-in” signalling or SIRT1 has a direct effect on actin polymerisation via deacetylation of ABPs remains unclear. As a consequence, SIRT1 alters platelet actin cytoskeletal rearrangement, reducing platelet adhesion and spreading to both collagen and fibrinogen and decreasing clot retraction. Regarding the effects in endothelial cells, SRT1720 (1 μ M) increased the mRNA levels of eNOS and DDAH1 in healthy and dysfunctional HCAECs, respectively. SRT1720 also increased THBD transcription in both healthy and LPS-treated HCAEC, which indicates that SIRT1 activation negatively regulates coagulation. LPS-treated HCAEC. Finally, higher doses of SRT1720 (3 μ M) diminished HCAEC migration in a gap closure assay. However, the mechanism behind this effect is still unknown. Overall, SIRT1 activation has an antithrombotic effect, which was demonstrated in our *in vitro* arterial thrombus formation experiments on both collagen and LPS-treated HCAEC. Created in BioRender.com

6.2 Limitations and future directions

There were limitations associated with the time and resources available for the development of this project, which will be addressed in bullet points for convenience.

- A major limitation of this project is the overreliance on SRT1720 as a SIRT1 activator. The rationale for this project stemmed from previous work by our research group, in which activation of SIRT1 with SRT1720 of human vascular smooth muscle cells reduced osteogenic differentiation in hyperglycaemic conditions (Bartoli-Leonard et al., 2019). In this study, treatment with SRT1720 was associated with more than a 10-fold increase in SIRT1 mRNA and protein, which can be consulted in Figure S11 of the supplementary information. Moreover, other investigations have demonstrated that SRT1720 activates SIRT1 using activity assays (Minor et al., 2011; Sung et al., 2020). In the future, repeating the same experiments with other SIRT1 selective agonists, such as SRT2104 (Hoffmann et al., 2013), and performing a SIRT1 activity assay would support that the results observed in this project when treating platelets or HCAEC with SRT1720 are due to SIRT1 activation.
- The lack of adequate controls in some of the experiments. For instance, no secondary antibody controls were included in the Western Blotting experiments. Including lysates obtained from cells in which expression of the target proteins has already been confirmed would also be useful as a positive control. In the case of the study of SIRT1 expression in platelets and HCAECs, HEK293 whole cell lysates would be a great positive control (W. Zhang et al., 2020). Moreover, although a TRAP-6 positive control was included in the F-actin measurements in platelet samples (section 4.3.3), no negative controls were conducted. An appropriate negative control could have been latrunculin A, which prevents actin polymerization by binding to the actin monomers (Woronowicz et al., 2010).
- To confirm the effect of SRT1720 on actin polymerisation in platelets, other techniques apart from flow cytometry and immunoblotting, such as fluorescence microscopy using fluorescently labelled phalloidin (Zonderland et al., 2019), could have been performed.

- Considering that SIRT1 activation with SRT1720 (10 μ M) decreased clot retraction *in vitro* (section 4.3.5), tail bleeding assays should be performed to evaluate whether this treatment could increase the bleeding time and, thus, potentially cause adverse bleeding events.
- Collagen I was used as an adhesive surface in the *in vitro* arterial thrombus formation assay plus the platelet adhesion and spreading assays. However, the ECM is formed by many other proteins entangled in a complex structure. Therefore, the effect of SIRT1 activation should be evaluated in a more representative model in the future, in which a confluent HCAEC monolayer would be treated and decellularized to allow the evaluation of thrombus formation or platelet adhesion/spreading in the ECM.
- The effect of SRT1720 in the formation of the platelet plug was investigated in this project. However, the role of SIRT1 in coagulation was not assessed from a platelet perspective. Using a coagulation analyser and human PRP, the impact of SIRT1 pharmacological activation in activated partial thromboplastin time (aPTT) and prothrombin time (PT) could be tested in the future.
- A major limitation of this project was the lack of commercialised anti-acetylated lysine antibodies. As a consequence, activation of most of the signalling pathways explored to determine the mechanism behind the effects of SRT1720 in platelets was assessed via phosphorylation changes, as SIRT1 could deacetylate an intermediate kinase or phosphatase involved in those routes. Moreover, the changes in the phosphorylation status of the platelet proteins investigated in section 4.3.6 have been robustly associated with platelet activation by previous studies (Valentijn et al., 2011; Senis, 2013), while the effect of acetylation of these proteins in platelet activation remains unclear. The fact that SRT1720 did not change the phosphorylation status of the targets explored in section 4.3.6 does not mean that acetylation levels remained unchanged. Therefore, acetylation of integrin α IIb β 3, MLC2, FAK, cofilin and other potential SIRT1 targets involved in the regulation of actin polymerisation, cytoskeletal reorganisation and platelet adhesion (S. Sun et al., 2022), should be tested in the future using either immunoprecipitation or mass spectrometry to

elucidate the molecular pathways modulated by SIRT1 in basal and activated platelets.

- As most of the effects of SRT1720 in platelets were observed in spread cells, lysates from platelets treated with vehicle or SRT1720 and spread in different adhesive surfaces, such as CRP-XL, collagen and fibrinogen, will be generated in the future. Then, acetylated lysine levels will be evaluated in key proteins involved in platelet cytoskeletal rearrangements to investigate the signalling behind the treatment with SRT1720 using the appropriate negative and positive controls via mass spectrometry.
- Considering that SRT1720 did not affect the phosphorylation of any of the targets explored in section 4.3.6 and that it reduced both integrin $\alpha\text{IIb}\beta\text{3}$ function platelets response to collagen, the signalling pathway affected by SIRT1 activation in platelets remains unclear. For future experiments, using selective agonists for the collagen receptors in all experiments, such as CRP-XL (Sang et al., 2019), or blocking the integrin $\alpha\text{IIb}\beta\text{3}$ signalling using eptifibatide (Safi et al., 2024) and evaluating changes in platelet function or signalling markers in the presence and absence of SRT1720 would be a good strategy to identify which pathway is affected by SIRT1 activation.
- In experiments with platelets, SRT1720 was used at 10 μM , as most of these tests were performed in PRP, in which the percentage of drug binding to plasma proteins is considerably high. Although microscopy images of platelets treated with SRT1720 demonstrate that a 10 μM dose of this drug is not toxic for platelets, performing a cytotoxicity test such as an MTS or Annexin V assay would have been ideal.
- In this project, only HCAECs obtained from male donors were used as a model of endothelial cells, due to lack of commercially available HCAECs from female donors. Moreover, the age of the donors was between 50 and 75 years old. In the future, using a more inclusive research approach to test the effects of SRT1720 in arterial endothelial cells from women and other age populations would be ideal.

- The lack of response from HCAECs to conventional inflammatory mediators in atherosclerosis (section 5.3.5.1) is one of the main limitations of this study and requires troubleshooting.

LPS (100 ng/mL) failed to induce or reduce the expression of the genes evaluated in section 5.3.5, which are widely considered markers of endothelial dysfunction. However, the same concentration and batch of LPS successfully induced thrombus formation in the *in vitro* arterial thrombosis model (section 5.3.4.1). One explanation for this event is that some of the cell batches were not responding to endothelial dysfunction inducers. The isolation process of HCAECs is complex and depending on the number of successive divisions required to reach confluency cells can be less reactive, which causes high variability in the results. Excluding irresponsive donors while performing more replicates in responsive cell batches would be necessary. Another potential explanation would be that the expression of all genes was evaluated at the same time point using the same concentration of LPS, while the time required for up or downregulation is variable depending on the specific gene. Therefore, performing a time course with healthy and LPS-treated cells to identify the mRNA peak or bottom would be necessary to obtain significant changes in all the genes of the panel. Moreover, culturing HCAECs under arterial flow might help to maximise transcriptional changes, as observed in investigations by Satta et al. (2023) with TNF- α (Satta et al., 2023).

When using TNF- α (10 ng/mL) in HCAEC, NF- κ B nuclear translocation was successfully induced after 4 hours. However, actin polymerisation and permeability were not increased after 24 hours with 10 ng/mL and 1 μ g/mL of TNF- α , respectively. TNF- α (10 ng/mL) also failed to change the mRNA expression of genes that codify endothelial regulators of haemostasis, including VCAM, NOS3 and PTGS2. Although the reason behind this lack of effect upon TNF- α -induced inflammation is yet unknown, it is likely linked to the HCAECs rather than the TNF- α , as different batches were used, obtaining the same results. As mentioned in the previous paragraph, culturing the HCAECs changes the expression profile in healthy and TNF- α -treated HCAECs (Satta et al., 2023). Thus,

evaluating the effects of TNF- α in HCAECs grown under arterial flow might offer different results.

- As mentioned in section 5.4 , evidence in the literature demonstrates that subclinical levels of LPS that cause chronic inflammation responses contribute to the development of atherosclerotic plaques (Violi et al., 2023), hence why an LPS treatment was performed in HCAECs to explore the role of SIRT1 in atherosclerosis in this project. However, considering that atherosclerosis is a multifactorial disease (Mahmoudi, 2022), future experiments should evaluate the impact of SRT1720 in a more complex model of endothelial dysfunction. For instance, high glucose or oxidised LDL, apart from an inflammatory cocktail including TNF- α or IL-6, could be used to mimic diabetes (Poznyak et al., 2020) and obesity (Henning, 2021) *in vitro*.
- Regarding the transcriptional effects of SIRT1 in HCAECs (section 5.3.5):
 - The reduction in thrombus formation on LPS-treated HCAEC was partially attributed to an increase in THBD expression (Figure 5.12). However, only mRNA levels were evaluated. Future experiments would involve evaluating THBD protein levels in healthy and LPS-treated HCAEC in the presence and absence of SRT1720 (1 μ M) using Western Blotting. Moreover, it is unlikely that this is the only mechanism behind the decrease in thrombus formation observed in the model, as blood was obtained in sodium citrate tubes and not re-calcified. Therefore, coagulation would be limited. Performing the same experiment using re-calcified blood and testing THBD protein expression instead of mRNA would be required to fully assess the importance of this mechanism in SIRT1-mediated antithrombotic effects.
 - Although the expression of PTGS1 (Figure 5.10C) and PTGS2 (Figure 5.10D) mRNA was evaluated in this study, additional transcripts downstream of the COX enzymes that could have been investigated are TxA2 synthase and PGI₂ synthase, which would alter the ratio of TXA₂, a platelet activator and vasoconstrictor (Rucker and Dhamoon, 2023), and PGI₂, a platelet inhibitor and vasodilator (Braune et al., 2020).

- VWF synthesis was evaluated in this project (Figure 5.11), but not its release. Thus, future experiments should evaluate whether SIRT1 activation could affect Weibel Palade body release (Valentijn et al., 2011), as this would constitute another potential mechanism through which SIRT1 could reduce thromboinflammation.
- Previous work by Breitenstein et al. (2011) revealed that SIRT1 downregulation in HAECs enhanced TF protein and mRNA expression (Breitenstein et al., 2011). TF is expressed and released from endothelial cells only in response to inflammatory cytokines, such as TNF- α or LPS (Szotowski et al., 2005). Therefore, future work will involve evaluating whether SRT1720 can prevent TF overexpression in LPS-treated HCAEC. Moreover, a TF surface activity assay in HCAECs could also be performed to confirm that this translates into decreased TF protein expression.
- Future work would involve culturing HCAECs under flow and re-assess the mRNA or protein levels of the endothelial regulators of haemostasis evaluated in section 5.3.5.1 in these cells, as the transcription profile changes significantly.
- In this study, the effect of SRT1720 in thrombus formation on dysfunctional endothelial cells was evaluated (Figure 5.8), but not in coagulation. Considering that SIRT1 activation reduced THBD expression, experiments to evaluate whether SIRT1 can reduce the procoagulant phenotype of dysfunctional endothelial cells should be performed in the future. For instance, HCAECs could be treated with PBS or LPS in the presence and absence of SRT1720 and the supernatant would be isolated and stored. Then, this supernatant would be added to PRP and the impact of the supernatant in the aPTT would be evaluated using a coagulation analyser.
- Considering the findings of this thesis, we hypothesise that SIRT1 activators could potentially be used as novel therapeutics to enhance the performance of current antithrombotic treatments while promoting a healthy endothelial phenotype (section 6.1.6). However, to empirically determine whether SIRT1 selective activation potentiates the effect of antiplatelet drugs, thrombus formation

should be evaluated using our endothelialised in vitro model in the presence of aspirin or clopidogrel. First, platelets would be treated with SRT1720 or vehicle plus one of the mentioned antithrombotic drugs or vehicle and thrombus formation would be tested on healthy and dysfunctional HCAECs and collagen. Then, platelets would only be treated with aspirin, clopidogrel or vehicle and thrombus formation would be assessed in SRT1720 or vehicle-treated healthy and dysfunctional HCAECs and collagen. Although this experiment was considered in the grant for this project, it could not be performed due to limited time and it is part of our future plan.

- In this project, it was identified that SRT1720 (3 μ M) reduce HCAEC migration in a gap closure assay (section 5.3.3.2). However, the mechanism behind this effect is still unknown. Although some potential targets were mentioned in section 6.1.5, the reduction in integrin α IIb β 3 activation observed in SRT1720 treated-platelets indicates that SIRT1 activation could disrupt the signalling that allows the conformational change required for integrin binding to substrates (section 3.3.3). In the case of platelets and endothelial cells, integrins are crucial proteins for anchorage to the ECM, which mediates spreading (Bennett et al., 2009) and migration (R. Silva et al., 2008), respectively. Therefore, the effect of SRT1720 on integrin pathways in platelets and HCAECs should be investigated in the future (Pang et al., 2023).
- Findings from this study identified that SRT1720 causes HCAEC death at doses of 10 μ M or higher (Figure 5.2), but the cytotoxicity mechanisms behind these observations remain unclear. Previous reports identified that treatment with SRT1720 of cardiomyocytes (G. Luo et al., 2019), bladder cancer cells (L. Li et al., 2024) and leukaemia T-cells (Heshmati et al., 2020) induced autophagy. Knowing that mild adaptive autophagy is protective against the progression of atherosclerotic lesions, while excessive autophagy leads to plaque instability (Ni et al., 2021), exploring in depth which mechanism of death is triggered by SRT1720 and whether this would disrupt autophagic homeostasis in endothelial cells would be required before considering SIRT1 agonists as potential treatments for atherosclerosis.

- On the one hand, studies in mice demonstrated that administration of the selective SIRT1 inhibitor EX-527 reduced the platelet count (Kumari et al., 2015), which indicates that SIRT1 inhibition might impair thrombopoiesis. On the other hand, our investigations revealed that SIRT1 decreased integrin $\alpha\text{IIb}\beta\text{3}$ activation (Figure 3.6) and fibrinogen binding (Figure 3.5) and commercialised integrin $\alpha\text{IIb}\beta\text{3}$ antagonists have been associated with thrombocytopenia (J. Huang et al., 2019; van den Kerkhof et al., 2021). Moreover, SIRT1 activation disrupted actin cytoskeletal reorganisation (Figure 4.3 and Figure 4.4), which is crucial for proplatelet formation (Italiano et al., 2007; Becker et al., 2024). Therefore, the effect of SRT1720 on megakaryocyte function and thrombopoiesis should be investigated in the future.
- Finally, a general limitation of this project was that no G-Power calculations were performed. Before publication of these results, it would be ideal to calculate the appropriate sample size to confirm all experiments are not under or overpowered, ensuring the rigor of our findings (Kang, 2021).

6.3 Conclusion

The initial aim of this project was to identify whether SIRT1-specific pharmacological activation could reduce platelet reactivity while promoting an antithrombotic phenotype on endothelial cells, which has been achieved successfully. Our investigations provide a novel alternative to current antiplatelet agents and a potential adjuvant drug that could be used to potentiate the effect of fibrinolytic therapy. Additionally, the findings of this thesis indicate that SIRT1 agonists might be useful drugs in the prevention of endothelial dysfunction and reveal the unmet need to further investigate the signalling mechanisms behind the effects of SRT1720 in platelets and endothelial cells using mass spectrometry. Future work also involves evaluating the impact of SIRT1 activation in thrombopoiesis.

Chapter 7. References

- Aburima, A., Wraith, K. S., Raslan, Z., Law, R., Magwenzi, S. and Naseem, K. M. (2013) 'cAMP signaling regulates platelet myosin light chain (MLC) phosphorylation and shape change through targeting the RhoA-Rho kinase-MLC phosphatase signaling pathway.' *Blood*, 122(20) pp. 3533-3545.
- Aghajanian, A., Wittchen, E. S., Allingham, M. J., Garrett, T. A. and Burridge, K. (2008) 'Endothelial cell junctions and the regulation of vascular permeability and leukocyte transmigration.' *Journal of Thrombosis and Haemostasis*, 6(9), 2008/09/01/, pp. 1453-1460.
- Ahmed, A., Fujisawa, T., Niu, X. L., Ahmad, S., Al-Ani, B., Chudasama, K., Abbas, A., Potluri, R., et al. (2009) 'Angiopoietin-2 confers Atheroprotection in apoE^{-/-} mice by inhibiting LDL oxidation via nitric oxide.' *Circ Res*, 104(12), Jun 19, 20090521, pp. 1333-1336.
- Ajjan, R., Storey, R. F. and Grant, P. J. (2008) 'Aspirin resistance and diabetes mellitus.' *Diabetologia*, 51(3), 2008/03/01, pp. 385-390.
- Aksnes, H., Marie, M., Arnesen, T. and Drazic, A. (2018) 'Actin polymerization and cell motility are affected by NAA80-mediated posttranslational N-terminal acetylation of actin.' *Commun Integr Biol*, 11(4) 20181021, p. e1526572.
- Al-Amer, O. M. (2022) 'The role of thrombin in haemostasis.' *Blood Coagul Fibrinolysis*, 33(3), Apr 1, 20220302, pp. 145-148.
- Alaskhar Alhamwe, B., Khalaila, R., Wolf, J., von Bülow, V., Harb, H., Alhamdan, F., Hii, C. S., Prescott, S. L., et al. (2018) 'Histone modifications and their role in epigenetics of atopy and allergic diseases.' *Allergy, Asthma & Clinical Immunology*, 14(1), 2018/05/23, p. 39.
- Ali, R. A., Wuescher, L. M. and Worth, R. G. (2015) 'Platelets: essential components of the immune system.' *Curr Trends Immunol*, 16 pp. 65-78.
- Alonso-Herranz, L., Albarrán-Juárez, J. and Bentzon, J. F. (2023) 'Mechanisms of fibrous cap formation in atherosclerosis.' *Frontiers in Cardiovascular Medicine*, 10, 2023-August-21,

Alp, N. J. and Channon, K. M. (2004) 'Regulation of endothelial nitric oxide synthase by tetrahydrobiopterin in vascular disease.' *Arterioscler Thromb Vasc Biol*, 24(3), Mar, 20031204, pp. 413-420.

Alper, J. D., Decker, F., Agana, B. and Howard, J. (2014) 'The motility of axonemal dynein is regulated by the tubulin code.' *Biophys J*, 107(12), Dec 16, pp. 2872-2880.

Anand, P. and Harper, A. G. S. (2020) 'Human platelets use a cytosolic Ca²⁺ nanodomain to activate Ca²⁺-dependent shape change independently of platelet aggregation.' *Cell Calcium*, 90, 2020/09/01/, p. 102248.

Andersen, H., Greenberg, D. L., Fujikawa, K., Xu, W., Chung, D. W. and Davie, E. W. (1999) 'Protease-activated receptor 1 is the primary mediator of thrombin-stimulated platelet procoagulant activity.' *Proceedings of the National Academy of Sciences*, 96(20) pp. 11189-11193.

Andrews, R. K., Gardiner, E. E., Shen, Y., Whisstock, J. C. and Berndt, M. C. (2003) 'Glycoprotein Ib-IX-V.' *The International Journal of Biochemistry & Cell Biology*, 35(8), 2003/08/01/, pp. 1170-1174.

Angiolillo, D. J. (2012) 'The evolution of antiplatelet therapy in the treatment of acute coronary syndromes: from aspirin to the present day.' *Drugs*, 72(16), Nov 12, pp. 2087-2116.

Antonipillai, J., Rigby, S., Bassler, N., Peter, K. and Bernard, O. (2018) 'Inhibition of platelet function by targeting the platelet cytoskeleton via the LIMK-signaling pathway.' *bioRxiv*, p. 438051.

Arce, N. A., Cao, W., Brown, A. K., Legan, E. R., Wilson, M. S., Xu, E.-R., Berndt, M. C., Emsley, J., et al. (2021) 'Activation of von Willebrand factor via mechanical unfolding of its discontinuous autoinhibitory module.' *Nature Communications*, 12(1), 2021/04/21, p. 2360.

Ardeshtna, D., Khare, S., Jagadish, P. S., Bhattad, V., Cave, B. and Khouzam, R. N. (2019) 'The dilemma of aspirin resistance in obese patients.' *Annals of Translational Medicine*, 7(17) p. 404.

Asada, Y., Yamashita, A., Sato, Y. and Hatakeyama, K. (2020) 'Pathophysiology of atherothrombosis: Mechanisms of thrombus formation on disrupted atherosclerotic plaques.' *Pathol Int*, 70(6), Jun, 20200313, pp. 309-322.

Aslan, J. E., Rigg, R. A., Nowak, M. S., Loren, C. P., Baker-Groberg, S. M., Pang, J., David, L. L. and McCarty, O. J. (2015) 'Lysine acetyltransferase supports platelet function.' *J Thromb Haemost*, 13(10), Oct, 20150829, pp. 1908-1917.

ATC. (2009) 'Aspirin in the primary and secondary prevention of vascular disease: collaborative meta-analysis of individual participant data from randomised trials.' *The Lancet*, 373(9678) pp. 1849-1860.

Avvakumov, N. and Côté, J. (2007) 'The MYST family of histone acetyltransferases and their intimate links to cancer.' *Oncogene*, 26(37), Aug 13, pp. 5395-5407.

Baaten, C. C. F. M. J., Nagy, M., Bergmeier, W., Spronk, H. M. H. and van der Meijden, P. E. J. (2024) 'Platelet biology and function: plaque erosion vs. rupture.' *European Heart Journal*, 45(1) pp. 18-31.

Badimon, L., Padró, T. and Vilahur, G. (2012) 'Atherosclerosis, platelets and thrombosis in acute ischaemic heart disease.' *Eur Heart J Acute Cardiovasc Care*, 1(1), Apr, pp. 60-74.

Bai, B., Man, A. W., Yang, K., Guo, Y., Xu, C., Tse, H. F., Han, W., Bloksgaard, M., et al. (2016) 'Endothelial SIRT1 prevents adverse arterial remodeling by facilitating HERC2-mediated degradation of acetylated LKB1.' *Oncotarget*, 7(26), Jun 28, pp. 39065-39081.

Bai, W. and Zhang, X. (2016) 'Nucleus or cytoplasm? The mysterious case of SIRT1's subcellular localization.' *Cell Cycle*, 15(24), Dec 16, 20160929, pp. 3337-3338.

Barrachina, M. N., Hermida-Nogueira, L., Moran, L. A., Casas, V., Hicks, S. M., Sueiro, A. M., Di, Y., Andrews, R. K., et al. (2021) 'Phosphoproteomic Analysis of Platelets in Severe Obesity Uncovers Platelet Reactivity and Signaling Pathways Alterations.' *Arterioscler Thromb Vasc Biol*, 41(1), Jan, 20201105, pp. 478-490.

Bartoli-Leonard, F., Wilkinson, F. L., Schiro, A., Inglott, F. S., Alexander, M. Y. and Weston, R. (2019) 'Suppression of SIRT1 in Diabetic Conditions Induces Osteogenic

Differentiation of Human Vascular Smooth Muscle Cells via RUNX2 Signalling.' *Scientific Reports*, 9(1), 2019/01/29, p. 878.

Bartoli-Leonard, F., Wilkinson, F. L., Schiro, A., Serracino Inglott, F., Alexander, M. Y. and Weston, R. (2021) 'Loss of SIRT1 in diabetes accelerates DNA damage-induced vascular calcification.' *Cardiovasc Res*, 117(3), Feb 22, pp. 836-849.

Bastid, J., Cottalorda-Regairaz, A., Alberici, G., Bonnefoy, N., Eliaou, J. F. and Bensussan, A. (2013) 'ENTPD1/CD39 is a promising therapeutic target in oncology.' *Oncogene*, 32(14), 2013/04/01, pp. 1743-1751.

Battinelli, E. M. (2015) 'Procoagulant Platelets.' *Circulation*, 132(15), 2015/10/13, pp. 1374-1376.

Batty, M., Bennett, M. R. and Yu, E. (2022) 'The Role of Oxidative Stress in Atherosclerosis.' *Cells*, 11(23) p. 3843.

Baumgartner, J. T., Habeeb Mohammad, T. S., Czub, M. P., Majorek, K. A., Arolli, X., Variot, C., Anonick, M., Minor, W., et al. (2021) 'Gcn5-Related N-Acetyltransferases (GNATs) With a Catalytic Serine Residue Can Play Ping-Pong Too.' *Front Mol Biosci*, 8 20210412, p. 646046.

Bearer, E. L., Prakash, J. M. and Li, Z. (2002) 'Actin dynamics in platelets.' *Int Rev Cytol*, 217 pp. 137-182.

Becker, I. C., Wilkie, A. R., Unger, B. A., Sciaudone, A. R., Fatima, F., Tsai, I. T., Xu, K., Machlus, K. R., et al. (2024) 'Dynamic actin/septin network in megakaryocytes coordinates proplatelet elaboration.' *Haematologica*, 109(3), Mar 1, 20240301, pp. 915-928.

Bedalov, A., Gatbonton, T., Irvine, W. P., Gottschling, D. E. and Simon, J. A. (2001) 'Identification of a small molecule inhibitor of Sir2p.' *Proc Natl Acad Sci U S A*, 98(26), Dec 18, pp. 15113-15118.

Bendall, J. K., Douglas, G., McNeill, E., Channon, K. M. and Crabtree, M. J. (2014) 'Tetrahydrobiopterin in cardiovascular health and disease.' *Antioxid Redox Signal*, 20(18), Jun 20, 20140314, pp. 3040-3077.

Bendas, G. and Schlesinger, M. (2022) 'The GPIb-IX complex on platelets: insight into its novel physiological functions affecting immune surveillance, hepatic thrombopoietin generation, platelet clearance and its relevance for cancer development and metastasis.' *Experimental Hematology & Oncology*, 11(1), 2022/04/02, p. 19.

Bender, M. and Palankar, R. (2021) 'Platelet Shape Changes during Thrombus Formation: Role of Actin-Based Protrusions.' *Hamostaseologie*, 41(1), Feb, 20210215, pp. 14-21.

Bender, M., Hagedorn, I. and Nieswandt, B. (2011) 'Genetic and antibody-induced glycoprotein VI deficiency equally protects mice from mechanically and FeCl₃ - induced thrombosis.' *J Thromb Haemost*, 9(7), Jul, pp. 1423-1426.

Bennett, J. S., Berger, B. W. and Billings, P. C. (2009) 'The structure and function of platelet integrins.' *J Thromb Haemost*, 7 Suppl 1, Jul, pp. 200-205.

Bettiol, A., Urban, M. L., Emmi, G., Galora, S., Argento, F. R., Fini, E., Borghi, S., Bagni, G., et al. (2023) 'SIRT1 and thrombosis.' *Front Mol Biosci*, 10 20240118, p. 1325002.

Bhatia, K., Jain, V., Aggarwal, D., Vaduganathan, M., Arora, S., Hussain, Z., Uberoi, G., Tafur, A., et al. (2021) 'Dual Antiplatelet Therapy Versus Aspirin in Patients With Stroke or Transient Ischemic Attack: Meta-Analysis of Randomized Controlled Trials.' *Stroke*, 52(6), 2021/06/01, pp. e217-e223.

Bishopric, N. H. (2013) 'Toward a Genomic Definition of Aspirin Resistance*.' *Journal of the American College of Cardiology*, 62(14), 2013/10/01, pp. 1277-1279.

Bishton, M. J., Gardiner, E. E., Harrison, S. J., Prince, H. M. and Johnstone, R. W. (2013) 'Histone deacetylase inhibitors reduce glycoprotein VI expression and platelet responses to collagen related peptide.' *Thrombosis Research*, 131(6) pp. 514-520.

Bledzka, K., Smyth, S. S. and Plow, E. F. (2013) 'Integrin α IIb β 3: from discovery to efficacious therapeutic target.' *Circ Res*, 112(8), Apr 12, pp. 1189-1200.

Blokhin, I. O. and Lentz, S. R. (2013) 'Mechanisms of thrombosis in obesity.' *Curr Opin Hematol*, 20(5), Sep, pp. 437-444.

Bogatcheva, N. V. and Verin, A. D. (2008) 'The role of cytoskeleton in the regulation of vascular endothelial barrier function.' *Microvasc Res*, 76(3), Nov, 20080628, pp. 202-207.

Bonaventura, A., Vecchié, A., Dagna, L., Martinod, K., Dixon, D. L., Van Tassell, B. W., Dentali, F., Montecucco, F., et al. (2021) 'Endothelial dysfunction and immunothrombosis as key pathogenic mechanisms in COVID-19.' *Nature Reviews Immunology*, 21(5), 2021/05/01, pp. 319-329.

Borst, O. and Gawaz, M. (2021) 'Glycoprotein VI - novel target in antiplatelet medication.' *Pharmacol Ther*, 217, Jan, 20200716, p. 107630.

Botts, S. R., Fish, J. E. and Howe, K. L. (2021) 'Dysfunctional Vascular Endothelium as a Driver of Atherosclerosis: Emerging Insights Into Pathogenesis and Treatment.' *Front Pharmacol*, 12 20211222, p. 787541.

Bouras, T., Fu, M., Sauve, A. A., Wang, F., Quong, A. A., Perkins, N. D., Hay, R. T., Gu, W., et al. (2005) 'SIRT1 deacetylation and repression of p300 involves lysine residues 1020/1024 within the cell cycle regulatory domain 1.' *J Biol Chem*, 280(11), Mar 18, 20050104, pp. 10264-10276.

Braganza, D. M. and Bennett, M. R. (2001) 'New insights into atherosclerotic plaque rupture.' *Postgrad Med J*, 77(904), Feb, pp. 94-98.

Brass, L. F., Stalker, T. J., Zhu, L. and Woulfe, D. S. (2007) 'CHAPTER 16 - Signal Transduction During Platelet Plug Formation.' In Michelson, A. D. (ed.) *Platelets (Second Edition)*. Burlington: Academic Press, pp. 319-346. <https://www.sciencedirect.com/science/article/pii/B9780123693679507783>

Brass, L. F., Vassallo, R. R., Jr., Belmonte, E., Ahuja, M., Cichowski, K. and Hoxie, J. A. (1992) 'Structure and function of the human platelet thrombin receptor. Studies using monoclonal antibodies directed against a defined domain within the receptor N terminus.' *J Biol Chem*, 267(20), Jul 15, pp. 13795-13798.

Braune, S., Küpper, J.-H. and Jung, F. (2020) 'Effect of Prostanoids on Human Platelet Function: An Overview.' *International Journal of Molecular Sciences*, 21, [Online] 23. [Accessed 10.3390/ijms21239020

Breitenstein, A., Stein, S., Holy, E. W., Camici, G. G., Lohmann, C., Akhmedov, A., Spescha, R., Elliott, P. J., et al. (2011) 'Sirt1 inhibition promotes in vivo arterial thrombosis and tissue factor expression in stimulated cells.' *Cardiovasc Res*, 89(2), Feb 1, 20101026, pp. 464-472.

Broos, K., Feys, H. B., De Meyer, S. F., Vanhoorelbeke, K. and Deckmyn, H. (2011) 'Platelets at work in primary hemostasis.' *Blood Rev*, 25(4), Jul, 20110414, pp. 155-167.

Broussy, S., Laaroussi, H. and Vidal, M. (2020) 'Biochemical mechanism and biological effects of the inhibition of silent information regulator 1 (SIRT1) by EX-527 (SEN0014196 or selisistat).' *J Enzyme Inhib Med Chem*, 35(1), Dec, pp. 1124-1136.

Burkhart, J. M., Gambaryan, S., Watson, S. P., Jurk, K., Walter, U., Sickmann, A., Heemskerk, J. W. and Zahedi, R. P. (2014) 'What can proteomics tell us about platelets?' *Circ Res*, 114(7), Mar 28, pp. 1204-1219.

Burkhart, J. M., Vaudel, M., Gambaryan, S., Radau, S., Walter, U., Martens, L., Geiger, J., Sickmann, A., et al. (2012) 'The first comprehensive and quantitative analysis of human platelet protein composition allows the comparative analysis of structural and functional pathways.' *Blood*, 120(15), Oct 11, 20120806, pp. e73-82.

Burleigh, M. E., Babaev, V. R., Oates, J. A., Harris, R. C., Gautam, S., Riendeau, D., Marnett, L. J., Morrow, J. D., et al. (2002) 'Cyclooxygenase-2 Promotes Early Atherosclerotic Lesion Formation in LDL Receptor-Deficient Mice.' *Circulation*, 105(15), 2002/04/16, pp. 1816-1823.

Caldwell, R. B., Toque, H. A., Narayanan, S. P. and Caldwell, R. W. (2015) 'Arginase: an old enzyme with new tricks.' *Trends Pharmacol Sci*, 36(6), Jun, 20150427, pp. 395-405.

Camaré, C., Pucelle, M., Nègre-Salvayre, A. and Salvayre, R. (2017) 'Angiogenesis in the atherosclerotic plaque.' *Redox Biol*, 12, Aug, 20170201, pp. 18-34.

Campbell, C. L., Smyth, S., Montalescot, G. and Steinhubl, S. R. (2007) 'Aspirin dose for the prevention of cardiovascular disease: a systematic review.' *Jama*, 297(18), May 9, pp. 2018-2024.

Cao, J. and Yan, Q. (2012) 'Histone ubiquitination and deubiquitination in transcription, DNA damage response, and cancer.' *Front Oncol*, 2 20120312, p. 26.

Cao, W., Wei, W., Qiu, B., Liu, Y., Xie, S., Fang, Q. and Li, X. (2024) 'Ultrasound-powered hydrogen peroxide-responsive Janus micromotors for targeted thrombolysis and recurrence inhibition.' *Chemical Engineering Journal*, 483, 2024/03/01/, p. 149187.

Capra, V., Bäck, M., Angiolillo, D. J., Cattaneo, M. and Sakariassen, K. S. (2014) 'Impact of vascular thromboxane prostanoid receptor activation on hemostasis, thrombosis, oxidative stress, and inflammation.' *Journal of Thrombosis and Haemostasis*, 12(2) pp. 126-137.

Carnemolla, R., Shuvaev, V. V. and Muzykantov, V. R. (2010) 'Targeting antioxidant and antithrombotic biotherapeutics to endothelium.' *Semin Thromb Hemost*, 36(3), Apr, 20100520, pp. 332-342.

Carnevale, R., Nocella, C., Petrozza, V., Cammisotto, V., Pacini, L., Sorrentino, V., Martinelli, O., Irace, L., et al. (2018) 'Localization of lipopolysaccharide from Escherichia Coli into human atherosclerotic plaque.' *Scientific Reports*, 8(1), 2018/02/26, p. 3598.

Carrizzo, A., Iside, C., Nebbioso, A., Carafa, V., Damato, A., Sciarretta, S., Frati, G., Di Nonno, F., et al. (2022) 'SIRT1 pharmacological activation rescues vascular dysfunction and prevents thrombosis in MTHFR deficiency.' *Cell Mol Life Sci*, 79(8), Jul 11, 20220711, p. 410.

Casey, M., Latario, C. J., Pickrell, L. E. and Higgs, H. N. (2020) 'Lysine acetylation of cytoskeletal proteins: Emergence of an actin code.' *J Cell Biol*, 219(12), Dec 7,

Chan, B. P. L., Wong, L. Y. H., Tan, B. Y. Q., Yeo, L. L. L. and Venketasubramanian, N. (2024) 'Dual Antiplatelet Therapy for the Acute Management and Long-term Secondary Prevention of Ischemic Stroke and Transient Ischemic Attack, An Updated Review.' *J Cardiovasc Dev Dis*, 11(2), Jan 31, 20240131,

Chan, M. V., Armstrong, P. C. and Warner, T. D. (2018) '96-well plate-based aggregometry.' *Platelets*, 29(7), 2018/10/03, pp. 650-655.

Chan, S. H., Hung, C.-H., Shih, J.-Y., Chu, P.-M., Cheng, Y.-H., Lin, H.-C. and Tsai, K.-L. (2017) 'SIRT1 inhibition causes oxidative stress and inflammation in patients with coronary artery disease.' *Redox Biology*, 13, 2017/10/01/, pp. 301-309.

Chapin, J. C. and Hajjar, K. A. (2015) 'Fibrinolysis and the control of blood coagulation.' *Blood Rev*, 29(1), Jan, 20140916, pp. 17-24.

Chari, R., Kim, S., Murugappan, S., Sanjay, A., Daniel, J. L. and Kunapuli, S. P. (2009) 'Lyn, PKC-delta, SHIP-1 interactions regulate GPVI-mediated platelet-dense granule secretion.' *Blood*, 114(14), Oct 1, 20090708, pp. 3056-3063.

Chatterjee, M. and Gawaz, M. (2017) 'Platelets in Atherosclerosis.' In Gresele, P., Kleiman, N. S., Lopez, J. A. and Page, C. P. (eds.) *Platelets in Thrombotic and Non-Thrombotic Disorders: Pathophysiology, Pharmacology and Therapeutics: an Update*. Cham: Springer International Publishing, pp. 993-1013. https://doi.org/10.1007/978-3-319-47462-5_66

Chauhan, D., Bandi, M., Singh, A. V., Ray, A., Raje, N., Richardson, P. and Anderson, K. C. (2011) 'Preclinical evaluation of a novel SIRT1 modulator SRT1720 in multiple myeloma cells.' *Br J Haematol*, 155(5), Dec, 20110926, pp. 588-598.

Chen, C. A., Wang, T. Y., Varadharaj, S., Reyes, L. A., Hemann, C., Talukder, M. A., Chen, Y. R., Druhan, L. J., et al. (2010) 'S-glutathionylation uncouples eNOS and regulates its cellular and vascular function.' *Nature*, 468(7327), Dec 23, pp. 1115-1118.

Chen, T., Dai, S.-H., Li, X., Luo, P., Zhu, J., Wang, Y.-H., Fei, Z. and Jiang, X.-F. (2018) 'Sirt1-Sirt3 axis regulates human blood-brain barrier permeability in response to ischemia.' *Redox Biology*, 14, 2018/04/01/, pp. 229-236.

Chen, Y., Yuan, Y. and Li, W. (2018) 'Sorting machineries: how platelet-dense granules differ from α -granules.' *Bioscience Reports*, 38(5) p. BSR20180458.

Chen, Y., Zhang, H., Ji, S., Jia, P., Chen, Y., Li, Y. and Wang, T. (2021) 'Resveratrol and its derivative pterostilbene attenuate oxidative stress-induced intestinal injury by improving mitochondrial redox homeostasis and function via SIRT1 signaling.' *Free Radical Biology and Medicine*, 177, 2021/12/01/, pp. 1-14.

Chen, Y., Ju, L. A., Zhou, F., Liao, J., Xue, L., Su, Q. P., Jin, D., Yuan, Y., et al. (2019) 'An integrin α IIb β 3 intermediate affinity state mediates biomechanical platelet aggregation.' *Nature Materials*, 18(7), 2019/07/01, pp. 760-769.

Cheng, Y., Di, S., Fan, C., Cai, L., Gao, C., Jiang, P., Hu, W., Ma, Z., et al. (2016) 'SIRT1 activation by pterostilbene attenuates the skeletal muscle oxidative stress injury and mitochondrial dysfunction induced by ischemia reperfusion injury.' *Apoptosis*, 21(8), Aug, pp. 905-916.

Chiang, Y.-C., Wu, Y.-S., Kang, Y.-F., Wang, H.-C., Tsai, M.-C. and Wu, C.-C. (2022) '3,5,2',4'-Tetramethoxystilbene, a fully methylated resveratrol analog, prevents platelet aggregation and thrombus formation by targeting the protease-activated receptor 4 pathway.' *Chemico-Biological Interactions*, 357, 2022/04/25/, p. 109889.

Chin, S. M., Hatano, T., Sivashanmugam, L., Suchenko, A., Kashina, A. S., Balasubramanian, M. K. and Jansen, S. (2022) 'N-terminal acetylation and arginylation of actin determines the architecture and assembly rate of linear and branched actin networks.' *J Biol Chem*, 298(11), Nov, 20220922, p. 102518.

Chistiakov, D. A., Orekhov, A. N. and Bobryshev, Y. V. (2015) 'Endothelial Barrier and Its Abnormalities in Cardiovascular Disease.' *Front Physiol*, 6 20151209, p. 365.

Chiu, J. J. and Chien, S. (2011) 'Effects of disturbed flow on vascular endothelium: pathophysiological basis and clinical perspectives.' *Physiol Rev*, 91(1), Jan, pp. 327-387.

Choi, J. H., Nam, K. H., Kim, J., Baek, M. W., Park, J. E., Park, H. Y., Kwon, H. J., Kwon, O. S., et al. (2005) 'Trichostatin A exacerbates atherosclerosis in low density lipoprotein receptor-deficient mice.' *Arterioscler Thromb Vasc Biol*, 25(11), Nov, 20050901, pp. 2404-2409.

Choudhary, C., Kumar, C., Gnad, F., Nielsen, M. L., Rehman, M., Walther, T. C., Olsen, J. V. and Mann, M. (2009) 'Lysine acetylation targets protein complexes and co-regulates major cellular functions.' *Science*, 325(5942), Aug 14, 20090716, pp. 834-840.

Cimmino, G., Natale, F., Alfieri, R., Cante, L., Covino, S., Franzese, R., Limatola, M., Marotta, L., et al. (2023) 'Non-Conventional Risk Factors: "Fact" or "Fake" in Cardiovascular Disease Prevention?' *Biomedicines*, 11, [Online] 9. [Accessed 10.3390/biomedicines11092353

Claesson-Welsh, L., Dejana, E. and McDonald, D. M. (2021) 'Permeability of the Endothelial Barrier: Identifying and Reconciling Controversies.' *Trends in Molecular Medicine*, 27(4), 2021/04/01/, pp. 314-331.

Clark, S. J., Falchi, M., Olsson, B., Jacobson, P., Cauchi, S., Balkau, B., Marre, M., Lantieri, O., et al. (2012) 'Association of sirtuin 1 (SIRT1) gene SNPs and transcript expression levels with severe obesity.' *Obesity (Silver Spring)*, 20(1), Jan, 20110714, pp. 178-185.

Clemetson, K. J. (2012) 'Platelets and primary haemostasis.' *Thromb Res*, 129(3), Mar, 20111216, pp. 220-224.

Co, A. D., Lagomarsino, M. C., Caselle, M. and Osella, M. (2017) 'Stochastic timing in gene expression for simple regulatory strategies.' *Nucleic Acids Res*, 45(3), Feb 17, pp. 1069-1078.

Cosen-Binker, L. I. and Kapus, A. (2006) 'Cortactin: The Gray Eminence of the Cytoskeleton.' *Physiology*, 21(5) pp. 352-361.

Costantino, S., Mengozzi, A., Velagapudi, S., Mohammed, S. A., Gorica, E., Akhmedov, A., Mongelli, A., Pugliese, N. R., et al. (2023) 'Treatment with recombinant Sirt1 rewires the cardiac lipidome and rescues diabetes-related metabolic cardiomyopathy.' *Cardiovascular Diabetology*, 22(1), 2023/11/13, p. 312.

Coughlin, S. R. (1999) 'How the protease thrombin talks to cells.' *Proc Natl Acad Sci U S A*, 96(20), Sep 28, pp. 11023-11027.

Coughlin, S. R. (2005) 'Protease-activated receptors in hemostasis, thrombosis and vascular biology.' *J Thromb Haemost*, 3(8), Aug, pp. 1800-1814.

Crabtree, M. J., Tatham, A. L., Al-Wakeel, Y., Warrick, N., Hale, A. B., Cai, S., Channon, K. M. and Alp, N. J. (2009) 'Quantitative regulation of intracellular endothelial nitric-oxide synthase (eNOS) coupling by both tetrahydrobiopterin-eNOS stoichiometry and biopterin redox status: insights from cells with tet-regulated GTP cyclohydrolase I expression.' *J Biol Chem*, 284(2), Jan 9, 20081114, pp. 1136-1144.

Csiszar, A., Labinsky, N., Podlutzky, A., Kaminski, P. M., Wolin, M. S., Zhang, C., Mukhopadhyay, P., Pacher, P., et al. (2008) 'Vasoprotective effects of resveratrol and SIRT1: attenuation of cigarette smoke-induced oxidative stress and proinflammatory phenotypic alterations.' *Am J Physiol Heart Circ Physiol*, 294(6), Jun, 20080418, pp. H2721-2735.

Cuenca-Zamora, E. J., Ferrer-Marín, F., Rivera, J. and Teruel-Montoya, R. (2019) 'Tubulin in Platelets: When the Shape Matters.' *International Journal of Molecular Sciences*, 20(14) p. 3484.

Cuiping, F., Hao, S., Xu, X., Zhou, J., Liu, Z., Lu, H., Wang, L., Jin, W., et al. (2019) 'Activation of SIRT1 ameliorates LPS-induced lung injury in mice via decreasing endothelial tight junction permeability.' *Acta Pharmacologica Sinica*, 40(5), 2019/05/01, pp. 630-641.

Cylwik, D., Mogielnicki, A. and Buczko, W. (2005) 'L-arginine and cardiovascular system.' *Pharmacol Rep*, 57(1), Jan-Feb, pp. 14-22.

Cyr, A. R., Huckaby, L. V., Shiva, S. S. and Zuckerbraun, B. S. (2020) 'Nitric Oxide and Endothelial Dysfunction.' *Crit Care Clin*, 36(2), Apr, pp. 307-321.

da Costa Martins, P., García-Vallejo, J.-J., van Thienen, J. V., Fernandez-Borja, M., van Gils, J. M., Beckers, C., Horrevoets, A. J., Hordijk, P. L., et al. (2007) 'P-Selectin Glycoprotein Ligand-1 Is Expressed on Endothelial Cells and Mediates Monocyte Adhesion to Activated Endothelium.' *Arteriosclerosis, Thrombosis, and Vascular Biology*, 27(5), 2007/05/01, pp. 1023-1029.

Dahlbäck, B. (2005) 'Blood coagulation and its regulation by anticoagulant pathways: genetic pathogenesis of bleeding and thrombotic diseases.' *Journal of Internal Medicine*, 257(3), 2005/03/01, pp. 209-223.

Dai, H., Sinclair, D. A., Ellis, J. L. and Steegborn, C. (2018) 'Sirtuin activators and inhibitors: Promises, achievements, and challenges.' *Pharmacol Ther*, 188, Aug, 20180322, pp. 140-154.

Dai, Y., Rahmani, M., Dent, P. and Grant, S. (2005) 'Blockade of histone deacetylase inhibitor-induced RelA/p65 acetylation and NF-kappaB activation potentiates apoptosis in leukemia cells through a process mediated by oxidative damage, XIAP downregulation, and c-Jun N-terminal kinase 1 activation.' *Mol Cell Biol*, 25(13), Jul, pp. 5429-5444.

Damman, P., Woudstra, P., Kuijt, W. J., de Winter, R. J. and James, S. K. (2012) 'P2Y12 platelet inhibition in clinical practice.' *J Thromb Thrombolysis*, 33(2), Feb, pp. 143-153.

Dasgupta, S. K. and Thiagarajan, P. (2020) 'Cofilin-1-induced actin reorganization in stored platelets.' *Transfusion*, 60(4), Apr, 20200311, pp. 806-814.

de Gregorio, E., Colell, A., Morales, A. and Marí, M. (2020) 'Relevance of SIRT1-NF- κ B Axis as Therapeutic Target to Ameliorate Inflammation in Liver Disease.' *Int J Mol Sci*, 21(11), May 29, 20200529,

de Ruijter, A. J., van Gennip, A. H., Caron, H. N., Kemp, S. and van Kuilenburg, A. B. (2003) 'Histone deacetylases (HDACs): characterization of the classical HDAC family.' *Biochem J*, 370(Pt 3), Mar 15, pp. 737-749.

De Servi, S., Landi, A., Savonitto, S., De Luca, L., De Luca, G., Morici, N., Montalto, C., Crimi, G., et al. (2023) 'Tailoring oral antiplatelet therapy in acute coronary syndromes: from guidelines to clinical practice.' *Journal of Cardiovascular Medicine*, 24(2)

De Silva, E., Hong, F., Falet, H. and Kim, H. (2022) 'Filamin A in platelets: Bridging the (signaling) gap between the plasma membrane and the actin cytoskeleton.' *Frontiers in Molecular Biosciences*, 9, 2022-December-20,

de Souza Brito, F. and Tricoci, P. (2013) 'Novel Anti-platelet Agents: Focus on Thrombin Receptor Antagonists.' *Journal of Cardiovascular Translational Research*, 6(3), 2013/06/01, pp. 415-424.

Dean, L. and Kane, M. (2012) 'Clopidogrel Therapy and CYP2C19 Genotype.' In Pratt, V. M., Scott, S. A., Pirmohamed, M., Esquivel, B., Kattman, B. L. and Malheiro, A. J. (eds.) *Medical Genetics Summaries*. Bethesda (MD): National Center for Biotechnology Information (US),

Delcuve, G. P., Khan, D. H. and Davie, J. R. (2012) 'Roles of histone deacetylases in epigenetic regulation: emerging paradigms from studies with inhibitors.' *Clinical Epigenetics*, 4(1), 2012/03/12, p. 5.

Dong, G., Wang, B., An, Y., Li, J., Wang, X., Jia, J. and Yang, Q. (2018) 'SIRT1 suppresses the migration and invasion of gastric cancer by regulating ARHGAP5 expression.' *Cell Death & Disease*, 9(10), 2018/09/24, p. 977.

Dowal, L., Yang, W., Freeman, M. R., Steen, H. and Flaumenhaft, R. (2011) 'Proteomic analysis of palmitoylated platelet proteins.' *Blood*, 118(13), Sep 29, 20110802, pp. e62-73.

Drazic, A., Aksnes, H., Marie, M., Boczkowska, M., Varland, S., Timmerman, E., Foyn, H., Glomnes, N., et al. (2018) 'NAA80 is actin's N-terminal acetyltransferase and regulates cytoskeleton assembly and cell motility.' *Proceedings of the National Academy of Sciences*, 115(17) pp. 4399-4404.

Drysdale, A., Blanco-Lopez, M., White, S. J., Unsworth, A. J. and Jones, S. (2024) 'Differential Proteoglycan Expression in Atherosclerosis Alters Platelet Adhesion and Activation.' *Int J Mol Sci*, 25(2), Jan 12, 20240112,

Du, Y., Xu, X.-X., Yu, S.-X., Wang, Y.-R., Liu, Y., Liu, F., Liu, W., Li, X.-L., et al. (2024) 'Dynamics of endothelial cells migration in nature-mimicking blood vessels.' *Talanta*, 277, 2024/09/01/, p. 126415.

Dubois-Deruy, E., El Masri, Y., Turkieh, A., Amouyel, P., Pinet, F. and Annicotte, J.-S. (2022) 'Cardiac Acetylation in Metabolic Diseases.' *Biomedicines*, 10, [Online] 8. [Accessed 10.3390/biomedicines10081834

Duong, C. N. and Vestweber, D. (2020) 'Mechanisms Ensuring Endothelial Junction Integrity Beyond VE-Cadherin.' *Frontiers in Physiology*, 11, 2020-May-21,

Durrant, T. N., van den Bosch, M. T. and Hers, I. (2017) 'Integrin $\alpha(\text{IIb})\beta(3)$ outside-in signaling.' *Blood*, 130(14), Oct 5, 20170809, pp. 1607-1619.

Eckenstaler, R., Ripperger, A., Hauke, M., Petermann, M., Hemkemeyer, S. A., Schwedhelm, E., Ergün, S., Frye, M., et al. (2022) 'A Thromboxane A2 Receptor-Driven COX-2-Dependent Feedback Loop That Affects Endothelial Homeostasis and Angiogenesis.' *Arteriosclerosis, Thrombosis, and Vascular Biology*, 42(4), 2022/04/01, pp. 444-461.

Edgar, L. T., Park, H., Crawshaw, J. R., Osborne, J. M., Eichmann, A. and Bernabeu, M. O. (2022) 'Traffic Patterns of the Migrating Endothelium: How Force

Transmission Regulates Vascular Malformation and Functional Shunting During Angiogenic Remodelling.' *Frontiers in Cell and Developmental Biology*, 10, 2022-May-19,

Egot, M., Kauskot, A., Lasne, D., Gaussem, P. and Bachelot-Loza, C. (2013) 'Biphasic myosin II light chain activation during clot retraction.' *Thromb Haemost*, 110(6), Dec, 20130822, pp. 1215-1222.

Eikelboom, J. W. and Hirsh, J. (2007) 'Combined antiplatelet and anticoagulant therapy: clinical benefits and risks.' *Journal of Thrombosis and Haemostasis*, 5, 2007/07/01/, pp. 255-263.

Engholm-Keller, K. and Larsen, M. R. (2013) 'Technologies and challenges in large-scale phosphoproteomics.' *PROTEOMICS*, 13(6), 2013/03/01, pp. 910-931.

Espinola-Klein, C. (2022) 'When and How to Combine Antiplatelet and Anticoagulant Drugs?' *Hamostaseologie*, 42(1), Feb, 20220223, pp. 73-79.

Fabre, J. E., Nguyen, M., Latour, A., Keifer, J. A., Audoly, L. P., Coffman, T. M. and Koller, B. H. (1999) 'Decreased platelet aggregation, increased bleeding time and resistance to thromboembolism in P2Y1-deficient mice.' *Nat Med*, 5(10), Oct, pp. 1199-1202.

Falet, H. (2017) 'Anatomy of the Platelet Cytoskeleton.' In Gresele, P., Kleiman, N. S., Lopez, J. A. and Page, C. P. (eds.) *Platelets in Thrombotic and Non-Thrombotic Disorders: Pathophysiology, Pharmacology and Therapeutics: an Update*. Cham: Springer International Publishing, pp. 139-156. https://doi.org/10.1007/978-3-319-47462-5_11

Falet, H., Chang, G., Brohard-Bohn, B., Rendu, F. and Hartwig, J. H. (2005) 'Integrin α IIb β 3 signals lead cofilin to accelerate platelet actin dynamics.' *American Journal of Physiology-Cell Physiology*, 289(4) pp. C819-C825.

Fatkhullina, A. R., Peshkova, I. O. and Koltsova, E. K. (2016) 'The Role of Cytokines in the Development of Atherosclerosis.' *Biochemistry (Mosc)*, 81(11), Nov, pp. 1358-1370.

Feng, Y., Ye, D., Wang, Z., Pan, H., Lu, X., Wang, M., Xu, Y., Yu, J., et al. (2022) 'The Role of Interleukin-6 Family Members in Cardiovascular Diseases.' *Frontiers in Cardiovascular Medicine*, 9, 2022-March-23,

Fiorentino, F., Mautone, N., Menna, M., D'Acunzo, F., Mai, A. and Rotili, D. (2022) 'Sirtuin modulators: past, present, and future perspectives.' *Future Med Chem*, 14(12), Jun, 20220518, pp. 915-939.

FitzGerald, G. A. (2003) 'COX-2 and beyond: approaches to prostaglandin inhibition in human disease.' *Nature Reviews Drug Discovery*, 2(11), 2003/11/01, pp. 879-890.

Flaumenhaft, R. and De Ceunynck, K. (2017) 'Targeting PAR1: Now What?' *Trends Pharmacol Sci*, 38(8), Aug, 20170527, pp. 701-716.

Flaumenhaft, R. and Sharda, A. (2019) '19 - Platelet Secretion.' In Michelson, A. D. (ed.) *Platelets (Fourth Edition)*. Academic Press, pp. 349-370.
<https://www.sciencedirect.com/science/article/pii/B9780128134566000199>

Förstermann, U. and Sessa, W. C. (2012) 'Nitric oxide synthases: regulation and function.' *Eur Heart J*, 33(7), Apr, 20110901, pp. 829-837, 837a-837d.

Fox, J. E. (2001) 'Cytoskeletal proteins and platelet signaling.' *Thromb Haemost*, 86(1), Jul, pp. 198-213.

Franchi, F. and Angiolillo, D. J. (2015) 'Novel antiplatelet agents in acute coronary syndrome.' *Nat Rev Cardiol*, 12(1), Jan, 20141007, pp. 30-47.

Fredenburgh, J. C. and Weitz, J. I. (2018) 'Chapter 122 - Overview of Hemostasis and Thrombosis.' In Hoffman, R., Benz, E. J., Silberstein, L. E., Heslop, H. E., Weitz, J. I., Anastasi, J., Salama, M. E. and Abutalib, S. A. (eds.) *Hematology (Seventh Edition)*. Elsevier, pp. 1831-1842.
<https://www.sciencedirect.com/science/article/pii/B9780323357623001220>

Fu, C., Hao, S., Xu, X., Zhou, J., Liu, Z., Lu, H., Wang, L., Jin, W., et al. (2019) 'Activation of SIRT1 ameliorates LPS-induced lung injury in mice via decreasing endothelial tight junction permeability.' *Acta Pharmacologica Sinica*, 40(5), 2019/05/01, pp. 630-641.

Fu, X., Liang, C., Li, F., Wang, L., Wu, X., Lu, A., Xiao, G. and Zhang, G. (2018) 'The Rules and Functions of Nucleocytoplasmic Shuttling Proteins.' *Int J Mol Sci*, 19(5), May 12, 20180512,

Fujii, J., Homma, T. and Osaki, T. (2022) 'Superoxide Radicals in the Execution of Cell Death.' *Antioxidants (Basel)*, 11(3), Mar 4, 20220304,

Gager, G. M., Biesinger, B., Hofer, F., Winter, M.-P., Hengstenberg, C., Jilma, B., Eyileten, C., Postula, M., et al. (2020) 'Interleukin-6 level is a powerful predictor of long-term cardiovascular mortality in patients with acute coronary syndrome.' *Vascular Pharmacology*, 135, 2020/12/01/, p. 106806.

Gao, D., Sun, C. W., Woodley, A. B. and Dong, J. F. (2023) 'Clot Retraction and Its Correlation with the Function of Platelet Integrin $\alpha(\text{IIb})\beta(3)$.' *Biomedicines*, 11(9), Aug 23, 20230823,

Gawaz, M., Langer, H. and May, A. E. (2005) 'Platelets in inflammation and atherogenesis.' *J Clin Invest*, 115(12), Dec, pp. 3378-3384.

Gelbenegger, G. and Jilma, B. (2022) 'Clinical pharmacology of antiplatelet drugs.' *Expert Rev Clin Pharmacol*, 15(10), Oct, 20220911, pp. 1177-1197.

Gelens, L. and Saurin, A. T. (2018) 'Exploring the Function of Dynamic Phosphorylation-Dephosphorylation Cycles.' *Dev Cell*, 44(6), Mar 26, pp. 659-663.

Ghoshal, K. and Bhattacharyya, M. (2014) 'Overview of platelet physiology: its hemostatic and nonhemostatic role in disease pathogenesis.' *ScientificWorldJournal*, 2014 20140303, p. 781857.

Giantini, A., Timan, I. S., Dharma, R., Sukmawan, R., Setiabudy, R., Alwi, I., Harahap, A. R., Listiyaningsih, E., et al. (2023) 'The role of clopidogrel resistance-related genetic and epigenetic factors in major adverse cardiovascular events among patients with acute coronary syndrome after percutaneous coronary intervention.' *Frontiers in Cardiovascular Medicine*, 9, 2023-February-08,

Gimbrone, M. A. and García-Cardeña, G. (2016) 'Endothelial Cell Dysfunction and the Pathobiology of Atherosclerosis.' *Circulation Research*, 118(4), 2016/02/19, pp. 620-636.

GlaxoSmithKline. (2010) 'A Clinical Study to Assess the Safety, Tolerability, and Activity of Oral SRT2104 Capsules Administered for 28 Days to Subjects With Type 2 Diabetes Mellitus.' [Online]. [Accessed on 29/05/2024] <https://clinicaltrials.gov/study/NCT01018017?intr=SRT2104&rank=5>

GlaxoSmithKline. (2011) 'A Clinical Study to Assess the Effects of SRT2104 Upon Immobilization-Induced Skeletal Muscle Atrophy in Healthy Human Volunteers.' [Online]. [Accessed on 29/05/2024] <https://clinicaltrials.gov/study/NCT01039909?intr=SRT2104&rank=6>

Godier, A., Albaladejo, P. and On Perioperative Haemostasis Gihp Group, T. (2020) 'Management of Bleeding Events Associated with Antiplatelet Therapy: Evidence, Uncertainties and Pitfalls.' *J Clin Med*, 9(7), Jul 21, 20200721,

Golebiewska, E. M. and Poole, A. W. (2015) 'Platelet secretion: From haemostasis to wound healing and beyond.' *Blood Rev*, 29(3), May, 20141031, pp. 153-162.

Gomaa, A. A., El-Abhar, H. S., Abdallah, D. M., Awad, A. S. and Soubh, A. A. (2021) 'Prasugrel anti-ischemic effect in rats: Modulation of hippocampal SUMO2/3-I κ B α /Ubc9 and SIRT-1/miR-22 trajectories.' *Toxicology and Applied Pharmacology*, 426, 2021/09/01/, p. 115635.

Gorabi, A. M., Kiaie, N., Khosrojerdi, A., Jamialahmadi, T., Al-Rasadi, K., Johnston, T. P. and Sahebkar, A. (2022) 'Implications for the role of lipopolysaccharide in the development of atherosclerosis.' *Trends in Cardiovascular Medicine*, 32(8), 2022/11/01/, pp. 525-533.

Gorenne, I., Kumar, S., Gray, K., Figg, N., Yu, H., Mercer, J. and Bennett, M. (2013) 'Vascular Smooth Muscle Cell Sirtuin 1 Protects Against DNA Damage and Inhibits Atherosclerosis.' *Circulation*, 127(3), 2013/01/22, pp. 386-396.

Green, H. L. H., Zuidschewoude, M., Alenazy, F., Smith, C. W., Bender, M. and Thomas, S. G. (2020) 'SMIFH2 inhibition of platelets demonstrates a critical role for formin proteins in platelet cytoskeletal dynamics.' *J Thromb Haemost*, 18(4), Apr, 20200217, pp. 955-967.

Greer, E. L. and Shi, Y. (2012) 'Histone methylation: a dynamic mark in health, disease and inheritance.' *Nature Reviews Genetics*, 13(5), 2012/05/01, pp. 343-357.

Gremmel, T., Calatzis, A., Steiner, S., Kaider, A., Seidinger, D., Koppensteiner, R., Kopp, C. W. and Panzer, S. (2010) 'Is TRAP-6 suitable as a positive control for platelet reactivity when assessing response to clopidogrel?' *Platelets*, 21(7) pp. 515-521.

Gresele, P. (2013) 'Antiplatelet agents in clinical practice and their haemorrhagic risk.' *Blood Transfus*, 11(3), Jul, 20130509, pp. 349-356.

Grover, S. P. and Mackman, N. (2019) 'Intrinsic Pathway of Coagulation and Thrombosis.' *Arteriosclerosis, Thrombosis, and Vascular Biology*, 39(3), 2019/03/01, pp. 331-338.

Guidetti, Canobbio, I. and Torti, M. (2015) 'PI3K/Akt in platelet integrin signaling and implications in thrombosis.' *Advances in Biological Regulation*, 59, 2015/09/01/, pp. 36-52.

Guidetti, Torti, M. and Canobbio, I. (2019) 'Focal Adhesion Kinases in Platelet Function and Thrombosis.' *Arterioscler Thromb Vasc Biol*, 39(5), May, pp. 857-868.

Gurbel, P. A. and Tantry, U. S. (2010) 'Combination antithrombotic therapies.' *Circulation*, 121(4), Feb 2, pp. 569-583.

Habib, S. and Ali, A. (2011) 'Biochemistry of nitric oxide.' *Indian J Clin Biochem*, 26(1), Jan, 20110203, pp. 3-17.

Hackeng, T. M., Maurissen, L. F., Castoldi, E. and Rosing, J. (2009) 'Regulation of TFPI function by protein S.' *J Thromb Haemost*, 7 Suppl 1, Jul, pp. 165-168.

Hadi, H. A., Carr, C. S. and Al Suwaidi, J. (2005) 'Endothelial dysfunction: cardiovascular risk factors, therapy, and outcome.' *Vasc Health Risk Manag*, 1(3) pp. 183-198.

Hamilos, M., Petousis, S. and Parthenakis, F. (2018) 'Interaction between platelets and endothelium: from pathophysiology to new therapeutic options.' *Cardiovasc Diagn Ther*, 8(5), Oct, pp. 568-580.

Han, C., Gu, Y., Shan, H., Mi, W., Sun, J., Shi, M., Zhang, X., Lu, X., et al. (2017) 'O-GlcNAcylation of SIRT1 enhances its deacetylase activity and promotes cytoprotection under stress.' *Nat Commun*, 8(1), Nov 14, 20171114, p. 1491.

Hankey, G. J. and Eikelboom, J. W. (2006) 'Aspirin resistance.' *Lancet*, 367(9510), Feb 18, pp. 606-617.

Harper, M. T. (2019) 'Platelets, fourth edition (Ed. Michelson, Cattaneo, Frelinger & Newman).' *Platelets*, 30(7), 2019/10/03, pp. 935-935.

Hartwig, J. H. (2013) 'Chapter 8 - The Platelet Cytoskeleton.' In Michelson, A. D. (ed.) *Platelets (Third Edition)*. Academic Press, pp. 145-168.
<https://www.sciencedirect.com/science/article/pii/B9780123878373000080>

Hashemzadeh, M., Haseefa, F., Peyton, L., Shadmehr, M., Niyas, A. M., Patel, A., Krđi, G. and Movahed, M. R. (2023) 'A comprehensive review of the ten main platelet receptors involved in platelet activity and cardiovascular disease.' *Am J Blood Res*, 13(6) 20231225, pp. 168-188.

He, R. and Chen, D. (2019) 'Chapter 142 - Confirmatory Testing for Diagnosis of Platelet Disorders.' In Shaz, B. H., Hillyer, C. D. and Reyes Gil, M. (eds.) *Transfusion Medicine and Hemostasis (Third Edition)*. Elsevier, pp. 841-848.
<https://www.sciencedirect.com/science/article/pii/B9780128137260001422>

Healy, S., Khan, P., He, S. and Davie, J. R. (2012) 'Histone H3 phosphorylation, immediate-early gene expression, and the nucleosomal response: a historical perspective.' *Biochem Cell Biol*, 90(1), Feb, 20120117, pp. 39-54.

Heijnen, H. and van der Sluijs, P. (2015) 'Platelet secretory behaviour: as diverse as the granules ... or not?' *J Thromb Haemost*, 13(12), Dec, 20151023, pp. 2141-2151.

Heiss and Dirsch, V. M. (2014) 'Regulation of eNOS enzyme activity by posttranslational modification.' *Curr Pharm Des*, 20(22) pp. 3503-3513.

Heiss, C., Rodriguez-Mateos, A. and Kelm, M. (2015) 'Central role of eNOS in the maintenance of endothelial homeostasis.' *Antioxid Redox Signal*, 22(14), May 10, 20141210, pp. 1230-1242.

Henderson, S. J., Weitz, J. I. and Kim, P. Y. (2018) 'Fibrinolysis: strategies to enhance the treatment of acute ischemic stroke.' *Journal of Thrombosis and Haemostasis*, 16(10), 2018/10/01/, pp. 1932-1940.

Henning, R. J. (2021) 'Obesity and obesity-induced inflammatory disease contribute to atherosclerosis: a review of the pathophysiology and treatment of obesity.' *Am J Cardiovasc Dis*, 11(4) 20210815, pp. 504-529.

Heshmati, M., Soltani, A., Sanaei, M. J., Nahid-Samiei, M., Shirzad, H., Jami, M. S. and GhatrehSamani, M. (2020) 'Ghrelin induces autophagy and CXCR4 expression via the SIRT1/AMPK axis in lymphoblastic leukemia cell lines.' *Cell Signal*, 66, Feb, 20191203, p. 109492.

Hitchcock, I. S., Fox, N. E., Prévost, N., Sear, K., Shattil, S. J. and Kaushansky, K. (2008) 'Roles of focal adhesion kinase (FAK) in megakaryopoiesis and platelet function: studies using a megakaryocyte lineage-specific FAK knockout.' *Blood*, 111(2), 2008/01/15/, pp. 596-604.

Hoffbrand, A. V., Higgs, D. R., Keeling, D. M. and Mehta, A. B. (2016) *Postgraduate haematology*. John Wiley & Sons.

Hoffmann, E., Wald, J., Lavu, S., Roberts, J., Beaumont, C., Haddad, J., Elliott, P., Westphal, C., et al. (2013) 'Pharmacokinetics and tolerability of SRT2104, a first-in-class small molecule activator of SIRT1, after single and repeated oral administration in man.' *Br J Clin Pharmacol*, 75(1), Jan, pp. 186-196.

Hori, D., Nomura, Y., Nakano, M., Han, M., Bhatta, A., Chen, K., Akiyoshi, K. and Pandey, D. (2020) 'Endothelial-Specific Overexpression of Histone Deacetylase 2 Protects Mice against Endothelial Dysfunction and Atherosclerosis.' *Cell Physiol Biochem*, 54(5), Sep 26, pp. 947-958.

Horii, K., Brooks, M. T. and Herr, A. B. (2009) 'Convulxin Forms a Dimer in Solution and Can Bind Eight Copies of Glycoprotein VI: Implications for Platelet Activation.' *Biochemistry*, 48(13), 2009/04/07, pp. 2907-2914.

Horita, H., Law, A. and Middleton, K. (2018) 'Utilizing Optimized Tools to Investigate PTM Crosstalk: Identifying Potential PTM Crosstalk of Acetylated Mitochondrial Proteins.' *Proteomes*, 6, [Online] 2. [Accessed 10.3390/proteomes6020024

Hosseini, E., Mohtashami, M. and Ghasemzadeh, M. (2019) 'Down-regulation of platelet adhesion receptors is a controlling mechanism of thrombosis, while also affecting post-transfusion efficacy of stored platelets.' *Thrombosis Journal*, 17(1), 2019/10/23, p. 20.

Huang, Lin, K.-C., Hsia, C.-W., Hsia, C.-H., Chen, T.-Y., Bhavan, P. S., Sheu, J.-R. and Hou, S.-M. (2021) 'The Antithrombotic Agent Pterostilbene Interferes with Integrin $\alpha\text{IIb}\beta\text{3}$ -Mediated Inside-Out and Outside-In Signals in Human Platelets.' *International Journal of Molecular Sciences*, 22, [Online] 7. [Accessed 10.3390/ijms22073643

Huang, Li, X., Shi, X., Zhu, M., Wang, J., Huang, S., Huang, X., Wang, H., et al. (2019) 'Platelet integrin $\alpha\text{IIb}\beta\text{3}$: signal transduction, regulation, and its therapeutic targeting.' *J Hematol Oncol*, 12(1), Mar 7, 20190307, p. 26.

Huang, J., Li, X., Shi, X., Zhu, M., Wang, J., Huang, S., Huang, X., Wang, H., et al. (2019) 'Platelet integrin $\alpha\text{IIb}\beta\text{3}$: signal transduction, regulation, and its therapeutic targeting.' *Journal of Hematology & Oncology*, 12(1), 2019/03/07, p. 26.

Huilcaman, R., Venturini, W., Fuenzalida, L., Cayo, A., Segovia, R., Valenzuela, C., Brown, N. and Moore-Carrasco, R. (2022) 'Platelets, a Key Cell in Inflammation and Atherosclerosis Progression.' *Cells*, 11(6), Mar 17, 20220317,

Huizinga, E. G., Tsuji, S., Romijn, R. A., Schiphorst, M. E., de Groot, P. G., Sixma, J. J. and Gros, P. (2002) 'Structures of glycoprotein Iba α and its complex with von Willebrand factor A1 domain.' *Science*, 297(5584), Aug 16, pp. 1176-1179.

Hung, C. H., Chan, S. H., Chu, P. M. and Tsai, K. L. (2015) 'Quercetin is a potent anti-atherosclerotic compound by activation of SIRT1 signaling under oxLDL stimulation.' *Mol Nutr Food Res*, 59(10), Oct, 20150826, pp. 1905-1917.

Hunter, T. S., Robison, C. and Gerbino, P. P. (2015) 'Emerging evidence in NSAID pharmacology: important considerations for product selection.' *Am J Manag Care*, 21(7 Suppl), Apr, pp. S139-147.

Hynes, R. O. (2002) 'Integrins: Bidirectional, Allosteric Signaling Machines.' *Cell*, 110(6), 2002/09/20/, pp. 673-687.

Immanuel, J. and Yun, S. (2023) 'Vascular Inflammatory Diseases and Endothelial Phenotypes.' *Cells*, 12(12), Jun 15, 20230615,

Induruwa, I., Jung, S. M. and Warburton, E. A. (2016) 'Beyond antiplatelets: The role of glycoprotein VI in ischemic stroke.' *Int J Stroke*, 11(6), Aug, 20160616, pp. 618-625.

Intengan, H. D. and Schiffrin, E. L. (2001) 'Vascular Remodeling in Hypertension.' *Hypertension*, 38(3) pp. 581-587.

Italiano, J. E., Patel-Hett, S. and Hartwig, J. H. (2007) 'Mechanics of proplatelet elaboration.' *Journal of Thrombosis and Haemostasis*, 5, 2007/07/01/, pp. 18-23.

Iwahara, N., Azekami, K., Hosoda, R., Nojima, I., Hisahara, S. and Kuno, A. (2022) 'Activation of SIRT1 promotes membrane resealing via cortactin.' *Scientific Reports*, 12(1), 2022/09/12, p. 15328.

Iwahara, N., Azekami, K., Hosoda, R., Nojima, I., Hisahara, S. and Kuno, A. (2022) 'Activation of SIRT1 promotes membrane resealing via cortactin.' *Sci Rep*, 12(1), Sep 12, 20220912, p. 15328.

Izaguirre, G., Aguirre, L., Hu, Y. P., Lee, H. Y., Schlaepfer, D. D., Aneskievich, B. J. and Haimovich, B. (2001) 'The cytoskeletal/non-muscle isoform of alpha-actinin is phosphorylated on its actin-binding domain by the focal adhesion kinase.' *J Biol Chem*, 276(31), Aug 3, 20010521, pp. 28676-28685.

Jackson, S. P. (2007) 'The growing complexity of platelet aggregation.' *Blood*, 109(12), Jun 15, 20070220, pp. 5087-5095.

Jakaria, M., Azam, S., Jo, S. H., Kim, I. S., Dash, R. and Choi, D. K. (2019) 'Potential Therapeutic Targets of Quercetin and Its Derivatives: Its Role in the Therapy of Cognitive Impairment.' *J Clin Med*, 8(11), Oct 25, 20191025,

Janaszak-Jasiecka, A., Płoska, A., Wierońska, J. M., Dobrucki, L. W. and Kalinowski, L. (2023) 'Endothelial dysfunction due to eNOS uncoupling: molecular mechanisms as potential therapeutic targets.' *Cellular & Molecular Biology Letters*, 28(1), 2023/03/09, p. 21.

Jang, J. Y., Min, J. H., Wang, S. B., Chae, Y. H., Baek, J. Y., Kim, M., Ryu, J.-S. and Chang, T.-S. (2015) 'Resveratrol inhibits collagen-induced platelet stimulation through suppressing NADPH oxidase and oxidative inactivation of SH2 domain-

containing protein tyrosine phosphatase-2.' *Free Radical Biology and Medicine*, 89, 2015/12/01/, pp. 842-851.

Jansen, E. E. and Hartmann, M. (2021) 'Clot Retraction: Cellular Mechanisms and Inhibitors, Measuring Methods, and Clinical Implications.' *Biomedicines*, 9, [Online] 8. [Accessed 10.3390/biomedicines9081064

Jantzen, H. M., Gousset, L., Bhaskar, V., Vincent, D., Tai, A., Reynolds, E. E. and Conley, P. B. (1999) 'Evidence for two distinct G-protein-coupled ADP receptors mediating platelet activation.' *Thromb Haemost*, 81(1), Jan, pp. 111-117.

Janus-Bell, E. and Mangin, P. H. (2023) 'The relative importance of platelet integrins in hemostasis, thrombosis and beyond.' *Haematologica*, 108(7), Jul 1, 20230701, pp. 1734-1747.

Jenkins, N. T., Padilla, J., Boyle, L. J., Credeur, D. P., Laughlin, M. H. and Fadel, P. J. (2013) 'Disturbed blood flow acutely induces activation and apoptosis of the human vascular endothelium.' *Hypertension*, 61(3), Mar, 20130114, pp. 615-621.

Jerka, D., Bonowicz, K., Piekarska, K., Gokyer, S., Derici, U. S., Hindy, O. A., Altunay, B. B., Yazgan, I., et al. (2024) 'Unraveling Endothelial Cell Migration: Insights into Fundamental Forces, Inflammation, Biomaterial Applications, and Tissue Regeneration Strategies.' *ACS Applied Bio Materials*, 7(4), 2024/04/15, pp. 2054-2069.

Jiang, Q., Hao, R., Wang, W., Gao, H. and Wang, C. (2016) 'SIRT1/Atg5/autophagy are involved in the antiatherosclerosis effects of ursolic acid.' *Mol Cell Biochem*, 420(1-2), Sep, 20160811, pp. 171-184.

Johnson, G. J., Leis, L. A., Krumwiede, M. D. and White, J. G. (2007) 'The critical role of myosin IIA in platelet internal contraction.' *Journal of Thrombosis and Haemostasis*, 5(7), 2007/07/01/, pp. 1516-1529.

Johnson, K. E. and Wilgus, T. A. (2014) 'Vascular Endothelial Growth Factor and Angiogenesis in the Regulation of Cutaneous Wound Repair.' *Adv Wound Care (New Rochelle)*, 3(10), Oct 1, pp. 647-661.

Ju, L., Chen, Y., Zhou, F., Lu, H., Cruz, M. A. and Zhu, C. (2015) 'Von Willebrand factor-A1 domain binds platelet glycoprotein Iba in multiple states with distinctive force-dependent dissociation kinetics.' *Thromb Res*, 136(3), Sep, 20150620, pp. 606-612.

Jung, S. B., Kim, C. S., Naqvi, A., Yamamori, T., Mattagajasingh, I., Hoffman, T. A., Cole, M. P., Kumar, A., et al. (2010) 'Histone deacetylase 3 antagonizes aspirin-stimulated endothelial nitric oxide production by reversing aspirin-induced lysine acetylation of endothelial nitric oxide synthase.' *Circ Res*, 107(7), Oct 1, 20100812, pp. 877-887.

Jurk, K. (2017) 'Platelet granules - secretory and secretive.' *Hamostaseologie*, 37(3), Aug 7, 20160921, pp. 208-210.

Justice, C. N., Derbala, M. H., Baich, T. M., Kempton, A. N., Guo, A. S., Ho, T. H. and Smith, S. A. (2018) 'The Impact of Pazopanib on the Cardiovascular System.' *J Cardiovasc Pharmacol Ther*, 23(5), Sep, 20180429, pp. 387-398.

Kang, H. (2021) 'Sample size determination and power analysis using the G*Power software.' *J Educ Eval Health Prof*, 18 20210730, p. 17.

Kanthi, Y. M., Sutton, N. R. and Pinsky, D. J. (2014) 'CD39: Interface between vascular thrombosis and inflammation.' *Curr Atheroscler Rep*, 16(7), Jul, p. 425.

Kao, C. L., Chen, L. K., Chang, Y. L., Yung, M. C., Hsu, C. C., Chen, Y. C., Lo, W. L., Chen, S. J., et al. (2010) 'Resveratrol protects human endothelium from H₂O₂-induced oxidative stress and senescence via SirT1 activation.' *J Atheroscler Thromb*, 17(9), Sep 30, 20100713, pp. 970-979.

Kato, K., Kanaji, T., Russell, S., Kunicki, T. J., Furihata, K., Kanaji, S., Marchese, P., Reininger, A., et al. (2003) 'The contribution of glycoprotein VI to stable platelet adhesion and thrombus formation illustrated by targeted gene deletion.' *Blood*, 102(5), Sep 1, 20030508, pp. 1701-1707.

Katsi, V., Zerdes, I., Manolakou, S., Makris, T., Nihoyannopoulos, P., Tousoulis, D. and Kallikazaros, I. (2014) 'Anti-VEGF Anticancer Drugs: Mind the Hypertension.' *Recent Adv Cardiovasc Drug Discov*, 9(2) pp. 63-72.

Kaur, R., Singh, V., Kumari, P., Singh, R., Chopra, H. and Emran, T. B. (2022) 'Novel insights on the role of VCAM-1 and ICAM-1: Potential biomarkers for cardiovascular diseases.' *Ann Med Surg (Lond)*, 84, Dec, 20221031, p. 104802.

Kautbally, S., Lepropre, S., Onselaer, M.-B., Le Rigoleur, A., Ginion, A., De Meester de Ravenstein, C., Ambroise, J., Boudjeltia, K. Z., et al. (2019) 'Platelet Acetyl-CoA Carboxylase Phosphorylation: A Risk Stratification Marker That Reveals Platelet-Lipid Interplay in Coronary Artery Disease Patients.' *JACC: Basic to Translational Science*, 4(5), 2019/09/01/, pp. 596-610.

Keularts, I. M., van Gorp, R. M., Feijge, M. A., Vuist, W. M. and Heemskerk, J. W. (2000) ' α (2A)-adrenergic receptor stimulation potentiates calcium release in platelets by modulating cAMP levels.' *J Biol Chem*, 275(3), Jan 21, pp. 1763-1772.

Keuren, J. F. W., Magdeleyns, E. J. P., Govers-Riemslog, J. W. P., Lindhout, T. and Curvers, J. (2006) 'Effects of storage-induced platelet microparticles on the initiation and propagation phase of blood coagulation.' *British Journal of Haematology*, 134(3), 2006/08/01, pp. 307-313.

Kiechl, S., Egger, G., Mayr, M., Wiedermann, C. J., Bonora, E., Oberhollenzer, F., Muggeo, M., Xu, Q., et al. (2001) 'Chronic Infections and the Risk of Carotid Atherosclerosis.' *Circulation*, 103(8) pp. 1064-1070.

Kietadisorn, R., Juni, R. P. and Moens, A. L. (2012) 'Tackling endothelial dysfunction by modulating NOS uncoupling: new insights into its pathogenesis and therapeutic possibilities.' *American Journal of Physiology-Endocrinology and Metabolism*, 302(5) pp. E481-E495.

Kilic, U., Gok, O., Bacaksiz, A., Izmirli, M., Elibol-Can, B. and Uysal, O. (2014) 'SIRT1 gene polymorphisms affect the protein expression in cardiovascular diseases.' *PLoS One*, 9(2) 20140228, p. e90428.

Kim, Kim, J. R. and Choi, H. C. (2018) 'Quercetin-Induced AMP-Activated Protein Kinase Activation Attenuates Vasoconstriction Through LKB1-AMPK Signaling Pathway.' *J Med Food*, 21(2), Feb, 20171016, pp. 146-153.

Kim, C. W., Oh, E. T. and Park, H. J. (2021) 'A strategy to prevent atherosclerosis via TNF receptor regulation.' *Faseb j*, 35(3), Mar, p. e21391.

Kim, M., Park, C., Jung, J. and Yeo, S. G. (2019) 'The histone deacetylase class I, II inhibitor trichostatin A delays peripheral neurodegeneration.' *J Mol Histol*, 50(2), Apr, 20190122, pp. 167-178.

Kim, S. and Kunapuli, S. P. (2011) 'P2Y12 receptor in platelet activation.' *Platelets*, 22(1) pp. 56-60.

Kim, Y. H., Bae, J. U., Kim, I. S., Chang, C. L., Oh, S. O. and Kim, C. D. (2016) 'SIRT1 prevents pulmonary thrombus formation induced by arachidonic acid via downregulation of PAF receptor expression in platelets.' *Platelets*, 27(8), Dec, 20160608, pp. 735-742.

King, S. L., Joshi, H. J., Schjoldager, K. T., Halim, A., Madsen, T. D., Dziegiel, M. H., Woetmann, A., Vakhrushev, S. Y., et al. (2017) 'Characterizing the O-glycosylation landscape of human plasma, platelets, and endothelial cells.' *Blood Adv*, 1(7), Feb 28, 20170223, pp. 429-442.

Kitada, M. and Koya, D. (2013) 'SIRT1 in Type 2 Diabetes: Mechanisms and Therapeutic Potential.' *Diabetes Metab J*, 37(5), Oct, pp. 315-325.

Kitada, M., Ogura, Y. and Koya, D. (2016) 'The protective role of Sirt1 in vascular tissue: its relationship to vascular aging and atherosclerosis.' *Aging (Albany NY)*, 8(10), Oct 15, pp. 2290-2307.

Klein, M. D., Williams, A. K., Lee, C. R. and Stouffer, G. A. (2019) 'Clinical Utility of CYP2C19 Genotyping to Guide Antiplatelet Therapy in Patients With an Acute Coronary Syndrome or Undergoing Percutaneous Coronary Intervention.' *Arteriosclerosis, Thrombosis, and Vascular Biology*, 39(4), 2019/04/01, pp. 647-652.

Kluft, C., Sidelmann, J. J. and Gram, J. B. (2017) 'Assessing Safety of Thrombolytic Therapy.' *Semin Thromb Hemost*, 43(03), 2017/03/27, 2016/06/06, pp. 300-310.

Kobsar, A. and Eigenthaler, M. (2006) 'The Cytoskeleton of the Platelet.' *In Advances in Molecular and Cell Biology*. Vol. 37. Elsevier, pp. 1-23.
<https://www.sciencedirect.com/science/article/pii/S1569255806370014>

Kobylka, P., Kucinska, M., Kujawski, J., Lazewski, D., Wierchowski, M. and Murias, M. (2022) 'Resveratrol Analogues as Selective Estrogen Signaling Pathway Modulators: Structure-Activity Relationship.' *Molecules*, 27(20), Oct 17, 20221017,

Kong, P., Cui, Z.-Y., Huang, X.-F., Zhang, D.-D., Guo, R.-J. and Han, M. (2022) 'Inflammation and atherosclerosis: signaling pathways and therapeutic intervention.' *Signal Transduction and Targeted Therapy*, 7(1), 2022/04/22, p. 131.

Kosuru, R., Rai, U., Prakash, S., Singh, A. and Singh, S. (2016) 'Promising therapeutic potential of pterostilbene and its mechanistic insight based on preclinical evidence.' *European Journal of Pharmacology*, 789, 2016/10/15/, pp. 229-243.

Koukouritaki, S. B., Vardaki, E. A., Papakonstanti, E. A., Lianos, E., Stournaras, C. and Emmanouel, D. S. (1999) 'TNF- α Induces Actin Cytoskeleton Reorganization in Glomerular Epithelial Cells Involving Tyrosine Phosphorylation of Paxillin and Focal Adhesion Kinase.' *Molecular Medicine*, 5(6), 1999/06/01, pp. 382-392.

Kouzarides, T. (2000) 'Acetylation: a regulatory modification to rival phosphorylation?' *Embo j*, 19(6), Mar 15, pp. 1176-1179.

Kriek, N., Nock, S. H., Sage, T., Khalifa, B., Bye, A. P., Mitchell, J. L., Thomson, S., McLaughlin, M. G., et al. (2022) 'Cucurbitacins Elicit Anti-Platelet Activity via Perturbation of the Cytoskeleton and Integrin Function.' *Thromb Haemost*, 122(7), Jul, 20220304, pp. 1115-1129.

Krishnan, K., Nguyen, T. N., Appleton, J. P., Law, Z. K., Caulfield, M., Cabrera, C. P., Lenthall, R., Hewson, D., et al. (2023) 'Antiplatelet Resistance: A Review of Concepts, Mechanisms, and Implications for Management in Acute Ischemic Stroke and Transient Ischemic Attack.' *Stroke: Vascular and Interventional Neurology*, 3(3), 2023/05/01, p. e000576.

Krüger-Genge, A., Blocki, A., Franke, R.-P. and Jung, F. (2019) 'Vascular Endothelial Cell Biology: An Update.' *International Journal of Molecular Sciences*, 20, [Online] 18. [Accessed 10.3390/ijms20184411

Kulkarni, S. S. and Cantó, C. (2015) 'The molecular targets of resveratrol.' *Biochimica et Biophysica Acta (BBA) - Molecular Basis of Disease*, 1852(6), 2015/06/01/, pp. 1114-1123.

Kumar, P., Shen, Q., Pivetti, C. D., Lee, E. S., Wu, M. H. and Yuan, S. Y. (2009) 'Molecular mechanisms of endothelial hyperpermeability: implications in inflammation.' *Expert Rev Mol Med*, 11, Jun 30, 20090630, p. e19.

Kumari, S., Chaurasia, S. N., Nayak, M. K., Mallick, R. L. and Dash, D. (2015) 'Sirtuin Inhibition Induces Apoptosis-like Changes in Platelets and Thrombocytopenia.' *J Biol Chem*, 290(19), May 8, 20150331, pp. 12290-12299.

Kuroda, Y. T., Komamura, K., Tatsumi, R., Mori, K., Yoneda, K., Katayama, Y., Shigemoto, S., Miyatake, K., et al. (2001) 'Vascular cell adhesion molecule-1 as a biochemical marker of left ventricular mass in the patients with hypertension.' *Am J Hypertens*, 14(9 Pt 1), Sep, pp. 868-872.

Lamalice, L., Le Boeuf, F. and Huot, J. (2007) 'Endothelial Cell Migration During Angiogenesis.' *Circulation Research*, 100(6) pp. 782-794.

Lan, F., Weikel, K. A., Cacicedo, J. M. and Ido, Y. (2017) 'Resveratrol-Induced AMP-Activated Protein Kinase Activation Is Cell-Type Dependent: Lessons from Basic Research for Clinical Application.' *Nutrients*, 9(7), Jul 14, 20170714,

Latorre, A. and Moscardó, A. (2016) 'Regulation of Platelet Function by Acetylation/Deacetylation Mechanisms.' *Curr Med Chem*, 23(35) pp. 3966-3974.

Lechner, K., von Schacky, C., McKenzie, A. L., Worm, N., Nixdorff, U., Lechner, B., Kränkel, N., Halle, M., et al. (2020) 'Lifestyle factors and high-risk atherosclerosis: Pathways and mechanisms beyond traditional risk factors.' *Eur J Prev Cardiol*, 27(4), Mar, 20190813, pp. 394-406.

Lee, van de Ven, R. A. H., Zaganjor, E., Ng, M. R., Barakat, A., Demmers, J., Finley, L. W. S., Gonzalez Herrera, K. N., et al. (2018) 'Inhibition of epithelial cell migration and Src/FAK signaling by SIRT3.' *Proc Natl Acad Sci U S A*, 115(27), Jul 3, 20180618, pp. 7057-7062.

Lee, D. D. and Schwarz, M. A. (2020) 'Cell-Cell Communication Breakdown and Endothelial Dysfunction.' *Crit Care Clin*, 36(2), Apr, 20200131, pp. 189-200.

Lee, H. and Hamilton, J. R. (2012) 'Physiology, pharmacology, and therapeutic potential of protease-activated receptors in vascular disease.' *Pharmacology & Therapeutics*, 134(2), 2012/05/01/, pp. 246-259.

Lee, H. T., Oh, S., Ro, D. H., Yoo, H. and Kwon, Y. W. (2020) 'The Key Role of DNA Methylation and Histone Acetylation in Epigenetics of Atherosclerosis.' *J Lipid Atheroscler*, 9(3), Sep, 20200921, pp. 419-434.

Lee, I. H., Cao, L., Mostoslavsky, R., Lombard, D. B., Liu, J., Bruns, N. E., Tsokos, M., Alt, F. W., et al. (2008) 'A role for the NAD-dependent deacetylase Sirt1 in the regulation of autophagy.' *Proc Natl Acad Sci U S A*, 105(9), Mar 4, 20080222, pp. 3374-3379.

Lefrançais, E., Ortiz-Muñoz, G., Caudrillier, A., Mallavia, B., Liu, F., Sayah, D. M., Thornton, E. E., Headley, M. B., et al. (2017) 'The lung is a site of platelet biogenesis and a reservoir for haematopoietic progenitors.' *Nature*, 544(7648), Apr 6, 20170322, pp. 105-109.

Leon, C., Ravanat, C., Freund, M., Cazenave, J. P. and Gachet, C. (2003) 'Differential involvement of the P2Y1 and P2Y12 receptors in platelet procoagulant activity.' *Arterioscler Thromb Vasc Biol*, 23(10), Oct 1, 20030821, pp. 1941-1947.

Léon, C., Hechler, B., Freund, M., Eckly, A., Vial, C., Ohlmann, P., Dierich, A., LeMeur, M., et al. (1999) 'Defective platelet aggregation and increased resistance to thrombosis in purinergic P2Y(1) receptor-null mice.' *J Clin Invest*, 104(12), Dec, pp. 1731-1737.

Lewandrowski, U., Zahedi, R. P., Moebius, J., Walter, U. and Sickmann, A. (2007) 'Enhanced N-glycosylation site analysis of sialoglycopeptides by strong cation exchange prefractionation applied to platelet plasma membranes.' *Mol Cell Proteomics*, 6(11), Nov, 20070727, pp. 1933-1941.

Li, H. (2014) 'Sirtuin 1 (SIRT1) and Oxidative Stress.' In Laher, I. (ed.) *Systems Biology of Free Radicals and Antioxidants*. Berlin, Heidelberg: Springer Berlin Heidelberg, pp. 417-435. https://doi.org/10.1007/978-3-642-30018-9_17

Li, L., Fu, S., Wang, J., Lu, J., Tao, Y., Zhao, L., Fu, B., Lu, L., et al. (2024) 'SRT1720 inhibits bladder cancer cell progression by impairing autophagic flux.' *Biochem Pharmacol*, 222, Apr, 20240307, p. 116111.

Li, M., Qian, M., Kyler, K. and Xu, J. (2018) 'Endothelial–Vascular Smooth Muscle Cells Interactions in Atherosclerosis.' *Frontiers in Cardiovascular Medicine*, 5, 2018-October-23,

Li, P., Ge, J. and Li, H. (2020) 'Lysine acetyltransferases and lysine deacetylases as targets for cardiovascular disease.' *Nature Reviews Cardiology*, 17(2), 2020/02/01, pp. 96-115.

Li, Q., Zhang, Q., Kim, Y.-R., Gaddam, R. R., Jacobs, J. S., Bachschmid, M. M., Younis, T., Zhu, Z., et al. (2023) 'Deficiency of endothelial sirtuin1 in mice stimulates skeletal muscle insulin sensitivity by modifying the secretome.' *Nature Communications*, 14(1), 2023/09/11, p. 5595.

Li, R. and Emsley, J. (2013) 'The organizing principle of the platelet glycoprotein Ib–IX–V complex.' *Journal of Thrombosis and Haemostasis*, 11(4), 2013/04/01/, pp. 605-614.

Li, Y., Li, C., Sun, L., Chu, G., Li, J., Chen, F., Li, G. and Zhao, Y. (2013) 'Role of p300 in regulating neuronal nitric oxide synthase gene expression through nuclear factor- κ B-mediated way in neuronal cells.' *Neuroscience*, 248, Sep 17, 20130627, pp. 681-689.

Li, Z., Delaney, M. K., O'Brien, K. A. and Du, X. (2010) 'Signaling during platelet adhesion and activation.' *Arterioscler Thromb Vasc Biol*, 30(12), Dec, 20101111, pp. 2341-2349.

Libby, P. (2021) 'The changing landscape of atherosclerosis.' *Nature*, 592(7855), Apr, 20210421, pp. 524-533.

Lin, K. Y., Ito, A., Asagami, T., Tsao, P. S., Adimoolam, S., Kimoto, M., Tsuji, H., Reaven, G. M., et al. (2002) 'Impaired nitric oxide synthase pathway in diabetes mellitus: role of asymmetric dimethylarginine and dimethylarginine dimethylaminohydrolase.' *Circulation*, 106(8), Aug 20, pp. 987-992.

Lin, Q., Geng, Y., Zhao, M., Lin, S., Zhu, Q. and Tian, Z. (2017) 'MiR-21 Regulates TNF- α -Induced CD40 Expression via the SIRT1-NF- κ B Pathway in Renal Inner Medullary Collecting Duct Cells.' *Cellular Physiology and Biochemistry*, 41(1) pp. 124-136.

Lin, Y., Li, L., Liu, J., Zhao, X., Ye, J., Reinach, P. S., Qu, J. and Yan, D. (2018) 'SIRT1 Deletion Impairs Retinal Endothelial Cell Migration Through Downregulation of VEGF-A/VEGFR-2 and MMP14.' *Invest Ophthalmol Vis Sci*, 59(13), Nov 1, pp. 5431-5440.

Lin, Y., Liu, Q., Li, L., Yang, R., Ye, J., Yang, S., Luo, G., Reinach, P. S., et al. (2022) 'Sirt1 Regulates Corneal Epithelial Migration by Deacetylating Cortactin.' *Invest Ophthalmol Vis Sci*, 63(12), Nov 1, p. 14.

Liu, Fassett, J., Wei, Y. and Chen, Y. (2013) 'Regulation of DDAH1 as a Potential Therapeutic Target for Treating Cardiovascular Diseases.' *Evid Based Complement Alternat Med*, 2013 20130626, p. 619207.

Liu, T., Zhang, L., Joo, D. and Sun, S.-C. (2017) 'NF- κ B signaling in inflammation.' *Signal Transduction and Targeted Therapy*, 2(1), 2017/07/14, p. 17023.

Liu, Y., Wang, T., Zhou, Q., Xin, G., Niu, H., Li, F., Wang, Y., Li, S., et al. (2023) 'Endogenous SIRT6 in platelets negatively regulates platelet activation and thrombosis.' *Front Pharmacol*, 14 20231218, p. 1268708.

Livak, K. J. and Schmittgen, T. D. (2001) 'Analysis of relative gene expression data using real-time quantitative PCR and the 2(-Delta Delta C(T)) Method.' *Methods*, 25(4), Dec, pp. 402-408.

Lockyer, S., Okuyama, K., Begum, S., Le, S., Sun, B., Watanabe, T., Matsumoto, Y., Yoshitake, M., et al. (2006) 'GPVI-deficient mice lack collagen responses and are protected against experimentally induced pulmonary thromboembolism.' *Thromb Res*, 118(3) 20050902, pp. 371-380.

Loyau, S., Dumont, B., Ollivier, V., Boulaftali, Y., Feldman, L., Ajzenberg, N. and Jandrot-Perrus, M. (2012) 'Platelet Glycoprotein VI Dimerization, an Active Process Inducing Receptor Competence, Is an Indicator of Platelet Reactivity.' *Arteriosclerosis, Thrombosis, and Vascular Biology*, 32(3), 2012/03/01, pp. 778-785.

Luo, G., Jian, Z., Zhu, Y., Zhu, Y., Chen, B., Ma, R., Tang, F. and Xiao, Y. (2019) 'Sirt1 promotes autophagy and inhibits apoptosis to protect cardiomyocytes from hypoxic stress.' *Int J Mol Med*, 43(5), 2019/05/01, pp. 2033-2043.

Luo, X., Lv, Y., Bai, X., Qi, J., Weng, X., Liu, S., Bao, X., Jia, H., et al. (2021) 'Plaque Erosion: A Distinctive Pathological Mechanism of Acute Coronary Syndrome.' *Frontiers in Cardiovascular Medicine*, 8, 2021-September-28,

Lüscher, T. F. and Corti, R. (2004) 'Flow: the signal of life.' *Circ Res*, 95(8), Oct 15, pp. 749-751.

- Ma, L. and Li, Y. (2015) 'SIRT1: Role in cardiovascular biology.' *Clinica Chimica Acta*, 440, 2015/02/02/, pp. 8-15.
- Ma, Y., Jiang, Q., Yang, B., Hu, X., Shen, G., Shen, W. and Xu, J. (2023) 'Platelet mitochondria, a potent immune mediator in neurological diseases.' *Front Physiol*, 14 20230901, p. 1210509.
- Machlus, K. R. and Italiano, J. E., Jr. (2013) 'The incredible journey: From megakaryocyte development to platelet formation.' *J Cell Biol*, 201(6), Jun 10, pp. 785-796.
- MacTaggart, B. and Kashina, A. (2021) 'Posttranslational modifications of the cytoskeleton.' *Cytoskeleton (Hoboken)*, 78(4), Apr, 20210702, pp. 142-173.
- Mahmoudi, M. (2022) 'The pathogenesis of atherosclerosis.' *Medicine*, 50(7), 2022/07/01/, pp. 395-398.
- Mai, A., Valente, S., Meade, S., Carafa, V., Tardugno, M., Nebbioso, A., Galmozzi, A., Mitro, N., et al. (2009) 'Study of 1,4-Dihydropyridine Structural Scaffold: Discovery of Novel Sirtuin Activators and Inhibitors.' *Journal of Medicinal Chemistry*, 52(17), 2009/09/10, pp. 5496-5504.
- Maiese, K. (2021) 'Targeting the core of neurodegeneration: FoxO, mTOR, and SIRT1.' *Neural Regen Res*, 16(3), Mar, pp. 448-455.
- Majithia, A. and Bhatt, D. L. (2019) 'Novel Antiplatelet Therapies for Atherothrombotic Diseases.' *Arteriosclerosis, Thrombosis, and Vascular Biology*, 39(4), 2019/04/01, pp. 546-557.
- Mammadova-Bach, E., Jaeken, J., Gudermann, T. and Braun, A. (2020) 'Platelets and Defective N-Glycosylation.' *Int J Mol Sci*, 21(16), Aug 6, 20200806,
- Man, A. W. C., Li, H. and Xia, N. (2019) 'The Role of Sirtuin1 in Regulating Endothelial Function, Arterial Remodeling and Vascular Aging.' *Front Physiol*, 10 20190912, p. 1173.

Marcus, A. J., Broekman, M. J., Drosopoulos, J. H. F., Pinsky, D. J., Islam, N., Gayle, R. B. and Maliszewski, C. R. (2001) 'Thromboregulation by Endothelial Cells.' *Arteriosclerosis, Thrombosis, and Vascular Biology*, 21(2), 2001/02/01, pp. 178-182.

Marumo, M., Ekawa, K. and Wakabayashi, I. (2020) 'Resveratrol inhibits Ca²⁺ signals and aggregation of platelets.' *Environmental Health and Preventive Medicine*, 25(1), 2020/11/07, p. 70.

Massberg, S., Gawaz, M., Grüner, S., Schulte, V., Konrad, I., Zohlnhöfer, D., Heinzmann, U. and Nieswandt, B. (2003) 'A crucial role of glycoprotein VI for platelet recruitment to the injured arterial wall in vivo.' *J Exp Med*, 197(1), Jan 6, pp. 41-49.

Mattagajasingh, I., Kim, C. S., Naqvi, A., Yamamori, T., Hoffman, T. A., Jung, S. B., DeRicco, J., Kasuno, K., et al. (2007) 'SIRT1 promotes endothelium-dependent vascular relaxation by activating endothelial nitric oxide synthase.' *Proc Natl Acad Sci U S A*, 104(37), Sep 11, 20070904, pp. 14855-14860.

Matus, V., Valenzuela, G., Sáez, C. G., Hidalgo, P., Lagos, M., Aranda, E., Panes, O., Pereira, J., et al. (2013) 'An adenine insertion in exon 6 of human GP6 generates a truncated protein associated with a bleeding disorder in four Chilean families.' *J Thromb Haemost*, 11(9), Sep, pp. 1751-1759.

Maurea, N., Coppola, C., Piscopo, G., Galletta, F., Riccio, G., Esposito, E., De Lorenzo, C., De Laurentiis, M., et al. (2016) 'Pathophysiology of cardiotoxicity from target therapy and angiogenesis inhibitors.' *J Cardiovasc Med (Hagerstown)*, 17 Suppl 1, May, pp. S19-26.

Maynard, D. M., Heijnen, H. F., Gahl, W. A. and Gunay-Aygun, M. (2010) 'The α -granule proteome: novel proteins in normal and ghost granules in gray platelet syndrome.' *J Thromb Haemost*, 8(8), Aug, 20100527, pp. 1786-1796.

Mazighi, M., Köhrmann, M., Lemmens, R., Lyrer, P. A., Molina, C. A., Richard, S., Toni, D., Plétan, Y., et al. (2024) 'Safety and efficacy of platelet glycoprotein VI inhibition in acute ischaemic stroke (ACTIMIS): a randomised, double-blind, placebo-controlled, phase 1b/2a trial.' *Lancet Neurol*, 23(2), Feb, pp. 157-167.

Mazzarello, P., Calligaro, A. L. and Calligaro, A. (2001) 'Giulio Bizzozero: a pioneer of cell biology.' *Nat Rev Mol Cell Biol*, 2(10), Oct, pp. 776-781.

McFadyen, J. D., Schaff, M. and Peter, K. (2018) 'Current and future antiplatelet therapies: emphasis on preserving haemostasis.' *Nat Rev Cardiol*, 15(3), Mar, 20180103, pp. 181-191.

McKellar, G. E., McCarey, D. W., Sattar, N. and McInnes, I. B. (2009) 'Role for TNF in atherosclerosis? Lessons from autoimmune disease.' *Nature Reviews Cardiology*, 6(6), 2009/06/01, pp. 410-417.

Mega, J. L. and Simon, T. (2015) 'Pharmacology of antithrombotic drugs: an assessment of oral antiplatelet and anticoagulant treatments.' *Lancet*, 386(9990), Jul 18, 20150314, pp. 281-291.

Menzies, K. J., Zhang, H., Katsyuba, E. and Auwerx, J. (2016) 'Protein acetylation in metabolism - metabolites and cofactors.' *Nat Rev Endocrinol*, 12(1), Jan, 20151027, pp. 43-60.

Michaelis, U. R. (2014) 'Mechanisms of endothelial cell migration.' *Cell Mol Life Sci*, 71(21), Nov, 20140720, pp. 4131-4148.

Michno, A., Gruzewska, K., Ronowska, A., Gul-Hinc, S., Zyśk, M. and Jankowska-Kulawy, A. (2022) 'Resveratrol Inhibits Metabolism and Affects Blood Platelet Function in Type 2 Diabetes.' *Nutrients*, 14(8), Apr 14, 20220414,

Millington-Burgess, S. L. and Harper, M. T. (2022) 'Maintaining flippase activity in procoagulant platelets is a novel approach to reducing thrombin generation.' *J Thromb Haemost*, 20(4), Apr, 20220130, pp. 989-995.

Milne, J. C. and Denu, J. M. (2008) 'The Sirtuin family: therapeutic targets to treat diseases of aging.' *Curr Opin Chem Biol*, 12(1), Feb, 20080307, pp. 11-17.

Milne, J. C., Lambert, P. D., Schenk, S., Carney, D. P., Smith, J. J., Gagne, D. J., Jin, L., Boss, O., et al. (2007) 'Small molecule activators of SIRT1 as therapeutics for the treatment of type 2 diabetes.' *Nature*, 450(7170), Nov 29, pp. 712-716.

Min, J. S., Kim, J. C., Kim, J. A., Kang, I. and Ahn, J. K. (2018) 'SIRT2 reduces actin polymerization and cell migration through deacetylation and degradation of HSP90.' *Biochimica et Biophysica Acta (BBA) - Molecular Cell Research*, 1865(9), 2018/09/01/, pp. 1230-1238.

Ministrini, S., Puspitasari, Y. M., Beer, G., Liberale, L., Montecucco, F. and Camici, G. G. (2021) 'Sirtuin 1 in Endothelial Dysfunction and Cardiovascular Aging.' *Front Physiol*, 12 20211006, p. 733696.

Minor, R. K., Baur, J. A., Gomes, A. P., Ward, T. M., Csiszar, A., Mercken, E. M., Abdelmohsen, K., Shin, Y.-K., et al. (2011) 'SRT1720 improves survival and healthspan of obese mice.' *Scientific Reports*, 1(1), 2011/08/18, p. 70.

Mitchell, J. A., Ali, F., Bailey, L., Moreno, L. and Harrington, L. S. (2008) 'Role of nitric oxide and prostacyclin as vasoactive hormones released by the endothelium.' *Experimental Physiology*, 93(1), 2008/01/01, pp. 141-147.

Mitchell, S. J., Martin-Montalvo, A., Mercken, E. M., Palacios, H. H., Ward, T. M., Abulwerdi, G., Minor, R. K., Vlasuk, G. P., et al. (2014) 'The SIRT1 activator SRT1720 extends lifespan and improves health of mice fed a standard diet.' *Cell Rep*, 6(5), Mar 13, 20140227, pp. 836-843.

Mohar, D. S. and Malik, S. (2012) 'The Sirtuin System: The Holy Grail of Resveratrol?' *J Clin Exp Cardiol*, 3(11), Nov,

Moroi, M. and Jung, S. M. (2004) 'Platelet glycoprotein VI: its structure and function.' *Thrombosis Research*, 114(4), 2004/01/01/, pp. 221-233.

Moscardó, A., Vallés, J., Latorre, A., Jover, R. and Santos, M. T. (2015) 'The histone deacetylase sirtuin 2 is a new player in the regulation of platelet function.' *J Thromb Haemost*, 13(7), Jul, 20150611, pp. 1335-1344.

Moschonas, I. C., Goudevenos, J. A. and Tselepis, A. D. (2015) 'Protease-activated receptor-1 antagonists in long-term antiplatelet therapy. Current state of evidence and future perspectives.' *International Journal of Cardiology*, 185, 2015/04/15/, pp. 9-18.

Moskalensky, A. E., Yurkin, M. A., Muliukov, A. R., Litvinenko, A. L., Nekrasov, V. M., Chernyshev, A. V. and Maltsev, V. P. (2018) 'Method for the simulation of blood platelet shape and its evolution during activation.' *PLoS Comput Biol*, 14(3), Mar, 20180308, p. e1005899.

Motonishi, S., Nangaku, M., Wada, T., Ishimoto, Y., Ohse, T., Matsusaka, T., Kubota, N., Shimizu, A., et al. (2015) 'Sirtuin1 Maintains Actin Cytoskeleton by Deacetylation

of Cortactin in Injured Podocytes.' *J Am Soc Nephrol*, 26(8), Aug, 20141125, pp. 1939-1959.

Mu, A., Latario, C. J., Pickrell, L. E. and Higgs, H. N. (2020) 'Lysine acetylation of cytoskeletal proteins: Emergence of an actin code.' *J Cell Biol*, 219(12), Dec 7,

Mundi, S., Massaro, M., Scoditti, E., Carluccio, M. A., van Hinsbergh, V. W. M., Iruela-Arispe, M. L. and De Caterina, R. (2018) 'Endothelial permeability, LDL deposition, and cardiovascular risk factors-a review.' *Cardiovasc Res*, 114(1), Jan 1, pp. 35-52.

Mussbacher, M., Salzmann, M., Brostjan, C., Hoesel, B., Schoergenhofer, C., Datler, H., Hohensinner, P., Basílio, J., et al. (2019) 'Cell Type-Specific Roles of NF- κ B Linking Inflammation and Thrombosis.' *Front Immunol*, 10 20190204, p. 85.

Nagy, M., Perrella, G., Dalby, A., Becerra, M. F., Garcia Quintanilla, L., Pike, J. A., Morgan, N. V., Gardiner, E. E., et al. (2020) 'Flow studies on human GPVI-deficient blood under coagulating and noncoagulating conditions.' *Blood Adv*, 4(13), Jul 14, pp. 2953-2961.

Naotoshi, I., Azekami, K., Hosoda, R., Nojima, I., Hisahara, S. and Kuno, A. (2022) 'Activation of SIRT1 promotes membrane resealing via cortactin.' *Scientific Reports*, 12(1), 2022/09/12, p. 15328.

Nasrin, N., Kaushik, V. K., Fortier, E., Wall, D., Pearson, K. J., de Cabo, R. and Bordone, L. (2009) 'JNK1 phosphorylates SIRT1 and promotes its enzymatic activity.' *PLoS One*, 4(12), Dec 22, 20091222, p. e8414.

Navarro-Núñez, L., Lozano, M. L., Martínez, C., Vicente, V. and Rivera, J. (2010) 'Effect of quercetin on platelet spreading on collagen and fibrinogen and on multiple platelet kinases.' *Fitoterapia*, 81(2), Mar, 20090815, pp. 75-80.

Neubauer, K. and Zieger, B. (2022) 'Endothelial cells and coagulation.' *Cell and Tissue Research*, 387(3), 2022/03/01, pp. 391-398.

Neubauer, K. and Zieger, B. (2022) 'Endothelial cells and coagulation.' *Cell Tissue Res*, 387(3), Mar, 20210520, pp. 391-398.

Ni, D., Mo, Z. and Yi, G. (2021) 'Recent insights into atherosclerotic plaque cell autophagy.' *Exp Biol Med (Maywood)*, 246(24), Dec, 20210818, pp. 2553-2558.

Nieman, M. T. and Schmaier, A. H. (2007) 'Interaction of thrombin with PAR1 and PAR4 at the thrombin cleavage site.' *Biochemistry*, 46(29), Jul 24, 20070627, pp. 8603-8610.

Nieswandt, B., Varga-Szabo, D. and Elvers, M. (2009) 'Integrins in platelet activation.' *J Thromb Haemost*, 7 Suppl 1, Jul, pp. 206-209.

Nieswandt, B., Brakebusch, C., Bergmeier, W., Schulte, V., Bouvard, D., Mokhtari-Nejad, R., Lindhout, T., Heemskerk, J. W., et al. (2001) 'Glycoprotein VI but not alpha2beta1 integrin is essential for platelet interaction with collagen.' *Embo j*, 20(9), May 1, pp. 2120-2130.

North, B. J., Marshall, B. L., Borra, M. T., Denu, J. M. and Verdin, E. (2003) 'The human Sir2 ortholog, SIRT2, is an NAD⁺-dependent tubulin deacetylase.' *Mol Cell*, 11(2), Feb, pp. 437-444.

Nurden, A. T. (2023) 'Molecular basis of clot retraction and its role in wound healing.' *Thromb Res*, 231, Nov, 20220819, pp. 159-169.

O'Donoghue, M. and Wiviott, S. D. (2006) 'Clopidogrel response variability and future therapies: clopidogrel: does one size fit all?' *Circulation*, 114(22), Nov 28, pp. e600-606.

Offermanns, S. (2006) 'Activation of Platelet Function Through G Protein–Coupled Receptors.' *Circulation Research*, 99(12), 2006/12/08, pp. 1293-1304.

Oldham, W. M. and Hamm, H. E. (2008) 'Heterotrimeric G protein activation by G-protein-coupled receptors.' *Nature Reviews Molecular Cell Biology*, 9(1), 2008/01/01, pp. 60-71.

Oppenheimer, H., Gabay, O., Meir, H., Haze, A., Kandel, L., Liebergall, M., Gagarina, V., Lee, E. J., et al. (2012) '75-kd sirtuin 1 blocks tumor necrosis factor α -mediated apoptosis in human osteoarthritic chondrocytes.' *Arthritis Rheum*, 64(3), Mar, pp. 718-728.

Ornelas, A., Zacharias-Millward, N., Menter, D. G., Davis, J. S., Lichtenberger, L., Hawke, D., Hawk, E., Vilar, E., et al. (2017) 'Beyond COX-1: the effects of aspirin on platelet biology and potential mechanisms of chemoprevention.' *Cancer Metastasis Rev*, 36(2), Jun, pp. 289-303.

Pahl, A. (2008) 'Thromboxane-A Synthase.' In Enna, S. J. and Bylund, D. B. (eds.) *xPharm: The Comprehensive Pharmacology Reference*. New York: Elsevier, pp. 1-6.
<https://www.sciencedirect.com/science/article/pii/B978008052323636888>

Pandey, D., Goyal, P., Bamburg, J. R. and Siess, W. (2006) 'Regulation of LIM-kinase 1 and cofilin in thrombin-stimulated platelets.' *Blood*, 107(2), Jan 15, 20051011, pp. 575-583.

Pang, X., He, X., Qiu, Z., Zhang, H., Xie, R., Liu, Z., Gu, Y., Zhao, N., et al. (2023) 'Targeting integrin pathways: mechanisms and advances in therapy.' *Signal Transduction and Targeted Therapy*, 8(1), 2023/01/02, p. 1.

Pardo, P. S. and Boriek, A. M. (2020) 'SIRT1 Regulation in Ageing and Obesity.' *Mechanisms of Ageing and Development*, 188, 2020/06/01/, p. 111249.

Park, J. A., Park, S., Park, W. Y., Han, M. K. and Lee, Y. (2019) 'Splitomicin, a SIRT1 Inhibitor, Enhances Hematopoietic Differentiation of Mouse Embryonic Stem Cells.' *Int J Stem Cells*, 12(1), Mar 30, pp. 21-30.

Parsa-kondelaji, M. and Mansouritorghabeh, H. (2023) 'Aspirin and clopidogrel resistance; a neglected gap in stroke and cardiovascular practice in Iran: a systematic review and meta-analysis.' *Thrombosis Journal*, 21(1), 2023/07/27, p. 79.

Patel-Hett, S., Wang, H., Begonja, A. J., Thon, J. N., Alden, E. C., Wandersee, N. J., An, X., Mohandas, N., et al. (2011) 'The spectrin-based membrane skeleton stabilizes mouse megakaryocyte membrane systems and is essential for proplatelet and platelet formation.' *Blood*, 118(6), Aug 11, 20110512, pp. 1641-1652.

Patel, S., Khan, H. and Majumdar, A. (2022) 'Crosstalk between Sirtuins and Nrf2: SIRT1 activators as emerging treatment for diabetic neuropathy.' *Metabolic Brain Disease*, 37(7), 2022/10/01, pp. 2181-2195.

Patrono, C. (2023) 'Fifty years with aspirin and platelets.' *Br J Pharmacol*, 180(1), Jan, 20221103, pp. 25-43.

Paven, E., Dillinger, J. G., Bal dit Sollier, C., Vidal-Trecan, T., Berge, N., Dautry, R., Gautier, J. F., Drouet, L., et al. (2020) 'Determinants of aspirin resistance in patients with type 2 diabetes.' *Diabetes & Metabolism*, 46(5), 2020/10/01/, pp. 370-376.

Pepin, M. E. and Gupta, R. M. (2024) 'The Role of Endothelial Cells in Atherosclerosis: Insights from Genetic Association Studies.' *The American Journal of Pathology*, 194(4), 2024/04/01/, pp. 499-509.

Periyah, M. H., Halim, A. S. and Mat Saad, A. Z. (2017) 'Mechanism Action of Platelets and Crucial Blood Coagulation Pathways in Hemostasis.' *Int J Hematol Oncol Stem Cell Res*, 11(4), Oct 1, pp. 319-327.

Petheő, G. L., Kerekes, A., Mihálffy, M., Donkó, Á., Bodrogi, L., Skoda, G., Baráth, M., Hoffmann, O. I., et al. (2021) 'Disruption of the NOX5 Gene Aggravates Atherosclerosis in Rabbits.' *Circulation Research*, 128(9), 2021/04/30, pp. 1320-1322.

Petronek, M. S., Bayanbold, K., Amegble, K., Tomanek-Chalkley, A. M., Allen, B. G., Spitz, D. R. and Bailey, C. K. (2023) 'Evaluating the iron chelator function of sirtinol in non-small cell lung cancer.' *Front Oncol*, 13 20230615, p. 1185715.

Phillips, D. R., Nannizzi-Alaimo, L. and Prasad, K. S. (2001) 'Beta3 tyrosine phosphorylation in alphaIIb beta3 (platelet membrane GP IIb-IIIa) outside-in integrin signaling.' *Thromb Haemost*, 86(1), Jul, pp. 246-258.

Pickett, J. R., Wu, Y., Zacchi, L. F. and Ta, H. T. (2023) 'Targeting endothelial vascular cell adhesion molecule-1 in atherosclerosis: drug discovery and development of vascular cell adhesion molecule-1-directed novel therapeutics.' *Cardiovascular Research*, 119(13) pp. 2278-2293.

Pober, J. S. and Sessa, W. C. (2007) 'Evolving functions of endothelial cells in inflammation.' *Nat Rev Immunol*, 7(10), Oct, pp. 803-815.

Podoplelova, N. A., Sveshnikova, A. N., Kotova, Y. N., Eckly, A., Receveur, N., Nechipurenko, D. Y., Obydennyi, S. I., Kireev, II, et al. (2016) 'Coagulation factors bound to procoagulant platelets concentrate in cap structures to promote clotting.' *Blood*, 128(13), Sep 29, 20160718, pp. 1745-1755.

Polanowska-Grabowska, R., Gibbins, J. M. and Gear, A. R. (2003) 'Platelet adhesion to collagen and collagen-related peptide under flow: roles of the $\alpha 2\beta 1$ integrin, GPVI, and Src tyrosine kinases.' *Arterioscler Thromb Vasc Biol*, 23(10), Oct 1, 20030717, pp. 1934-1940.

Pollitt, A. Y., Hughes, C. E. and Watson, S. P. (2013) 'Chapter 11 - GPVI and CLEC-2.' In Michelson, A. D. (ed.) *Platelets (Third Edition)*. Academic Press, pp. 215-231. <https://www.sciencedirect.com/science/article/pii/B9780123878373000110>

Poulter, N. S., Pollitt, A. Y., Davies, A., Malinova, D., Nash, G. B., Hannon, M. J., Pikramenou, Z., Rappoport, J. Z., et al. (2015) 'Platelet actin nodules are podosome-like structures dependent on Wiskott–Aldrich syndrome protein and ARP2/3 complex.' *Nature Communications*, 6(1), 2015/06/01, p. 7254.

Poznyak, A., Grechko, A. V., Poggio, P., Myasoedova, V. A., Alfieri, V. and Orekhov, A. N. (2020) 'The Diabetes Mellitus-Atherosclerosis Connection: The Role of Lipid and Glucose Metabolism and Chronic Inflammation.' *Int J Mol Sci*, 21(5), Mar 6, 20200306,

Pradhan, A., Tiwari, A., Caminiti, G., Salimei, C., Muscoli, S., Sethi, R. and Perrone, M. A. (2022) 'Ideal P2Y₁₂ Inhibitor in Acute Coronary Syndrome: A Review and Current Status.' *Int J Environ Res Public Health*, 19(15), Jul 23, 20220723,

Presneau, N., Duhamel, L. A., Ye, H., Tirabosco, R., Flanagan, A. M. and Eskandarpour, M. (2017) 'Post-translational regulation contributes to the loss of LKB1 expression through SIRT1 deacetylase in osteosarcomas.' *British Journal of Cancer*, 117(3), 2017/07/01, pp. 398-408.

Puccini, M., Rauch, C., Jakobs, K., Friebel, J., Hassanein, A., Landmesser, U. and Rauch, U. (2023) 'Being Overweight or Obese Is Associated with an Increased Platelet Reactivity Despite Dual Antiplatelet Therapy with Aspirin and Clopidogrel.' *Cardiovasc Drugs Ther*, 37(4), Aug, 20220225, pp. 833-837.

Puylaert, P., Zurek, M., Rayner, K. J., De Meyer, G. R. Y. and Martinet, W. (2022) 'Regulated Necrosis in Atherosclerosis.' *Arteriosclerosis, Thrombosis, and Vascular Biology*, 42(11), 2022/11/01, pp. 1283-1306.

Qiang, L., Sample, A., Liu, H., Wu, X. and He, Y. (2017) 'Epidermal SIRT1 regulates inflammation, cell migration, and wound healing.' *Sci Rep*, 7(1), Oct 26, 20171026, p. 14110.

Qin, R., Zhang, L., Lin, D., Xiao, F. and Guo, L. (2019) 'Sirt1 inhibits HG-induced endothelial injury: Role of Mff-based mitochondrial fission and F-actin homeostasis-mediated cellular migration.' *Int J Mol Med*, 44(1), Jul, 20190508, pp. 89-102.

Quach, M. E. and Li, R. (2020) 'Structure-function of platelet glycoprotein Ib-IX.' *J Thromb Haemost*, 18(12), Dec, 20200824, pp. 3131-3141.

Radenković, M., Stojanović, M., Potpara, T. and Prostran, M. (2013) 'Therapeutic Approach in the Improvement of Endothelial Dysfunction: The Current State of the Art.' *BioMed Research International*, 2013(1), 2013/01/01, p. 252158.

Rajendran, A., Minhas, A. S., Kazzi, B., Varma, B., Choi, E., Thakkar, A. and Michos, E. D. (2023) 'Sex-specific differences in cardiovascular risk factors and implications for cardiovascular disease prevention in women.' *Atherosclerosis*, 384, Nov, 20230904, p. 117269.

Rand, M. L., Le Breton, G. C., Paton, T., Pai, M. K., Chan, A. K. C., Blanchette, V. S. and Kahr, W. H. (2005) 'A Novel Inherited Platelet Function Disorder Involving the Thromboxane A2 Pathway of Platelet Activation.' *Blood*, 106(11) pp. 2175-2175.

Randriamboavonjy, V., Isaak, J., Frömel, T., Viollet, B., Fisslthaler, B., Preissner, K. T. and Fleming, I. (2010) 'AMPK α 2 subunit is involved in platelet signaling, clot retraction, and thrombus stability.' *Blood*, 116(12), Sep 23, 20100617, pp. 2134-2140.

Rashdan, N. A., Shrestha, B. and Pattillo, C. B. (2020) 'S-glutathionylation, friend or foe in cardiovascular health and disease.' *Redox Biol*, 37, Oct, 20200822, p. 101693.

Rashedi, S., Greason, C. M., Sadeghipour, P., Talasaz, A. H., O'Donoghue, M. L., Jimenez, D., Monreal, M., Anderson, C. D., et al. (2024) 'Fibrinolytic Agents in Thromboembolic Diseases: Historical Perspectives and Approved Indications.' *Semin Thromb Hemost*, 50(05), 2024/03/01, pp. 773-789.

Ray, S. (2014) 'Clopidogrel resistance: the way forward.' *Indian Heart J*, 66(5), Sep-Oct, 20141007, pp. 530-534.

Razick, D. I., Akhtar, M., Wen, J., Alam, M., Dean, N., Karabala, M., Ansari, U., Ansari, Z., et al. (2023) 'The Role of Sirtuin 1 (SIRT1) in Neurodegeneration.' *Cureus*, 15(6), Jun, 20230615, p. e40463.

Reddy, M. A., Sahar, S., Villeneuve, L. M., Lanting, L. and Natarajan, R. (2009) 'Role of Src tyrosine kinase in the atherogenic effects of the 12/15-lipoxygenase pathway in vascular smooth muscle cells.' *Arterioscler Thromb Vasc Biol*, 29(3), Mar, 20081218, pp. 387-393.

Ren, G., Rimando, A. M. and Mathews, S. T. (2018) 'AMPK activation by pterostilbene contributes to suppression of hepatic gluconeogenic gene expression and glucose production in H4IIE cells.' *Biochemical and Biophysical Research Communications*, 498(3), 2018/04/06/, pp. 640-645.

Ribba, A.-S., Batzenschlager, M., Rabat, C., Buchou, T., Moog, S., Khochbin, S., Bourova-Flin, E., Lafanechère, L., et al. (2021) 'Marginal band microtubules are acetylated by α TAT1.' *Platelets*, 32(4), 2021/05/19, pp. 568-572.

Rivera, J., Lozano, M. L., Navarro-Núñez, L. and Vicente, V. (2009) 'Platelet receptors and signaling in the dynamics of thrombus formation.' *Haematologica*, 94(5), 04/30, pp. 700-711.

Robaux, V., Kautbally, S., Ginion, A., Dechamps, M., Lejeune, S., Menghoum, N., Bertrand, L., Pouleur, A. C., et al. (2023) 'Dual antiplatelet therapy is associated with high α -tubulin acetylation in circulating platelets from coronary artery disease patients.' *Platelets*, 34(1), Dec, p. 2250002.

Rodríguez, A., Rodríguez, M., Córdoba, J. J. and Andrade, M. J. (2015) 'Design of Primers and Probes for Quantitative Real-Time PCR Methods.' In Basu, C. (ed.) *PCR Primer Design*. New York, NY: Springer New York, pp. 31-56. https://doi.org/10.1007/978-1-4939-2365-6_3

Romero, S., Le Clainche, C. and Gautreau, A. M. (2020) 'Actin polymerization downstream of integrins: signaling pathways and mechanotransduction.' *Biochem J*, 477(1), Jan 17, pp. 1-21.

Rothgiesser, K. M., Fey, M. and Hottiger, M. O. (2010) 'Acetylation of p65 at lysine 314 is important for late NF-kappaB-dependent gene expression.' *BMC Genomics*, 11, Jan 11, 20100111, p. 22.

Rucker, D. and Dhamoon, A. S. (2023) *Physiology, Thromboxane A2*. StatPearls Publishing, Treasure Island (FL).

Ruijie, Q., Zhang, L., Lin, D., Xiao, F. and Guo, L. (2019) 'Sirt1 inhibits HG-induced endothelial injury: Role of Mff-based mitochondrial fission and F-actin homeostasis-mediated cellular migration Retraction in /10.3892/ijmm.2024.5390.' *Int J Mol Med*, 44(1), 2019/07/01, pp. 89-102.

Russo, I., Barale, C., Melchionda, E., Penna, C. and Pagliaro, P. (2023) 'Platelets and Cardioprotection: The Role of Nitric Oxide and Carbon Oxide.' *International Journal of Molecular Sciences*, 24, [Online] 7. [Accessed 10.3390/ijms24076107

Rutledge, N. S. and Muller, W. A. (2020) 'Understanding Molecules that Mediate Leukocyte Extravasation.' *Current Pathobiology Reports*, 8(2), 2020/06/01, pp. 25-35.

Rwibasira Rudinga, G., Khan, G. J. and Kong, Y. (2018) 'Protease-Activated Receptor 4 (PAR4): A Promising Target for Antiplatelet Therapy.' *Int J Mol Sci*, 19(2), Feb 14, 20180214,

Sacitharan, P. K., Bou-Gharios, G. and Edwards, J. R. (2020) 'SIRT1 directly activates autophagy in human chondrocytes.' *Cell Death Discovery*, 6(1), 2020/05/29, p. 41.

Sadoul, Wang, J., Diagouraga, B., Vitte, A.-L., Buchou, T., Rossini, T., Polack, B., Xi, X., et al. (2012) 'HDAC6 controls the kinetics of platelet activation.' *Blood*, 120(20) pp. 4215-4218.

Sadoul, K. (2015) 'New explanations for old observations: marginal band coiling during platelet activation.' *J Thromb Haemost*, 13(3), Mar, 20150123, pp. 333-346.

Sadoul, K., Wang, J., Diagouraga, B., Vitte, A. L., Buchou, T., Rossini, T., Polack, B., Xi, X., et al. (2012) 'HDAC6 controls the kinetics of platelet activation.' *Blood*, 120(20), Nov 15, 20120906, pp. 4215-4218.

Safi, M., Nazari, R., Senobari, N., Taheri, H. and Ebrahimi, P. (2024) 'A woman with eptifibatide (integrilin)-induced thrombocytopenia following treatment of a clot in her coronary artery: A case report and literature review.' *Clinical Case Reports*, 12(4) p. e8694.

Sang, Y., Roest, M., de Laat, B., de Groot, P. G. and Huskens, D. (2021) 'Interplay between platelets and coagulation.' *Blood Rev*, 46, Mar, 20200712, p. 100733.

Sang, Y., Huskens, D., Wichapong, K., de Laat, B., Nicolaes, G. A. F. and Roest, M. (2019) 'A Synthetic Triple Helical Collagen Peptide as a New Agonist for Flow Cytometric Measurement of GPVI-Specific Platelet Activation.' *Thromb Haemost*, 119(12), Dec, 20191021, pp. 2005-2013.

Santini, S. J., Cordone, V., Mijit, M., Bignotti, V., Aimola, P., Dolo, V., Falone, S. and Amicarelli, F. (2019) 'SIRT1-Dependent Upregulation of Antiglycative Defense in HUVECs Is Essential for Resveratrol Protection against High Glucose Stress.' *Antioxidants (Basel)*, 8(9), Sep 1, 20190901,

Satta, S., Beal, R., Smith, R., Luo, X., Ferris, G. R., Langford-Smith, A., Teasdale, J., Ajime, T. T., et al. (2023) 'A Nrf2-OSGIN1&2-HSP70 axis mediates cigarette smoke-induced endothelial detachment: implications for plaque erosion.' *Cardiovasc Res*, 119(9), Aug 7, pp. 1869-1882.

Scherlinger, M., Richez, C., Tsokos, G. C., Boilard, E. and Blanco, P. (2023) 'The role of platelets in immune-mediated inflammatory diseases.' *Nature Reviews Immunology*, 23(8), 2023/08/01, pp. 495-510.

Schilling, B., Meyer, J. G., Wei, L., Ott, M. and Verdin, E. (2019) 'High-Resolution Mass Spectrometry to Identify and Quantify Acetylation Protein Targets.' *Methods Mol Biol*, 1983 pp. 3-16.

Schlesinger, M. (2018) 'Role of platelets and platelet receptors in cancer metastasis.' *Journal of Hematology & Oncology*, 11(1), 2018/10/11, p. 125.

Schnoor, M., Stradal, T. E. and Rottner, K. (2018) 'Cortactin: Cell Functions of A Multifaceted Actin-Binding Protein.' *Trends in Cell Biology*, 28(2), 2018/02/01/, pp. 79-98.

Schoenwaelder, S. M., Yuan, Y., Josefsson, E. C., White, M. J., Yao, Y., Mason, K. D., O'Reilly, L. A., Henley, K. J., et al. (2009) 'Two distinct pathways regulate platelet phosphatidylserine exposure and procoagulant function.' *Blood*, 114(3) pp. 663-666.

Schuijt, T. J., Bakhtiari, K., Daffre, S., Deponte, K., Wielders, S. J., Marquart, J. A., Hovius, J. W., van der Poll, T., et al. (2013) 'Factor Xa activation of factor V is of paramount importance in initiating the coagulation system: lessons from a tick salivary protein.' *Circulation*, 128(3), Jul 16, 20130701, pp. 254-266.

Scridon, A. (2022) 'Platelets and Their Role in Hemostasis and Thrombosis-From Physiology to Pathophysiology and Therapeutic Implications.' *Int J Mol Sci*, 23(21), Oct 23, 20221023,

Searles, C. D. (2006) 'Transcriptional and posttranscriptional regulation of endothelial nitric oxide synthase expression.' *Am J Physiol Cell Physiol*, 291(5), Nov, 20060531, pp. C803-816.

Sebbagh, M., Olschwang, S., Santoni, M. J. and Borg, J. P. (2011) 'The LKB1 complex-AMPK pathway: the tree that hides the forest.' *Fam Cancer*, 10(3), Sep, pp. 415-424.

Selvadurai, M. V. and Hamilton, J. R. (2018) 'Structure and function of the open canalicular system – the platelet's specialized internal membrane network.' *Platelets*, 29(4), 2018/05/19, pp. 319-325.

Senis, Y. A. (2013) 'Protein-tyrosine phosphatases: a new frontier in platelet signal transduction.' *J Thromb Haemost*, 11(10), Oct, pp. 1800-1813.

Sessa, W. C. (2004) 'eNOS at a glance.' *J Cell Sci*, 117(Pt 12), May 15, pp. 2427-2429.

Shao, F., Lee, P. W., Li, H., Hsieh, K. and Wang, T. H. (2023) 'Emerging platforms for high-throughput enzymatic bioassays.' *Trends Biotechnol*, 41(1), Jan, 20220718, pp. 120-133.

Shao, Y., Saredy, J., Yang, W. Y., Sun, Y., Lu, Y., Saaoud, F., Drummer, C. t., Johnson, C., et al. (2020) 'Vascular Endothelial Cells and Innate Immunity.' *Arterioscler Thromb Vasc Biol*, 40(6), Jun, 20200527, pp. e138-e152.

Shattil, S. J. and Newman, P. J. (2004) 'Integrins: dynamic scaffolds for adhesion and signaling in platelets.' *Blood*, 104(6), Sep 15, 20040617, pp. 1606-1615.

Shen, D.-S., Yang, Y.-J., Kong, X.-J., Ma, N., Liu, X.-W., Li, S.-H., Jiao, Z.-H., Qin, Z., et al. (2019) 'Aspirin eugenol ester inhibits agonist-induced platelet aggregation in

vitro by regulating PI3K/Akt, MAPK and Sirt 1/CD40L pathways.' *European Journal of Pharmacology*, 852, 2019/06/05/, pp. 1-13.

Shentu, T.-P., He, M., Sun, X., Zhang, J., Zhang, F., Gongol, B., Marin, T. L., Zhang, J., et al. (2016) 'AMP-Activated Protein Kinase and Sirtuin 1 Coregulation of Cortactin Contributes to Endothelial Function.' *Arteriosclerosis, Thrombosis, and Vascular Biology*, 36(12), 2016/12/01, pp. 2358-2368.

Shin, E. K., Park, H., Noh, J. Y., Lim, K. M. and Chung, J. H. (2017) 'Platelet Shape Changes and Cytoskeleton Dynamics as Novel Therapeutic Targets for Anti-Thrombotic Drugs.' *Biomol Ther (Seoul)*, 25(3), May 1, pp. 223-230.

Sieve, I., Ricke-Hoch, M., Kasten, M., Battmer, K., Stapel, B., Falk, C. S., Leisegang, M. S., Haverich, A., et al. (2018) 'A positive feedback loop between IL-1 β , LPS and NEU1 may promote atherosclerosis by enhancing a pro-inflammatory state in monocytes and macrophages.' *Vascular Pharmacology*, 103-105, 2018/04/01/, pp. 16-28.

Silva, R., D'Amico, G., Hodivala-Dilke, K. M. and Reynolds, L. E. (2008) 'Integrins.' *Arteriosclerosis, Thrombosis, and Vascular Biology*, 28(10), 2008/10/01, pp. 1703-1713.

Silva, T., Jäger, W., Neuss-Radu, M. and Sequeira, A. (2020) 'Modeling of the early stage of atherosclerosis with emphasis on the regulation of the endothelial permeability.' *Journal of Theoretical Biology*, 496, 2020/07/07/, p. 110229.

Sim, D. S., Dilks, J. R. and Flaumenhaft, R. (2007) 'Platelets possess and require an active protein palmitoylation pathway for agonist-mediated activation and in vivo thrombus formation.' *Arterioscler Thromb Vasc Biol*, 27(6), Jun, 20070215, pp. 1478-1485.

Singh, C. K., Chhabra, G., Ndiaye, M. A., Garcia-Peterson, L. M., Mack, N. J. and Ahmad, N. (2018) 'The Role of Sirtuins in Antioxidant and Redox Signaling.' *Antioxid Redox Signal*, 28(8), Mar 10, 20171020, pp. 643-661.

Sirtris, G. (2011) 'Study of the Clinical Activity, Safety, and Tolerability of SRT2104 in Subjects With Moderate to Severe Plaque-Type Psoriasis.' [Online]. [Accessed on 29/05/2024]

<https://clinicaltrials.gov/study/NCT01154101?intr=SRT2104&rank=9#more-information>

Sirtris, G. (2013) 'A Phase 1b Study to Assess the Safety and Anti-inflammatory Effects of Two Different Doses of SRT2104 in Patients With Ulcerative Colitis.' [Online]. [Accessed on 29/05/2024] <https://clinicaltrials.gov/study/NCT01453491?intr=SRT2104&rank=1>

Sitia, S., Tomasoni, L., Atzeni, F., Ambrosio, G., Cordiano, C., Catapano, A., Tramontana, S., Perticone, F., et al. (2010) 'From endothelial dysfunction to atherosclerosis.' *Autoimmunity Reviews*, 9(12), 2010/10/01/, pp. 830-834.

Skoge, R. H., Dölle, C. and Ziegler, M. (2014) 'Regulation of SIRT2-dependent α -tubulin deacetylation by cellular NAD levels.' *DNA Repair (Amst)*, 23, Nov, 20140510, pp. 33-38.

Slater, A., Khattak, S. and Thomas, M. R. (2024) 'GPVI inhibition: Advancing antithrombotic therapy in cardiovascular disease.' *European Heart Journal - Cardiovascular Pharmacotherapy*, 10(5) pp. 465-473.

Smethurst, P. A., Onley, D. J., Jarvis, G. E., O'Connor, M. N., Knight, C. G., Herr, A. B., Ouwehand, W. H. and Farndale, R. W. (2007) 'Structural basis for the platelet-collagen interaction: the smallest motif within collagen that recognizes and activates platelet Glycoprotein VI contains two glycine-proline-hydroxyproline triplets.' *J Biol Chem*, 282(2), Jan 12, 20061102, pp. 1296-1304.

Smith, L. E. and White, M. Y. (2014) 'The role of post-translational modifications in acute and chronic cardiovascular disease.' *Proteomics Clin Appl*, 8(7-8), Aug, pp. 506-521.

Smith, S. A. and Morrissey, J. H. (2019) '21 - Interactions Between Platelets and the Coagulation System.' In Michelson, A. D. (ed.) *Platelets (Fourth Edition)*. Academic Press, pp. 393-400. <https://www.sciencedirect.com/science/article/pii/B9780128134566000217>

Soehnlein, O. and Libby, P. (2021) 'Targeting inflammation in atherosclerosis — from experimental insights to the clinic.' *Nature Reviews Drug Discovery*, 20(8), 2021/08/01, pp. 589-610.

Sonmez, O. and Sonmez, M. (2017) 'Role of platelets in immune system and inflammation.' *Porto Biomedical Journal*, 2(6) pp. 311-314.

Soodi, D., VanWormer, J. J. and Rezkalla, S. H. (2020) 'Aspirin in Primary Prevention of Cardiovascular Events.' *Clin Med Res*, 18(2-3), Aug, 20200624, pp. 89-94.

Spange, S., Wagner, T., Heinzl, T. and Krämer, O. H. (2009) 'Acetylation of non-histone proteins modulates cellular signalling at multiple levels.' *Int J Biochem Cell Biol*, 41(1), Jan, 20080902, pp. 185-198.

Springer, T. A., Zhu, J. and Xiao, T. (2008) 'Structural basis for distinctive recognition of fibrinogen gammaC peptide by the platelet integrin alphaIIb beta3.' *J Cell Biol*, 182(4), Aug 25, 20080818, pp. 791-800.

Stamatovic, S. M., Martinez-Revollar, G., Hu, A., Choi, J., Keep, R. F. and Andjelkovic, A. V. (2019) 'Decline in Sirtuin-1 expression and activity plays a critical role in blood-brain barrier permeability in aging.' *Neurobiol Dis*, 126, Jun, 20180906, pp. 105-116.

Stark, R. J., Koch, S. R., Stothers, C. L., Pourquoi, A., Lamb, C. K., Miller, M. R. and Choi, H. (2022) 'Loss of Sirtuin 1 (SIRT1) potentiates endothelial dysfunction via impaired glycolysis during infectious challenge.' *Clinical and Translational Medicine*, 12(9) p. e1054.

Stef, G., Csiszar, A., Lerea, K., Ungvari, Z. and Veress, G. (2006) 'Resveratrol Inhibits Aggregation of Platelets from High-risk Cardiac Patients with Aspirin Resistance.' *Journal of Cardiovascular Pharmacology*, 48(2)

Stefanini, L. and Bergmeier, W. (2018) 'Negative regulators of platelet activation and adhesion.' *J Thromb Haemost*, 16(2), Feb, 20171226, pp. 220-230.

Sun, H. J., Wu, Z. Y., Nie, X. W. and Bian, J. S. (2019) 'Role of Endothelial Dysfunction in Cardiovascular Diseases: The Link Between Inflammation and Hydrogen Sulfide.' *Front Pharmacol*, 10 20200121, p. 1568.

Sun, J., Zhang, M., Chen, K., Chen, B., Zhao, Y., Gong, H., Zhao, X. and Qi, R. (2018) 'Suppression of TLR4 activation by resveratrol is associated with STAT3 and Akt inhibition in oxidized low-density lipoprotein-activated platelets.' *European Journal of Pharmacology*, 836, 2018/10/05/, pp. 1-10.

Sun, S., Qiao, B., Han, Y., Wang, B., Wei, S. and Chen, Y. (2022) 'Posttranslational modifications of platelet adhesion receptors.' *Pharmacol Res*, 183, Sep, 20220823, p. 106413.

Sun, X. and Liu, B. (2022) 'Donepezil ameliorates oxygen-glucose deprivation/reoxygenation-induced brain microvascular endothelial cell dysfunction via the SIRT1/FOXO3a/NF- κ B pathways.' *Bioengineered*, 13(3), 2022/03/01, pp. 7760-7770.

Sun, X. J., Man, N., Tan, Y., Nimer, S. D. and Wang, L. (2015) 'The Role of Histone Acetyltransferases in Normal and Malignant Hematopoiesis.' *Front Oncol*, 5 20150526, p. 108.

Sung, J. Y., Kim, S. G., Cho, D. H., Kim, J.-R. and Choi, H. C. (2020) 'SRT1720-induced activation of SIRT1 alleviates vascular smooth muscle cell senescence through PKA-dependent phosphorylation of AMPK α at Ser485.' *FEBS Open Bio*, 10(7) pp. 1316-1325.

Surin, W. R., Barthwal, M. K. and Dikshit, M. (2008) 'Platelet collagen receptors, signaling and antagonism: Emerging approaches for the prevention of intravascular thrombosis.' *Thrombosis Research*, 122(6), 2008/01/01/, pp. 786-803.

Szotowski, B., Antoniak, S., Poller, W., Schultheiss, H.-P. and Rauch, U. (2005) 'Procoagulant Soluble Tissue Factor Is Released From Endothelial Cells in Response to Inflammatory Cytokines.' *Circulation Research*, 96(12), 2005/06/24, pp. 1233-1239.

Tabatabaei, M. S. and Ahmed, M. (2022) 'Enzyme-Linked Immunosorbent Assay (ELISA).' In Christian, S. L. (ed.) *Cancer Cell Biology: Methods and Protocols*. New York, NY: Springer US, pp. 115-134. https://doi.org/10.1007/978-1-0716-2376-3_10

Tafrova, J. I. and Tafrov, S. T. (2014) 'Human histone acetyltransferase 1 (Hat1) acetylates lysine 5 of histone H2A in vivo.' *Mol Cell Biochem*, 392(1-2), Jul, 20140329, pp. 259-272.

Tang, B. L. (2010) 'Sirt1 and cell migration.' *Cell Adh Migr*, 4(2), Apr-Jun, 20100418, pp. 163-165.

Tang, W. H., Wang, Z., Cho, L., Brennan, D. M. and Hazen, S. L. (2009) 'Diminished global arginine bioavailability and increased arginine catabolism as metabolic profile of increased cardiovascular risk.' *J Am Coll Cardiol*, 53(22), Jun 2, pp. 2061-2067.

Tanno, M., Sakamoto, J., Miura, T., Shimamoto, K. and Horio, Y. (2007) 'Nucleocytoplasmic shuttling of the NAD⁺-dependent histone deacetylase SIRT1.' *J Biol Chem*, 282(9), Mar 2, 20061230, pp. 6823-6832.

Tantry, U. S., Bliden, K. P., Chaudhary, R., Novakovic, M., Rout, A. and Gurbel, P. A. (2020) 'Vorapaxar in the treatment of cardiovascular diseases.' *Future Cardiol*, 16(5), Sep, 20200420, pp. 373-384.

Tenopoulou, M. and Doulias, P. T. (2020) 'Endothelial nitric oxide synthase-derived nitric oxide in the regulation of metabolism.' *F1000Res*, 9 20201001,

Thachil, J. (2016) 'Antiplatelet therapy - a summary for the general physicians.' *Clin Med (Lond)*, 16(2), Apr, pp. 152-160.

Thayse, K., Kindt, N., Laurent, S. and Carlier, S. (2020) 'VCAM-1 Target in Non-Invasive Imaging for the Detection of Atherosclerotic Plaques.' *Biology (Basel)*, 9(11), Oct 29, 20201029,

Thomas, S. G. (2019) '3 - The Structure of Resting and Activated Platelets.' In Michelson, A. D. (ed.) *Platelets (Fourth Edition)*. Academic Press, pp. 47-77. <https://www.sciencedirect.com/science/article/pii/B9780128134566000035>

Thon, J. N. and Italiano, J. E. (2012) 'Platelets: Production, Morphology and Ultrastructure.' In Gresele, P., Born, G. V. R., Patrono, C. and Page, C. P. (eds.) *Antiplatelet Agents*. Berlin, Heidelberg: Springer Berlin Heidelberg, pp. 3-22. https://doi.org/10.1007/978-3-642-29423-5_1

Thon, J. N., Peters, C. G., Machlus, K. R., Aslam, R., Rowley, J., Macleod, H., Devine, M. T., Fuchs, T. A., et al. (2012) 'T granules in human platelets function in TLR9 organization and signaling.' *J Cell Biol*, 198(4), Aug 20, pp. 561-574.

Tomaiuolo, M., Brass, L. F. and Stalker, T. J. (2017) 'Regulation of Platelet Activation and Coagulation and Its Role in Vascular Injury and Arterial Thrombosis.' *Interv Cardiol Clin*, 6(1), Jan, pp. 1-12.

Tong, C., Wang, Y., Li, J., Cen, W., Zhang, W., Zhu, Z., Yu, J. and Lu, B. (2021) 'Pterostilbene inhibits gallbladder cancer progression by suppressing the PI3K/Akt pathway.' *Sci Rep*, 11(1), Feb 23, 20210223, p. 4391.

Toniolo, A., Buccellati, C., Pinna, C., Gaion, R. M., Sala, A. and Bolego, C. (2013) 'Cyclooxygenase-1 and prostacyclin production by endothelial cells in the presence of mild oxidative stress.' *PLoS One*, 8(2) 20130218, p. e56683.

Toro, T. B., Bornes, K. E. and Watt, T. J. (2023) 'Lysine Deacetylase Substrate Selectivity: Distinct Interaction Surfaces Drive Positive and Negative Selection for Residues Following Acetyllysine.' *Biochemistry*, 62(9), 2023/05/02, pp. 1464-1483.

Tricoci, P., Huang, Z., Held, C., Moliterno, D. J., Armstrong, P. W., Werf, F. V. d., White, H. D., Aylward, P. E., et al. (2012) 'Thrombin-Receptor Antagonist Vorapaxar in Acute Coronary Syndromes.' *New England Journal of Medicine*, 366(1) pp. 20-33.

Trisciuglio, D., Di Martile, M. and Del Bufalo, D. (2018) 'Emerging Role of Histone Acetyltransferase in Stem Cells and Cancer.' *Stem Cells Int*, 2018 20181216, p. 8908751.

Troncoso, M. F., Ortiz-Quintero, J., Garrido-Moreno, V., Sanhueza-Olivares, F., Guerrero-Moncayo, A., Chiong, M., Castro, P. F., García, L., et al. (2021) 'VCAM-1 as a predictor biomarker in cardiovascular disease.' *Biochim Biophys Acta Mol Basis Dis*, 1867(9), Sep 1, 20210514, p. 166170.

Tsai, H.-J., Cheng, J.-C., Kao, M.-L., Chiu, H.-P., Chiang, Y.-H., Chen, D.-P., Rau, K.-M., Liao, H.-R., et al. (2021) 'Integrin α IIb β 3 outside-in signaling activates human platelets through serine 24 phosphorylation of Disabled-2.' *Cell & Bioscience*, 11(1), 2021/02/08, p. 32.

Tsao, C. W., Aday, A. W., Almarzooq, Z. I., Anderson, C. A. M., Arora, P., Avery, C. L., Baker-Smith, C. M., Beaton, A. Z., et al. (2023) 'Heart Disease and Stroke Statistics—2023 Update: A Report From the American Heart Association.' *Circulation*, 147(8), 2023/02/21, pp. e93-e621.

Tsikas, D. (2007) 'Analysis of nitrite and nitrate in biological fluids by assays based on the Griess reaction: appraisal of the Griess reaction in the L-arginine/nitric oxide area of research.' *J Chromatogr B Analyt Technol Biomed Life Sci*, 851(1-2), May 15, 20060906, pp. 51-70.

Tucker, K. L., Sage, T. and Gibbins, J. M. (2012) 'Clot retraction.' *Methods Mol Biol*, 788 pp. 101-107.

Uniprot. (2022) 'The Uniprot Consortium: the Universal Protein Knowledgebase in 2023.' *Nucleic Acids Research*, 51(D1) pp. D523-D531.

Unsworth, A. J., Flora, G. D. and Gibbins, J. M. (2018) 'Non-genomic effects of nuclear receptors: insights from the anucleate platelet.' *Cardiovasc Res*, 114(5), Apr 1, pp. 645-655.

Unsworth, A. J., Bombik, I., Pinto-Fernandez, A., McGouran, J. F., Konietzny, R., Zahedi, R. P., Watson, S. P., Kessler, B. M., et al. (2019) 'Human Platelet Protein Ubiquitylation and Changes following GPVI Activation.' *Thromb Haemost*, 119(1), Jan, 20181231, pp. 104-116.

Vaidya, A. R., Wolska, N., Vara, D., Mailer, R. K., Schröder, K. and Pula, G. (2021) 'Diabetes and Thrombosis: A Central Role for Vascular Oxidative Stress.' *Antioxidants (Basel)*, 10(5), Apr 29, 20210429,

Vaklavas, C., Lenihan, D., Kurzrock, R. and Tsimberidou, A. M. (2010) 'Anti-vascular endothelial growth factor therapies and cardiovascular toxicity: what are the important clinical markers to target?' *Oncologist*, 15(2) 20100205, pp. 130-141.

Valentijn, K. M., Sadler, J. E., Valentijn, J. A., Voorberg, J. and Eikenboom, J. (2011) 'Functional architecture of Weibel-Palade bodies.' *Blood*, 117(19) pp. 5033-5043.

van den Kerkhof, D. L., van der Meijden, P. E. J., Hackeng, T. M. and Dijkgraaf, I. (2021) 'Exogenous Integrin α IIb β 3 Inhibitors Revisited: Past, Present and Future Applications.' *Int J Mol Sci*, 22(7), Mar 25, 20210325,

Van Dyke, M. W. (2014) 'Lysine deacetylase (KDAC) regulatory pathways: an alternative approach to selective modulation.' *ChemMedChem*, 9(3), Mar, 20140121, pp. 511-522.

van Hinsbergh, V. W. (2012) 'Endothelium--role in regulation of coagulation and inflammation.' *Semin Immunopathol*, 34(1), Jan, 20110804, pp. 93-106.

Vane, J. R. and Botting, R. M. (2003) 'The mechanism of action of aspirin.' *Thromb Res*, 110(5-6), Jun 15, pp. 255-258.

Vega, M. E., Kastberger, B., Wehrle-Haller, B. and Schwarzbauer, J. E. (2020) 'Stimulation of Fibronectin Matrix Assembly by Lysine Acetylation.' *Cells*, 9(3), Mar 8, 20200308,

Velnar, T. and Gradisnik, L. (2018) 'Tissue Augmentation in Wound Healing: the Role of Endothelial and Epithelial Cells.' *Med Arch*, 72(6), Dec, pp. 444-448.

Verdone, L., Agricola, E., Caserta, M. and Di Mauro, E. (2006) 'Histone acetylation in gene regulation.' *Briefings in Functional Genomics*, 5(3) pp. 209-221.

Versteeg, H. H., Heemskerk, J. W., Levi, M. and Reitsma, P. H. (2013) 'New fundamentals in hemostasis.' *Physiol Rev*, 93(1), Jan, pp. 327-358.

Vestweber, D. (2008) 'VE-Cadherin.' *Arteriosclerosis, Thrombosis, and Vascular Biology*, 28(2) pp. 223-232.

Violi, F., Cammisotto, V., Bartimoccia, S., Pignatelli, P., Carnevale, R. and Nocella, C. (2023) 'Gut-derived low-grade endotoxaemia, atherothrombosis and cardiovascular disease.' *Nature Reviews Cardiology*, 20(1), 2023/01/01, pp. 24-37.

Virani, S. S., Newby, L. K., Arnold, S. V., Bittner, V., Brewer, L. C., Demeter, S. H., Dixon, D. L., Fearon, W. F., et al. (2023) '2023 AHA/ACC/ACCP/ASPC/NLA/PCNA Guideline for the Management of Patients With Chronic Coronary Disease: A Report of the American Heart Association/American College of Cardiology Joint Committee on Clinical Practice Guidelines.' *Circulation*, 148(9), 2023/08/29, pp. e9-e119.

Vlad, M. L., Manea, S. A., Lazar, A. G., Raicu, M., Muresian, H., Simionescu, M. and Manea, A. (2019) 'Histone Acetyltransferase-Dependent Pathways Mediate Upregulation of NADPH Oxidase 5 in Human Macrophages under Inflammatory Conditions: A Potential Mechanism of Reactive Oxygen Species Overproduction in Atherosclerosis.' *Oxid Med Cell Longev*, 2019 20190902, p. 3201062.

W., Z., Zhang, Y., Guo, X., Zeng, Z., Wu, J., Liu, Y., He, J., Wang, R., et al. (2017) 'Sirt1 Protects Endothelial Cells against LPS-Induced Barrier Dysfunction.' *Oxid Med Cell Longev*, 2017 20171025, p. 4082102.

Wallentin, L., Becker, R. C., Budaj, A., Cannon, C. P., Emanuelsson, H., Held, C., Horrow, J., Husted, S., et al. (2009) 'Ticagrelor versus clopidogrel in patients with acute coronary syndromes.' *N Engl J Med*, 361(11), Sep 10, 20090830, pp. 1045-1057.

Wallerath, T., Deckert, G., Ternes, T., Anderson, H., Li, H., Witte, K. and Förstermann, U. (2002) 'Resveratrol, a polyphenolic phytoalexin present in red wine, enhances expression and activity of endothelial nitric oxide synthase.' *Circulation*, 106(13), Sep 24, pp. 1652-1658.

Wandall, H. H., Rumjantseva, V., Sørensen, A. L., Patel-Hett, S., Josefsson, E. C., Bennett, E. P., Italiano, J. E., Jr., Clausen, H., et al. (2012) 'The origin and function of platelet glycosyltransferases.' *Blood*, 120(3), Jul 19, 20120521, pp. 626-635.

Wang, Hao, H., Leeper, N. J. and Zhu, L. (2018) 'Thrombotic Regulation From the Endothelial Cell Perspectives.' *Arteriosclerosis, Thrombosis, and Vascular Biology*, 38(6), 2018/06/01, pp. e90-e95.

Wang, Wu, L., Chen, J., Dong, L., Chen, C., Wen, Z., Hu, J., Fleming, I., et al. (2021) 'Metabolism pathways of arachidonic acids: mechanisms and potential therapeutic targets.' *Signal Transduction and Targeted Therapy*, 6(1), 2021/02/26, p. 94.

Wang, X. and He, B. (2024) 'Endothelial dysfunction: molecular mechanisms and clinical implications.' *MedComm*, 5(8), 2024/08/01, p. e651.

Watson, S. P., Asazuma, N., Atkinson, B., Berlanga, O., Best, D., Bobe, R., Jarvis, G., Marshall, S., et al. (2001) 'The role of ITAM- and ITIM-coupled receptors in platelet activation by collagen.' *Thromb Haemost*, 86(1), Jul, pp. 276-288.

Wautier, J. L. and Wautier, M. P. (2020) 'Cellular and Molecular Aspects of Blood Cell-Endothelium Interactions in Vascular Disorders.' *Int J Mol Sci*, 21(15), Jul 27, 20200727,

Weaver, A. M., Karginov, A. V., Kinley, A. W., Weed, S. A., Li, Y., Parsons, J. T. and Cooper, J. A. (2001) 'Cortactin promotes and stabilizes Arp2/3-induced actin filament network formation.' *Current Biology*, 11(5), 2001/03/06/, pp. 370-374.

Weis, W. I. and Kobilka, B. K. (2018) 'The Molecular Basis of G Protein-Coupled Receptor Activation.' *Annu Rev Biochem*, 87, Jun 20, pp. 897-919.

Wettschureck, N., Moers, A. and Offermanns, S. (2004) 'Mouse models to study G-protein-mediated signaling.' *Pharmacol Ther*, 101(1), Jan, pp. 75-89.

Weyrich, A. S., Schwertz, H., Kraiss, L. W. and Zimmerman, G. A. (2009) 'Protein synthesis by platelets: historical and new perspectives.' *J Thromb Haemost*, 7(2), Feb, 20081029, pp. 241-246.

White, J., Derheimer, F. A., Jensen-Pergakes, K., O'Connell, S., Sharma, S., Spiegel, N. and Paul, T. A. (2024) 'Histone lysine acetyltransferase inhibitors: an emerging class of drugs for cancer therapy.' *Trends in Pharmacological Sciences*, 45(3), 2024/03/01/, pp. 243-254.

WHO. (2021) *Cardiovascular diseases (CVDs)*. [Online] [Accessed on 08/10/2024] <https://www.who.int/news-room/fact-sheets/detail/cardiovascular-diseases-cvds>

Wijns, W., Kolh, P., Danchin, N., Di Mario, C., Falk, V., Folliguet, T., Garg, S., Huber, K., et al. (2010) 'Guidelines on myocardial revascularization.' *Eur Heart J*, 31(20), Oct, 20100829, pp. 2501-2555.

Wilcox, C. S. (2012) 'Asymmetric Dimethylarginine and Reactive Oxygen Species.' *Hypertension*, 59(2), 2012/02/01, pp. 375-381.

Winnik, S., Auwerx, J., Sinclair, D. A. and Matter, C. M. (2015) 'Protective effects of sirtuins in cardiovascular diseases: from bench to bedside.' *European Heart Journal*, 36(48) pp. 3404-3412.

Winter, P. M., Neubauer, A. M., Caruthers, S. D., Harris, T. D., Robertson, J. D., Williams, T. A., Schmieder, A. H., Hu, G., et al. (2006) 'Endothelial $\alpha(v)\beta_3$ integrin-targeted fumagillin nanoparticles inhibit angiogenesis in atherosclerosis.' *Arterioscler Thromb Vasc Biol*, 26(9), Sep, 20060706, pp. 2103-2109.

Witjas, F. M. R., van den Berg, B. M., van den Berg, C. W., Engelse, M. A. and Rabelink, T. J. (2019) 'Concise Review: The Endothelial Cell Extracellular Matrix Regulates Tissue Homeostasis and Repair.' *Stem Cells Transl Med*, 8(4), Apr, 20181211, pp. 375-382.

Woronowicz, K., Dilks, J. R., Rozenvayn, N., Dowal, L., Blair, P. S., Peters, C. G., Woronowicz, L. and Flaumenhaft, R. (2010) 'The platelet actin cytoskeleton associates with SNAREs and participates in alpha-granule secretion.' *Biochemistry*, 49(21), Jun 1, pp. 4533-4542.

Woulfe, D. S. (2005) 'REVIEW ARTICLES: Platelet G protein-coupled receptors in hemostasis and thrombosis.' *Journal of Thrombosis and Haemostasis*, 3(10) pp. 2193-2200.

Wu, Zhang, T.-N., Chen, H.-H., Yu, X.-F., Lv, J.-L., Liu, Y.-Y., Liu, Y.-S., Zheng, G., et al. (2022) 'The sirtuin family in health and disease.' *Signal Transduction and Targeted Therapy*, 7(1), 2022/12/29, p. 402.

Wu, M. D., Atkinson, T. M. and Lindner, J. R. (2017) 'Platelets and von Willebrand factor in atherogenesis.' *Blood*, 129(11), Mar 16, 20170207, pp. 1415-1419.

Wu, M. Y., Li, C. J., Hou, M. F. and Chu, P. Y. (2017) 'New Insights into the Role of Inflammation in the Pathogenesis of Atherosclerosis.' *Int J Mol Sci*, 18(10), Sep 22, 20170922,

Wu, Q., Hu, Y., Jiang, M., Wang, F. and Gong, G. (2019) 'Effect of Autophagy Regulated by Sirt1/FoxO1 Pathway on the Release of Factors Promoting Thrombosis from Vascular Endothelial Cells.' *Int J Mol Sci*, 20(17), Aug 24, 20190824,

Wu, Z., Liu, M.-C., Liang, M. and Fu, J. (2012) 'Sirt1 protects against thrombomodulin down-regulation and lung coagulation after particulate matter exposure.' *Blood*, 119(10) pp. 2422-2429.

Xia, N., Strand, S., Schluffer, F., Siuda, D., Reifenberg, G., Kleinert, H., Förstermann, U. and Li, H. (2013) 'Role of SIRT1 and FOXO factors in eNOS transcriptional activation by resveratrol.' *Nitric Oxide*, 32, 2013/08/01/, pp. 29-35.

Xia, N., Daiber, A., Habermeier, A., Closs, E. I., Thum, T., Spanier, G., Lu, Q., Oelze, M., et al. (2010) 'Resveratrol reverses endothelial nitric-oxide synthase uncoupling in apolipoprotein E knockout mice.' *J Pharmacol Exp Ther*, 335(1), Oct, 20100707, pp. 149-154.

Xin, H. Y., Jiang, D. J., Jia, S. J., Song, K., Wang, G. P., Li, Y. J. and Chen, F. P. (2007) 'Regulation by DDAH/ADMA pathway of lipopolysaccharide-induced tissue factor expression in endothelial cells.' *Thromb Haemost*, 97(5), May, pp. 830-838.

Xiong, Y., Uys, J. D., Tew, K. D. and Townsend, D. M. (2011) 'S-glutathionylation: from molecular mechanisms to health outcomes.' *Antioxid Redox Signal*, 15(1), Jul 1, 20110525, pp. 233-270.

Yanagisawa, S., Baker, J. R., Vuppusetty, C., Koga, T., Colley, T., Fenwick, P., Donnelly, L. E., Barnes, P. J., et al. (2018) 'The dynamic shuttling of SIRT1 between cytoplasm and nuclei in bronchial epithelial cells by single and repeated cigarette smoke exposure.' *PLoS One*, 13(3) 20180306, p. e0193921.

Yang, Liu, Y., Wang, Y., Chao, Y., Zhang, J., Jia, Y., Tie, J. and Hu, D. (2022) 'Regulation of SIRT1 and Its Roles in Inflammation.' *Front Immunol*, 13 20220311, p. 831168.

Yang, Zhou, R., Yu, S., Yu, S., Cui, Z., Hu, P., Liu, J., Qiao, Q., et al. (2019) 'Cytoplasmic SIRT1 inhibits cell migration and invasion by impeding epithelial-mesenchymal transition in ovarian carcinoma.' *Mol Cell Biochem*, 459(1-2), Sep, 20190717, pp. 157-169.

Yang, H., Zhang, W., Pan, H., Feldser, H. G., Lainez, E., Miller, C., Leung, S., Zhong, Z., et al. (2012) 'SIRT1 Activators Suppress Inflammatory Responses through Promotion of p65 Deacetylation and Inhibition of NF- κ B Activity.' *PLOS ONE*, 7(9) p. e46364.

Yang, J., Mapelli, C., Wang, Z., Sum, C. S., Hua, J., Lawrence, R. M., Ni, Y. and Seiffert, D. A. (2022) 'An optimized agonist peptide of protease-activated receptor 4 and its use in a validated platelet-aggregation assay.' *Platelets*, 33(7), Oct 3, 20220328, pp. 979-986.

Yang, T., Zhou, R., Yu, S., Yu, S., Cui, Z., Hu, P., Liu, J., Qiao, Q., et al. (2019) 'Cytoplasmic SIRT1 inhibits cell migration and invasion by impeding epithelial-mesenchymal transition in ovarian carcinoma.' *Mol Cell Biochem*, 459(1-2), Sep, 20190717, pp. 157-169.

Yang, X., Yu, W., Shi, L., Sun, L., Liang, J., Yi, X., Li, Q., Zhang, Y., et al. (2011) 'HAT4, a Golgi Apparatus-Anchored B-Type Histone Acetyltransferase, Acetylates Free Histone H4 and Facilitates Chromatin Assembly.' *Molecular Cell*, 44(1), 2011/10/07/, pp. 39-50.

Yang, X. D., Tajkhorshid, E. and Chen, L. F. (2010) 'Functional interplay between acetylation and methylation of the RelA subunit of NF-kappaB.' *Mol Cell Biol*, 30(9), May, 20100216, pp. 2170-2180.

Yeung, F., Hoberg, J. E., Ramsey, C. S., Keller, M. D., Jones, D. R., Frye, R. A. and Mayo, M. W. (2004) 'Modulation of NF-kappaB-dependent transcription and cell survival by the SIRT1 deacetylase.' *Embo j*, 23(12), Jun 16, 20040520, pp. 2369-2380.

Yip, J., Shen, Y., Berndt, M. C. and Andrews, R. K. (2005) 'Primary platelet adhesion receptors.' *IUBMB Life*, 57(2), Feb, pp. 103-108.

Zampetaki, A., Zeng, L., Margariti, A., Xiao, Q., Li, H., Zhang, Z., Pepe, A. E., Wang, G., et al. (2010) 'Histone Deacetylase 3 Is Critical in Endothelial Survival and Atherosclerosis Development in Response to Disturbed Flow.' *Circulation*, 121(1), 2010/01/05, pp. 132-142.

Zaninetti, C., Sachs, L. and Palankar, R. (2020) 'Role of Platelet Cytoskeleton in Platelet Biomechanics: Current and Emerging Methodologies and Their Potential Relevance for the Investigation of Inherited Platelet Disorders.' *Hamostaseologie*, 40(3), Aug, 20200729, pp. 337-347.

Zarbock, A., Ley, K., McEver, R. P. and Hidalgo, A. (2011) 'Leukocyte ligands for endothelial selectins: specialized glycoconjugates that mediate rolling and signaling under flow.' *Blood*, 118(26), Dec 22, 20111020, pp. 6743-6751.

Zhang, Cui, G., Wang, Y., Gong, Y. and Wang, Y. (2019) 'SIRT1 activation alleviates brain microvascular endothelial dysfunction in peroxisomal disorders.' *Int J Mol Med*, 44(3), Sep, 20190620, pp. 995-1005.

Zhang, Wang, Z., Chen, H. Z., Zhou, S., Zheng, W., Liu, G., Wei, Y. S., Cai, H., et al. (2008) 'Endothelium-specific overexpression of class III deacetylase SIRT1 decreases atherosclerosis in apolipoprotein E-deficient mice.' *Cardiovasc Res*, 80(2), Nov 1, 20080809, pp. 191-199.

Zhang, C. (2008) 'The role of inflammatory cytokines in endothelial dysfunction.' *Basic Res Cardiol*, 103(5), Sep, 20080703, pp. 398-406.

Zhang, J. (2022) 'Biomarkers of endothelial activation and dysfunction in cardiovascular diseases.' *RCM*, 23(2), 2022-02-24,

Zhang, R., Chen, H. Z., Liu, J. J., Jia, Y. Y., Zhang, Z. Q., Yang, R. F., Zhang, Y., Xu, J., et al. (2010) 'SIRT1 suppresses activator protein-1 transcriptional activity and cyclooxygenase-2 expression in macrophages.' *J Biol Chem*, 285(10), Mar 5, 20091230, pp. 7097-7110.

Zhang, W., Huang, Q., Zeng, Z., Wu, J., Zhang, Y. and Chen, Z. (2017) 'Sirt1 Inhibits Oxidative Stress in Vascular Endothelial Cells.' *Oxidative Medicine and Cellular Longevity*, 2017(1), 2017/01/01, p. 7543973.

Zhang, W., Zhang, Y., Guo, X., Zeng, Z., Wu, J., Liu, Y., He, J., Wang, R., et al. (2017) 'Sirt1 Protects Endothelial Cells against LPS-Induced Barrier Dysfunction.' *Oxid Med Cell Longev*, 2017 20171025, p. 4082102.

Zhang, W., Feng, Y., Guo, Q., Guo, W., Xu, H., Li, X., Yi, F., Guan, Y., et al. (2020) 'SIRT1 modulates cell cycle progression by regulating CHK2 acetylation–phosphorylation.' *Cell Death & Differentiation*, 27(2), 2020/02/01, pp. 482-496.

Zhang, X., Ameer, F. S., Azhar, G. and Wei, J. Y. (2021) 'Alternative Splicing Increases Sirtuin Gene Family Diversity and Modulates Their Subcellular Localization and Function.' *International Journal of Molecular Sciences*, 22(2) p. 473.

Zhang, Y., Ehrlich, S. M., Zhu, C. and Du, X. (2022) 'Signaling mechanisms of the platelet glycoprotein Ib-IX complex.' *Platelets*, 33(6), Aug 18, 20220526, pp. 823-832.

Zhang, Y., Cui, G., Wang, Y., Gong, Y. and Wang, Y. (2019) 'SIRT1 activation alleviates brain microvascular endothelial dysfunction in peroxisomal disorders.' *Int J Mol Med*, 44(3), 2019/09/01, pp. 995-1005.

Zhao, Y. and Liu, Y. S. (2021) 'Longevity Factor FOXO3: A Key Regulator in Aging-Related Vascular Diseases.' *Front Cardiovasc Med*, 8 20211223, p. 778674.

Zhou, C., Tan, Y., Xu, B., Wang, Y. and Cheang, W. S. (2022) '3,4',5-Trimethoxy-trans-stilbene Alleviates Endothelial Dysfunction in Diabetic and Obese Mice via Activation of the AMPK/SIRT1/eNOS Pathway.' *Antioxidants (Basel)*, 11(7), Jun 28, 20220628,

Zhou, D. W., Fernández-Yagüe, M. A., Holland, E. N., García, A. F., Castro, N. S., O'Neill, E. B., Eyckmans, J., Chen, C. S., et al. (2021) 'Force-FAK signaling coupling at individual focal adhesions coordinates mechanosensing and microtissue repair.' *Nature Communications*, 12(1), 2021/04/21, p. 2359.

Zhou, R., Barnes, K., Gibson, S. and Fillmore, N. (2024) 'Dual-edged role of SIRT1 in energy metabolism and cardiovascular disease.' *American Journal of Physiology-Heart and Circulatory Physiology*, 327(5), 2024/11/01, pp. H1162-H1173.

Zhu, L., Liu, Y.-P., Huang, Y.-T., Zhou, Z.-J., Liu, J.-F., Yu, L.-M. and Wang, H.-S. (2024) 'Cellular and molecular biology of posttranslational modifications in cardiovascular disease.' *Biomedicine & Pharmacotherapy*, 179, 2024/10/01/, p. 117374.

Zonderland, J., Wieringa, P. and Moroni, L. (2019) 'A quantitative method to analyse F-actin distribution in cells.' *MethodsX*, 6, 2019/01/01/, pp. 2562-2569.

Zubčić, K., Radovanović, V., Vlainić, J., Hof, P. R., Oršolić, N., Šimić, G. and Jazvinščak Jembrek, M. (2020) 'PI3K/Akt and ERK1/2 Signalling Are Involved in Quercetin-Mediated Neuroprotection against Copper-Induced Injury.' *Oxid Med Cell Longev*, 2020 20200711, p. 9834742.

Appendices

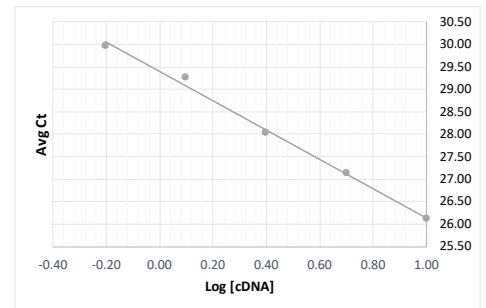
Appendix A - Primer efficiencies

DDAH1

Ct 1	Ct 2	Ct 3	Avg Ct
26.45	25.56	26.36	26.12
27.31	26.95	27.14	27.13
28.21	27.73	28.14	28.03
29.23	29.12	29.44	29.26
29.80	30.02	30.09	29.97

[cDNA] (ng)	Log [cDNA]
10.0000	1.00
5.0000	0.70
2.5000	0.40
1.2500	0.10
0.6250	-0.20

Dilution Factor	2
Slope	-3.262426785
R Squared	0.9951
Efficiency (%)	102.54

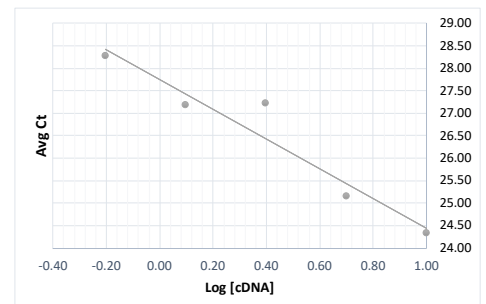


ENTPD1

Ct 1	Ct 2	Ct 3	Avg Ct
24.44	24.32	24.18	24.31
25.13	25.10	25.21	25.15
26.18	26.26	29.19	27.21
27.16	27.09	27.28	27.18
28.29	28.17	28.37	28.27

[cDNA] (ng)	Log [cDNA]
10.0000	1.00
5.0000	0.70
2.5000	0.40
1.2500	0.10
0.6250	-0.20

Dilution Factor	2
Slope	-3.305025046
R Squared	0.9260
Efficiency (%)	100.71



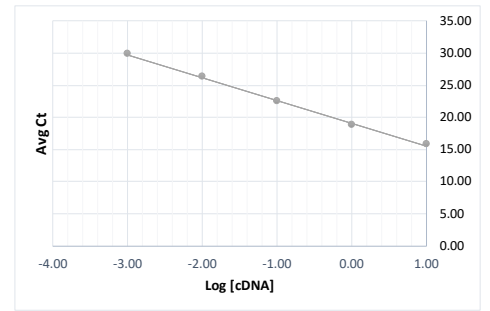
GAPDH

Ct 1	Ct 2	Ct 3	Avg Ct
15.89	15.86	15.81	15.85
18.77	18.75	18.72	18.75
22.29	22.40	22.60	22.43
26.47	26.15	26.37	26.33
30.05	29.75	29.83	29.87

[cDNA] (ng)	Log [cDNA]
10.0000	1.00
1.0000	0.00
0.1000	-1.00
0.0100	-2.00
0.0010	-3.00

Dilution Factor

Slope -3.562768344
R Squared 0.9977
Efficiency (%) **90.84**

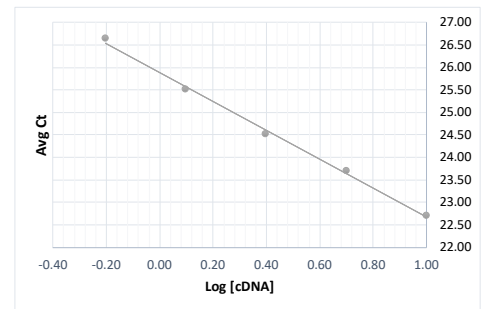
**NOS3**

Ct 1	Ct 2	Ct 3	Avg Ct
22.73	22.69	22.67	22.70
23.80	23.67	23.59	23.69
24.51	24.49	24.51	24.50
25.57	25.44	25.48	25.50
26.59	26.51	26.82	26.64

[cDNA] (ng)	Log [cDNA]
10.0000	1.00
5.0000	0.70
2.5000	0.40
1.2500	0.10
0.6250	-0.20

Dilution Factor

Slope -3.221029736
R Squared 0.9968
Efficiency (%) **104.39**

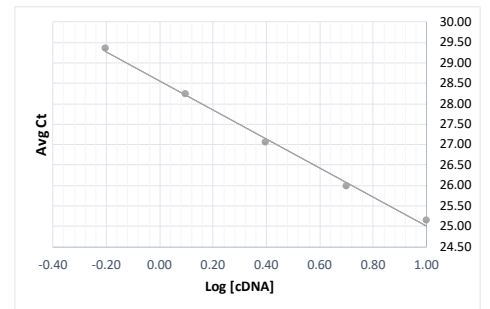
**PTGS1**

Ct 1	Ct 2	Ct 3	Avg Ct
25.21	25.07	25.12	25.13
26.13	25.95	25.87	25.98
27.05	27.06	27.00	27.04
28.18	28.22	28.31	28.24
29.06	29.42	29.55	29.34

[cDNA] (ng)	Log [cDNA]
10.0000	1.00
5.0000	0.70
2.5000	0.40
1.2500	0.10
0.6250	-0.20

Dilution Factor

Slope -3.545949945
R Squared 0.9964
Efficiency (%) **91.43**

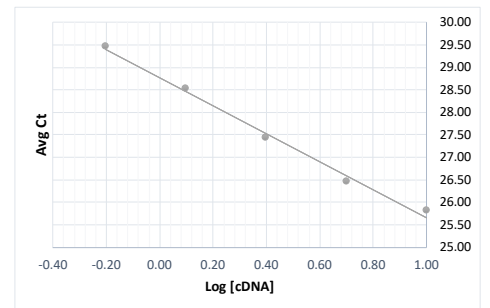
**PTGS2**

Ct 1	Ct 2	Ct 3	Avg Ct
25.95	25.79	25.68	25.81
26.40	26.56	26.40	26.45
27.52	27.36	27.42	27.43
28.43	28.44	28.72	28.53
29.43	29.47	29.46	29.46

[cDNA] (ng)	Log [cDNA]
10.0000	1.00
5.0000	0.70
2.5000	0.40
1.2500	0.10
0.6250	-0.20

Dilution Factor

Slope -3.111976006
R Squared 0.9934
Efficiency (%) **109.57**

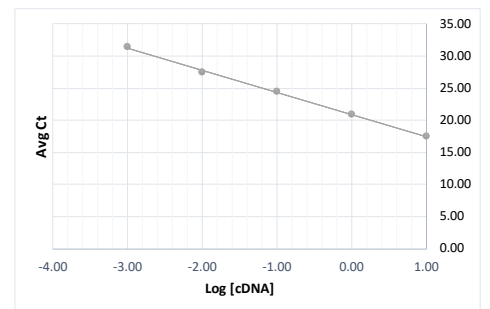
**RPLPO**

Ct 1	Ct 2	Avg Ct
17.37	17.53	17.45
20.56	21.08	20.82
24.21	24.64	24.42
27.30	27.60	27.45
31.33	31.53	31.43

[cDNA] (ng)	Log [cDNA]
10.0000	1.00
1.0000	0.00
0.1000	-1.00
0.0100	-2.00
0.0010	-3.00

Dilution Factor

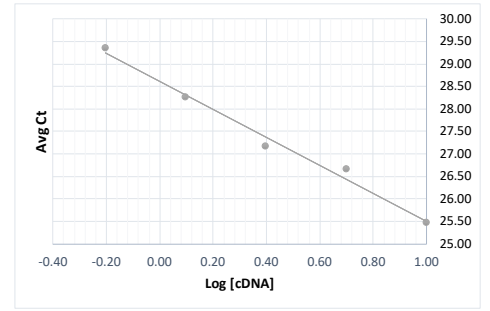
Slope -3.458901756
R Squared 0.9987
Efficiency (%) **94.58**



SIRT1			
Ct 1	Ct 2	Ct 3	Avg Ct
25.48	25.38	25.49	25.45
26.47	26.82	26.64	26.64
27.30	27.03	27.16	27.16
28.10	28.39	28.25	28.25
29.45	29.25	29.35	29.35

[cDNA] (ng)	Log [cDNA]
10.0000	1.00
5.0000	0.70
2.5000	0.40
1.2500	0.10
0.6250	-0.20

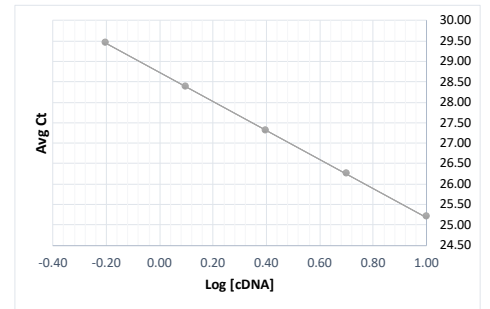
Dilution Factor	2
Slope	-3.121700724
R Squared	0.9884
Efficiency (%)	109.09



THBD			
Ct 1	Ct 2	Ct 3	Avg Ct
25.21	25.22	25.14	25.19
26.22	26.22	26.31	26.25
27.34	27.44	27.16	27.31
28.35	28.44	28.36	28.38
29.56	29.38	29.42	29.45

[cDNA] (ng)	Log [cDNA]
10.0000	1.00
5.0000	0.70
2.5000	0.40
1.2500	0.10
0.6250	-0.20

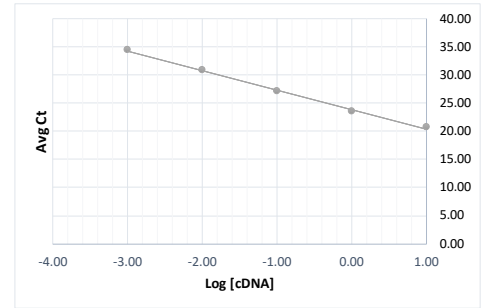
Dilution Factor	2
Slope	-3.541998456
R Squared	1.0000
Efficiency (%)	91.57



VCAM			
Ct 1	Ct 2	Ct 3	Avg Ct
20.75	20.74	20.68	20.72
23.57	23.43	23.71	23.57
26.87	27.16	27.05	27.03
30.85	30.93	31.01	30.93
35.56	34.56	33.42	34.51

[cDNA] (ng)	Log [cDNA]
10.0000	1.00
1.0000	0.00
0.1000	-1.00
0.0100	-2.00
0.0010	-3.00

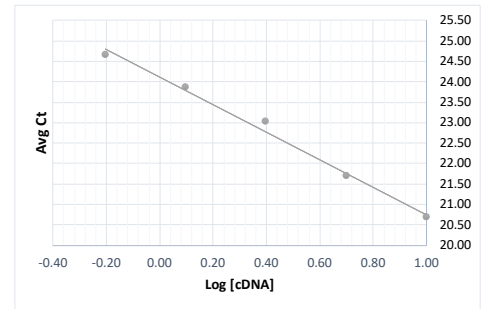
Dilution Factor	2
Slope	-3.494702587
R Squared	0.9971
Efficiency (%)	93.26



VWF			
Ct 1	Ct 2	Avg Ct	
21.15	20.20	20.68	
21.77	21.60	21.68	
23.01	23.01	23.01	
23.75	23.97	23.86	
24.49	24.82	24.65	

[cDNA] (ng)	Log [cDNA]
10.0000	1.00
5.0000	0.70
2.5000	0.40
1.2500	0.10
0.6250	-0.20

Dilution Factor	2
Slope	-3.364065685
R Squared	0.9910
Efficiency (%)	98.27



Appendix B – Live HCAEC migration

The following videos, in which HCAEC motility and migration in a gap closure assay in the presence of vehicle or SRT1720 can be observed, are complementary to the data presented in Figure 5.4.



Vehicle.mp4



SRT1720 0.3 μM.mp4



SRT1720 1 μM.mp4



SRT1720 3 μM.mp4

